



Wissenschaftszentrum Weihenstephan für Ernährung, Landnutzung und Umwelt

Lehrstuhl für Botanik

**Identification and characterization of a novel component
involved in water deficit stress and abscisic acid signaling in
*Arabidopsis thaliana***

Jin Huang

Vollständiger Abdruck der von der Fakultät Wissenschaftszentrum Weihenstephan für Ernährung, Landnutzung und Umwelt der Technischen Universität München zur Erlangung des akademischen Grades eines

Doktors der Naturwissenschaften

genehmigten Dissertation.

Vorsitzender: Univ.-Prof. Dr. Ralph Hückelhoven

Prüfer der Dissertation:

1. Univ.-Prof. Dr. Erwin Grill
2. Univ.-Prof. Dr. Kay Schneitz

Die Dissertation wurde am 28.10.2014 bei der Technischen Universität München eingereicht und durch die Fakultät Wissenschaftszentrum Weihenstephan für Ernährung, Landnutzung und Umwelt am 27.11.2014 angenommen.

Contents

SUMMARY	13
ZUSAMMENFASSUNG	15
1. INTRODUCTION	17
1.1 PHYSIOLOGICAL RESPONSES TO WATER DEFICIT	17
1.1.1 Drought escape.....	18
1.1.2 Low water potential/dehydration avoidance	19
1.1.3 Dehydration tolerance	20
1.1.4 Integrated stressresponses	21
1.2 WATER DEFICIT PERCEPTION AND TRANSDUCTION.....	23
1.2.1 Two-component systems	25
1.2.2 Mechanosensor	26
1.2.3 Cell wall integrity (CWI) sensor.....	28
1.2.4 Upstream signal transduction	29
1.3 ABA-DEPENDENT SIGNALING PATHWAY.....	31
1.3.1 ABA metabolism	31
1.3.2 ABA transport	35
1.3.3 ABA perception and core ABA signaling	36
1.3.4 Signal transduction and the targets of SnRK2s.....	40
1.3.5 Ca ²⁺ -dependent ABA signaling.....	44
1.4 ABA-INDEPENDENT WATER DEFICIT SIGNALING	45
1.5 THE AIM OF THIS WORK	47
2. MATERIALS AND METHODS	49
2.1 MATERIALS.....	49
2.1.1 Plant materials.....	49
2.1.2 Reagents.....	49
2.1.3 Microorganisms	50
2.1.4 Oligonucleotides and plasmids	50
2.1.5 Medium and sterilization.....	50
2.2 METHODS	55
2.2.1 Plant growth condition	55
2.2.2 Seed sterilization and seedling growth condition	55
2.2.3 Quantification of ABA-dependent luciferase activity.....	55
2.2.4 Map-based cloning	56
2.2.5 Next generation sequencing (NGS).....	58
2.2.6 Methods for plant analysis	58
2.2.7 Protoplasts expression in <i>Arabidopsis thaliana</i>	61
2.2.8 Floral dip of <i>Arabidopsis thaliana</i>	64
2.2.9 Standard molecular biology methods.....	65
2.2.10 High-throughput yeast two-hybrid screen	68

3. RESULTS	75
3.1 ISOLATION OF A NOVEL ABA-HYPERSENSITIVE MUTANT <i>AHR11</i>	75
3.2 MAP-BASED CLONING AND NEXT GENERATION SEQUENCING	78
3.2.1 <i>Generation of mapping population</i>	78
3.2.2 <i>First-pass mapping</i>	80
3.2.3 <i>Fine-scale mapping</i>	82
3.2.4 <i>Pre-selection of candidate genes</i>	84
3.2.5 <i>Next generation sequencing</i>	85
3.3 IDENTIFICATION OF <i>AHR11</i> GENE	87
3.3.1 <i>Ectopic expression in Arabidopsis thaliana protoplasts</i>	87
3.3.2 <i>Ectopic expression in plants</i>	90
3.3.3 <i>T-DNA knockout mutants of candidate gene</i>	94
3.4 PHYSIOLOGICAL ANALYSES OF <i>AHR11</i>	97
3.4.1 <i>Transpiration and leaf temperature under well-watered condition</i>	97
3.4.2 <i>Water loss of detached shoots</i>	99
3.4.3 <i>Stomatal closure and ABA</i>	100
3.4.4 <i>Seed dormancy</i>	104
3.4.5 <i>Seed Germination</i>	105
3.4.6 <i>Root growth</i>	106
3.4.7 <i>Developmental phenotypes of ahr11</i>	108
3.5 PHYSIOLOGICAL ANALYSES OF <i>AHR11</i> MUTANT IN <i>ABA2-1</i> AND <i>ABI1-1</i> GENOME BACKGROUND	111
3.5.1 <i>Crosses of ahr11 to aba2-1 and abi1-1 mutants</i>	111
3.5.2 <i>Physiological analyses of double mutants ahr11/aba2-1 and ahr11/abi1-1</i>	111
3.6 FUNCTIONAL ANALYSIS OF <i>AHR11</i>	113
3.6.1 <i>Subcellular localization of wild type AHR11 and of truncated protein Δahr11</i>	113
3.6.2 <i>ABA biosynthesis and distribution under water deficit</i>	113
3.7 YEAST TWO-HYBRID SCREEN FOR PROTEINS INTERACTING WITH <i>AHR11</i>	119
3.7.1 <i>Generation of expression plasmids and identification of autoactivators</i>	119
3.7.2 <i>Yeast-two-hybrid screen and verification of putative interactions</i>	120
3.7.3 <i>Analysis of potential interacting candidates</i>	122
4. DISCUSSIONS	125
4.1 IDENTIFICATION OF <i>AHR11</i> USING A FORWARD GENETIC APPROACH	125
4.2 FUNCTION OF <i>AHR11</i> IN PLANTS	127
4.2.1 <i>AHR11 protein</i>	127
4.2.2 <i>AHR11 negatively regulates ABA-induced gene expression</i>	132
4.2.3 <i>Physiological function of AHR11 under water deficit</i>	133
4.3 <i>AHR11</i> AS A COMPONENT OF A REGULATORY NETWORK	140
4.3.1 <i>Network of genes co-regulated with AHR11</i>	140
4.3.2 <i>Yeast two-hybrid interactome screen for interacting partners of AHR11</i>	143
4.4 MULTIPLE FUNCTIONS OF <i>AHR11</i> IN DEVELOPMENT AND NON-ABA HORMONE SIGNALING PATHWAYS	153
5. APPENDIX	155
5.1 OLIGO NUCLEOTIDES USED IN THIS WORK	155

5.1.1	<i>Primers for mapping</i>	155
5.1.2	<i>Primers for Cloning and genotyping</i>	157
5.1.3	<i>Primers for Real Time-PCR</i>	160
5.2	STRAINS USED IN THIS WORK	161
5.3	GENOTYPING OF MUTANTS AND TRANSFORMANTS OF <i>ARABIDOPSIS THALIANA</i>	164
5.3.1	<i>EMS-induced mutant ahr11</i>	164
5.3.2	<i>ABA-reporter line pATHB6::LUC</i>	165
5.3.3	<i>ABA-deficient mutant aba2-1</i>	166
5.3.4	<i>ABA-insensitive mutant abi1-1</i>	167
5.4	AHR11-INTERACTING CANDIDATES IN YEAST TWO-HYBRID SCREEN	168
6.	REFERENCES	169
	LEBENS LAUF	205
	ACKNOWLEDGMENTS	207

List of Figures and Tables

Figures

Figure 1-1: Conceptual diagram of the responses of plants to water deficit stress

Figure 1-2: A simplified model of the water deficit sensing and signaling pathway

Figure 1-3: Hydraulic sensors and sensor candidates in different organisms

Figure 1-4: Overview of the ABA-dependent water deficit stress signaling pathway

Figure 3-1: Activation of the LUC reporter in wild type and *ahr11* seedlings harboring the *pATHB6::LUC* ABA-reporter construct by water deficit stress and exogenous ABA

Figure 3-2: ABA-induced activation of the LUC-reporter in wild type *pATHB6::LUC* and mutant *ahr11* seedlings grown in liquid culture

Figure 3-3: Hypersensitivity of *ahr11* to water deficit stress is a recessive trait

Figure 3-4: Phenotyping of *Ler* x *ahr11* F₃ progenies

Figure 3-5A: Schematic representation of first-pass mapping marker set

Figure 3-5B: Bulked segregant analysis of *ahr11* mutant

Figure 3-6: Recombination events of 17 individuals in *Ler* x *ahr11* F₂ mapping population

Figure 3-7: Map-based cloning of the *AHR11* gene in *ahr11*

Figure 3-8: SNPs of *ahr11* detected by NGS in interest region on chromosome V

Figure 3-9: Schematic representation of *AHR11* and of changes in *ahr11* mutant alleles

Figure 3-10: The ABA-induced luciferase activity measured in *ahr11* protoplasts specifically results from the ABA-reporter construct *pRD29B::LUC*

Figure 3-11: The *ahr11* mutant allele confers ABA-hypersensitivity to *Arabidopsis* protoplasts

Figure 3-12: ABA-dependent luciferase activity in response to water deficit stress and ABA of transgenic *ahr11* mutant and wild type *pAtHB6::LUC*

Figure 3-13: Morphological phenotype of transgenic *ahr11* mutant and wild type *pAtHB6::LUC*

Figure 3-14: Selection and characterization of *AHR11* homozygous T-DNA knockout mutants

Figure 3-15: The ABA-induced and water-deficit-induced activation of the ABA-reporter in *AHR11* T-DNA knockout mutants harboring the *pATHB6::LUC* ABA-reporter construct

Figure 3-16: Protoplasts of *AHR11* T-DNA knockout mutants show ABA-hypersensitivity which is complemented by the wild type allele

Figure 3-17: Enhanced transpiration rate of *ahr11* under well-watered conditions

Figure 3-18: Comparison of leaf temperature of *ahr11* and *pAtHB6::LUC* under well-watered condition

Figure 3-19: Enhanced water loss of detached *ahr11* shoots

Figure 3-20: The stomatal response of *ahr11* to root-inflicted water deficit and ABA

Figure 3-21: Hypersensitive and rapid response to exogenous ABA of detached rosette leaf stomatal closure of *ahr11*

Figure 3-22: The seeds of *ahr11* show an extended dormancy

Figure 3-23: Water deficit stress and exogenous ABA inhibit germination of *ahr11* and *pAtHB6::LUC* seeds to a similar extent

Figure 3-24: Contrasting sensitivity of *ahr11* root growth to water deficit stress and to exogenous ABA

Figure 3-25: Development of *ahr11* compared to *pAtHB6::LUC*

Figure 3-26: Chlorophyll content of *ahr11* and *pATHB6::LUC*

Figure 3-27: Enhanced senescence of *ahr11* compared to *pAtHB6::LUC*

Figure 3-28: Response of germination of ABA-deficient *aba2-1*, ABA-insensitive *abi1-1*, as well as double mutants *ahr11/aba2-1* and *ahr11/abi1-1* to water deficit stress and ABA

Figure 3-29: Subcellular localization of eGFP::AHR11 and eGFP:: Δ ahr11 fusion protein in protoplasts

Figure 3-30: The ABA biosynthesis in *ahr11* under water deficit is similar to wild type *pATHB6::LUC*

Figure 3-31: ABA content in fresh seeds of *ahr11* and *pATHB6::LUC*

Figure 3-32: Distribution of water-deficit-induced active ABA in cotyledon of *ahr11* and *pATHB6::LUC*

Figure 3-33: Distribution of exogenous ABA in cotyledon of *ahr11* and *pATHB6::LUC*

Figure 3-34: The expression of ABA transporters in *ahr11* under water deficit stress

Figure 3-35: Schematic representation of fragmented AHR11 ORFs used as baits in the yeast two-hybrid screen and identification of autoactivators

Figure 3-36: Interaction between fragmented AHR11 and candidate proteins in Y2H

Figure 3-37: Grouping of AHR11-interacting candidates

Figure 4-1: Similarity analysis of AHR11 protein in the kingdom

Figure 4-2: Schematic evolutionary tree representing AHR11 radiation

Figure 4-3: Alignment of amino acid sequences of AHR11 orthologs from different species

Figure 4-4: Conserved domains of the AHR11 protein

Figure 4-5: Schematic view of hypothetical function of AHR11 in ABA intercellular transmission

Figure 4-6: Expression pattern of AHR11 during *Arabidopsis thaliana* Col-0 plant development

Figure 4-7: Gene expression pattern during seed development

Figure 4-8: Gene expression pattern during imbibition

Figure 4-9: Hypothetical function of AHR11 in germination under water deficit stress

Figure 4-10: *ABI1* as part of a network of putatively co-regulated genes

Figure 4-11: *AHR11* as part of a network of putatively co-regulated genes

Figure 4-12: Protein-protein interactions of AHR11

Figure 4-13: functions of MYC2 and JAMs in JA signaling and osmotic response

Figure 4-14: Model of Auxin-regulated transcription

Figure 4-15: Model of JA-regulated transcription

Figure 4-16: Hypothetical model of AHR11-regulated transcription

Figure 5-1: Genotyping of EMS-induced mutant *ahr11*

Figure 5-2: Genotyping of ABA-reporter line *pATHB6::LUC* harboring the *pATHB6::LUC* ABA-reporter construct

Figure 5-3: Genotyping of ABA-deficient mutant *aba2-1*

Figure 5-4: Genotyping of ABA-deficient mutant *abi1-1*

Tables

Table 3-1: Genotype of 28 recombinants

Table3-2: Description of detected SNPs of *ahr11*

Table 3-3: The transgenic plants isolation and identification

Table 3-4: Early flowering time of *ahr11* compared to wild type *pATHB6::LUC*

Table 3-5: List of candidate proteins interacting with AHR11 in yeast

Abbreviations

ABA	Abscisic Acid
3AT	3-amino-1,2,4-triazole
AAO	Abscisic aldehyde oxidase
ABA-GE	ABA glucose ester
ABA-GTase	ABA-glucosyltransferase
ABAR/ CHLH/ GUN5	ABA-binding protein/H subunit of Mg-chelatase/Genomes uncoupled 5
ABC transporter	ATP-binding cassette transporter
ABI1/2	ABA INSENSITIVE 1/2; A type PP2C
ABI3	ABA INSENSITIVE 3; B3 domain TF
ABI4	ABA INSENSITIVE 4; APETALA 2 (AP2) domain TF
ABI5	ABA INSENSITIVE 5; bZIP TF
ABRE	ABA-responsive element
AD	Activation Domain
AFP	ABI5-binding protein
AHG1/3	Hypersensitive germination 1/3
AHR11	ABA-Hypersensitive Response 11
AIB/JAM1	ABA-inducible bHLH transcription factor/Jasmonate-associated MYC2-like 1
AIL1	ABA-inducible LEA
AIT1/NRT1.2	ABA-IMPORTING TRANSPORTER 1/NITRATE TRANSPORTER 1.2
AKT1	<i>Arabidopsis</i> Potassium Transporter 1
Amp	Ampicillin
ARE	Auxin-responsive element
AREBs/ABFs	ABRE-binding proteins/factors
ARF	Auxin response TF
AtCSP3	<i>Arabidopsis</i> COLD SHOCK DOMAIN (CSD) PROTEIN 3
ATHB6	<i>Arabidopsis</i> HOMEBOX PROTEIN 6; HD-ZIP TF
Bet v 1	Major birch pollen allergen of <i>Betula verrucosa</i> 1
BG	β -glucosidase
bHLH TF	basic helix-loop-helix transcriptional factor
BiFC	Bimolecular fluorescence complementation
BL	Bright light
bZIP TF	Basic leucine zipper transcription factor
CAM and CaMK	Calmoduline and calmodulin-dependent protein kinase
CaMV	Cauliflower Mosaic Virus
CAPs	Cleaved amplified polymorphic sequence
CBL and CIPK	Calcineurin B-like protein and CBL interacting protein kinase
CCaMK	Calmodulin dependent protein kinases
CDPK/CPK and CRK	Ca ²⁺ -dependent protein kinase and CDPK-related kinase
CDS	Coding sequence
CE	Coupling element
CHX	Cycloheximide
CK	Cytokinin
CKI1/2	CYTOKININ-INDEPENDENT 1/2
COI1	CORONATINE INSENSITIVE 1
CPL3	C-terminal domain phosphatase-like 3
CRD domain	cysteine-rich domain at N-terminus of Wsc sensors
CRE1	CYTOKININ RESPONSE 1
CTAB	Hexadecyl trimethyl-ammonium bromide
CTLH	C-terminal to lissencephaly homology domain of TPL
CWI	Cell wall integrity
DB	DNA binding Domain

dCAP	Derived cleaved amplified polymorphic sequence
DCP	mRNA decapping protein
DLC	Dynein light chain protein
DNA_pol_viral_N	DNA-polymerase N-terminal domain of virus
DPA	Dihydrophaseic acid
DRE/CRT	Dehydration-responsive <i>cis</i> -element/C-Repeat
DREB/CBF	DRE-binding protein/C-repeat-binding factor
DSDS	Days of seed dry storage
DST	Drought and salt tolerance C2H2-type TF
DTT	Dithiothreitol
EAR-motif	Ethylene response factor-associated amphiphilic repression motif
ECM	Extracellular matrix
EDTA	Ethylenediaminetetraacetic acid
EIN4	ETHYLENE INSENSITIVE 4
EMS	Ethylmethanesulfonate
ER	Endoplasmic reticulum
ERD1	EARLY RESPONSIVE TO DEHYDRATION 1
ERS1/2	ETHYLENE SENSOR 1/2
EtBr	Ethidium bromide
ETR1/2	ETHYLENE RESPONSE 1/2
GA	Gibberellic acid
GC-MS	Gas chromatography mass spectrometry
GCR2	G-protein coupled receptor 2
GTG1/2	G-protein coupled receptor (GPCR)-type G protein 1/2
HAB1/2	Homology to ABI1 1/2; A type PP2C
HAI1/2/3	Highly ABA-induced PP2C 1/2/3; A type PP2C
HBV	Hepatitis B virus
HDA19	HISTONE DEACETYLASE 19
HK	Histidine kinase
HOG pathway	High osmolarity glycerol pathway
HPt	Histidine-containing phosphotransfer protein
Hsf	Heat shock TF
I _{Ca}	Hyperpolarization-activated Ca ²⁺ -permeable cation channel
InDels	Insertions/deletions DNA polymorphisms
JA	Jasmonic acid
JAM	Jasmonate-associated MYC2-like protein; bHLH TF
JAZ	JASMONATE-ZIM DOMAIN protein
JID	JAZ interaction domain
Kan	Kanamycin
KAT1/2	POTASSIUM CHANNEL IN ARABIDOPSIS THALIANA 1/2
KEG	KEEP ON GOING
LEA	Late embryogenesis abundant protein
LecRLK	L-type lectin receptor-like kinase
LUC	<i>Photinus pyralis</i> luciferase
MAPK	Mitogen-activated protein kinase
MAPKK	MAPK kinase
MAPKKK	MAPK kinase kinase
MCA1/2	<i>mid1</i> -complementing activity 1/2
MID1	Mating pheromone-induced death 1
MoCoSu	Molybdenum cofactor sulfurase
MR	Mutual rank value
MS ion channel	Mechanosensitive ion channel
MscS and MscL	mechanosensitive channel of small and large conductance

MSL	MscS-Like protein
MUG	4-Methylumbelliferyl-b-D-Glucuronid
NADPH oxidase	Nicotinamide adenine dinucleotide phosphate-oxidase
NCBI-CDD	National Center for Biotechnology Information-Conserved domain database
NCED	9- <i>cis</i> -epoxycarotenoid dioxygenase
NGS	Next generation sequencing
NINJA	Novel interactor of JAZ
NLS	Nuclear localization signal
OST1	OPTEN STOMATA 1
PA	Phaseic acid
PERK	Proline-rich extension-like receptor kinase
PP2C	Type 2C protein phosphatase
PPFD	Photosynthetic photon flux density
qRT-PCR	Quantitative Real-Time PCR
QUAC1	QUICK-ACTIVATING ANION CHANNEL 1
RAB18	RESPONSE TO ABA 18
RCARs/PYR1/PYLs	Regulatory Components of ABA Receptors/ Pyrabactin Resistance Protein 1/PYR-Like proteins
RD22	RESPONSIVE TO DESSICATION 22
RD29A	RESPONSIVE TO DESSICATION 29A
RD29B/LTI65	RESPONSIVE TO DESSICATION 29B/LOW-TEMPERATURE-INDUCED 65
RH	Relative humidity
RKP	Related to KPC1 protein
RLK	Receptor-like kinase
RLU	Relative luminescence unit
RNAP II	RNA polymerase II
ROS	Reactive oxygen species
RR	Response regulator
S/R-type anion channel	Voltage-independent slow/rapid-type anion channel
SA	Salicylic acid
SDR1	Short chain dehydrogenase/reductase-like enzyme
SIAH	SINA (SEVEN IN ABSENTIA) mammalian homolog
SIMK	Stress-inducible MAP kinase
SIMKK	SIMK kinase
SINAT-like	SINA plant homolog like protein
SINAT	SINA (SEVEN IN ABSENTIA) plant homolog
SIPK	Salicylic acid-induced protein kinase
SIPKK	SIPK kinase
SL	Strigolactone
SLAC1/SLAH3	SLOW ANION CHANNEL-ASSOCIATED 1/SLAC1 HOMOLOGUE 3
SNPs	Single nucleotide polymorphisms
SnRK2	Subfamily 2 of sucrose nonfermenting 1 (SNF1)-related kinase
SOS pathway	Salt overly sensitive pathway
SSLPs	Simple sequence length polymorphisms
TIR1	TRANSPORT INHIBITOR RESPONSE 1
TMD	Transmembrane domain
TPL/TPRs	TOPLESS/TOPLESS-related proteins
VDE	Violaxanthin de-epoxidase
VWC	Volumetric water content
WAK	Wall-associated kinase
WRKY	WRKYGQK domain TF
ZEP	Zeaxanthin epoxidase
ψ_w	Water potential

Summary

Water deficit stress is one of the greatest environmental challenges to plant survival and reproduction in nature. After stress perception, plant responses are regulated by complex multicomponent signaling pathways, in which the abscisic acid (ABA) signaling pathway plays a pivotal role. In plants suffering from drought or salt stress a hydraulic signal is generated which immediately propagates throughout the plant to trigger biosynthesis of ABA, accompanied by stomatal closure and a massive change in gene expression which results in adaptive physiological responses.

In this work, an EMS (ethylmethanesulfonate)-induced mutant *ahr11* (*ABA-hypersensitive response 11*) was studied which exhibits a hypersensitive activation of the ABA-reporter construct *pATHB6::LUC* under water deficit. Using map-based cloning and next generation sequencing (NGS), the hypersensitivity was assigned to a lesion in *Arabidopsis AHR11* gene (*ABA Hypersensitive Response 11*, *At5g13590*) which encodes a protein of 1168 amino acid residues with yet unknown function. In the mutant *ahr11*, the AHR11 is prematurely terminated resulting in a truncated *ahr11* protein (247 amino acid residues). Three lines of evidence confirmed the mutation in *AHR11* being responsible for the mutant phenotype. (I) Ectopic expression of *AHR11* rescued the ABA-hypersensitivity of *ahr11* in protoplasts. (II) Introducing the wild type *AHR11* gene into the mutant restored water deficit and ABA responses. (III) Knockout mutants of *AHR11* displayed also the hypersensitive response to water deficit and exogenous ABA as *ahr11*.

The functional analyses revealed that AHR11 is a nuclear protein and negatively regulates transcription of ABA-induced genes such as *HB6* and *RD29B*. Water deficit-induced ABA action was not detectable in *ahr11* guard cells but in mesophyll cells and epidermal cells, resulting in *ahr11* guard cells being insensitive to water deficit. Therefore, the role of AHR11 is likely involved in ABA distribution.

The double mutant *ahr11/abi1-1* had a decreased sensitivity to water deficit compared with the WT or the single mutants *ahr11* and *abi1-1* during seed germination indicating that AHR11 and ABI1 additively control this developmental process.

AHR11-interacting candidates from *Arabidopsis* libraries were identified and included a bHLH-TF JAM2 (AT1G01260), and two transcriptional corepressors TPL (AT1G15750) and TPR2 (AT3G16830). Based on these results, a possible hypothetical model of AHR11-mediated transcriptional repression is supposed that AHR11 bound to JAM2 acts as an adaptor protein to recruit TPL/TPR corepressors thereby inhibiting the transcription of JAM2 target genes.

Zusammenfassung

Für das Überleben und die Fortpflanzung stellt in der freien Natur Trockenstress als Umweltfaktor eine der größten Herausforderungen für Pflanzen dar. Nach der Wahrnehmung der Stresseinwirkung wird die Reaktion der Pflanze durch komplexe Signalwege aus zahlreichen Komponenten reguliert wobei der Abscisinsäure (ABA)-Signalweg eine Schlüsselrolle übernimmt. Bei Belastung durch Trockenstress oder Salzstress wird in Pflanzen ein hydraulisches Signal generiert, das sich sehr schnell in der gesamten Pflanze ausbreitet und die Biosynthese von ABA induziert. Durch den gestiegenen ABA-Spiegel kommt es zum Spaltenschluß sowie zu einer starken Veränderung des Genexpressionsmusters was letztendlich zu physiologischen Anpassungsreaktionen führt.

In dieser Arbeit wurde die durch Ethylmethansulfonat (EMS)-Behandlung generierte Mutante *ahr11* (*ABA-hypersensitive response 11*) untersucht, die bei Wasserstress eine hypersensitive Aktivierung des ABA-Reporterkonstrukts *pAtHB6::LUC* zeigt. Mit Hilfe des kartierungsgestützten Klonierens sowie des *Next Generation Sequencing* (NGS) gelang es, die hypersensitive Reaktion der Mutante auf eine Läsion im Arabidopsis-Gen *AHR11* (*ABA Hypersensitive Response 11*, *At5g13590*) zurückzuführen. Diese Gen codiert für ein Protein aus 1168 Aminosäuren mit noch nicht bekannter Funktion. In der Mutante *ahr11* liegt *AHR11* als trunkiertes Protein *ahr11* aus 247 Aminosäuren vor. Drei Befunde sprechen dafür, dass die Mutation in *AHR11* für den beobachteten Phänotyp verantwortlich ist: (I) Eine Überexpression von *AHR11* hebt die ABA-Hypersensitivität von *ahr11* in Protoplasten auf. (II) Die Transfektion der Mutante mit dem Wildtyp-Gen *AHR11* führt zur Wiederherstellung der normalen Reaktion auf Wasserdefizit und auf ABA. (III) *Knockout*-Mutanten von *AHR11* zeigen wie *ahr11* ebenfalls eine hypersensitive Reaktion auf Wasserdefizit und ABA.

Die funktionelle Analyse ergab dass es sich bei *AHR11* um ein kernlokalisiertes Protein handelt, das die Transkription ABA-induzierter Gene wie *HB6* und *RD29B* negativ reguliert. Wasserdefizit-induzierte ABA-Aktivität ließ sich in Schließzellen von *ahr11* nicht nachweisen, wohl aber in Mesophyll- und Epidermiszellen, was erklärt warum die Schließzellen von *ahr11* gegenüber Wasserdefizit insensitiv reagieren. *AHR11* spielt damit vermutlich eine Rolle bei der ABA-Verteilung.

Eine *ahr11/abi1-1* Doppelmutante zeigte hinsichtlich der Keimung eine verringerte Sensitivität gegenüber Wasserdefizit verglichen mit den Einzelmutanten *ahr11* und *abi1-1*, was dafür spricht, dass *AHR11* und *ABI1* diesen Entwicklungsprozess auf additive Weise beeinflussen.

Mögliche *AHR11*-Interaktoren wurden aus genomischen Arabidopsis-DNA-Banken isoliert. Darunter befinden sich ein bHLH-Transkriptionsfaktor, *JAM2* (*AT1G01260*) sowie zwei Transkriptionelle Co-Repressoren, *TPL* (*AT1G15750*) und *TPR2* (*AT3G16830*). Aufgrund dieses Ergebnisses wird ein hypothetisches Modell für die *AHR11*-vermittelte transkriptionelle Repression vorgeschlagen, in dem an *JAM2* gebundenes *AHR11* als Adaptorprotein für die *TPL/TPR*-Co-Repressoren fungiert und auf diese Weise die Transkription der *JAM2*-Zielgene inhibiert.

1. Introduction

Plants, with their sessile lifestyle in natural habitats, constantly suffer from various abiotic environmental stresses, such as drought, high salinity, and low temperature. Among these adverse environmental conditions, drought is considered a major abiotic stress with water deficiency impairing plant growth and development in > 50% of the Earth's surface area. It has long been recognized, *e.g.* in ancient Egypt thousands of years ago, that high crop yield can be obtained by appropriate water supply. To date, however, water shortage has become a critical bottleneck in improvement of worldwide crop productivity. In the future, the situation is expected to be even worse because of the global climate change and over exploitation of underground water (Gleeson et al., 2012).

Plant water deficit tolerance or susceptibility is a complex phenomenon, because stress can occur at different growth stages with varying sensitivity, and moreover, multiple stresses may affect plants simultaneously. Drought, high salinity and low temperature challenge the water status of plants, and plants have gradually evolved sophisticated acclimation mechanisms to sense, transduce and respond to the restricted water availability (Mahajan and Tuteja, 2005). In recent decades, physiological bases for plant responses to water deficit have become the subject of intense research (Medrano et al., 2002, Ober and Sharp, 2003, Flexas et al., 2004, Rosado et al., 2006, Christmann et al., 2007). Stomatal conductance, leaf water potential and turgor pressure are the common parameters to assess the water deficit response (Medrano et al., 2002, Ache et al., 2010, Tardieu, 2012). At the molecular level, important drought-related signaling pathways have been unraveled and numerous drought-responsive genes have been discovered (Bray, 2002, Verslues and Bray, 2006, Chen et al., 2009, Hayano-Kanashiro et al., 2009, Lim et al., 2009, Chen et al., 2010a, Fujii and Zhu, 2012). However, some key aspects such as water deficit signal perception and early signal transduction are still little understood.

1.1 Physiological responses to water deficit

Plant water deficit may result from a number of different abiotic stresses such as drought, salinity and cold (Mahajan and Tuteja, 2005). The availability of soil water to the plant primarily depends on the quantity of water stored in the soil and to the soil water potential (ψ_w). ψ_w is the chemical potential of water divided by the partial molar volume (Boyer and Kramer, 1995, Kramer and Boyer, 1995). In essence, the ψ_w gradient among soil, plant and atmosphere determines the direction of free water movement. During daytime, the low value of ψ_w in the atmosphere pulls up water from the soil through root and stem into the leaf where it diffuses into the air *via* the stomata. However, this pathway requires (I) that root ψ_w is more negative than soil ψ_w and (II) that a ψ_w gradient is maintained within the plant with most negative ψ_w occurring in the leaves. A decrease of soil ψ_w during drought periods may lower or even reverse the plant-soil ψ_w gradient thereby impeding water uptake or even causing a loss of water. To describe the plant's adaptive strategy to water deficit, the terminologies

such as drought escape, low ψ_w /dehydration avoidance and dehydration tolerance were employed (Levitt, 1972, Verslues and Juenger, 2011).

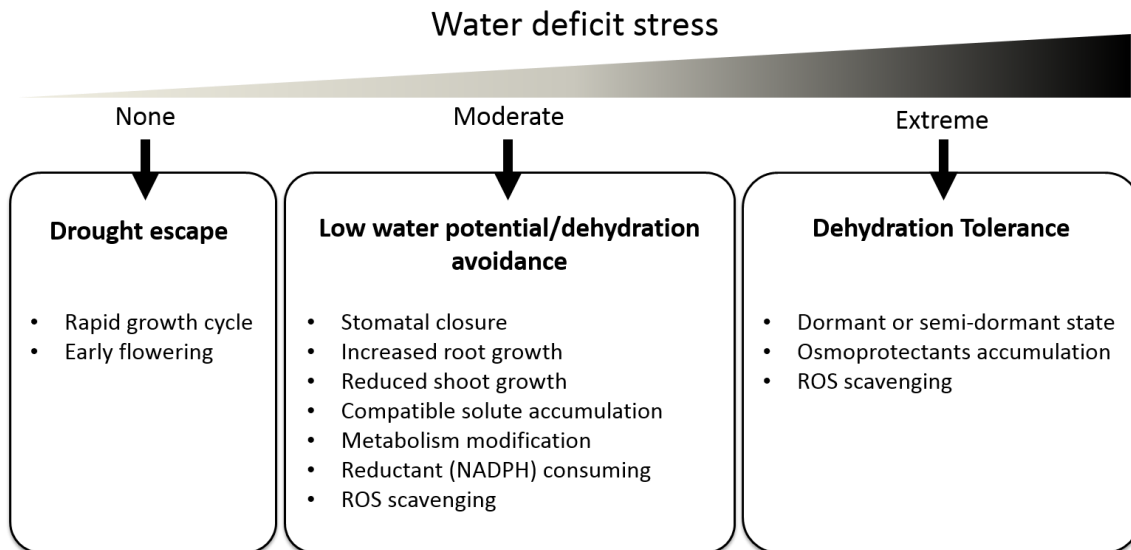


Figure 1-1: **Conceptual diagram of the responses of plants to water deficit stress**

Water deficit adaptation strategies of plant are termed drought escape, low ψ_w avoidance and dehydration tolerance (Verslues and Juenger, 2011). Some desert plants adopt drought escape by rapid completion of the growth cycle when the environment is suitable, while *Arabidopsis* may to some degree escape stressful conditions by early flowering. Low ψ_w avoidance strategies may be followed by dehydration tolerance strategies in certain plant species. However, *Arabidopsis* is not tolerant to severe dehydration. Modified from Verslues and Juenger (2011).

1.1.1 Drought escape

To cope with seasonal water limitation, certain plant species adjust their development to complete their life cycle in a timely manner. This is a strategy adopted e.g. by some desert plants with very rapid growth after rain. When water is not limiting, further development may slow down resulting in high seed yield, whereas under the influence of stress, plants including *Arabidopsis* often prematurely transit to reproductive development to generate stress-tolerant seeds before severe stress leads to the death of the mother plant. A general variation of flowering time has been found among natural accessions of *Arabidopsis thaliana* (McKay et al., 2003). In drought stress experiments, the ecotypes *Columbia* and *Landsberg* commonly exhibited early flowering. A screen of different flowering time mutants under conditions triggering drought-escape (DE) revealed GIGANTEA (GI), FLOWERING LOCUS T (FT) and TWIN SISTER OF FT (TSF) as central components of the DE response and showed that the phytohormone ABA and long days are required for DE (Riboni et al., 2013). From an agricultural viewpoint, drought escape saves water but also reduces cumulative photosynthesis during the life cycle, which leads to a trade-off between stress escape and potential yields (Tardieu, 2012, Tardieu, 2013).

1.1.2 Low water potential/dehydration avoidance

Under mild water deficit, the principal responses of plants help to avoid low ψ_w and maintain tissue water balance (water/osmotic homeostasis) close to the unstressed level by reducing water loss and/or increasing water uptake. Water loss mainly takes place through transpiration *via* stomatal pores in aerial tissues and is accompanied by CO₂ uptake. Hence, plants quickly close the stomata to minimize transpiration as a short-term response to mild water deficit. At the whole plant level, gain of above-ground biomass decreases in response to water deficit due to changes of carbon usage (Hummel et al., 2010). An attenuated shoot development is an efficacious way to limit leaf area and thereby transpirational water loss. With water shortage, *Arabidopsis* leaf rosette growth has been shown to decrease more than photosynthesis, leading to an increase in carbon availability to promote root growth and osmotic adjustment (Hummel et al., 2010). Correspondingly, the sensitivity to low soil ψ_w is distinct between the root and the shoot (Hsiao and Xu, 2000, Mahajan and Tuteja, 2005). Compared to the stress-limited shoot development, the root system is generally more resistant to stress. Mild water deficit even promotes axial root elongation and lateral root development, which allows to explore the soil for yet unexploited water sources (Sharp et al., 2004, Yamaguchi et al., 2009, Yamaguchi and Sharp, 2010). Still, the trade-off associated with a reduced transpiration rate is a decrease of photosynthesis, which means an overall diminished carbon assimilation and shoot growth.

When water homeostasis cannot be maintained by the low ψ_w avoidance response mentioned above, a decrease tissue ψ_w , particularly in the root, is the next adaptative step. Of the different components of ψ_w , which is the osmotic potential ψ_s , the pressure potential ψ_p and the gravitational potential ψ_g (Christmann et al., 2013), only ψ_s may be altered by the plant (few exceptions exist where also ψ_p is modified) which, however, indirectly also affects ψ_p . The ψ_s is substantially lowered by an increase in solute concentration. While an increase of anorganic ions and organic acid ions is observed in the vacuole, ψ_s in the cytoplasm is adjusted with the help of a number of small molecules named osmoprotectants or compatible solutes, which do not interfere with cellular function and help organisms to survive extreme osmotic stress (Lang, 2007). Osmotic adjustment of the root may be achieved by uptake of inorganic ions such as K⁺, Cl⁻ and Na⁺ from the soil with K⁺ uptake mediated by K⁺ channels playing a key role (Sze et al., 2004, Osakabe et al., 2013, Wang et al., 2013). Adjustment was shown to be fast with hyperosmotically-stressed root cells of *Arabidopsis* recovering their turgor within 40 to 50 min (Shabala and Lew, 2002). Enhanced ion uptake is accompanied by synthesis of osmoprotectants such as the amino acids proline, non-reducing sugars (Suc and trehalose), polyols (mannitol and sorbitol) and quaternary amines (such as glycine betaine) under water deficit stress (Nakayama et al., 2000, Rontein et al., 2002, Iordachescu and Imai, 2008, Hayat et al., 2012, Wani et al., 2013). The most striking property of these solutes is the lack of a negative influence on cellular metabolism and function.

The pressure potential ψ_p of living cells is the cell turgor pressure which is thought to be at or above zero while in non-living water-conducting cells with thick, lignified walls, ψ_p usually is negative and is then called tension. Under water deficit stress, cell wall extensibility is reduced as part of the water deficit response (Moore et al., 2008). Studies of drought effects on the cell walls in roots of maize (*Zea*

mays) revealed that cell wall hardening occurs in the basal part of the root elongation zone, and is accompanied by alterations in metabolism and accumulation of cell wall proteins, such as expansins, xyloglucan endotransglycosylases, glucanases, dehydrins and other proteins of carbohydrate and amino acid metabolism (Wu and Cosgrove, 2000, Fan and Neumann, 2004, Sharp et al., 2004, Fan et al., 2006, Poroyko et al., 2007, Zhu et al., 2007a, Spollen et al., 2008). And similar proteomic analyses of root cell wall were also performed in soybean and common bean (Yamaguchi et al., 2009, Yang et al., 2013).

If soil ψ_w becomes still more negative, additional mechanisms become important, such as leaf area adjustment by shedding of leaves to reduce transpiration or a premature termination of the plant's life cycle. Abscission of leaves is preceded by leaf senescence, a programmed aging process during which important nutrients are redistributed from the senescing leaves to actively growing tissues or storage organs. Senescence is regulated by plant hormones with ethylene functioning as the major senescence-promoting hormone and cytokinin as the major senescence-inhibiting hormone and may be prematurely induced by abiotic stresses through an effect on hormone homeostasis (Buchanan-Wollaston et al., 2005). Although the promotion of senescence by different signals may involve distinct signal transduction pathways, similar senescence-associated genes (SAGs) are induced by different stresses. Therefore the initiated senescence processes may share common execution events (Guo and Gan, 2012). The premature termination of the life cycle may be understood as a premature initiation of whole-plant senescence where redistribution of nutrients into reproductive structures ensures the production of the next generation.

1.1.3 Dehydration tolerance

In order to colonize the land, the early land plants with their very simple architecture must have been desiccation-tolerant in both vegetative and reproductive stages to survive the dehydrating atmospheres of land habitats (Oliver et al., 2005). Vegetative desiccation tolerance is common in less complex plants such as bryophytes (Proctor and Pence, 2002), but only about 300 species with vegetative desiccation tolerance are found in vascular plants (Porembski and Barthlott, 2000). These vascular plants, also named resurrection plants (Gaff, 1971), can recover from an extreme dehydration and resume normal growth when water is available (Phillips et al., 2008). *Craterostigma plantagineum* has been employed as a model system to unveil the mechanisms of desiccation tolerance because desiccation tolerance can be studied both in undifferentiated callus cultures and in differentiated plants (Bartels, 2005, Rodriguez et al., 2010, Alcazar et al., 2011). Plants which are not desiccation-tolerant in the vegetative stage often show dehydration tolerance during reproductive stages. Seed dehydration tolerance is associated with seed dormancy and is of great importance for survival. Until the environmental conditions are suitable to establish a new plant generation, the seed enters a dormant stage to survive even extended periods of unfavorable conditions (Koornneef et al., 2002, Finch-Savage and Leubner-Metzger, 2006, Bentsink and Koornneef, 2008, Holdsworth et al., 2008). Seed dormancy is controlled by genetic factors as well by environmental factors such as light, temperature and water availability and also by the time elapsed since initiation of dormancy.

At the molecular level, the response of resurrection plants to vegetative desiccation and the sequence of events during the late stage of seed development in non-tolerant plants share some similarities: (I) Accumulation of ABA-regulated transcripts is a early response to dehydration and ABA-related stress responses are up-regulated; (II) the cellular structures are protected by protective proteins such as dehydrins and other late-embryogenesis abundant (LEA) type proteins; (III) photosynthesis and nitrogen and carbon metabolism are reduced, but carbohydrates such as sucrose, hexoses and malate are accumulated as osmoprotectants; and (IV) the level of reactive oxygen species (ROS) is tightly controlled and ROS scavenging capacity increase (Bartels, 2005, Ndimba et al., 2005, Rodriguez et al., 2010, Alcazar et al., 2011).

1.1.4 Integrated stressresponses

After half a century of research into survival strategies initiated when a plant is exposed to low ψ_w , it became clear that the responses of stressed plants do not fit a linear progression from mild stress, moderate stress, to extreme stress, or from short-term responses to long-term responses. Also, separating the stress-induced events in time is difficult, because these show a spatio-temporal patten. For example, while stomata close to prevent water loss from the shoot, accumulation of compatible solutes is also initiated in the root. Additionally, synthesis of protective proteins such as dehydrins and LEA protein may be initialted before significant dehydration occurs. In recent years it turned out that some of the low ψ_w -initiated responses events have additional beneficial effects. Compatible solutes like proline and glycine betaine, for example, do not only function as osmoprotectants but also stabilize certain protein complexes or cell memberane structures and act as ROS scavengers (Hayat et al., 2012, Wani et al., 2013). Similarly, protection of proteins by dehydrins specifically seems to enhance the antioxidative capacity during drought stress (Imamura et al., 2013).

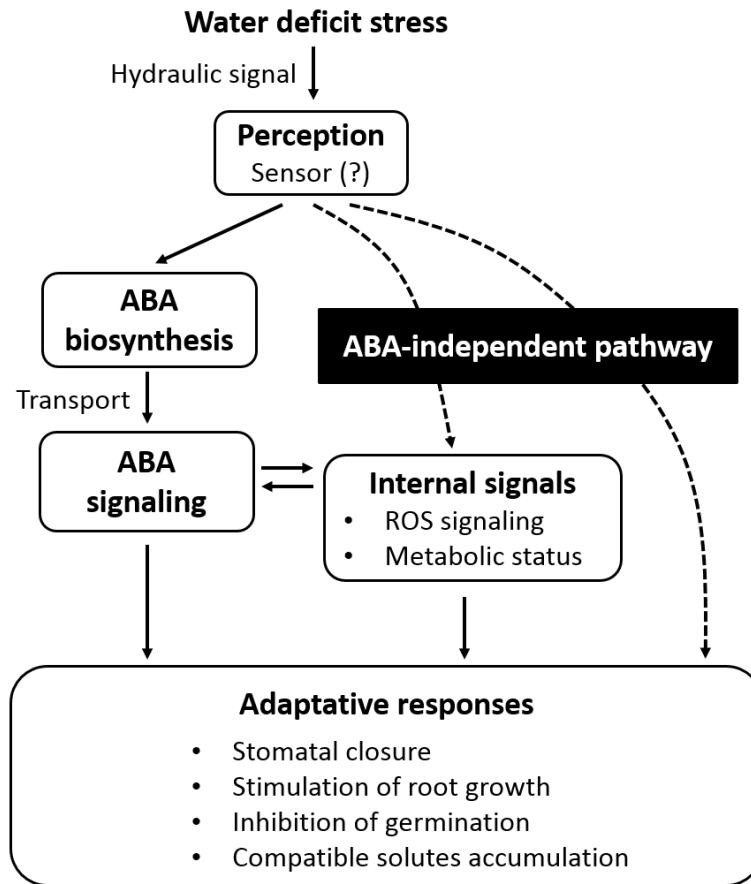


Figure 1-2: **A simplified model of the water deficit sensing and signaling pathway**

The water deficit stress is sensed by some unknown sensors and converted into endogenous signals, which subsequently initiate a series of adaptative responses of the plant *via* ABA-dependent and ABA-independent signaling pathways.

Therefore, the water deficit response of plants comprises a complex regulatory network which integrates external and internal stimuli, such as alterations in water status, cell turgor, hormone levels, ROS production, and of levels of sugar, and other metabolic products. Water deficit perception and signaling and can be conceptually divided into 3 phases (Figure 1-2): stress transduction to remote plant organs, stress perception and conversion into an internal signal which is the plant hormone ABA and ABA signaling. An ABA-independent signaling pathway also operates and internal signals such as ROS and metabolic status modify the output of ABA-dependent and independent signaling (Verslues and Zhu, 2005). To date, although the perception of water deficit and signaling upstream of ABA biosynthesis are still not uncovered, the ABA signaling cascade in the center of this response model is well known and plays a key regulatory role mediating stomatal closure (Schroeder et al., 2001, Kim et al., 2010b, Joshi-Saha et al., 2011b, Bauer et al., 2013) and adaptative root growth (Sharp and LeNoble, 2002, Ober and Sharp, 2003, Yamaguchi and Sharp, 2010) as well as compatible solute accumulation, synthesis of protective proteins and control of ROS levels (Stewart and Voetberg, 1985, Strizhov et al., 1997, Verslues and Bray, 2006, Sharma and Verslues, 2010). The ABA-independent water deficit

signaling pathway also stimulates stress adaptation of plants, but its precise role and the structure of the respective signaling network are still much less clear.

1.2 Water deficit perception and transduction

The water deficit response of plants starts with sensing of external stimuli, which is low soil ψ_w . The external signals are both converted into endogenous signals and transmitted to plant parts distal from the site of perception. Low soil ψ_w induces a drop in ψ_w of root cells which causes a loss of turgor in these cells. After a lag phase, responses are observed in remote plant parts like the shoot. It was suggested that a decrease in soil ψ_w was converted into an internal chemical signal in the root with ABA being the likely candidate. The plant hormone is supposed to be then transmitted to the shoot *via* the xylem (Wilkinson and Davies, 2002). This hypothesis was recently challenged by studies which used reciprocal grafting of wild type and ABA-deficient mutants of *Arabidopsis* and tomato. According to these studies, root exposure to water deficit induces ABA biosynthesis in the shoot and shoot-biosynthesized ABA is necessary and sufficient to mediate drought-induced responses (Holbrook et al., 2002, Christmann et al., 2007). It was further demonstrated that water deficit stress results in generation of a hydraulic signal which is rapidly transmitted to the shoot. Attenuation of the hydraulic signal by feeding water to leaves abolished ABA-dependent responses like stomatal closure (Christmann et al., 2007). Water feeding to leaves would not attenuate chemical signals or electrical signals which have also been suggested as long-distance signals relayed from roots (Grams et al., 2007, Gil et al., 2008). Accordingly a hydraulic signal plays a crucial role in the water deficit response (Christmann et al., 2007, Christmann et al., 2013). In essence, a drought-induced hydraulic signal is a drop in ψ_w , which in living cells where the signal is decoded comprises a decrease of the cell turgor and of the osmotic potential. To date the hydraulic sensors in plant as well as the early steps in the signaling cascade initiated by the hydraulic signal are still unknown. In theory any cellular component that monitors turgor-dependent parameters such as cell wall tension or changes in osmotic potential is a promising candidate for a hydraulic sensor. Also, candidate sensors could be homologs of osmosensors or mechanosensors of bacteria, fungi, and metazoans. The term hydraulic sensor will be used here to cover sensors for which the mode of action is unknown or has not been proven and that putatively monitor changes in turgor, solute concentration or cell wall-plasma membrane associated tension.

1.2.1 Two-component systems

The two-component regulatory system is an evolutionarily ancient system where the phosphorylation status of sensor and target proteins is altered during stress signal perception and transduction in both prokaryotes and eukaryotes. The EnvZ-OmpR system found in *Escherichia coli* is the simplest form of a two-component system (Forst et al., 1987, Slauch et al., 1988), which consists of a membrane sensor histidine kinase (HK) EnvZ and a cytoplasmic response regulator (RR) OmpR (Figure 1-3A). Under conditions of hyperosmolarity, the inner membrane protein EnvZ autophosphorylates on a histidine residue. Phosphorylated EnvZ then phosphorylates and thereby activates OmpR. Phospho-OmpR binds to the promoter regions of the porin genes *ompF* and *ompC* to trigger their expression (Slauch et al., 1988, Roberts et al., 1994, Head et al., 1998, King and Kenney, 2007). A recent *in vivo* analysis reveals that the transmembrane domain of EnvZ is not necessary but the N-terminal cytoplasmic domain of EnvZ is sufficient to respond to changes in concentration of osmolytes, e.g. sucrose and NaCl (Wang et al., 2012b).

Compared with the *E. Coli* EnvZ-OmpR regulatory system, a more elaborated osmosensing and signal transduction system has evolved in budding yeast (*Saccharomyces cerevisiae*), termed the high osmolarity glycerol (HOG) pathway (Boguslawski, 1992, Brewster et al., 1993, Maeda et al., 1994). The HOG pathway consists of a two-component system and a mitogen-activated protein kinase (MAPK) cascade (Figure 1-3A), which is composed of three MAPKKs (Ssk2p, Ssk22p, and Ste11p), a MAPKK (Pbs2p) and a MAPK (Hog1p). Two distinct upstream signal transducer branches Sln1p and Sho1p independently sense (probably) a decrease in turgor pressure to activate the HOG1 MAPK cascade. In the Sln1-Ypd1-Ssk1 branch, the plasmamembrane-associated histidine kinase Sln1p has the ability to autophosphorylate on a conserved histidine residue, and initiates a multistep of His-to-Asp phosphoryl transfer among the sensor kinase Sln1p, the phosphotransferase Ypd1p and the response regulator Ssk1p (Posas et al., 1996, Janiak-Spens et al., 1999, Tao et al., 2002, Chooback and West, 2003, Xu et al., 2003). In the *sln1* and *ypd1* yeast mutants, the HOG1 MAPK cascade is constitutively activated resulting in cell death. Therefore, the Sln1p branch negatively regulates the HOG1 pathway. Sln1p monitors turgor changes in yeast cells (Tamas et al., 2000, Reiser et al., 2003) and in the absence of hyperosmotic stress the HOG1 MAPK cascade is repressed by phospho-Ssk1p, whereas hyperosmotic stress results in dephosphorylation and inactivation of Ssk1p. Once Ssk1p is inactive, the HOG1-MAPK cascade becomes active which results in an increase of glycerol levels in the cell to restore osmotic balance. In the Sho1p branch, two mucin-like proteins Hkr1p and Msb2p redundantly or synergistically sense either a turgor decrease or an increase in osmotic potential *via* their high-glycosylated domains imbedded in the cell wall, which affects interaction with the plasmamembrane-localized adaptor protein Sho1p (Tatebayashi et al., 2007). The key function of Sho1p is to recruit the kinase cascade complex Ste11-Ste50-Pbs2-Hog1 to the cytoplasmic membrane at the areas of polarized growth of yeast *via* its C-terminal SH3 domain (Maeda et al., 1995, Raitt et al., 2000, Reiser et al., 2000, Tatebayashi et al., 2006). It has been demonstrated that in response to hyperosmotic shock, this kinase cascade complex is subsequently activated by a GTPase protein, the Cdc42-bound membrane kinase Ste20 (Raitt et al., 2000).

In the yeast *Debaryomyces hansenii*, a novel cytosolic osmotensor DhNik1 has been identified with 5 repeats of a specific N-terminus HAMP domain (Aravind and Ponting, 1999) that currently occurs in histidine kinases, adenylyl cyclases, methyl accepting chemotaxis proteins, and phosphatases. The possible mechanism of osmotic sensing by DhNik1 is the “on-off” switch of the alternative interaction among these HAMP domains (Meena et al., 2010).

Although no plant homologs of Hkr1p and Msb2p exist in plant, proteins with significant sequence similarities to other elements of yeast two-component systems have been identified (Lohrmann and Harter, 2002, Mizuno, 2005, Schaller et al., 2008), including sensor histidine kinases (HKs), histidine-containing phosphotransfer proteins (HPts) and response regulators (RRs) (Figure 1-3A). In *Arabidopsis* the perception and transduction of ethylene, a well-characterized plant two-component regulatory system is involved. The ethylene receptor family which comprises 5 members, ETHYLENE RESPONSE 1 (ETR1), ETR2, ETHYLENE INSENSITIVE 4 (EIN4), ETHYLENE SENSOR 1 (ERS1) and ERS2, belongs to the *Arabidopsis* sensor histidine kinases (AHKs) (Yoo et al., 2009, Lin et al., 2009, Liu and Wen, 2012). Another subgroup of AHKs, nonethylene receptor HKs (NER HKs) includes AHK1, AHK2, AHK3, CYTOKININ RESPONSE 1 (CRE1)/AHK4, CYTOKININ-INDEPENDENT 1 (CKI1), and CKI2/AHK5 (Nongpiur et al., 2012), of which AHK2, AHK3 and CRE1/AHK4 have been identified as receptors of the phytohormone cytokinin (To and Kieber, 2008, Perilli et al., 2009). The complementation analyses in yeast reveal that AHK1, AHK2, AHK3, and CRE1 can complement the lethal phenotype of the double mutant *sln1sho1* by conferring phosphotransfer to the HOG1 MAPK cascade under high-salinity conditions (Urao et al., 1999, Reiser et al., 2003, Hao et al., 2004). Analyses of transgenic plants over-expressing AHK1 and of *ahk1* knockdown mutants indicate that AHK1 positively regulates both ABA-dependent and ABA-independent signaling pathways in response to osmotic stress (Tran et al., 2007b, Wohlbach et al., 2008). Hence, AHK1 has been predicted as an osmosensor and positive regulator of hyperosmotic resistance in plant for a long time. Five signaling intermediate phosphotransfer proteins (AHPts) (Miyata et al., 1998, Suzuki et al., 1998) and 23 response regulators (ARRs) (Imamura et al., 1999, Schaller et al., 2007) are found in *Arabidopsis*, and thoroughly researched in cytokinin signaling (Hutchison et al., 2006, To et al., 2007). It's known that AHK1 can interact with Histidine-containing Phosphotransfer protein 1 (HPt1) (Dortay et al., 2006). Similarly the interaction between rice ortholog OsHK3b and OsHPt2 is also predicted by interactome network (Kushwaha et al., 2013). However, recently, the osmosensor role of AHK1 is challenged by a study of the *ahk1-1* (Nos-0) mutant, in which expression of AHK1 enhances drought tolerance through modulating stomata density to control water loss and to avoid tissue dehydration, but not through accumulating osmoprotectants (e.g. Pro) and ABA (Kumar et al., 2013). Therefore, AHK1 may not be the main plant osmosensor involved in sensing low ψ_w stress.

1.2.2 Mechanosensor

Mechanosensitive (MS) ion channels are membrane-located protein pores evolved for sensing mechanical forces. The change of membrane tension could cause these pores to open thereby rapidly releasing solutes and water from the cell (Haswell et al., 2011, Martinac, 2011). Tension-responsive

ion channel activities have been reported in a number of plant cell types, such as mesophyll cells, guard cells, and pollen tubes, but no channel responsive for these activities has yet been identified (Falke et al., 1988, Cosgrove and Hedrich, 1991, Ding and Pickard, 1993, Dutta and Robinson, 2004). In bacteria, two families of MS channels of small conductance and large conductance (MscS and MscL), respectively, were identified and demonstrated to play a role in solute release in response to excessive turgor (Sukharev et al., 1993, Sukharev et al., 1994, Levina et al., 1999, Pivetti et al., 2003) (Figure 1-3B). MscL is usually found as a single copy gene in a bacterial genome, and homologs of MscL are ubiquitous in bacteria and are also found in a number of fungi and oomycetes but are absent in plants. In contrast, the MscS family is quite diverse and broadly exists not only in bacteria and archaea but also in plants, however MscS homologs are not present in animals (Kloda and Martinac, 2002, Pivetti et al., 2003, Haswell and Meyerowitz, 2006). The studies on structure and function of bacterial MscL and MscS channels give us the opportunity to understand the function of MS channels in plants (Figure 1-3B).

In *Arabidopsis*, totally 10 MscS-like proteins (MSLs) are grouped into two clusters: (I) MscS-like proteins from both prokaryotes and eukaryotes (MSL1-3); (II) eukaryotic MscS-like proteins from rice, yeast, and green algae (MSL4-10). The closely related MSL2 and MSL3 share an N-terminus chloroplast transit peptide, 5 transmembrane (TM) helices, and a C-terminus cytoplasmic β -domain (Haswell and Meyerowitz, 2006). A complementation analysis of MSL3 in the mutant of *E. coli* lacking the three mechanosensitive ion channels MscS, MscL and MscK has indicated that MSL3 can serve as a MS ion channel in *E. coli* to regulate the cell volume. Both MSL2 and MSL3 are localized to the plastid envelope and, the knockout mutants *msl2-1* and *msl3-1* have enlarged chloroplasts in mesophyll cells compatible with a role of these channels in regulation of plastid volume (Haswell and Meyerowitz, 2006). Functional analysis of conserved motifs in MSL2 revealed that a PN(X)₉N motif at the top of the cytoplasmic β -domain is required for proper intraplasmic localization, and for maintaining normal plastid and leaf morphology (Jensen and Haswell, 2012). Maintenance of plastid volume is continuously challenged by hypoosmotic conditions in the cytoplasm and the plastid-localized MS ion channels MSL2 and MSL3 are critical for preservation of plastid size and shape (Veley et al., 2012). In MSL cluster II, *MSL9* and *MSL10* probably encode chloride channels on the plasma membrane of root cells and function both separately in monomeric and combinatorially in heteromultimeric complexes. The function as an MS ion channel has been clearly demonstrated for MSL10 (Maksaev and Haswell, 2012), but neither the double mutant *msl9/msl10* nor the quintuple mutant *msl4/msl5/msl6/msl9/msl10* displays a specific phenotype under stress conditions. Therefore, the physiological role of MSL9 and MSL10, as well as of their homologs, remains to be determined (Qi et al., 2004, Peyronnet et al., 2008, Haswell et al., 2008).

In yeast, the Ca²⁺ influx during mating is mediated by the calcium-permeable, stretch-activated (SA) nonselective cation channel MID1 (mating pheromone-induced death 1), which in response to mechanical stress exhibits an increased Ca²⁺ conductance which results in an increase in the concentration of cytosolic free Ca²⁺ (Iida et al., 1994, Kanzaki et al., 1999) (Figure 1-3B). The putative *Arabidopsis* Ca²⁺ SA influx channel MCA1 (*mid1*-complementing activity 1), as well as its homolog

MCA2, have been identified by a functional complementation screening of the yeast mutant *mid1* (Nakagawa et al., 2007). The expression of MCA1 and MCA2 complements the lethal phenotype of the *mid1* mutant, and mediates the stretch activated Ca^{2+} uptake in yeast (Nakagawa et al., 2007). Also, MCA1-dependent MS cation currents were observed in *Xenopus laevis* oocytes (Furuichi et al., 2012). MCA1 is present in the plasma membrane of root cells, and in yeast, too, MCA1 localizes to the yeast plasma membrane as an integral membrane protein. MCA2 shows an overlapping but also distinct spatial expression pattern compared to MCA1. Both single mutants *mca1-null* and *mca2-null* are defective in Ca^{2+} uptake from the roots, but only the primary roots of *mca1-null* seedling are impaired in penetrating a harder agar medium from a softer (Yamanaka et al., 2010). Therefore, MCA1 and MCA2 are putative MS ion channels which differentially mediate Ca^{2+} uptake in *Arabidopsis* (Figure 1-3B).

1.2.3 Cell wall integrity (CWI) sensor

Cell wall remodeling during growth and upon extracellular stress has been extensively studied in yeast. The signal transduction pathway uncovered by such studies has been designated cell wall integrity (CWI) pathway, which essentially is composed of the cell wall-associated cell surface sensors, the GDP/GTP exchange factors (GEFs), and the small GTPases (Rhos) (Levin, 2005, Levin, 2011). The yeast genome encodes five CWI sensors belonging to two subgroups (Figure 1-3C): the Wsc-type sensors (Wsc1, Wsc2 and Wsc3) and the Mid-type sensors (Mid2 and Mtl1). All of them share a single transmembrane domain (TMD), a short cytoplasmic tail (CT) and a large extracellular region (Rodicio and Heinisch, 2010). In the extracellular region the highly O-mannosylated serine- and threonine-rich (STR) sequences form a nanospring-like structure that is capable of resisting high mechanical force and of responding to cell surface stress (Dupres et al., 2009). In addition, the specific cysteine-rich domain (CRD) at the N-terminus of Wsc sensors transiently interacts with glucan chains in the cell wall. Although Mid-type sensors lack the CRD domain, an N-glycosylated asparagine near the N-terminus may serve a similar function as CRD domain (Hutzler et al., 2008). Consequently, strain either on the cell wall or on the plasma membrane should generate a mechanical force on the extracellular nanospring-like structure. The strain-induced conformational changes of CWI sensors could then signal to GEFs, which directly activate the Rho GTPases, and then trigger the sole yeast protein kinase C (PKC1)-activated MAPK cascade (Garcia et al., 2006).

Similar to the STR sequences in Wsc1, the ankyrin repeat motifs have also been postulated to form nanospring structures which, when coupled to an ion channel are thought to transmit mechanical forces to the channel thereby altering channel open state probability (Howard and Bechstedt, 2004, Lee et al., 2006b). Accordingly, the plant proteins containing ankyrin repeats (Becerra et al., 2004) including kinases and potassium channels might be involved in hydraulic sensing.

Proteins putatively involved in sensing of plant cell wall integrity include the L-type lectin receptor-like kinases (LecRLKs) and the proline-rich extension-like receptor kinases (PERKs) (Figure 1-3C). LecRLKs were identified in a screen for tripeptidic integrin-recognition motif Arg-Gly-Asp (RGD)-binding proteins (Gouget et al., 2006). Integrins are central components of metazoan plasma

membrane-localized protein complexes thought to function in mechanosensing of shear stress (Shyy and Chien, 2002) and the LecRLKs seem to play a structural and signaling role at the plant cell surfaces through protein-protein interactions with plant RGD-containing proteins (Gouget et al., 2006). Further members of the receptor-like kinase family (RLKs) whose extracellular domains mediate carbohydrate ligand binding in the cell wall have recently been linked cell wall integrity sensing during vegetative and reproductive development (Boisson-Dernier et al., 2011).

The *Arabidopsis* genome encodes 15 PERKs, of which PERK4 has been identified as a plasma membrane-associated protein which perturbs Ca^{2+} homeostasis during the early stage of ABA signaling to inhibit primary root cell elongation (Bai et al., 2009a, Bai et al., 2009b). Additionally, the receptor-like wall-associated kinases (WAKs) bind pectins in the cell wall, and are necessary both for cell expansion during development and for a response to pathogens and wounding. The type and concentration of pectins in the wall could lead to a WAK-dependent activation of different cytosolic MAPK signaling pathways (Kohorn and Kohorn, 2012).

In the nematode *Caenorhabditis elegans*, an eukaryotic MS sodium channel complex (MEC-4/MEC10) has been identified in a screen for mutants defective in the response to gentle touch (Chalfie and Au, 1989). The channel proteins have specialized extracellular matrix (ECM) and unique cytoskeletal elements to form the adhesions between the cell wall and the plasma membrane (Arnadottir and Chalfie, 2010). Similarly, the animal cell surface receptor integrins also have a dual-tethered adhesion structure, of which the extracellular domains of integrins bind to cell wall ligands, while the flexible internal tails interact with the actin cytoskeleton, to connect the interior of the cell to the extracellular environment and to bi-directionally transmit signals across the cell membrane (Wegener and Campbell, 2008, Shyy and Chien, 2002, Legate et al., 2009). Although the analysis of the *Arabidopsis* genome indicates that homologs of MEC-4/MEC-10 channels and integrins do not exist, plant genome encodes some integrin-like proteins that are structurally and functionally similar to animal integrins (Schindler et al., 1989). For instance, the *Zea mays* integrin-like proteins mediate the interaction between cell wall and plasma membrane as well as cell responses to osmotic stress (Lu et al., 2007). An *Arabidopsis* plasma membrane protein AT14A serves as a transmembrane linker between the cell wall and the cytoskeleton just as integrin complexes do in animals, and plays important roles in controlling polarity and morphogenesis (Lu et al., 2012). In addition, *Arabidopsis* integrin-like protein NON-RACE-SPECIFIC DISEASE RESISTANCE 1 (NDR1) has been demonstrated to play an essential role in plant disease resistance (Lu et al., 2013, Knepper et al., 2011). Taken together the plant integrin-like proteins have important roles of maintaining the integrity of the cell wall-plasma membrane connection and are involved in the cell wall strain perception and signal transduction during growth development and environmental stress.

1.2.4 Upstream signal transduction

Whatever the primary sensing mechanism, it must be linked to specific down-stream molecules that further transmit the signal. It has long been known that cytoplasmic free Ca^{2+} increases in *Arabidopsis* seedlings within seconds of osmotic stress (Knight et al., 1997) and under mechanical stimulation

(Monshausen et al., 2009). Some presumed hydraulic signal sensors such as MCA1 and MCA2 are calcium channel proteins which might directly mediate Ca^{2+} uptake (Yamanaka et al., 2010), while the sensor candidate PERK4 indirectly regulates Ca^{2+} homeostasis (Bai et al., 2009a). Hence, cytoplasmic Ca^{2+} transients have been considered to play a role in the early response to water deficit. However, Ca^{2+} transients are also involved in early ABA signaling (see section 1.3.5). Therefore, it is hard to discern of Ca^{2+} action upstream or downstream of ABA, or both.

The MAPK kinase pathway, an eukaryotic conserved signal transduction module which is activated as part of the HOG pathway in yeast. In *Arabidopsis*, 80 MAPKK kinases (MAPKKKs), 10 MAPK kinase (MAPKKs/MKKs) and 20 MAP kinases (MAPKs/MPKs) have been characterized (Ichimura et al., 2002). The MAPKKKs are probably the scaffolding proteins to recruit the MAPK cascade to the response sites. The diversity of MAPKKKs ensures that different external stimuli are precisely converted to initiate similar MAPK cascades, which finally activate the same downstream MAPK. Several hyperosmotic stress-activated plant MAPK cascades have been identified in many species, such as the cascades activating salt stress-inducible MAP kinase (SIMK) alfalfa (Munnik et al., 1999, Kiegerl et al., 2000), salicylic acid-induced protein kinase (SIPK) in tobacco (Droillard et al., 2000, Liu et al., 2000, Mikolajczyk et al., 2000), as well as MPK3, MPK4, MPK6 and MPK7 in *Arabidopsis* (Ichimura et al., 2000, Droillard et al., 2002, Colcombet and Hirt, 2008, Opdenakker et al., 2012). However, unlike in yeast, osmotic stress-dependent MAPK cascade activation in plants seems to be no early response directly triggered by osmosensing. Rather, these MAP kinase cascades appear to be activated H_2O_2 -dependently during ABA signaling (see section 1.3.4.3).

In spite of the limited knowledge about hydraulic signal perception and early signal transduction, the accumulation of endogenous ABA, which is followed by ABA signal transduction, is undoubtedly an output of upstream hydraulic signaling (see section 1.3). Concomitantly water deficit is also transduced *via* an ABA-independent pathway (see section 1.4).

1.3 ABA-dependent signaling pathway

The plant hormone abscisic acid (ABA) was discovered as abscisin II and dormin in 1960s (Liu and Carnsdagger, 1961, Ohkuma et al., 1963). ABA modulates many aspects of plant growth and development including embryo maturation, seed dormancy, germination, cell division, cell elongation, and floral induction (Finkelstein et al., 2002, Cutler et al., 2010, Takezawa et al., 2011, Seung et al., 2011). Correspondingly, the ABA-deficient mutant *aba1-1* displays a stunted growth phenotype (Sharp, 2002), a phenotype which can be rescued by exogenous ABA (Finkelstein et al., 2002). In addition, ABA is extensively studied as a 'stress hormone', because of its dramatical increase when plants are challenged by biotic and abiotic stresses (Schroeder et al., 2001, Zhu, 2002, Himmelbach et al., 2003, Christmann et al., 2006, Qin et al., 2011, Huang et al., 2011, Cao et al., 2011, Finkelstein, 2013). Under water deficit, ABA is recruited to regulate many aspects of adaptative responses, such as stomatal closure to reduce transpiration (Schroeder et al., 2001, Kim et al., 2010b, Joshi-Saha et al., 2011b, Bauer et al., 2013), maintenance of root growth to allow extraction of water from additional sources (Sharp and LeNoble, 2002, Ober and Sharp, 2003, Yamaguchi and Sharp, 2010), accumulation of compatible solutes and synthesis of protective proteins (Stewart and Voetberg, 1985, Strizhov et al., 1997, Verslues and Bray, 2006, Sharma and Verslues, 2010).

1.3.1 ABA metabolism

ABA is a sesquiterpenoid with a single chiral centre at C-1'. The naturally occurring compound is exclusively the S-(+)-enantiomer ABA (2-*cis*, 4-*trans* ABA) of which the 2-*cis* double bond is isomerized by light (UV light being most effective) resulting in an equilibrium of *cis*-ABA and *trans*-ABA. While *trans*-ABA is biologically inactive, R-(-)-ABA is weakly active in some processes, and has the ability to trigger biosynthesis of natural active S-(+)-ABA (Cutler et al., 2010). The level of locally active ABA in the plant is regulated by the balance of ABA biosynthesis and ABA catabolism, and further by compartmentation and transport.

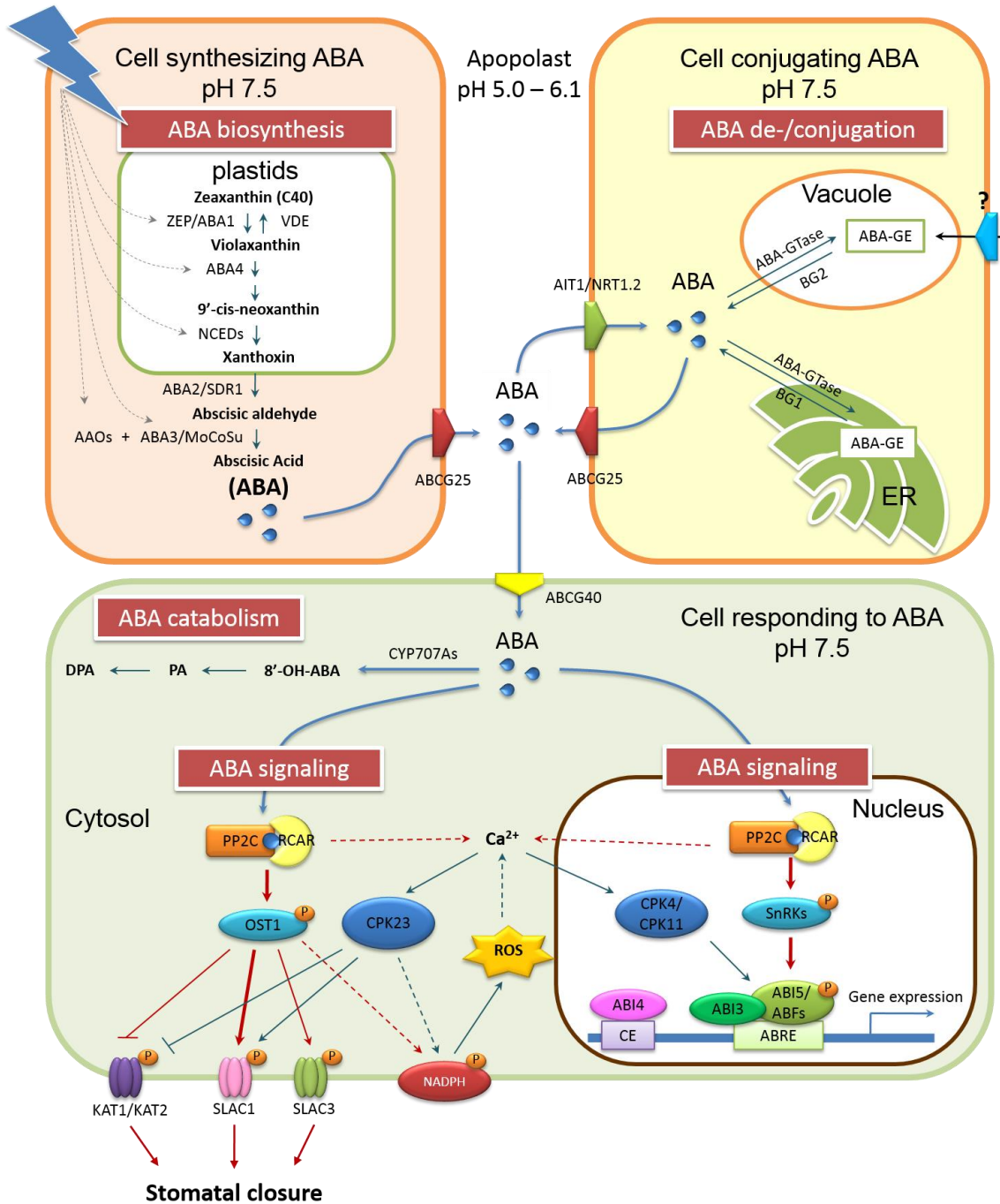


Figure 1-4: Overview of the ABA-dependent water deficit stress signaling pathway

Water deficit stress initiates ABA biosynthesis in vascular parenchyma cells. The expression of most of ABA biosynthetic enzymes is up-regulated by water deficit, except ABA2/SDR1. Both ABA conjugation and catabolism are activated to balance ABA levels. Active ABA is transported to perception sites or into the apoplast by ABA transporters, such as ABCG25, ABCG40 and AIT1/NRT1.2. At the ABA perception sites, the core ABA signaling (RCAR-ABA-PP2C-SnRK) governs ABA signaling responses in the nucleus and in the cytosol. Further signaling elements such as Ca^{2+} , H_2O_2 or CDPKs are modulating ABA signal transduction. Details are summarized in the text.

1.3.1.1 ABA biosynthesis

ABA biosynthesis pathway has been precisely revealed from a number of plant species and been detailedly reviewed in many publications (Xiong and Zhu, 2003, Schwartz et al., 2003, Nambara and Marion-Poll, 2005, Christmann et al., 2006, Wasilewska et al., 2008, Finkelstein, 2013). In higher plants the specific ABA biosynthesis starts from the oxidative cleavage of a C₄₀ epoxy-carotenoid precursor zeaxanthin to violaxanthin, which is catalyzed by a zeaxanthin epoxidase (ZEP) in plastids, firstly isolated in tobacco (Marin et al., 1996). The *Arabidopsis* ZEP is encoded by *ABA1* gene which was identified from the ABA-deficient mutant *aba1* (Koorneef et al., 1982). Meanwhile, a violaxanthin de-epoxidase (VDE) functions as an antagonism of ZEP to produce more photo-protective zeaxanthin in response to the intensive light (Bugos et al., 1998). Both mutations of ZEP and VDE can result in decreased zeaxanthin accumulation (Niyogi et al., 1998). A plastid membrane-localized protein ABA4 catalyzes the transforming from violaxanthin to primary ABA precursor neoxanthin (North et al., 2007). The rate-limiting step of ABA biosynthesis is catalyzed by 9-*cis*-epoxy-carotenoid dioxygenase (NCED) in plastids. NCED cleaves the xanthophylls (neoxanthin and/or violaxanthin) to C₁₅ compound xanthoxin/xanthoxal which is subsequently released into the cytosol (Schwartz et al., 1997). Then, xanthoxin is transformed into ABA by two oxidative steps. The short chain dehydrogenase/reductase-like (SDR1) enzyme encoded by *ABA2* firstly catalyzes the intermediate reaction to produce ABA aldehyde (Cheng et al., 2002). The final step of ABA converting is accomplished by abscisic aldehyde oxidases (AAOs) (Seo et al., 2000) and a molybdenum cofactor sulfurase (MoCoSu) encoded by *ABA3* (Xiong et al., 2001).

Because of these extremely defined ABA biosynthetic enzymes, we have the opportunity to investigate how the ABA biosynthesis is regulated during growth development and under environmental stresses (Xiong and Zhu, 2003). The biosynthetic enzymes *ZEP/ABA1*, *ABA4*, *SDR1/ABA2* and *MoCoSu/ABA3* are single copy genes, excepting that the AAOs and the NCEDs are encoded by small gene family, respectively. The *ZEP/ABA1* is abundantly expressed in all tissues, and is induced by drought stresses (Xiong et al., 2002). Although the impaired *ABA4* significantly reduces the ABA level in plant, the *aba4* mutant can also produce ABA *via* an alternative pathway using violaxanthin as a substrate (North et al., 2007). The AAO inactive phenotype of ABA-deficient mutant *aba3/los5* with impaired MoCoSu indicates that the ubiquitous MoCoSu/*ABA3* enzyme is prerequisite for AAOs activity (Xiong et al., 2001). AAO protein family contains four members (AAO1-to-4), in which AAO3 is the main abscisic aldehyde oxidase in seeds and leaves, even though high expression levels of AAO1 and AAO4 in the seed (Seo et al., 2004). And *Arabidopsis* genome encodes 9 NCEDs, of which NCED2, 3, 5, 6 and 9 are identified as plastid-localized functional NCEDs, but differ in binding activity of the thylakoid membrane (Tan et al., 2003). The roles of ABA during seed maturation and germination have been clearly studied (Finkelstein et al., 2002, Xiong and Zhu, 2003, Kanno et al., 2010, Finkelstein, 2013). Although the whole seed is considered to be involved in ABA biosynthesis, the functional NCEDs still display distinct expression patterns. For example, NCED2 and NCED3 are found in the surrounding maternal tissue of seed (Tan et al., 2003); NCED6 acts specifically in the endosperm (Lefebvre et al., 2006); and NCED9 locates in both endosperm and embryos (Lefebvre et

al., 2006). At the mid-stage of seed development, ABA is primarily synthesized in maternal tissues by NCED2 and NCED3, and subsequently transported into embryo to promote the synthesis of storage proteins in embryo. Then the second peak of ABA accumulation occurs during the desiccation phase to activate the producing of protective protein LEAs and initiate the seed dormancy. Here, the ABA is derived from the *de novo* synthesis catalyzed by NCED9 in embryo. A recent report indicates that upon imbibition the endosperm in dormant seed coat can synthesize ABA which is released to the non-dormant embryo to maintain the seed dormancy, while a DELLA protein RGL2 is required to promote this ABA synthesis (Lee et al., 2010).

Concerning the water deficit-induced ABA *de novo* synthesis, three important ABA biosynthetic enzymes, NCED3, ABA2 and AAO3, are co-localized in the vascular parenchyma cells (Cheng et al., 2002, Koiwai et al., 2004, Endo et al., 2008). The expression of *NCED3* is up-regulated by drought stress (Tan et al., 2003) *via* a stress-inducible NAC TF ATAF1 that directly binds the *NCED3* promoter (Jensen et al., 2008, Jensen et al., 2013). Therefore, Stress-induced ABA is predominately synthesized in the vascular tissue and subsequently transported into surrounding responsive cells. Recently, the research of stomatal response to dry air in ABA-deficient mutant *aba3-1* revealed that the guard cell may autonomously synthesize ABA to promote stomatal closure in response to low relative humidity (Bauer et al., 2013). For its high expression level, the ZEP/ABA1 seems not the rate-limiting enzyme of ABA biosynthesis, but is still up-regulated by drought stress. In *Arabidopsis*, tobacco, and tomato the ZEP/ABA1 is drought-induced in roots but not in leaves (Audran et al., 1998, Thompson et al., 2000), whereas the cowpea ZEP transcripts are not drought responsive at all (Iuchi et al., 2000). Only the SDR1/ABA2 expression appears not to be regulated by stress, but up-regulated by sugar (Cheng et al., 2002). In addition, ZEP/ABA1, AAO3 and MoCoSu in *Arabidopsis* are all up-regulated by ABA, meanwhile the ABA-induced up-regulation of *NCED3* is also found in the Landsberg background (Xiong et al., 2002). Therefore, the ABA biosynthesis is positively regulated by water deficit and ABA.

1.3.1.2 ABA catabolism and conjugation

Antagonizing to excessive ABA accumulation, the ABA level in cellular is balanced by catabolism and conjugation (Cutler and Krochko, 1999). The major ABA catabolic pathway is triggered by ABA 8'-hydroxylation and catalyzed by a cytochrome P450 CYP707A family (CYP707A1-4), whose transcripts are increased in response to water deficit stresses including salt, hyperosmotic and dehydration, as well as to exogenously applied ABA (Kushiro et al., 2004, Saito et al., 2004). The *cyp707a* mutant accumulates higher ABA content than wild type as well as the lines overexpressing ABA biosynthetic enzymes. The spatial analysis indicates the different expression patterns of CYP707As: the CYP707A3 plays a prominent role in ABA catabolism in the vegetative tissues of *Arabidopsis*, because it is the most abundantly protein induced by dehydration, especially highly expressed in leaves (Umezawa et al., 2006); the CYP707A1 is expressed in the embryo during the mid-maturation stage and decreased during the late-maturation stage, whereas the CYP707A2 in both embryo and endosperm plays a role during the late-maturation stage till seed germination (Okamoto et al., 2006). In subsequent step, the 8'-OH-ABA is isomerized to the phaseic acid (PA), which then converts to dihydrophaseic acid (DPA).

Actually, ABA can also be hydroxylated at the 7' or 9' positions. At least 9'-hydroxylation is a side pathway of CYP707As catalyzed ABA catabolism (Okamoto et al., 2011).

Compared with ABA catabolism, ABA conjugation is a reversible process to reduce active ABA level in cellular. ABA glucose ester (ABA-GE) is the predominant conjugate form and sequestered in apoplast tissues and vacuoles of mesophyll cells as an inactive storage ABA (Bray and Zeevaart, 1985, Cutler and Krochko, 1999). The glycosylation of ABA is catalyzed by the ABA-glucosyltransferase (ABA-GTase). Although the water stress- and ABA-inducible UDP-GTase identified from adzuki bean displays an ABA dependent GTase activity *in vitro* (Xu et al., 2002), over-expressing of the *Arabidopsis* GTase *UGT71B6* only mildly influences the free ABA content and the physiological phenotype, whereas the ABA-GE is massively accumulated in the over-expression lines (Priest et al., 2006). The possible reason is the functional redundancy of GTases in plant. The inactive storage ABA can be hydrolyzed by β -glucosidases (BGs). In *Arabidopsis*, the BG1 localizes in the endoplasmic reticulum (ER) (Lee et al., 2006c), and the BG2 (Xu et al., 2012) localized in the vacuole and quickly resorted by stresses. Under osmotic stress, Both BGs rapidly polymerize from lower to higher molecular weight forms to liberate active ABA. Therefore, ABA can be quickly restored from the storage ABA-GE by water deficit.

1.3.2 ABA transport

Besides the balancing of ABA biosynthesis and catabolism, cellular ABA content is also regulated by ABA intercellular translocation. The ABA flux between organs is explained as an 'ionic trap model' (Boursiac et al., 2013). The weak acidic ABA (pKa 4.7) is in an equilibrium between the anionic charged form (ABA⁻) and the protonated uncharged form (ABA-H). The uncharged ABA-H in apoplast (pH 5.0 to 6.1) can freely diffuse through the lipid bilayer of plasma membrane into cytosol, where the ABA-H is converted to the undiffusible charged form ABA⁻ for higher cytoplasmic pH (7.5). Therefore, the cytosol becomes a 'trap' for a constant ABA influx from xylem sap to surrounding cells. A big question is how the undiffusible ABA⁻ is exported from synthetic parenchyma cells to xylem sap over the ionic trap. Under environmental stresses, the xylem sap pH value rises up to 6.7, reducing the motive force for ABA-H uptake (Dietz et al., 2000).

The active transport of ABA has been investigated since 1970s, but the molecular bases of such transport are just isolated lately (Kuromori and Shinozaki, 2010, Kuromori et al., 2010, Kang et al., 2010, Kanno et al., 2012, Boursiac et al., 2013). ABCG25 and ABCG40, which were respectively identified from mutants *atabcg25* and *atabcg40*, belong to the G family of ATP-binding cassette (ABC) transporter (Kang et al., 2010, Kuromori et al., 2010). The ABC transporter family contains 130 members in *Arabidopsis*, but only few of them are functionally analyzed (Kang et al., 2012). The ABCG25 locates on the membrane of vascular parenchyma cells and plays a role during the ATP-dependent ABA export (Kuromori et al., 2010). Compared to ABCG25, the membrane-localized ABCG40 is broadly expressed in many tissues, including leaves of young plantlets, primary roots and lateral roots. It is remarkable that the expression level of *ABCG40* in guard cells is significantly higher than in mesophyll cells. And ABCG40 shows an ATP-dependent ABA import activity in yeast and tobacco BY2 cells (Kang et al., 2010). Hence, a simple model of ABA translocation is constructed: The

ABA-exporter ABCG25 works at ABA biosynthesizing cells for the ABA transport from inside to the bundle sheath cell apoplastic area over the ionic trap; Then ABA is diffused passively with the flow of water directed to the sites of transpiration; Subsequently, ABA is imported to guard cells by the ABA-importer ABCG40 to trigger the stomatal closure, particularly under stresses (Kuromori and Shinozaki, 2010). Since the discovery of ABCG25 and ABCG40, the ABCG group members of ABC transporter family are strong candidates for ABA transporters. Several ABCG proteins have also been reported to be involved in drought and salt tolerance, e.g. ABCG36 (Kim et al., 2010a) and ABCG22 (Kuromori et al., 2011), but the substrates transported by them have not been determined.

Recently, this model is improved by the third ABA transporter ABA-IMPORTING TRANSPORTER 1 (AIT1) which is found in yeast two-hybrid system using the ABA receptor complex (ABI1/PYR1 complex, see section 1.3.3.1) as a sensor (Kanno et al., 2012). AIT1 is also named NRT1.2 (NITRATE TRANSPORTER 1.2) identified as a low-affinity nitrate (NO_3^-) transporter in root epidermis and root hair (Huang et al., 1999). High activity of *AIT1/NRT1.2* promoter is detected in imbibed seeds as well as in vascular tissues of inflorescence stems, leaves and roots. In yeast and insect cells the expression of *AIT1/NRT1.2* enhanced ABA uptake (Kanno et al., 2012). Thus, the primary role of AIT1/NRT1.2 seems to be the ABA import from the vessels to epidermis and guard cells for the regulation of stomatal aperture in inflorescence stems (Kanno et al., 2012).

The conjugated storage ABA (ABA-GE) is also considered as a possible shuttle molecule of ABA signals, and is hypothesized to be transported into mesophyll vacuoles by ABC transporters (Sauter et al., 2002), two of which the vacuole-localized ABCC1 and ABCC2 exhibit an ABA-GE importing activity *in vitro* (Burla et al., 2013).

1.3.3 ABA perception and core ABA signaling

ABA signaling is initiated from the specific perception by receptor at the action site. The previous studies implied the presence of multiple types of ABA receptors on the cell surface as well as in the cytosol (Allan et al., 1994, Jeannette et al., 1999). Since 2009, a cytosol/nucleus Regulatory Components of ABA Receptors (RCAR1-14)/Pyrabactin Resistance Protein 1 (PYR 1)/PYR-Like (PYL1-13) have been independently identified and confirmed as cytosolic ABA receptors by several research groups (Ma et al., 2009, Park et al., 2009). In pace with this illustrious discovery, the essential core components of ABA signaling pathway from hormone perception to signal transduction have been identified: cytosolic ABA receptors (RCARs/PYR1/PYLs), clade A of type 2C serine/threonine protein phosphatases (PP2Cs), and subfamily 2 of SNF1-related kinases (SnRK2s). Subsequently a number of downstream targets, e.g. the ABA-activated basic leucine zipper transcription factors (bZIP TFs: ABFs/AREBs) and the guard cell specific SLOW ANION CHANNEL-ASSOCIATED 1 (SLAC1), are phosphorylated by SnRK2 kinases to organize the adaptative responses (Raghavendra et al., 2010, Joshi-Saha et al., 2011b, Qin et al., 2011). Transient expression of these components have successfully reconstituted the ABA signaling pathway in *Arabidopsis* protoplasts (Fujii et al., 2009).

1.3.3.1 ABA coreceptor complex: RCARs/PYR1/PYLs-PP2Cs

Since the first plant PP2C, ABA INSENSITIVE 1 (ABI1) was identified from an ABA-insensitive mutant *abi1-1* (Meyer et al., 1994, Leung et al., 1994), PP2Cs have been generally described as negative regulators of ABA signaling (Schweighofer et al., 2004). Accompanied with the identification of ABA receptor family RCARs/PYR1/PYLs, the role of PP2Cs during ABA perception has been investigated. Further researches revealed that PP2Cs play as coreceptor together with RCARs/PYR1/PYLs even though they do not make direct contacting with ABA (Szostkiewicz et al., 2009, Park et al., 2009, Ma et al., 2009, Nishimura et al., 2010).

The well known ABA-related ABI1 and its homolog ABI2 (Rodriguez et al., 1998, Leung et al., 1997) belong to the clade A of PP2Cs, whose phosphatase activity depends on the presence of Mg^{2+} and Mn^{2+} (Leube et al., 1998). *Arabidopsis* genome encodes 80 PP2Cs which are grouped into twelve subfamilies (from A to K) (Xue et al., 2008, Fuchs et al., 2012). In the ABA-insensitive mutants *abi1-1* and *abi2-1*, the amino acid residue converting in ABI1 (Gly¹⁸⁰Asp) and ABI2 (Gly¹⁶⁸Asp) leads to a hypermorphic mutation of ABI1 and ABI2, respectively, which cause a preferential accumulation of the mutated PP2Cs in the nucleus abolishing the interaction between ABI1/ABI2 and RCARs (Robert et al., 2006, Moes et al., 2008, Santiago et al., 2009b). As a result, both *abi1-1* and *abi2-1* mutants are dominantly insensitive to ABA. Conversely, loss-of-function alleles of *ABI1* and *ABI2* (*abi1-2*, *abi1-3*, and *abi2-1R*) are hypersensitive to ABA and drought stress (Merlot et al., 2001, Saez et al., 2006). Therefore, ABI1 and ABI2 negatively control a broad region of ABA signaling during plant development and stresses. In addition to prototypical ABI1 and ABI2, other members of clade A PP2Cs, e.g. PP2CA/ABA Hypersensitive germination 3 (AHG3) (Yoshida et al., 2006b, Kuhn et al., 2006), Homology to ABI1 1 (HAB1) (Saez et al., 2004), Homology to ABI1 2 (HAB2), Highly ABA-induced PP2C 1-3 (HAIs) (Bhaskara et al., 2012), and ABA Hypersensitive germination 1 (AHG1) (Nishimura et al., 2007), have been also characterized as negative regulators of ABA signaling. The extreme ABA hypersensitive phenotypes of multiple clade A PP2C knockouts revealed that these clade A PP2Cs redundantly regulate ABA response, and the fine-tuning of ABA sensitivity can be obtained through combined inactivation of these PP2Cs (Saez et al., 2006, Rubio et al., 2009).

The cytosolic ABA receptors RCAR1 (identical to PYL9) and RCAR3 (identical to PYL8) were initially identified as ABI1- and ABI2-interacting proteins in a yeast two-hybrid screen, and specifically bound to ABA (Ma et al., 2009, Szostkiewicz et al., 2009). RCARs/PYR1/PYLs family containing 14 members in *Arabidopsis* belongs to the Bet v 1 superfamily, of which the most distinctive feature is a large solvent accessible hydrophobic cavity (binding pocket) as a ligand binding site involved in binding and metabolism of large hydrophobic compounds such as lipids, hormones and antibiotics (Radauer et al., 2008). *In vitro* RCAR1 is required for ABA to completely block the phosphatase activity of ABI2. The binding assay of ABA and RCAR1-PP2C revealed that a 1:1 ratio heteromeric protein complex RCAR1-PP2C has single ABA binding site. The RCAR1 over-expressing lines displayed an ABA hypersensitivity with regard to the physiological ABA responses including the inhibition of seed germination and root elongation, as well as the stomatal closure (Ma et al., 2009). Compared to RCAR1, RCAR3 displayed greater ABA sensitivity to PP2C regulation, but less stringent stereo-selectivity for the (+)-ABA

(Szostkiewicz et al., 2009). In parallel, the ABA receptor roles of RCARs/PYR1/PYLs were independently discovered by several other groups. PYR1 (identical to RCAR11) was identified by chemical genetic screen of the mutant *pyr1* which is insensitive to the synthetic ABA agonist pyrabactin (Park et al., 2009). ABA-bound PYR1 inhibits the activity of PP2Cs *via* their physical interaction. For functional redundancy, the single mutant *pyr1* displays a normal ABA sensitivity, whereas the triple mutant *pyr1/pyl1/pyl4* and the quadruple mutant *pyr1/pyl1/pyl2/pyl4* are strongly insensitive to ABA (Park et al., 2009). PYL5, PYL6 and PYL8 interact with HAB1 in a yeast two-hybrid screen (Santiago et al., 2009b). The over-expressing analysis and ABA-binding assay of PYL5 proved that ABA-bound PYL5 inhibits the activity of clade A PP2Cs to activate ABA signaling (Santiago et al., 2009b). Furthermore, the mass-spectrometric (MS) analyses of ABI1-interacting proteins in *Arabidopsis* also confirmed the interaction between RCARs and PP2Cs which is quickly stimulated by ABA (Nishimura et al., 2010). These results indicate that *Arabidopsis* RCARs/PYR1/PYLs have the ability to bind ABA and PP2Cs, and inhibit phosphatase activity of PP2Cs in a combinatorial manner.

According to crystallographic structure analyses of ABA binding and protein phosphatase inhibition, the RCARs/PYR1/PYLs are separated into three distinct subclasses (Hao et al., 2011, Dupeux et al., 2011, Zhang et al., 2012), including *cis*-dimeric receptors (PYR1, PYL1 and PYL2), *trans*-dimeric receptor (PYL3) and monomeric receptors (PYL4-6, PYL8-10). In the absence of ABA, PYR1 and PYL1-2 proteins exist as a *cis*-homodimer which means that the ABA binding pocket of each subunit is towards the same direction. Surrounding the ABA binding pocket, two highly conserved surface loops CL2 serve as a 'gate' and a 'latch' of the open ligand-binding pocket (Melcher et al., 2009). The CL2 loops are also thought to be involved in the dimer interface of PYL2 (Yin et al., 2009). Once ABA has bound, a conformational change in the CL2 loops leads to the closure of the gate and latch, as well as the dimer dissociation, subsequently creating a surface to interact with and competitively inhibit the active site of PP2C. A conserved tryptophan in PP2C serves as a 'lock' to stable the 1:1 heteroternary receptor-ABA-PP2C complex by inserting directly between the gate and latch (Yin et al., 2009, Miyazono et al., 2009, Nishimura et al., 2009, Santiago et al., 2009a, Melcher et al., 2010). PYL3/RCAR13 is the most distinctive ABA receptor proteins and exists in limited species. The ABA-bound PYL3/RCAR13 prefers to *trans*-homodimeric form, which can easily disassociates to the monomer compared to *cis*-dimers (Zhang et al., 2012). It seems that PYL3 exists in an equilibrium of monomer, *cis*-dimer and *trans*-dimer. In contrast, the crystal structure of monomeric PYL10 indicated that the CL2 loops of PYL10 are constitutively closed, leading to a high affinity of PYL10 to PP2Cs. Therefore, PLY10 ABA-independently inhibits the PP2C activity. Of cause, the presence of ABA increases the affinity of the receptor complex (Hao et al., 2011, Sun et al., 2012). RCAR7/PYL13 was considered as an inactive ABA receptor (Fujii et al., 2009). However, the crystal structure of PLY13-PP2CA indicated that RCAR7/PYL13 selectively inhibits PP2CA independent of ABA (Li et al., 2013). The RCAR7 over-expressing and knockout lines revealed a *bona fide* ABA receptor function for RCAR7/PYL13 (Fuchs et al., 2014). Therefore, all members of RCARs/PYR1/PYLs family may combine ABA into the ligand-binding pocket. But the ABA affinity of heteromeric receptor complexes is significantly higher. The K_d value of ABA binding to the heteromeric receptor complexe is around

nanomole level which is relevance to the physiological ABA level (Ma et al., 2009, Szostkiewicz et al., 2009). Therefore, the ABA receptor and the PP2C constitute an ABA coreceptor complex during ABA perception.

As mentioned in section 1.3.1, ABA has several enantiomers, of which S-(+)-ABA is the natural active ABA, and conversely *trans*-ABA is biologically inactive. The affinities of ABA receptors to ABA enantiomers have been investigated. Crystal structures of apo-PYL5, PYL3(-)-ABA and PYL9(+)-ABA showed that PYL5 strongly binds (-)-ABA, that PYL9 is a stringently exclusive (+)-ABA receptor, and that PYL3 may accept both ABA enantiomers. Differing (+)-ABA binding, the steric hindrance and hydrophobic interaction are the two key factors for (-)-ABA (Zhang et al., 2013). Taken together 14 RCARs/PYR1/PYLs and 9 clade A PP2Cs combinational recognize the ABA enantiomers.

Although the ABA coreceptor role of the heteromeric receptor complex RCARs/PYR1/PYLs-PP2Cs has been proved *via* structural, biochemical and site-directed mutagenesis studies, the existence of other probable ABA receptors still cannot be excluded. The reported ABA receptor candidates include the plastidic-localized ABA-binding protein (ABAR)/H subunit of Mg-chelatase (CHLH)/Genomes uncoupled 5 (GUN5) (Shen et al., 2006, Wu et al., 2009, Mochizuki et al., 2001) and the plasma membrane-localized G-protein coupled receptor 2 (GCR2) (Liu et al., 2007) and G-protein coupled receptor (GPCR)-type G protein 1 and 2 (GTG1/GTG2) (Pandey et al., 2009). However, the contradictory results of the ABA binding activities pointed out that it is still too early to conclude the natural role of these ABA receptor candidates in ABA signaling (Gao et al., 2007, Johnston et al., 2007, Risk et al., 2009, Tsuzuki et al., 2011). Thereby more robust method of determining ABA binding (e.g. isothermal titration calorimetry) is suggested in future research to prove the ABA binding abilities (Christmann and Grill, 2009, Risk et al., 2009).

Given the central role of RCARs/PYR1/PYLs-PP2Cs receptor complex in ABA signaling, the investigation of their target transducers becomes necessary to understand the ABA signal transduction. In addition to the proper activation of the positive regulators SnRK2 kinases, various PP2Cs members physically interact with a number of targets, including the homeodomain transcription factor HB6 which negatively regulates ABA signaling (Himmelbach et al., 2002), a plastid-associated lipid-binding protein fibrillin involved in the ABA-mediated photoprotection (Yang et al., 2006), the calcium binding proteins and protein kinases (see section 1.3.5) and the ion channels (Lee et al., 2009, Brandt et al., 2012). Therefore, the PP2Cs may play as a crucial hub that connects the ABA perception with other signaling pathways involved in abiotic stress.

1.3.3.2 Activation of SnRK2s by ABA coreceptor complex

SnRK2 kinases belong to a plant-specific serine/threonine kinase family sucrose nonfermenting 1 (SNF1)-related kinases (SnRKs) and have been identified to involved in general osmotic stress and plant development in many species such as tobacco (Mikolajczyk et al., 2000), fava bean (Li et al., 2000), maize (Huai et al., 2008), wheat (Mao et al., 2009), soybean (Monks et al., 2001), rice (Kobayashi et al., 2004) and *Arabidopsis* (Boudsocq et al., 2004). *Arabidopsis* genome encodes 10 SnRK2s (SnRK2.1-10) with three subgroups (Kulik et al., 2011). All SnRK2s share a N-terminal Ser/Thr

kinase domain and a C-terminal regulatory domain (Domain I) involved in ABA-independent osmotic stress response (Kobayashi et al., 2004, Belin et al., 2006). Specifically, the ABA-activated kinases of SnRK2 group 3, including SnRK2.2, SnRK2.3 and SnRK2.6, contain a C-terminal ABA-specific box (Domain II) (Yoshida et al., 2006a).

SnRK2.6, also named SnRK2E, was firstly discovered as OPTEN STOMATA 1 (OST1) and highly expressed in guard cells. The mutant *ost1* displays a wilted phenotype mainly due to its impaired stomatal closure, but a normal ABA responsiveness in seeds (Mustilli et al., 2002, Yoshida et al., 2002). Two homologs SnRK2.2 and SnRK2.3 are widely expressed in all tissues. The distinct expression pattern of SnRK2s is consistent with the critical role of SnRK2.6 in stomatal response, and the broad regulations of SnRK2.2 and SnRK2.3 in response to ABA during seed germination, dormancy and seedling growth (Fujii et al., 2007). Triple mutant *snrk2.2/3/6*, also named *snrk2d/e/l*, exhibits poor growth and few products, as well as extremely insensitive to ABA (Fujii and Zhu, 2009, Fujita et al., 2009, Nakashima et al., 2009a). Therefore SnRK2.6, SnRK2.2 and SnRK2.3 function redundantly as positive regulators in ABA signaling during plant development and stress tolerance.

As the important positive regulators of ABA signaling, SnRK2s of subgroup 3 are directly regulated by PP2Cs (Umezawa et al., 2009). Earlier researches have revealed some vital aspects of the regulation of SnRK2 kinases activity. Firstly, the conserved serine residue (Ser¹⁷⁵) in the activation loop plays a critical role for the kinase activity (Belin et al., 2006, Burza et al., 2006), and is dephosphorylated by PP2C in the absence of ABA (Umezawa et al., 2009, Vlad et al., 2009). Secondly, the ABA-specific box Domain II constantly interacts with PP2C, as is not affected by ABA (Yoshida et al., 2006a, Umezawa et al., 2009). The mimic crystal structures of the SnRK2.6-HAB1 complex and the receptor-PP2C complex clearly revealed the regulation mechanism of SnRK2s kinase activity by receptor-ABA-PP2C complex (Soon et al., 2011, Ng et al., 2011, Yunta et al., 2011). In the absence of ABA, the activation loop of SnRK2 mimics the ABA receptor gate to approach the catalytic domain of PP2C, and the dephosphorylation of Ser¹⁷⁵ by PP2C leads to the SnRK2 converting to basal activity form, then the conserved tryptophan of PP2C inserts into the kinase active cleft to completely block the kinase activity (Soon et al., 2011). Reversely, in the presence of ABA, the activation of SnRK2s is suggested as a two-step intramolecular kinase activation. The ABA-bound receptor competitively binds to PP2C resulting in the liberation and conversion of SnRK2 from PP2C-inhibited state to a partially active state, which is then fully activated by the phosphorylation of its activation loop (Ng et al., 2011).

1.3.4 Signal transduction and the targets of SnRK2s

Given the central role of SnRK2s, especially mention about ABA-activated SnRK2s, in ABA signaling, their downstream targets transmit the internal signals towards distinct directions, such as the ABA-activated transcription in nucleus, the ion channel-mediated stomata responses, and the accumulation of reactive oxygen species (ROS) production (Joshi-Saha et al., 2011a).

1.3.4.1 ABA-activated transcription in nucleus

The ABA-regulated gene expression is mainly managed at transcription level. The ABA-responsive element (ABRE)-binding proteins/factors (AREB1-3/ABF1-4) are well-characterized substrates of SnRK2s in nucleus (Fujita et al., 2012). The AREBs/ABFs belong to basic leucine zipper transcription factors (bZIP TFs) family (Choi et al., 2000, Uno et al., 2000), of which AREB1/ABF2, AREB2/ABF4, and ABF3 are strongly induced and activated by osmotic stress and ABA, and have largely overlapping functions in vegetative tissues (Kang et al., 2002, Kim et al., 2004, Fujita et al., 2005, Kobayashi et al., 2005, Yoshida et al., 2010). Another typical representative of ABA-activated bZIP TFs ABA-INSENSITIVE 5 (ABI5) especially regulates ABA-dependent seed dormancy and germination, as well as post-germination development (Finkelstein and Lynch, 2000, Lopez-Molina et al., 2001). The bZIP TFs share a conserved leucine zipper dimerization motif and a basic DNA binding region containing two α -helices (Schumacher et al., 2000, Lindemose et al., 2013). The SnRK2 kinases directly multiply phosphorylate the Ser/Thr residues of the R-X-X-S/T sites in N-terminal conserved region of bZIP TFs to fully activate the TFs (Kobayashi et al., 2005, Furihata et al., 2006, Johnson et al., 2002). The multi-phosphorylated homo- or hetero-dimeric AREBs/ABFs/ABI5 (Yoshida et al., 2010, Lindemose et al., 2013) bind to the ABA-responsive *cis*-element (ABRE: ACGTGT/GC) in the promoter region of ABA-induced genes to activate the transcription. ABRE element was firstly identified in the promoter region of wheat *Em* gene (Guiltinan et al., 1990) and of rice *Rab16* gene (Mundy et al., 1990). Actually, single ABRE element is not sufficient to initiate the ABA-activated transcription, and must cooperate with other ABREs or coupling elements (CEs) to accomplish this mission (Shen and Ho, 1995, Skriver et al., 1991). Most of the known CE elements have the similarity with ABRE and contain an A/GCGT motif (Hobo et al., 1999).

In addition to bZIP TFs, some other transcription factors are also involved in ABA- or stress-induced transcription. For instance, both the B3 domain TF ABA INSENSITIVE 3 (ABI3) (Giraudat et al., 1992, McCarty et al., 1991) and the APETALA 2 (AP2) domain TF ABA INSENSITIVE 4 (ABI4) (Finkelstein et al., 1998), synergistically cooperating with ABI5, are well-characterized positive regulators of seed-specific and/or ABA-inducible gene expression. ABI3 and ABI4 regulate the expression of ABI5 in seed development and maturing (Lopez-Molina et al., 2002, Bossi et al., 2009, Reeves et al., 2011). Some R2R3-MYB and bHLH-MYC TFs are implicated in ABA-mediated abiotic stress responses (Abe et al., 1997, Li et al., 2007, Dubos et al., 2010). MYB2 was induced by ABA and dehydration, and the over-expressing of MYC2 (bHLH TF) and/or MYB2 (R2R3-MYB TF) enhanced the ABA sensitivity and the drought tolerance (Abe et al., 1997, Abe et al., 2003). The HD-ZIP TF ATHB6 (Himmelbach et al., 2002), as well as its homologs ATHB7 and ATHB12 (Olsson et al., 2004), negatively regulates ABA-induced gene expression *via* the direct interaction with PP2C (Elhiti and Stasolla, 2009, Valdes et al., 2012). Furthermore, WRKYGQK domain (WRKY) TFs contrarily modulate ABA-dependent stress response. WRKY57 (Jiang et al., 2012), WRKY25 and WRKY33 (Jiang and Deyholos, 2009, Li et al., 2011) improve drought tolerance *via* ABA-dependent pathway, while WRKY18, WRKY40 and WRKY60 negatively regulate seed germination and post-germination development by inhibiting the expression of many ABA-responsive genes, e.g. *ABF4*, *ABI4*, *ABI5*, *DREB1A*, *MYB2*, and *RAB18* (Shang et al., 2010, Chen et al., 2010b).

Although it is hard to precisely construct the sophisticated regulation network, the comparisons of transcriptomes for *Arabidopsis* exposed to ABA and various abiotic stresses have reinforced the view that about 1-10% genes of the genome are affected, and split fairly evenly between induced and repressed genes (Zeller et al., 2009, Nakashima et al., 2009a, Nakashima et al., 2009b, Yoshida et al., 2010, Choudhury and Lahiri, 2010, Okamoto et al., 2010). Although the diversity of experiment conditions leads to differential gene regulation, about 50 ABA-induced genes are common to nearly all conditions (Wang et al., 2011). According to the biological functions, the core set ABA-induced proteins are roughly sorted into two types: (I) the protective proteins involved in stress tolerance, such as late embryogenesis abundant (LEA) proteins, ROS scavenge enzymes and compatible solute metabolism enzymes, and (II) the signaling regulators, including transcription factors, protein kinases and phosphatases.

LEA proteins were firstly found in cotton seeds, accumulating in late embryogenesis (Dure et al., 1981). *Arabidopsis* has 51 LEA proteins (Hundertmark and Hinch, 2008). The well-characterized LEA proteins, such as RD29B/LTI65 involved in desiccation and cold responses, dehydrin protein RAB18, stress- and cold-induced protein KIN2/COR6.6 and ABA-inducible LEA 1 (AIL1), are remarkably accumulated under ABA treatment (Fujita et al., 2005). The hydrophilic and unfolded structure of LEAs implies the probable role for counteracting crystallization of cellular components or the irreversibly damaging effects of increasing ionic strength (Hundertmark and Hinch, 2008). Besides the protective proteins, the negative regulators PP2Cs are also induced by ABA. Five members of group-Ab PP2C subfamily, including *AHG1*, *AHG3*, *HAI1*, *HAI2*, and *HAI3*, were significantly less expressed in the triple mutant *areb1/areb2/abf3* under water stress (Nakashima et al., 2009a). Furthermore, the ABA-upregulated TFs, e.g. MYBs (Ding et al., 2009), bHLHs (Abe et al., 2003, Li et al., 2007) and heat shock TFs (Hsfs) (Kotak et al., 2007), have been indicated to involve in drought stress response. In contrast, the ABA-repressed proteins are enriched for proteins associated with plant growth and development (Wang et al., 2011).

1.3.4.2 ABA signaling to ion channel

Guard cell is highly developed single cell that integrates both environmental and internal signals (Hetherington and Woodward, 2003, Sirichandra et al., 2009b). The ABA-induced stomatal closure and the ABA-inhibited stomatal opening are short-term responses to the mild water deficit, and are accomplished by the guard cell specific kinase-phosphatase pair OST1/SnRK2.6-PP2C, which directly regulate the activities of ion channels in plasma membrane by phosphorylation/dephosphorylation (Pandey et al., 2007, Joshi-Saha et al., 2011b, Lee et al., 2012).

To initiate stomatal closure, ABA activates the guard cell voltage-independent slow (S)-type anion channel and voltage-dependent rapid (R)-type anion channel to trigger a transient membrane depolarization. Subsequently, the Cl^- and malate²⁻ are released from guard cells to decrease the cytosolic osmotic potential, resulting in stomatal closure (Roelfsema et al., 2004). The guard cell S-type anion channel SLOW ANION CHANNEL-ASSOCIATED 1 (SLAC1) is activated by OST1/SnRK2.6 (Negi et al., 2008, Vahisalu et al., 2008). The recessive mutant *slac1* shows constitutively high stomatal

conductance and strong ABA-insensitivity, while the R-type anion currents and Ca^{2+} -permeable channel currents are not disrupted (Vahisalu et al., 2008, Geiger et al., 2011). *In vitro*, OST1/SnRK2.6 phosphorylates the N-terminus of SLAC1 to activate the anion channel currents, meanwhile, co-expressing of PP2Cs such as ABI1 and PP2CA successfully inhibits this activation (Lee et al., 2009, Geiger et al., 2009). The PP2Cs not only inhibit the OST1/SnRK2.6 kinase activity *via* physical interaction in the absence of ABA, but also directly dephosphorylate SLAC1 to inhibit the S-type anion currents (Lee et al., 2009, Brandt et al., 2012). It is already known that the R-type anion channel QUAC1 is also activated by ABA through the phosphorylation of OST1/SnRK2.6 (Imes et al., 2013). In addition to the activation by Ca^{2+} -independent kinases, the anion channels are also regulated by Ca^{2+} -dependent kinases (see section 1.3.5).

In guard cells the inward-rectifying potassium channel KAT1 and its homolog KAT2 form the heteromultimeric channels and mediate K^+ influx resulting in stomatal opening (Kwak et al., 2001, Pilot et al., 2001, Lebaudy et al., 2009). *In vitro*, OST1/SnRK2.6 phosphorylates two positions of the cytosolic C-terminus of KAT1 (Thr³⁰⁶ and Thr³⁰⁸), and further point mutation assay implied that the phosphorylation at Thr³⁰⁶ is responsible for the functional inhibition of KAT1 (Sato et al., 2009). Therefore the ion channel activity of KAT1 is inhibited by OST1/SnRK2.6 to keep the ABA-dependent stomatal closure.

1.3.4.3 ABA-induced ROS production

Reactive oxygen species (ROS) play a dual role in the response of plants to abiotic stresses, functioning as toxic by-products of stress metabolism and as signaling molecule in regulating diverse function in plants (Choudhury et al., 2013). The downstream signaling of ROS is likely to occur *via* calcium and protein phosphorylation (Kar, 2011). In guard cells the plasma membrane-bound NADPH oxidases encoded by *AtrbohD* and *AtrbohF* genes directly interact with OST1/SnRK2.6 and are phosphorylated at Ser¹³ and Ser¹⁷⁴ amino acid residues (Mustilli et al., 2002, Kwak et al., 2003, Sirichandra et al., 2009a). The phosphorylated active NADPH oxidases transfer electrons from cytoplasmic NADPH to O_2 to generate O_2^- and, subsequently, H_2O_2 (Torres and Dangl, 2005), which activates the hyperpolarization-activated Ca^{2+} -permeable cation channel (I_{Ca}) to increase the cytosolic free calcium ($[\text{Ca}^{2+}]_{\text{cyt}}$), then leading to the stomatal closure (Pei et al., 2000). The NADPH oxidase RBOH C in the epidermal cells of *Arabidopsis* root elongation zone mediates the tip-localized Ca^{2+} influx and cytosolic Ca^{2+} elevation during root hair growth (Foreman et al., 2003). The ROS-induced activation of calcium channel is a broad conserved signaling cassette in plant biology (Mori and Schroeder, 2004), whereas the intracellular Ca^{2+} elevation could also lead to the ROS producing in apoplast by directly stimulating NADPH oxidase (Takeda et al., 2008, Monshausen et al., 2009). Therefore, the Ca^{2+} elevation and ROS signaling constitute a positive feedback loop to generate an oxidative burst. In addition, the ABA-induced ROS production may inhibit the activities of ABI1 and ABI2 to turn up the ABA signaling pathway (Meinhard and Grill, 2001, Meinhard et al., 2002).

The ROS production such as H_2O_2 has been shown to activate several MAPK cascades (Desikan et al., 2000, Grant et al., 2000, Colcombet and Hirt, 2008). Many MAPK cascade components have been

illustrated to locate at downstream of ROS signaling, including the MAPKKKs, e.g. ANP1, MEKK1 and MKKK20 in *Arabidopsis* (Kim et al., 2011a), NPK1 in tobacco (Kovtun et al., 2000), DSM1 in rice (Ning et al., 2010) and OMTK1 in alfalfa (Nakagami et al., 2004), the MAPKKs, e.g. MKK1 (Teige et al., 2004), MKK4 (Ren et al., 2002) and MKK5 (Kovtun et al., 2000), and the MAPKs, e.g. MPK3/MPK6, MPK4, and MPK9/MPK12 (Jammes et al., 2011). H₂O₂ especially activates the *Arabidopsis* Raf-type MAPKKK ANP1, initiating the MPK3/MPK6 cascades (Kovtun et al., 2000). MEKK1-MKK1-MPK4 cascade is also responsible to H₂O₂ (Teige et al., 2004, Droillard et al., 2004, Nakagami et al., 2006). The ROS-activated MAPKs phosphorylate a variety of substrates, including transcription factors, transcription regulators, splicing factors and other protein kinases, to respond to biotic and abiotic stresses (Ichimura et al., 2002, Mishra et al., 2006). The ROS-induced genes seem to be involved in cellular repair/protection mechanisms or in the H₂O₂ stress response signal transduction pathway (Desikan et al., 2000, Desikan et al., 2001, Choudhury et al., 2013).

ROS production are common second messengers working downstream of many hormones such as salicylic acid (SA), ABA, jasmonic acid (JA) and ethylene during the protective responses in plants under abiotic stresses. The involvement of ROS in crosstalk among these signaling pathways has not been fully understood (Fujita et al., 2006).

1.3.5 Ca²⁺-dependent ABA signaling

In contrast to the Ca²⁺-independent SnRK2s activity, the Ca²⁺-dependent signaling connects to the core ABA signaling *via* a number of Ca²⁺ binding protein and protein kinase such as calcineurin B-like proteins (CBLs) and CBL interacting protein kinases (CIPKs), Ca²⁺-dependent protein kinases (CDPKs/CPKs) and CDPK-related kinases (CRKs), calmodulines (CAMs) and calmodulin-dependent protein kinases (CaMKs), and Ca²⁺- and calmodulin dependent protein kinases (CCaMKs) (Luan, 2009, Das and Pandey, 2010, Wurzing et al., 2011, Asano et al., 2012).

CIPKs belonging to the SnRK3 subfamily contain a SNF1-like kinase domain and two regulatory domains FISL and PPI, which are binding sites to CBLs and PP2Cs respectively (Ohta et al., 2003, Sanchez-Barrena et al., 2013). Therefore, the CBL-CIPK complex has been discussed as one of the important targets of PP2Cs involved in the plant response to abiotic stresses and ABA (Batistic and Kudla, 2004, Kolkusaoglu et al., 2004, Luan, 2009). The SCaBP5 (CBL1)-interacting kinase PKS3/CIPK15 physically interacts to ABI2 participating a calcium responsive negative regulatory loop to control ABA sensitivity (Guo et al., 2002). And the Ca²⁺-binding CBL1/9-CIPK26 complex phosphorylates the N-terminus of NADPH oxidase AtROBHF to induce the ROS signaling (Drerup et al., 2013, Lyzenga et al., 2013). The best known CBL-CIPK-PP2C network is the salt overly sensitive (SOS) pathway regulating sensitivity to salinity in *Arabidopsis* (Zhu, 2002, Ji et al., 2013). In the presence of Ca²⁺, the Ca²⁺-bound SOS3 activates the SOS2 kinase leading to the Na⁺/H⁺ antiporter SOS1 open, whereas the released ABI2 physically binds to the PPI domain of SOS3 to prevent the interaction between SOS2 and SOS3 (Ohta et al., 2003, Quintero et al., 2011, Sanchez-Barrena et al., 2013). The regulation of Na⁺/H⁺ antiporter SOS1 by SOS3/CBL4-SOS2/CIPK24-ABI2 network illustrates that the molecular on-off switches control the phosphorylation/dephosphorylation of plant ion transporters. Similarly,

Arabidopsis K⁺ transporter 1 (AKT1) is also regulated by the CBL1/9-CIPK23-PP2C pathway to involve in K⁺ uptake during stomatal opening (Li et al., 2006, Xu et al., 2006a, Cheong et al., 2007). Some members of CBLs can interact with PP2CA *in vitro* (Lan et al., 2011). Thus, it seems like that the activation of AKT1 by CBL1/9-CIPK23 is inhibited by PP2C, whereas certain CBLs can re-switch on the ion channels by binding to PP2Cs.

CDPKs/CPKs are also broadly announced as regulators of ABA-dependent signaling pathway (Harmon et al., 2000, Ludwig et al., 2004, Asano et al., 2012). The CPK32 (Choi et al., 2005), CPK4 and CPK11 (Zhu et al., 2007b), bind to and phosphorylate the bZIP TFs AREBs/ABFs at Ser residue of C2 conserved domain *in vitro*. The disruption of CDPKs reduces, but over-expression of the genes enhances, ABA sensitivity and the expression of ABA-regulated genes. In guard cell, CPK23 and CPK21, as well as CPK3 and CPK6, promote the ABA- and Ca²⁺-induced stomatal closure by activating the SLAC1, SLAH3, and I_{ca} channels (Mori et al., 2006, Geiger et al., 2010, Geiger et al., 2011, Brandt et al., 2012). The BiFC-based interaction analyses displayed that ABI1 physically binds to CPK23 and CPK21 to block the activation of SLAC1 and SLAH3 by CDPKs (Geiger et al., 2011). These results indicate that CDPKs are probably additional regulation targets of PP2Cs, and further activated by the cytosolic Ca²⁺ elevation. However, not all of CDPKs are positive regulator of ABA signaling. For evidence, CPK12 negatively regulates ABA signaling in seed germination and post-germination growth (Zhao et al., 2011a). CPK12 phosphorylates not only ABFs, e.g. ABF1 and ABF4, but also ABI2 to activate both positive and negative regulators of ABA-signaling (Zhao et al., 2011a). Therefore, it seems like that different members of CDPK family may constitute a regulatory loop by antagonistic functions, in which CPK12 plays as a balancer of ABA signal transduction (Zhao et al., 2011b).

In fact, although Ca²⁺ is a simple divalent cation, the diversity of cytosolic Ca²⁺ signaling arises from a wide range of Ca²⁺ concentration elevations. The redundancy of Ca²⁺-binding proteins and the different compositions of canonic and non canonic calcium binding sites seem to control the overall calcium affinity of the Ca²⁺ signals decoding. However, the mechanisms of specificity and fine-tuning of the Ca²⁺-dependent signaling must be investigated in future.

1.4 ABA-independent water deficit signaling

Although the crucial role of ABA-dependent signaling in water deficit response has been thoroughly comprehended, much less is understood on the more direct, ABA-independent osmosensing pathway. Studying ABA-independent signaling in general is hampered by the fact that, actually, none of the ABA-deficient mutants, e.g. *aba1* and *aba2*, and the ABA-insensitive mutants, e.g. *abi1-1* and *abi2-1* is completely deficient or insensitive to ABA. Even in the decuple mutant *snrk2.1/2/3/4/5/6/7/8/9/10*, in which all members of SnRK2s are disrupted, the osmotic stress-induced ABA increase is greatly reduced but not abolished (Fujii et al., 2011). Transcriptomic and proteomic analyses have exhibited the stress-responsive gene network involved in general physiological responses to water deficit stress (Yamaguchi-Shinozaki and Shinozaki, 2006, Shinozaki and Yamaguchi-Shinozaki, 2007, Abebe et al., 2009, Aprile et al., 2009, Jogaiah et al., 2012, Le et al., 2012). While most drought-induced genes are also ABA-induced, some drought stress responsive genes do not change expression in response to

exogenously applied ABA such as the *ERD1* gene encoding a Clp protease regulatory subunit D (ClpD) (Nakashima et al., 1997, Simpson et al., 2003). The differential regulation of certain genes by ABA or hyperosmotic stress such as the *RD29A* gene (Yamaguchi-Shinozaki and Shinozaki, 1994, Yamaguchi-Shinozaki and Shinozaki, 2005) has fostered detailed promoter analysis of such genes. The promoter sequence analysis of *RD29A* gene then uncovered two major *cis*-elements (Yamaguchi-Shinozaki and Shinozaki, 1993): ABA-responsive ABRE and dehydration-responsive *cis*-element (DRE)/C-Repeat (CRT) (Yamaguchi-Shinozaki and Shinozaki, 1994, Yamaguchi-Shinozaki and Shinozaki, 2005). The DRE *cis*-element (TACCGACAT) is recognized by drought-induced DRE-binding protein DREB2A and its single homolog (Liu et al., 1998, Sakuma et al., 2006), as well as low temperature-induced DREB1A/C-repeat-binding factor 3 (CBF3) and its two homologs (Liu et al., 1998, Akhtar et al., 2012). DREB2A regulates the expression of water deficit-induced genes particularly, some of which, are also targeted by DREB1A (Sakuma et al., 2006).

Indeed, these evidences demonstrate the presence of an ABA-independent regulatory pathway which, together with the ABA-dependent pathway, synergistically governs the water deficit responses. Going through the entire signal transduction process from perception to adaptable responses, it seems likely that the ABA-independent events exist on every step of the water deficit signal transduction.

Firstly, the heteromeric ABA coreceptor complexes RCARs/PP2Cs have approximately 80 combinations, which vary in their affinities to ABA thus allowing for the adjustment of ABA signaling. In contrast to the ABA-dependent construction of receptor-ABA-PP2C complexes, two monomeric ABA receptors PYL10 and PYL13, constitutively bind to PP2C in the absence of ABA, and antagonistically inhibit the phosphatase activity independent of ABA (Hao et al., 2011, Sun et al., 2012, Li et al., 2013). On the other hand, the HAI PP2Cs, particularly HAI1, interact with monomeric RCARs but not dimeric RCARs, and this interaction is unaffected or only moderately stimulated by ABA (Bhaskara et al., 2012). The *hai* mutants display increased low ψ_w -induced proline and osmoregulatory solute accumulation, as well as enhanced expression of dehydration-protective genes but reduced expression of defense genes (Bhaskara et al., 2012). These results imply that under low ψ_w conditions HAI PP2Cs are not inhibited in a RCAR-ABA-PP2C complex, and thus remain active to dephosphorylate undiscovered substrate proteins as regulators of the low ψ_w response (Bhaskara et al., 2012).

Secondly, almost SnRK2 kinase family proteins (except SnRK2.9) are activated by hyperosmotic stress, but only five of them (subgroup 2 and 3) are weakly or strongly activated by ABA. The ABA-independent SnRK2s (subgroup 1) do not interact with PP2C in yeast and contain a C-terminal Domain I involved in the ABA-independent osmotic response (Boudsocq et al., 2004). However, the role of ABA-independent SnRK2s is still unclear.

Given the Ca^{2+} -dependent signals, the CBL1 represents a integrator of multiple stress signals, and positively regulates salt and drought responses but negatively regulates cold response, while the expression of ABA-regulated genes is not affected (Cheong et al., 2003). In contrast, CBL9 that displays similar expression pattern to CBL1 is induced by ABA, and commonly regulates ABA biosynthesis (Pandey et al., 2004). Both CBL1 and CBL9 can interact with different CIPK kinases, such as CIPK1,

CIPK23 and CIPK24 (D'Angelo et al., 2006). The alternation of complex formations between CBL1-CIPK and CBL9-CIPK is a convergence point for ABA-dependent and ABA-independent gene expression and ion channel regulation.

MAPK cascades probably play a role in the early water deficit response with MPK6 being directly activated by drought, also in an ABA-deficient mutant *aba2-4*, and with exogenous ABA failing to suppress the rehydration-dependent inactivation of MPK6 (Tsugama et al., 2012). Thus the ROS-induced MPK6 activation appears to be ABA-independent. mRNA decapping protein DCP1, which forms a mRNA decapping complex with DCP2 and DCP5 to regulate postembryonic development (Xu et al., 2006b), has been identified as direct phosphorylation target of the dehydration stress activated MPK6 (Xu and Chua, 2012). Therefore, the MPK6-DCP1 pathway is suggested as a rapid ABA-independent response to water deficit stress in *Arabidopsis*.

1.5 The aim of this work

Water deficit is a central abiotic stress factor for wild plant species and agricultural crops. Limited access to water triggers ABA accumulation in plants and the plant hormone controls a number of essential stress-adaptative responses including stomatal closure, adjustment of vegetative growth, accumulation of osmolytes, and modification of gene expression. While the core ABA signaling pathway has been elucidated, the whole water deficit signaling network is still poorly understood.

The major interest of this work is to better understand the molecular mechanisms of water deficit signaling in *Arabidopsis*. Map-based cloning was recruited to identify a novel *Arabidopsis* mutant *ahr11* with an alternated water deficit response phenotype. To elucidate the function of the novel component AHR11, the protein was ectopically expressed in protoplasts and *in planta*. In addition, a screen for proteins interacting with AHR11 was performed using a yeast two-hybrid screen.

2. Materials and methods

2.1 Materials

2.1.1 Plant materials

Wild-type *Arabidopsis thaliana*

Two accessions of *Arabidopsis thaliana* Columbia (Col-0) and Landsberg *erecta* (*Ler*) were employed in this work as wild-type reference or source for protoplasts, DNA and RNA isolation. Landsberg *erecta* (*Ler*) was used as the paternal outcross line for generating mapping population. All accessions were received from the Arabidopsis Biological Resource Center (ABRC; <https://abrc.osu.edu>), Ohio, USA.

Transgenic *Arabidopsis thaliana*

Transgenic ABA-reporter line *pATHB6::LUC* (*Arabidopsis thaliana* Col-0 background) harboring the *Photinus pyralis* luciferase (LUC) reporter under control of the ABA-activated promoter of homeodomain protein *ATHB6* (*At2g22430*) was generated previously to monitor active ABA pools *in vivo* (Himmelbach et al., 2002, Christmann et al., 2005). In this work, the *pATHB6::LUC* ABA-reporter line was applied for generation of the EMS-mutagenized seed population by J. Berger and Dr. A. Christmann and as a reference for physiological analysis if not otherwise indicated.

***Arabidopsis thaliana* mutants**

T-DNA knockout mutants of *AHR11* SAIL_88_D02.v1 (Col-0 background; N804 for short) and GK_476H03 (Col-0 background; Δ 476 for short) served in this work for novel protein characterization. Meanwhile, the *pATHB6::LUC* ABA-reporter construct was introduced into these T-DNA mutants by crossing to the *pATHB6::LUC* reporter line.

ABA-deficient mutant *aba2-1* (Leon-Kloosterziel et al., 1996) and ABA-insensitive mutant *abi1-1* (Koorneef et al., 1984) were used for generating double mutants *ahr11/aba2-1* and *ahr11/abi1-1*, respectively.

All mutants were ordered from ABRC (<https://abrc.osu.edu>).

2.1.2 Reagents

The chemicals used in this work were purchased in p.a. quality from Fluka (Sigma-Aldrich GmbH, Munich), Roth (Carl Roth GmbH & Co. KG, Karlsruhe), Serva (Serva Electrophoresis GmbH, Heidelberg) and Qigen (Qigen GmbH, Hilden). The DNA ladders (1 kb, 100 bp and λ HindIII DNA ladders) were applied by Thermo scientific (Thermo scientific GmbH, Munich). The basic molecular biology enzymes (Restriction enzymes, T4-ligase/-kinase, alkaline phosphatase, GoTaq-polymerase, Phusion-HiFi-polymerase, Klenow-fragment polymerase, M-MuLV reverse transcriptase, and so on) were obtained from Thermo scientific (Thermo scientific GmbH, Munich) and/or New England Biolabs (NEB GmbH, Frankfurt a. M). The enzymes Macerozym R-10 and cellulose R-10 were acquired from Yakult (Yakult

Honshia Co. Ltd., Japan). The detergent Silvet L-77 was purchased from Lehle Seeds (Round Rock, Texas, USA).

2.1.3 Microorganisms

Bacterial strains

For routine cloning, *Escherichia coli* (*E. coli*) strains DH5 α (strain #2970; no resistant; Stratagene GmbH, Heidelberg) and/or XL1Blue (strain #3340; Tetracyclin-resistant; Stratagene GmbH, Heidelberg) were employed to propagate plasmids.

The *Agrobacterium tumefaciens* strain pGV3101 harboring plasmid *pMP90/pSOUP* (strain #625) (Hellens et al., 2000) was used for plant transformation by inflorescence dip (Harrison et al., 2006, Zhang et al., 2006).

Yeast strains

Yeast strains Y8800 (*MAT α*) and Y8930 (*MAT α*) in yeast two-hybrid screen were kindly donated by Dr. Pascal Braun from Department of Plant Systems Biology of Technische Universität München (TU München). These two strains were derived from pJ69-4 (James et al., 1996), which harbor the following genotype: *leu2-3,112 trp1-901 his3-200 ura3-52 gal4 Δ gal80 Δ GAL2-ADE2 LYS2:: GAL1-HIS3 MET2::GAL7-lacZ cyh2^R*. The Y8800 and Y8930 strains were transformed with *pDEST AD-Y* and *pDEST DB-X* constructs, respectively (Dreze et al., 2010).

2.1.4 Oligonucleotides and plasmids

All the oligonucleotides created and used in this work were listed in the appendix 5.1, stored at -20° C in the Institute's primer collection. The primers were synthesized by Eurofins MWG Operon (Ebersberg, Germany). All the constructs generated and used in this work were listed in the appendix 5.2. The clones harboring the respective plasmids were stored at -80°C in the institute's strain collection labeled with the numbers indicated in the list.

2.1.5 Medium and sterilization

2.1.5.1 Medium for plants

MS medium (Murashige and Skoog, 1962) (per 1000 ml)

10 x MS-Macrosalts solution	100 ml
400 x MS-Microsalts solution	2.5 ml
MES	1 g
Sucrose	10 g
Agar	10g (for solid medium only)
pH 5.8 (KOH)	

Autoclave to sterilize

MS-0.5x sucrose medium (MS_{0.5xsuc})

MS_{0.5xsuc} medium was prepared as the same way as MS medium mentioned above, but 5 g/l sucrose.

10 x MS-Macrosalts solution [g/l]

NH ₄ NO ₃	16.5
KNO ₃	19.0
CaCl ₂ ·2H ₂ O	4.4
KH ₂ PO ₄	1.7
MgSO ₄ ·7H ₂ O	3.7

400 x MS-Microsalts solution [g/l]

CoCl ₂ ·6H ₂ O	0.01
CuSO ₄ ·5H ₂ O	0.01
Na ₂ -EDTA	14.60
H ₃ BO ₄	1.20
KI	0.30
MnSO ₄ ·H ₂ O	4.00
Na ₂ MoO ₄ ·2H ₂ O	0.10
ZnSO ₄ ·7H ₂ O	0.80
FeSO ₄ ·7H ₂ O	11.12

pH 4.5

Store at -20°C

400 x B5-Vitamin solution [g/l]

Nicotinic acid	0.4
Pyridoxine	0.4
Thiamine	4.0
Myo-Inositol	40.0

Medium for bacteria

LB medium [g/l]

Bacto tryptone	10
Yeast extract	5
NaCl	10
Agar	10 (for solid medium only)
pH7.0 (NaOH)	
Autoclave to sterilize	

For preparation of selective medium, antibiotics were added in the appropriate concentration after cooling LB medium below 50°C.

E. coli were grown in LB medium with appropriate antibiotics at 37°C for 12-16 h, with shaking at 200 rpm. *Agrobacterium* were grown in LB medium with appropriate antibiotics at 30°C for 2 days, with shaking at 200 rpm.

2.1.5.2 Medium for Yeast

All yeast medium recipes were described by Matija Dreze (2010).

YEPD liquid medium [g/l] (nonselective rich yeast medium)

Yeast extract	10
Bacto-peptone	20
Autoclave to sterilize	

Before use add 50 ml 40% (w/v) autoclaved glucose and 15 ml 65 mM adenine solution.

YEPD agar plates

40 g agar and 950 ml mQ water were shaken well. 2 x YEPD medium and agar were mixed after autoclaving. Before pouring, 50 ml 40% (w/v) glucose and 15 ml 65 mM adenine solution were added into the medium. 15 cm diameter YEPD agar plates were dried and stored in room temperature.

2 x Sc medium (synthetic complete medium) (per 1000ml)

10 x Yeast-macrosalts solution	200 ml
1000 x Yeast-microsalts solution	2 ml
Amino acid powder	2.6 g
pH 5.9 (NaOH)	
Autoclave to sterile	

Add 8 ml each amino acid stock solution as needed (15 ml adenine solution).

Sc agar plates

40 g agar and 950 ml mQ water were shaken well. 2 x Sc medium and agar were mixed after autoclaving. Before pouring, 50 ml 40% (w/v) glucose and amino acid solution were added into the medium. 15 cm diameter Sc agar plates were dried and stored in room temperature.

Amino acid powder mix and stock solution

Mix 6 g of each of the following amino acids: alanine, arginine, aspartic acid, asparagine, cysteine, glutamic acid, glutamine, glycine, isoleucine, lysine, methionine, phenylalanine, proline, serine, threonine, tyrosine, valine and pyrimidine uracil.

The different amino acid stock solutions are prepared at the following concentrations:

Amino acids	Stock solution [mM]	Stock condition
Histidine-HCl	100	room temperature; light protected
Leucine	100	room temperature
Adenine sulfate	65	room temperature
Tryptophan	40	4°C; light protected

The concentrated amino acid stock solutions are used at 8 ml/l of medium, except for adenine which is used at 15 ml/l of medium.

10 x Yeast-macrosalts solution [g/l]

KH ₂ PO ₄	10
MgSO ₄ ·7H ₂ O	10.24
NaCl	1
MgCl ₂	1
(NH ₄) ₂ SO ₄	50

After autoclaving, the stock solution was stored at room temperature.

1000 x Yeast-microsalts solution [g/l]

Biotin	0.002
Pantothenic Calcium	0.4
Folic Acid	0.02
Myo-Inositol	2.0
Nicotinic Acid	0.4
p-Aminobenzoic Acid	0.02
Pyridoxine Hydrochlorid	0.4
Riboflavin	0.2
Thiamine HCl	0.4
H ₃ BO ₃	0.5
CuSO ₄ ·5H ₂ O	0.04
KI	0.1
FeCl ₃ ·6H ₂ O	0.2
MnSO ₄ ·H ₂ O	0.4
Na ₂ MoO ₄ ·2H ₂ O	0.2
ZnSO ₄	400

The stock solution was allocated into 50 ml Facon-tubes and stored at -20°C.

2.1.5.3 Antibiotics and hormones

Antibiotic	Final concentration [mg/l]	Stock solution [mg/ml]
Ampicillin	50	100 (in mQ H ₂ O)
Kanamycin	50	50 (in mQ H ₂ O)
Rifampicin	50	50 (in DMSO; light protection)
Gentamicin	25	25 (in mQ H ₂ O)
Hygromycin	50	50 (in mQ H ₂ O)
Chloromycetin	25	10 (in ethanol; light protection)

Stock solution of each antibiotic was dissolved in corresponding buffer, filtrated through 0.22 µM filter and stored at -20°C.

Hormone	Final concentration [µM]	Stock solution [mM]
ABA	0.01-30	5 (in 10 mM MES-KOH, pH7.0)

Stock solution of each hormone was dissolved in corresponding buffer, filtrated through 0.22 µM filter and stored at -20°C.

2.2 Methods

2.2.1 Plant growth condition

Arabidopsis thaliana plants were grown in a controlled phyto-chamber (Conviron, Canada) under the following long-day conditions: 16 h light (photosynthetic photon flux density [PPFD]: $200 \mu\text{mol m}^{-2} \text{s}^{-1}$, temperature [T]: 22°C , relative humidity [RH]: 50%) and 8 h dark (T: 18°C , RH: 50%). For certain experiments mentioned in context, *Arabidopsis thaliana* plants were grown in short-day conditions: 8 h light (PPFD: $200 \mu\text{mol m}^{-2} \text{s}^{-1}$, T: 22°C , RH: 50%) and 16 h dark (T: 18°C , RH: 50%).

2.2.2 Seed sterilization and seedling growth condition

Arabidopsis thaliana seeds were immersed within 1 ml of 80% ethanol containing 0.1% (v/v) Triton X-100 and incubated for 20 min under constant shaking at 600 rpm. After removing the supernatant, the seeds were washed with 1 ml of 3% sodium hypochlorite for 3 min. Then seeds were eventually cleaned by thorough washing with sterile mQ H_2O for 5 times in sterile bench. Finally, seeds were sown in 9 cm Petri dishes containing $\text{MS}_{0.5\text{suc}}$ solid medium. Then stratification was performed at 4°C for 2 days in the dark before germination. The seedlings were grown vertically in a culture room under continuous illumination (PPFD: $60 \mu\text{mol m}^{-2} \text{s}^{-1}$, T: 22°C) till suited development stage for further experiments.

2.2.3 Quantification of ABA-dependent luciferase activity

The ABA-reporter line *pATHB6::LUC* has been generated to quantitatively detect the active ABA pool *in vivo* (Christmann et al., 2005). The ABA-induced luciferase oxidizes luciferin to oxyluciferin and this process releases photons which can be sensitively detected by an intensified CCD camera (ORCAII ERG; Hamamatsu photonics, Hamamatsu City, Japan) adapted with a Schneider Xenon 0.95/25 Objective (Schneider, Kreuznach, Germany). Shortly, the seedlings harboring the ABA-reporter construct *pATHB6::LUC* were sprayed with luciferin solution*. After 10 min incubation in the dark, the light emission of luciferase activity was detected by the CCD camera in a dark box. The exposure time was 10 min and imaging was done with 4 x 4 pixel binning. The intensity of light emission was translated into a false-color spectrum. Quantitative determination of luciferase activity was performed with software Simple PCI 6.6.0.0 (Compix, Cranberry Township, PA). The gray levels of pixels within the measuring area corrected for background activity are referred to as CCD-RLU (Christmann et al., 2005).

Detection of luminescence on a cellular level was performed with an inverted microscope (Axiovert 200; Carl Zeiss, Germany) equipped with Fluar objectives and the CCD camera mounted to the microscope base port. Seedlings were placed in a drop of Luciferin solution in a small chamber that was sealed at the bottom with a coverslip. Seedlings were covered with a small piece nylon-net, and the whole chamber was loosely covered with a coverslip to reduce evaporation. Pixel binning was 4 x 4, and exposure times varied between 10 and 30 min as indicated.

*** luciferin solution**

luciferin (PJK, Kleinblittersdorf, Germany)	1 mM
MES-KOH (pH7.0)	10 mM
Tween-80	0.01% (v/v)

Luciferin solution was filtrated through 0.22 μ M filter, and allocated into 12 ml Facon-tubes and stored at -20°C in the dark.

2.2.4 Map-based cloning

The strategy of map-based cloning was designed and modified based on several previous researches (Lukowitz et al., 2000, Jander et al., 2002, Jander, 2006, Hou et al., 2010). The most commonly used *Arabidopsis thaliana* Columbia x Landsberg *erecta* (Col-0 x *Ler*) mapping combination system served in this work.

2.2.4.1 Generation of F₂ mapping population

The EMS-mutant (Col-0 background, with *pATHB6::LUC* ABA-reporter construct) was out-crossed to another diverged accession *Ler* to generate a mapping population. *Ler* plant was used as the egg donator and mutant plant was used as the sperm donator to be sure successful crossing *pATHB6::LUC* ABA-reporter construct from pollens of mutant. The ABA-dependent light emission from seedlings exposed to water deficit stress (-0.6 MPa, mannitol) served as the parameter to select homozygous mutant phenotypic F₂ individuals. Only the individuals whose F₃ progenies were homogenously hypersensitive to water deficit stress were included into the mapping population.

2.2.4.2 First-pass mapping

The bulked segregant analysis was employed in first-pass mapping (Michelmore et al., 1991). The genomic DNA samples of homozygous individuals were isolated from leaf tissue (see section 2.2.9.1) for mapping. DNA pool was constructed by mixing DNA samples isometrically. A mapping marker set with 24 simple sequence length polymorphisms (SSLPs) markers, spaced evenly every 20 centiMorgan (cM) on the whole genome of *Arabidopsis thaliana*, was kindly provided by Dr. Farhah Assaad (TU München). All markers are PCR based, co-dominant (fully informative) and relatively abundant. And the sequence information was listed in Appendix 5.1.1. The basic polymerase chain reaction (PCR) recipe and program were described as follows. The PCR products were separated by 2% agarose gel electrophoresis. The genotyping was identified by comparing with several references, including Col-0 DNA, *Ler* DNA and an isometric DNA mixture of Col-0 and *Ler*. The genotyping of mixture reference was heterozygous for all molecular markers.

PCR recipe (20 μ l)

Component	Final concentration	Volume [μ l]
5 x GoTaq Buffer	1 x	4
10 x dNTP (20mM for each)	2 mM	2
Primer-F (100 pmol/l)	1 μ M	0.1
Primer-R (100 pmol/l)	1 μ M	0.1
GoTaq Polymerase (Promega)	0.01-0.25 U/ μ l	0.05-0.2
Template DNA	0.1-20 ng	1
mQ H ₂ O		Up to 20

PCR program

1#	Initial denaturing	95°C	5 min	
2#	Denaturing	95°C	30 sec	
3#	Annealing	48-65°C	30 sec	
4#	Elongation	72°C	50 sec	Go to step 2#; 35 cycles
5#	Final elongation	72°C	10 min	

50 x TAE Buffer (per 1000 ml)

Tris-Base	242 g
Acetic acid	57.1 ml
EDTA (0.5 M, pH8.0)	100 ml

6 x Loading dye

Glycerol	50% (v/v)
Orange G	0.25% (w/v)
EDTA (pH8.0)	1 mM

EtBr stock solution

ErBr	10 mg
mQ H ₂ O	1 ml

2.2.4.3 Fine-scale mapping

Designed molecular markers based on Cereon Genomics (Cambridge, MA) database were grouped into three types, such as SSLP markers, cleaved amplified polymorphic sequences (CAPs) markers and derived CAPs (dCAPs; <http://helix.wustl.edu/dcaps/dcaps.html>) (Neff et al., 2002). The sequence information of primers was listed in Appendix 5.1.1. PCR reactions were performed as mentioned in first-pass mapping. The genotypes of all individuals from mapping population were collected to check

the recombination events in the mapping population. The genomic region of interest was flanked by two markers with lowest recombinant rate.

2.2.5 Next generation sequencing (NGS)

Genomic DNA samples for next generation sequencing (NGS) were isolated from root tissue of a liquid culture of seedlings (see section 2.2.9.2) to avoid chloroplast DNA contamination. NGS of the mutant was carried out on the ABI SOLiD 3G+ sequencing platform by Dr. Tim-Matthias Strom from Helmholtz Center Munich Human Genetic Institute. Data analysis was carried out using CLC Genomics Workbench version 3.7 (CLC bio; Aarhus, Denmark) and LUMA (Febit biomed). The crude sequence data obtained by NGS was aligned to the public reference *Arabidopsis thaliana* Col-0 genome (TAIR10).

2.2.6 Methods for plant analysis

2.2.6.1 Transpiration measurement

The long-term transpiration of intact plant was measured using a portable gas exchange fluorescence system (GFS-3000, Heinz Walz, Germany). The plant growth and measurement were performed in long-day conditions. The entire aerial portion of 3- to 4-week-old plant (before flowering) was sealed off into a gas exchange cuvette (ring-chamber, custom designed, Heinz Walz, Germany) equipped with GFS-3000. The conditions in the ring-chamber were kept constant with growing chamber: impeller: 9; flow: 750 $\mu\text{mol s}^{-1}$; H₂O: 12000 ppm; CO₂: 380 ppm; PPFD: 190 $\mu\text{mol m}^{-2}\text{s}^{-1}$; T: 28.5°C (light) and 22°C (night).

2.2.6.2 Thermal imaging

Plants for thermal imaging were grown in water-controlled pots, in which the volumetric water content (VWC)* was steadied to 80% by adding additional water every day. The thermal pictures were captured using a thermographic system (VarioCAM high resolution head, InfraTec, Germany) in long-day growth chamber. The leaf surface temperature was quantified *via* software (IRBIS v2.2, InfraTec, Germany).

* VWC = water weigh [g]/dry soil weigh [g] x soil bulk density (0.167) x 100%

2.2.6.3 Water loss of detached shoots

The entire aerial portion was excised from the roots of 3- to 4-week-old plants, and the decline of the fresh weight was measured at ambient conditions over time. The water loss* of the detached shoot was calculated as follows.

*Water loss [%] = (Fresh weigh₀-Fresh weigh_n)/Fresh weigh₀ x 100%

in which n = time after excision from the roots.

2.2.6.4 Stomatal response to root-inflicted water deficit and ABA

The root-inflicted stress analysis was described in previous research (Christmann et al., 2007). 5-day-old seedlings grown on $MS_{0.5xSuc}$ medium were water deficit stressed by exposing roots to $MS_{0.5xSuc}$ solid medium supplemented with mannitol to imitate low water potential for 24 h. For ABA responses, the indicated amount of ABA was not only added into $MS_{0.5xSuc}$ medium, but also sprayed evenly on the surface of seedlings. Then the stomata of the abaxial cotyledon surface were directly observed under a research microscope (HBO 50 Axioskop; Carl Zeiss, Germany). 5 biological replicates, which contained more than 100 stomata in total, were employed in each condition.

2.2.6.5 Stomatal response of rosette leaf to exogenous ABA

The ABA-dependent stomatal closure of rosette leaf was performed as described previously (Pei et al., 1997). The rosette leaves with same development stage clipped from 3-week-old *Arabidopsis thaliana* were floated on 3 ml of incubation solution*, and exposed to white light ($150 \mu\text{mol m}^{-2} \text{s}^{-1}$) filtered through a water jacket for 2 h, for stomatal opening. Then the indicated ABA was added to the incubation solution, and the leaves were kept under the same conditions for another 2 h before measuring the stomatal aperture. Subsequently, the abaxial epidermis was mounted onto a microscope slide with transparent adhesive tape. Stomata images were observed under a research microscope (HBO 50 Axioskop; Carl Zeiss, Germany). About 30 stomata with 16-22 μm edge height were measured in each condition. The ambient temperature was maintained at $25 \pm 1^\circ\text{C}$.

The experiment condition of Ca^{2+} dependency of ABA-induced leaf stomatal closure was as same as the method mentioned above. The free Ca^{2+} concentration in the incubation solution was buffered by EGTA.

* Incubation solution

KCl	10 mM
CaCl_2	0.2 mM
EGTA	0.1 mM
MES-KOH (pH 6.15)	10 mM

2.2.6.6 Computed analysis of stomatal aperture

All stomata detections were performed with a digital camera (Olympus UC30; Olympus, Japan) connected to a research microscope (HBO 50 Axioskop; Carl Zeiss, Germany). And the width and length measurements of stomatal pores were accomplished using image analysis software (Image J 1.42q; Wayne Rasband, National Institutes of Health, USA). The ratio of width/length (W/L) of stomatal aperture was analyzed as a functional parameter to demonstrate stomatal response to certain treatments. Statistical tests (one-way ANOVA) were performed using software SPSS 16.0.0 (IBM SPSS Statistics). $P < 0.05$ was defined as statistically significant difference.

2.2.6.7 Seed dormancy and germination

All seed batches for dormancy analysis were harvested at the same time from plants grown side by side. Seeds were regarded as being germinated when the radical ruptured the surrounding structures (Koornneef et al., 2002, Bentsink and Koornneef, 2008). The percentage of germinated seeds at particular timing was taken as a parameter of dormancy depth and the response to stress or hormones.

Dormancy analyses in mQ water under light were performed as described previously (Alonso-Blanco et al., 2003). Sterilized seeds (50-100) were sown on water soaked filter paper in 9 cm Petri dish. After 7 days incubation in culture room (T: 22°C, PPFD: 60 $\mu\text{mol m}^{-2}\text{s}^{-1}$, constantly) the number of germinated seeds was scored under a dissecting microscope (Stemi SVII; Carl Zeiss, Germany). Seed germination rate at a series of the days of seed dry storage (DSDS) from the harvest date was detected. Two replicates were employed for each seed batch.

Seeds of *Arabidopsis thaliana* for germination assay were harvested and stored in room temperature more than 6 months for after-ripen. Since the inhibition of high sucrose level on germination, the MS_{0.5xSUC} medium with half amount of sucrose was employed as basic medium in germination assay. 50-100 of sterilized seeds were evenly sown in 9 cm Petri dish with MS_{0.5xSUC} medium, which was supplemented with ABA or mannitol according to the germination condition examined. And seeds were stratified at 4°C in the dark for 2 days. The rate of germinated seeds was calculated after 2 days growth in culture room (T: 22°C, PPFD: 60 $\mu\text{mol m}^{-2}\text{s}^{-1}$, constantly). Three independent experiments were performed using different seed batches.

2.2.6.8 Root growth

The 4-day-old seedlings of *Arabidopsis thaliana* grown on MS_{0.5xSUC} medium were gently transferred onto and entirely exposed to MS_{0.5xSUC} medium supplemented with various concentrations mannitol to adjust medium water potential or with ABA, and then grown vertically in culture room (22°C, light constant) for 3 days. The position of root tip was marked every 24 h under a dissecting microscope (Stemi SVII; Carl Zeiss, Germany). Then the photographs were taken with a digital camera (Canon G10, Canon, Japan; camera control software: Canon Utilities Remote Capture DC ver. 3.1.0.5), and the root length was measured using an image analysis software (Image J 1.42q; Wayne Rasband, National Institutes of Health, USA). Statistical tests (one-way ANOVA) were performed using software SPSS 16.0.0 (IBM SPSS Statistics). $P < 0.05$ was defined as statistically significant difference.

2.2.6.9 ABA quantification

The fresh shoot tissue of 5-day-old *Arabidopsis thaliana* seedlings was harvested and frozen in liquid nitrogen for ABA quantification after exposed to root-inflicted water deficit stress (MS_{0.5xSUC} with mannitol). Two biological replicates were prepared for each condition. The gas chromatography mass spectrometry (GC-MS) analysis of ABA quantification was carried out by Prof. Dr. Jutta Ludwig-Müller from the Institut für Botanik of Technische Universität Dresden. The details of GC-MS analysis was described in previous reports (Martin-Rodriguez et al., 2011). ABA quantification was repeated three times for each biological replicate (equivalent to minimum 100 mg FW of shoot tissue).

2.2.6.10 Pigments analysis

Plant tissue samples were ground in liquid nitrogen, and dissolved in 1 ml cold methanol (100%), then incubated on ice for 5 min. The absorbance of the extract, which was clarified by centrifuging for 4 min at maximal speed, was measured with a spectrophotometer (Ultrospec 2000 UV/Visible, Pharmacia Biotech) at certain wave length. Because the spectrophotometer response was linear with pigment concentration up to an absorbance value of one, the solutions were diluted further when the absorbance exceeded one. Following formulae were used to calculate different pigments (Sims and Gamon, 2002, Lichtenthaler, 1987):

$$\text{Chlorophyll a } [\mu\text{g/ml extract}] = 16.72 \times A_{665} - 9.16 \times A_{652};$$

$$\text{Chlorophyll b } [\mu\text{g/ml extract}] = 34.09 \times A_{665} - 15.28 \times A_{652};$$

$$\text{Chlorophyll a + b } [\mu\text{g/ml extract}] = 1.44 \times A_{665} + 24.93 \times A_{652};$$

$$\text{Carotenoid } [\mu\text{g/ml extract}] = (1000 \times A_{470} - 1.63 \times \text{Chl a} - 104.96 \times \text{Chl b})/221;$$

where A_λ was the absorbance of the extract solution in a 1 cm path length cuvette at wave length λ .

The relative content of chlorophyll (a+b) to total carotenoid was employed here as a parameter of pigments in leaves.

2.2.7 Protoplasts expression in *Arabidopsis thaliana*

The protoplasts isolation and transfection protocol was modified by M. Meinhard and T. Hoffmann according to previous publication (Abel and Theologis, 1994).

2.2.7.1 Isolation of protoplasts from plant leaves

The 3- to 4-week-old *Arabidopsis thaliana* plants (before flowering) are suitable for protoplasts isolation. 0.5-1 g of leaves were incubated within 10 ml enzyme solution* on a vertical shaker (RotoShake; 30 rpm) at 23°C for 4 h. Digested protoplast suspension was filtrated through a 150 μm mesh nylon net. After centrifugation at 60 g for 2 min, the supernatant was carefully removed and discarded. And the pellet protoplasts were resuspended in 10 ml WIMK solution** by rolling the tube in the hands. The wash step was repeated once with 5 ml WIMK solution. After another centrifugation step the pellet was resuspended in an appropriate volume of MaMg solution*** with a concentration of $0.5\text{-}1.0 \times 10^6$ protoplasts/ml. The viability of the protoplasts was estimated by staining with FDA (1 mg/ml in Aceton). Before the subsequent transfection, the protoplasts suspension was cooled to 4°C for 30 min.

*** Enzyme solution**

Cellulase	1% (w/v)
Macerozyme	0.25% (w/v)
Mannitol	400 mM
CaCl ₂	8 mM
BSA (Fluka, #05488)	0.6% (w/v)
MES-KOH (pH 5.6)	5 mM

**** WIMK solution**

Mannitol	500 mM
MES-Tris (pH 5.8-6.0)	5 mM

***** Mannitol-Magnesium (MaMg) solution**

Mannitol	400 mM
MgCl ₂	15 mM
MES-KOH (pH 5.8)	5 mM

All solutions were allocated into 50 ml Facon-tubes and stored at -20°C.

2.2.7.2 Protoplasts transfection

Quality of plasmid DNA is the major issue for successful transfection. All plasmid DNA used in protoplasts transfection were purified according to the manufactures of Plasmid DNA midi preparation (JETSTAR plasmid purification kit, GENOMED).

For transfection, a mixture of the plasmids to be introduced into the protoplasts was provided in 2 ml reaction tubes as follows:

<i>pRD29B::LUC</i> ABA-reporter plasmid (#3041)	4 µl (4 µg DNA)
<i>p35S::GUS</i> GUS-reporter plasmid (#883)	2 µl (2 µg DNA)
effector plasmid/empty plasmid (#1337)	4 µl (4 µg DNA)
Mannitol (800 mM)	10 µl

Subsequently, 100 µl (0.5-1.0 x 10⁶) protoplasts suspension was transferred to the reaction tubes containing the DNA premix. After additional 120 µl of PEG solution*, the suspension was mixed immediately by gently inverting tubes 5 times and incubated in room temperature for 3-5 min. Then, the suspension was washed by 750 µl and 600 µl WIMK solution, orderly. After centrifugation (2500 rpm, 2 min), pellet cells were resuspended into 100 µl WIMK solution with or without the inductive substances such as ABA. The transfections were incubated on a horizontal shaker (Rotamax) at 50 rpm for 16 h.

*** PEG solution**

PEG-4000	40% (w/v)
CaCl ₂	300 mM
MES-Tris (pH5.8)	5 mM

PEG solution was allocated into 50 ml Facon-tubes and stored at -20°C.

2.2.7.3 Activity assay of reporter**GUS activity**

The 35S promoter driven GUS reporter was used to assess transformation efficiency and to normalize the luciferase activity of single samples. The GUS activity was measured as fluorescence signal derived from and correlating to the β -glucuronidase activity. 50 μ l aliquot of the protoplast suspension was transferred to black 96-well-microtiterplate (Greiner bio one). Then 100 μ l of 1.5 x MUG-solution* were added into each well. The GUS activity was measured at 37°C for 12 min in the microplate reader (Synergy 2, BioTek). GUS activity was calculated and given as relative fluorescence units (RFU)/sec.

Luciferase (LUC) activity

The luciferase activity was detected using luminometer (Flash'n'Glow, BERTHOLD). 50 μ l aliquot of the protoplast suspension was transferred into luminometer round bottom tubes (SARSTEDT). The sample tubes were automatically processed and 100 μ l of LAR substrate** were added automatically to start the luminescence reaction. Total luciferase activity was given as relative luminescence units (RLU) and allowed calculation of RLU/sec. The relative activity of LUC to GUS reflected the activation of signaling.

*** 1.5 x MUG-solution**

Na ₂ HPO ₄ /NaH ₂ PO ₄ (pH 7.0)	50 mM
Na ₂ EDTA	10 mM
Triton X-100	0.1% (v/v)
Dithiothreitol (DTT)	1 mM
4-Methylumbelliferyl-b-D-Glucuronid (MUG)	0.2 mM

**** LAR substrate**

Tricine/NaOH (pH 7.8)	20 mM
MgSO ₄	2.7 mM
Na ₂ EDTA	0.5 mM
DTT	30 mM
ATP	0.5 mM
(MgCO ₃) ₄ Mg(OH) ₂	1 mM
Coenzyme A	250 μM
Luciferin	500 μM
Triton X-100	1% (v/v)

CCLR

Tris-phosphate (pH 7.8)	25 mM
DTT	2 mM
1,2-diaminocyclohexane-N,N',N'-tetra acetic acid	2 mM
Glycerin	10% (v/v)

2.2.8 Floral dip of *Arabidopsis thaliana*

For stable transformation of *Arabidopsis thaliana* an agrobacterium-mediated floral dip transformation was performed according to previous reports (Zhang et al., 2006, Harrison et al., 2006). Recipient plants were grown under long-day conditions for 4 weeks until inflorescences were present but not yet opened. Agrobacterium strain pGV 3101 pMP90/pSOUP (#625) carrying desired plasmid (*pGreenII_AscI_Hygro* derivation) was cultivated in LB medium with Kanamycin (50 mg/l), Rifampicin (25 mg/l) and Gentamicin (25 mg/l) at 30°C for 2 days. The culture was amplified in 200 ml fresh LB medium without antibiotics at 30°C for another 2 days. Agrobacterium cells were pelleted and resuspended in infiltration medium*. The inflorescences were submerged into the agrobacterium suspension for 3 min assuring complete wetting of the stems and inflorescences. The infiltrated plants were irrigated with 1 x MS-macrosalts for nutrition. To improve transformation efficiency, the procedure was usually repeated once, 3 days after the first dipping.

Transgenic seeds of T₁ generation were screened according to the hygromycin (50 mg/l) resistance marker and presence of the transformed fragment was verified by PCR analysis of genomic DNA isolated from hygromycin resistant plants. The positive transformants were planted into soil for next generation. The sterilized T₂ transgenic seeds were placed on MS medium containing hygromycin (50 mg/l). The hygromycin-resistant T₂ lines with a segregation rate of approximately 1:3 were selected as transgenic plants with one copy insertion for further homozygous stable transformation screening. About 100 seeds of each T₃ line were sown on hygromycin-MS medium (50 mg/l) to select for homozygous T₃ populations with 100% hygromycin resistance.

*** Infiltration medium (per 1000 ml)**

10 x Macrosalts solution	50 ml
MES	0.5 g
Sucrose	100 g
BAP (1 mg/ml in EtOH)	10 μ l
VAC-IN-STUFF Silvet L-77	100 μ l
pH 5.8 (KOH)	

2.2.9 Standard molecular biology methods

The standard molecular biology methods used in this work were as described by the protocols provided by the manufacturers or according to the standard protocols (Sambrook and Russell, 2001). Modifications and adaptations of single protocols and experiments are separately mentioned.

- plasmid DNA mini-preparation (NucleoSpin[®] Plasmid, MACHEREY-NAGEL)
- Plasmid DNA midi-preparation (JETSTAR[®] plasmid purification kit, GENOMED)
- Polymerase chain reaction (GoTaq[®]DNA polymerase, Promega)
- High-fidelity PCR (Phusion High-Fidelity DNA polymerase, Thermo Scientific)
- Plant tissue PCR (KAPA3G plant PCR Kit, KAPABIOSYSTEMS)
- DNA restriction (NEB and Thermo Scientific)
- DNA fragment dephosphorylation (alkaline phosphatase, NEB)
- DNA ligation (T4 DNA ligase, Thermo Scientific)
- Agarose gel electrophoresis
- DNA gel extraction (PeqLab Gel Extraction kit, PEQLAB)
- Preparation of competent *E.coli* cells
- Preparation of competent *Agrobacterium* cells
- 'Heat-shock' plasmid transformation to chemical competent *E. coli* cells
- Plasmid electroporation to competent *Agrobacterium* cells

2.2.9.1 Genomic DNA isolation from leaves tissue

100 mg *Arabidopsis thaliana* leaves were collected and homogenized in 300 μ l 2x CTAB buffer*. After vigorously mixing and 30 min incubation at 65°C, 300 μ l of chloroform was added. Then two phases were separated by spinning down at 10,000 g speed for 5 min. The upper aqueous phase was transformed into a new reaction tube. Following precipitation from the upper aqueous phase by additional 300 μ l isopropanol, the DNA was washed by 80% ethanol and dried at 37°C. Finally, DNA was dissolved in 0.1 x TE buffer**, with 10 ng/ μ l RNase.

*** 2x CTAB buffer**

Hexadecyl trimethyl-ammonium bromide (CTAB)	2% (w/v)
Tris-HCl (pH 8.0)	200 mM
EDTA (pH 8.0)	50 mM
NaCl	2M

**** TE buffer**

Tris-HCl (pH 8.0)	10 mM
EDTA (pH 8.0)	1 mM

2.2.9.2 Genomic DNA isolation from root tissue

Genomic DNA was isolated from root tissue of a liquid culture of seedlings to avoid chloroplast DNA contamination. Sterilized *Arabidopsis* seeds were sown into a 100 ml flask with 50 ml modified MS liquid medium* and grown in dark at 22°C on a shaker (100 rpm) till enough root tissue gotten. During this period, fresh medium was substituted weekly. The isolation of high quality genomic DNA from root tissue was performed following the handbook of DNeasy Plant Maxi Kit (QIAGEN).

*** Modified-MS liquid medium (per 1000 ml)**

10 x MS-Macrosalts solution	100 ml
400 x MS-Microsalts solution	2.5 ml
400 x B5-vitamin solution	2.5 ml
MES	1 g
Sucrose	15g
pH 5.8 (KOH)	
Autoclave to sterilize	

2.2.9.3 RNA isolation

Total RNA was isolated from rosette leaves or 5-day-old seedlings of *Arabidopsis thaliana* following the handbook of RNeasy Mini Kit (QIAGEN). Stress treatments were supplied before isolation. To determine the RNA concentration and purity, UV spectroscopy was used. The absorbance of RNA was measured at 260 nm and 280 nm by a NanoDrop-Photometer (NanoPhotometer 7211, IMPLEN). The A_{260}/A_{280} ratio of 1.8-2.1 was an indication of highly purified RNA.

2.2.9.4 RT-PCR

RT-PCR process followed the handbook of RevertAid First Strand cDNA Synthesis Kit (#K1621; Thermo Scientific).

Removal of genomic DNA from RNA preparation

DNase I (RNase-free; #EN0521; Thermo Scientific) was employed for genomic DNA removal from RNA. The followings were mixed and incubated at 37°C for 30 min:

RNA	1 µg
10x Reaction Buffer with MgCl ₂	1 µl
DNase I, RNase-free	1 µl
Water, nuclease-free	Up to 10 µl

Additional 1 µl 50 mM EDTA and 10 min incubation at 65°C was performed to deactivate the DNase I.

Synthesis of the first strand cDNA

The product from above step was used as a template to synthesize the first strand cDNA. 1 µl oligo (dT)₁₈ primer was added and incubated at 65°C for 5 min. The following components were supplemented in the indicated order:

5 x Reaction Buffer	4 µl
RiboLock RNase Inhibitor	1 µl
10 mM dNTP mix	1 µl
RevertAid M-MuLV Reverse Transcriptase	1 µl

The reaction was incubated at 37°C for 1 h and stopped by heating at 70°C for 10 min.

Semi-quantitative RT-PCR

Conventional PCR was done by using 0.5 µl (about 25 ng) cDNA as template. To semi-quantify the transcriptional level of target gene, endogenous standards such as housekeeping genes, *β-Actin* and *Tubulin*, were used as internal references. The PCR products were separated by gel electrophoresis and quantified by software Image J. The relative expression level was achieved by comparing the amount of products amplified by the target gene and the endogenous standard.

2.2.9.5 Quantitative real-time PCR

Quantitative real-time PCR (qRT-PCR) reactions were performed using the iQTMSYBR[®] Green Supermix (#170-8880, Bio-Rad). A master mix for all reactions was prepared (on the ice or at room temperature) by adding all required components, except the cDNA template, as follows:

qRT-PCR recipe (10 µl)

iQ TM SYBR [®] Green Supermix (2 X)	5 µl
Primer-F (10 pmol/l)	0.1 µl
Primer-R (10 pmol/l)	0.1 µl
cDNA template	0.5 µl
H ₂ O	Up to 10 µl

Assay master mix was dispensed equal aliquots into each qPCR tubes. And the cDNA samples were added to the tubes as reaction template. The quantitative real-time PCR was accomplished using CFX96 Touch Real-time PCR Detection system (#185-5196, Bio-Rad).

qRT-PCR program

Initial denaturing	95°C	3 min	
Denaturing	95°C	15 sec	
Annealing and elongation	55°C	30 sec	Go to step 2; 40 cycles
Melt curve analysis	55-95°C	0.5°C increment 2-5 sec/step	

The data analysis was performed according to the CFX Manager software (184-5001, Bio-Rad). In this work, the expression level of housekeeping gene *UBC9* (*At4g27960*) was used as a reference (Czechowski et al., 2005).

For target genes, a common method for validating a real-time PCR assay involves constructing a primer standard curve, which helps to determine the primer efficiency (E^*), linear dynamic range, and reproducibility of the assay. 8 serial 2-fold dilutions of cDNAs were served as template to perform a qRT-PCR reaction described as above. The standard curve was set as a plot of C_t value to log dilution value. The sequence information of primer pairs was listed in Appendix 5.1.3.

$$*E=10^{-(1/\text{slope})}$$

where $90\% < E < 105\%$; and $R^2 > 0.98$

2.2.10 High-throughput yeast two-hybrid screen

High-throughput yeast two-hybrid screen was described previously by Dreze (2010).

2.2.10.1 Assembly of DB-X and AD-Y expression plasmids

The generation of expression plasmids was accomplished using gateway cloning system (Karimi et al., 2007, Walhout et al., 2000). Firstly, distinct ORFs of interest were inserted into the dual selection entry vector *pENTRTM 1A* (Kan^R and Cm^S; Catalog no. A10462; INVITROGEN) by the restrictionsites Sall and EcoRI. Additionally, a STOP code was added at the C-terminus of ORFs. Plasmid DNAs from positive clones were analyzed by restriction analysis, as well as by sequencing (primer: pENTR-seq-r #1919 in Appendix 5.1.2).

Secondly, ROFs of interest were recombined into the destination vectors *pDEST-DB* (Amp^R) and *pDEST-AD* (Amp^R), respectively, *via* a Gateway LR recombination reaction between the entry clones and destination vectors. For large (> 10 kb) entry clones or destination vectors, linearizing the vectors by restriction digestion (SmaI) may increase the recombination efficiency by up to 2-fold. The Gateway LR recombination reaction was performed according to the manual of Gateway LR clonase II Enzyme mix (Catalog no. 11790-020; INVITROGEN). Briefly, the following components were added to a 1.5 ml reaction tube at room temperature and mix.

Entry clone (50-150 ng)	1-7 μ l
Destination vector (150 ng/ μ l)	1 μ l
LR Clonase™ II enzyme mix	2 μ l
TE buffer (pH 8.0)	Up to 10 μ l

After 1 h incubation at 25°C, additional 1 μ l of the Proteinase K solution was added into samples, which were subsequently incubated at 37°C for 10 min to terminate the reaction.

Then the LR reaction products were transformed into *E.coli* DH5 α by ‘Heat-shock’ transformation. The positive clones with ampicillin resistance were analyzed by PCR analysis and sequencing. The vector specific primers pDEST-AD (#1916), pDEST-DB (#1917) and pDEST-term (#1918) were employed for analyses.

2.2.10.2 Yeast transformation

Yeast transformation is performed following the ‘High efficiency LiAc transformation’ published previously (Gietz and Woods, 2002). *pDEST-DB-X* and *pDEST-AD-Y* expression plasmid constructs were individually transformed into competent yeast strains Y8930 (*MAT α*) and Y8800 (*MAT α*), respectively.

Single yeast colonies were used to inoculate a 5 ml pre-culture in Sc medium supplemented with the corresponding amino acids and grown over night at 30°C. An aliquot of 5 ml yeast pre-culture was added into 50 ml YEPD full medium and incubated at 30°C on a shaker (200 rpm) till reaching an optimal OD₆₀₀ of 0.6-0.8 (3×10^7 cells). The yeast cells were harvested *via* centrifugation for 5 min at 1,000 x g. After washing the cells in 25 ml sterile mQ water, the pellet was resuspended in 1 ml of 1 x LiAc (100 mM) and transferred into a new reaction tube. Cells were subsequently pelleted by short spinning and dissolved in 400 μ l 1 x LiAc. For one transformation 50 μ l of competent yeast cell suspension were used. In reaction tube cells were pelleted by short spinning, and the supernatant was removed carefully. The followings were supplemented into competent cells, orderly:

PEG4000 (50% w/v)	240 μ l
10 x LiAc (1 M)	36 μ l
Carrier DNA* (10 μ g/ μ l)	10 μ l
DNA (100-500 ng/ μ l)	1 μ l
sterile mQ water	73 μ l

Transformation mixtures were resuspended and incubated at 42°C for 40 min. After heat-shocking the cells were harvested by centrifugation for 15 sec short spinning and resuspended in 100 μ l mQ water for subsequent plating on Sc selective medium. The transformed yeast on selective solid medium was incubated at 30°C for 2 days.

*** Carrier DNA**

Single stranded DNA derived from salmon testes was dissolved 10 mg/ml in 1 x TE buffer (pH 7.5), stirred for 3 h and ultrasonic-pulsed twice at max power for 30 sec. Then 1/10 volume of NaAc (3 M) was added to this solution. Subsequently, DNA was precipitated by mixing with 2.5 volume of EtOH (100%). The precipitated DNA is pelleted by centrifugation for 10 min at max speed and frozen for later use. The aliquots of carrier DNA to be used for transformation were again boiled at 95°C for 5 min and then cooled on ice prior to use.

2.2.10.3 Yeast colony PCR

A quick and easy yeast colony PCR was modified according to the ‘Yeast Colony PCR v 2.0 protocol’ from Blackburn lab in university of California San Francisco. For cell lysis, a small yeast colony was resuspended in 10 µl of 0.02 M NaOH in PCR tube. The suspension was incubated on a PCR machine at 99°C for 10 min, and then kept on ice or freeze for longer. Phusion High-fidelity DNA polymerase (Thermo Scientific) was applied for the PCR reaction, and a master mix for PCR reactions was prepared by adding all required components, except the cell lysis template, as follows:**PCR recipe (20 µl)**

Component	Final concentration	Volume [µl]
5 x Phusion HiFi polymerase buffer	1 x	4
10 x dNTP (20 mM for each)	2 mM	2
AD or DB primer (100 pmol/l)	1 µM	1
Term primer (100 pmol/l)	1 µM	1
Phusion HiFi DNA polymerase	0.25 U/µl	0.2
PCR Enhancer (100 x)	0.5-1 x	0.1-0.2
Cell lysis suspension template		1
mQ H ₂ O		Up to 20

PCR program

1#	Initial denaturing	98°C	30 sec	
2#	Denaturing	98°C	10 sec	
3#	Annealing	58°C	30 sec	
4#	Elongation	72°C	3 min	Go to step 2; 35 cycles
5#	Final elongation	72°C	10 min	

The PCR enhancer supplied in KAPA plant PCR Kit (KAPABIOSYSTEMS) was employed here to substitute the Q-solution in original protocol. The primer concentration was about ten-times more than standard PCR protocols. The PCR products were separated by 1% agarose gel electrophoresis, and DNA fragments of interest were extracted from agarose gel according to the manual of the PeqLab Gel Extraction Kit (PEQLAB), and subsequently sequenced by GATC Biotech.

2.2.10.4 Controls of yeast-two-hybrid

For reliable validation of protein interacting, 6 of real biophysical interactors served as interacting controls in yeast two-hybrid system (Table 2-1). All interactions that pass these controls were considered high-quality yeast-two-hybrid interactions.

Table 2-1: Yeast two-hybrid controls

Controls	Plasmid pairs	Protein	Interaction strength
1	<i>pDEST-AD</i> <i>pDEST-DB</i>	No insert No insert	None, background
2	<i>pDEST-AD-E2F1</i> <i>pDEST-DB-pRB</i>	Human E2F1 aa342-437 Human pRB aa 302-928	Weak (control for CHX control plates)
3	<i>pDEST-AD-Jun</i> <i>pDEST-DB-Fos</i>	Mouse Jun aa 250-325 Rat Fos aa 132-211	Moderately strong
4	<i>pDEST-AD</i> <i>pDEST-DB-Gal4</i>	No insert Yeast Gal4 aa 1-881	Very strong
5	<i>pDEST-AD-dE2F1</i> <i>pDEST-DB-dDP</i>	<i>Drosophila</i> E2F aa 225-433 <i>Drosophila</i> DP aa 1-337	Strong
6	<i>pDEST-AD-CYH2-dE2F1</i> <i>pDEST-DB-dDP</i>	<i>Drosophila</i> E2F aa 225-433 <i>Drosophila</i> DP aa 1-377	Strong (control for CHX plates)

Identities and description of expected phenotypes for the six controls used in every yeast two-hybrid experiment (Dreze et al., 2010).

2.2.10.5 Identification of autoactivators

Autoactivation of yeast-two-hybrid-inducible reporter genes is a common artifact of the yeast two-hybrid system. The identification of autoactivators was achieved in diploid yeast strains obtained by mating yeast strains Y8930 (DB-X) with the yeast strain Y8800 transformed with the AD encoding plasmid containing no insert (*pDEST-AD-emp*).

- The DB-X yeast strains and AD-emp yeast strain were incubated in fresh liquid mediums Sc-Leu and Sc-Trp, respectively, at 30°C for 72 h on a shaker.
- 5 µl of DB-X liquid cultures were spotted on a YEPE plate and allowed to dry for 30-60 min.
- 5 µl of AD-emp liquid cultures were spotted on top of the DB-X spots and allowed to dry for 30-60 min.
- The mating plates were incubated at 30°C for 14-18 h.
- The mating plates were replicated onto Sc-Leu-Trp plates to select for diploid cells, and incubated at 30°C for 14-18 h.
- Subsequently, the diploid cells on Sc-Leu-Trp plates were replicated onto Sc-Leu-Trp-His + 1 mM 3AT (3-amino-1,2,4-triazole) plates, where nonautoactivating yeast cells were not able to grow, and incubated at 30°C for 14-18 h.

- Replica-clean of the Sc-Leu-Trp-His + 1 mM 3AT plates were performed by pushing evenly the plate on a piece of sterilized velvet to remove excess yeast. Plates were incubated at 30°C for another 72 h.

All yeast strains on Sc-Leu-Trp-His + 1 mM 3AT plates showing a stronger growth phenotype than the 'no interaction' control (control 1) were considered autoactivators. To reliably identify autoactivators, two independent tests were performed, and the most stringent scores were accepted to ensure high quality of the starting material for subsequent interactome mapping. The chemical 3AT is a competitive inhibitor of the HIS3 gene product, therefore, when dealing with DB-X auto activators, higher 3AT concentrations could be used to circumvent autoactivator-dependent activity of GAL1-HIS3. All autoactivators of DB-X strains were excluded from the collection of DB-X.

Albeit much less frequent, autoactivation of AD-Y could also occur. The AD-Y autoactivator identification by use of mating between AD-Y yeast strains and DB-emp yeast strain was easily adapted.

2.2.10.6 Yeast two-hybrid primary screening

- 5 µl of glycerol stocks of the DB-X yeast strains and AD pools tested were inoculated in round bottom 96-well plates containing 160 µl selective medium in every well (Sc-Leu for DB-X, Sc-Trp for Ad pool) at 30°C for another 72 h for 72 h on a shaker.
- For each combination (AD-pool plate x DB-X plate), 5 µl/well of the respective AD-Y pool liquid culture were spotted onto a mating plate (YEED) using a liquid handling robot, and allowed to dry for 30-60 min.
- Then 5 µl of each DB-X were spotted on top of the AD pool spots, and allowed to dry for 30-60 min.
- Six controls of Y2H were spotted on every plate.
- After an incubation at 30°C for 14-18 h, mated yeast cells were replicated from mating plates onto screening plates (Sc-Leu-trp-His + 1 mM 3AT), meanwhile replicated onto CHX control plates (Sc-Leu-His + 1 mM3AT + 1 mg/l CHX), and incubated at 30°C for 14-18 h.
- All screening plates were cleaned by pressing plates onto a piece of velvet stretched over a replica-plating block and incubated at 30°C for 5 days.
- The colonies that grew better than background (control 1) and did not grow on CHX plates were considered primary positive colonies.
- Three colonies from each positive interacting spot were picked into a 96-well plate with round bottom (LOT: E13030FL; Greiner bio-one) containing 160 µl Sc-Leu-Trp medium per well, and incubating the culture plate at 30°C for 72 h on a shaker for subsequent phenotyping experiments.

2.2.10.7 Secondary phenotyping

5 µl of primary positive diploid yeast strains and Y2H controls were spotted onto Sc-Leu-Trp plates using a 96-well liquid handling robot and incubated at 30°C for 48 h. Positives were replicated onto fur phenotyping plates:

Sc-Leu-Trp-His + 1 mM 3AT	(His auxotrophy)
Sc-Leu-His + 1 mM 3AT + 1 mg/l CHX	(CHX control plate for His)
Sc-Leu-Trp-Ade	(Ade auxotrophy)
Sc-Leu-Ade + 1 mg/l CHX	(CHX control plate for Ade)

Plate cleaning was immediately performed after replica-plating to minimize background growth, and then the phenotyping plates were incubated at 30°C for 72 h.

During phenotyping, both reporter genes His and Ade were inspected, and any yeast spot showing growth on CHX plates should not be considered for further processing. All positives were patched and incubated on fresh Sc-Leu-Trp plates at 30°C for 48 h. The inserts of the AD-Y in positive colonies were amplified by yeast colony PCR for subsequent ORF identification by sequencing. Once sequencing data have been received and the candidate protein pairs have been identified, a list of unique candidate interacting pairs could be compiled.

2.2.10.8 Independent verification of candidate Y2H pairs

According to the list of candidate interacting pairs, the individual ORFs of candidates were subcloned into expression plasmid vector (*pDEST-AD*) and subsequently transformed into yeast strain Y8800 by Angela Alkofer from Department of Plant Systems Biology of TU München.

- 5 µl of glycerol stock of the DB-X yeast strain and AD-Y yeast strain of interest were inoculated in round bottom 96-well plates containing 160 µl/well selective medium (Sc-Leu for DB-X, Sc-Trp for AD pool) at 30°C for 72 h on a shaker.
- 5 µl/well of liquid cultures AD-Y and DB-X were mated on YEPD plate as described above and incubated at 30°C for 14-18 h.
- Then mated cells were replicated onto diploid selection plates Sc-Leu-Trp, and incubated 30°C for 14-18 h.
- Positives were replicated onto four phenotyping plates, and cleaned immediately.
- After 3 days incubation, the growth phenotype was scored in the same way as for secondary phenotyping.

The verification was performed at least three times independently.

3. Results

3.1 Isolation of a novel ABA-hypersensitive mutant *ahr11*

To better comprehend the mechanism of ABA-dependent water deficit stress signaling pathway, a noninvasive, cell-autonomous ABA-reporter system has been established previously, by which the spatial and temporal pattern of physiologically active ABA pools can be detected *in vivo* (Christmann et al., 2005). Transgenic *Arabidopsis* plants (*pATHB6::LUC*, Col-0 background) harboring the firefly luciferase (LUC) reporter gene under control of the promoter of homeodomain protein *ATHB6* were generated. The *ATHB6* promoter contains the ABA-responsive *cis*-element (ABRE), so the luciferase activity in *pATHB6::LUC* transgenic seedlings is induced over 1,000-fold by ABA (Himmelbach et al., 2002).

Subsequently, homozygous *pATHB6::LUC* seeds were mutagenized by using ethylmethanesulfonate (EMS). Different mutants were isolated from the M₂ generation of the mutated population by J. Berger and Dr. A. Christmann in a screen for mutants with a hypersensitive response to water deficit stress. The M₃ and M₄ generations were re-tested for stability of the water deficit-hypersensitive phenotype. According to the sensitivity to exogenous ABA, all of the water deficit-hypersensitive mutants were grouped into hypersensitive ABA response mutants and normal ABA response mutants. One of the ABA hypersensitive mutants, *ahr11* (*ABA hypersensitive response 11*), was selected for map-based cloning and further characterization in this work.

The 4-day-old seedlings from *ahr11* and *pATHB6::LUC* were selectively subjected to various water deficit stresses such that the shoot contact was prevented by narrow Parafilm strips. After 24 h treatment, the water deficit-induced luciferase activity in the mutant *ahr11* was confined to the shoot, and was detectable below a mannitol water potential $\psi = -0.4$ MPa. The maximal induction of luciferase activity in *ahr11* was up to 82.7 ± 7.8 CCD-RLU $\times 10^4$ at -0.8 MPa mannitol water potential, which was 18.3-fold of the induction in *pATHB6::LUC* (Figure 3-1A). When different concentrations of exogenous ABA were supplied, the luciferase activity response of *ahr11* to 30 μ M ABA was 19.4 ± 5.3 CCD-RLU $\times 10^4$ and obviously stronger than *pATHB6::LUC* (Figure 3-1B).

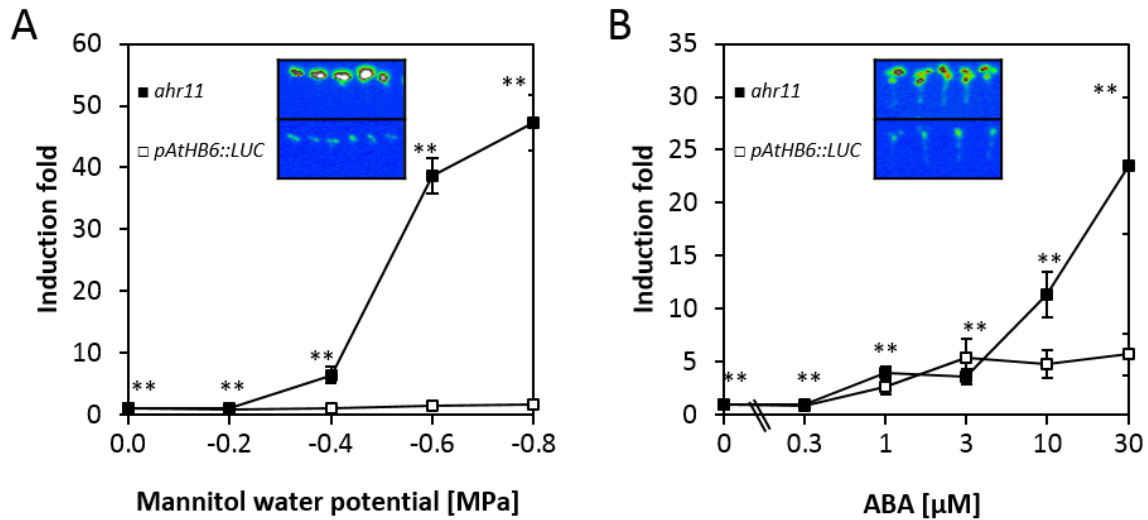


Figure 3-1: Activation of the LUC-reporter in wild type and *ahr11* seedlings harboring the *pATHB6::LUC* ABA-reporter construct by water deficit stress and exogenous ABA

4-day-old seedlings of mutant *ahr11* (black) and wild type *pATHB6::LUC* (white) were exposed to low water potentials modulated by supplementing the $MS_{0.5xSUC}$ medium with mannitol or $MS_{0.5xSUC}$ medium with different concentrations of ABA for 24 h. (A) ABA-dependent LUC-reporter responses to water deficit stress. The luciferase activities of *ahr11* (black) and *pATHB6::LUC* (white) were $1.7 \text{ CCD-RLU} \times 10^4$ and $2.7 \text{ CCD-RLU} \times 10^4$, respectively, under control condition ($MS_{0.5xSUC}$, without mannitol). (B) ABA-dependent LUC-reporter responses to exogenous ABA applied in solid $MS_{0.5xSUC}$ medium. The luciferase activities of *ahr11* (black) and *pATHB6::LUC* (white) were $0.8 \text{ CCD-RLU} \times 10^4$ and $0.3 \text{ CCD-RLU} \times 10^4$, respectively, under control condition ($MS_{0.5xSUC}$, without ABA). The ABA-dependent luciferase activity in terms of light emission was detected by a CCD camera (ORCAII ERG; Hamamatsu photonics, Hamamatsu City, Japan) and quantified using software Simple PCI 6.6.0.0 (Compix, Cranberry Township, PA). Exposure time was 10 min and imaging was done with 4×4 pixel binning. The data are means \pm SE ($n = 50$), and are subjected to one-way ANOVA via SPSS 16.0. ** $P < 0.01$; * $P < 0.05$. The luciferase activity of each line under control condition is taken as a reference and set to 1. Inserts show typical CCD images with intensity of light emission of seedlings at -0.8 MPa mannitol water potential (A) and $30 \mu\text{M}$ ABA (B) translated into a false-color spectrum.

In order to ensure uniform uptake of exogenous ABA, the liquid culture of *Arabidopsis* seedlings was employed in ABA response analysis. The luciferase activity in *ahr11* induced by $30 \mu\text{M}$ ABA was $216.4 \pm 10.1 \text{ CCD-RLU} \times 10^4$ which was 7 folds of the activity induced in *pATHB6::LUC* (Figure 3-2A). When seedlings were classified according to their luciferase activities using classes with a width of $50 \text{ CCD-RLU} \times 10^4$, most *pATHB6::LUC* seedlings were found in the class $50\text{-}100 \text{ CCD-RLU} \times 10^4$, whereas *ahr11* seedlings showed a broader distribution and were found in classes $100\text{-}500 \text{ CCD-RLU} \times 10^4$ up to $400\text{-}450 \text{ CCD-RLU} \times 10^4$ (Figure 3-2B). These results indicate that *ahr11* mutant is hypersensitive to water deficit as well as exogenous ABA, therefore, this novel *Arabidopsis* mutant is named *ahr11* (*ABA hypersensitive response11*).

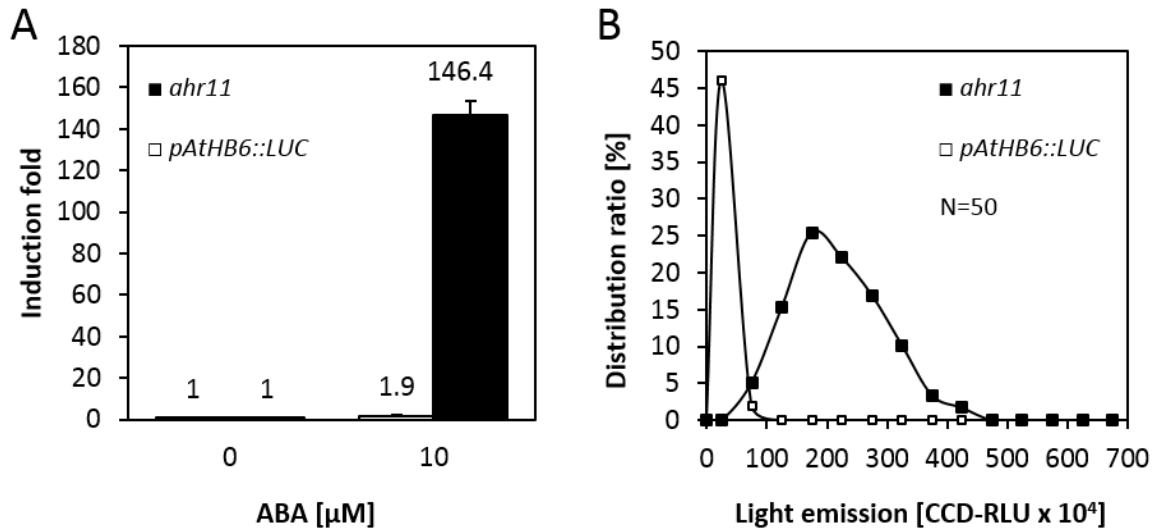


Figure 3-2: ABA-induced activation of the LUC-reporter in wild type *pATHB6::LUC* and mutant *ahr11* seedlings grown in liquid culture

Seedlings of mutant *ahr11* (black) and wild type *pATHB6::LUC* (white) were cultured in liquid 1/10 MS medium and then were exposed to 10 μM ABA for 24 h. The detection and calculation of luciferase activity of seedlings were performed as indicated in the Figure 3-1 legend. (A) ABA-induced LUC-reporter responses to exogenous ABA in liquid culture. The luciferase activities of *ahr11* (black) and *pATHB6::LUC* (white) under control condition (1/10 MS liquid medium, without ABA) were 1.5 CCD-RLU $\times 10^4$ and 12.7 CCD-RLU $\times 10^4$, respectively, and set to 1 ($n = 50$). The numbers above bars indicate the ABA induction fold. (B) Distribution plot of light emission under 10 μM ABA shown in (A). The width of each class is set to 50 CCD-RLU $\times 10^4$.

To avoid multi-mutation influences, *ahr11* was backcrossed to *pATHB6::LUC*. The ABA-dependent luciferase activity of backcrossed F₁ plants (*ahr11 BC1F1*; 1 x backcrossed) under water deficit (-0.6 MPa, mannitol) was then compared to the luciferase activity in *pATHB6::LUC* and in original *ahr11*. Although the *ahr11 BC1F1* seedlings displayed intermediate response to water deficit stress (Figure 3-3A), there was no significant difference between *ahr11 BC1F1* and *pATHB6::LUC* using statistical analysis ($P = 0.163 > 0.05$). Further distribution analysis of the water deficit-induced luciferase activity exhibited that 69.5% of the F₂ generation of *ahr11 BC3F2* (3 x backcrossed) had wild type-like response to water deficit (Figure 3-3B). These results indicate that a recessive mutation in a single nuclear gene leads to the altered (hypersensitive) response to water deficit stress in the *ahr11* mutant.

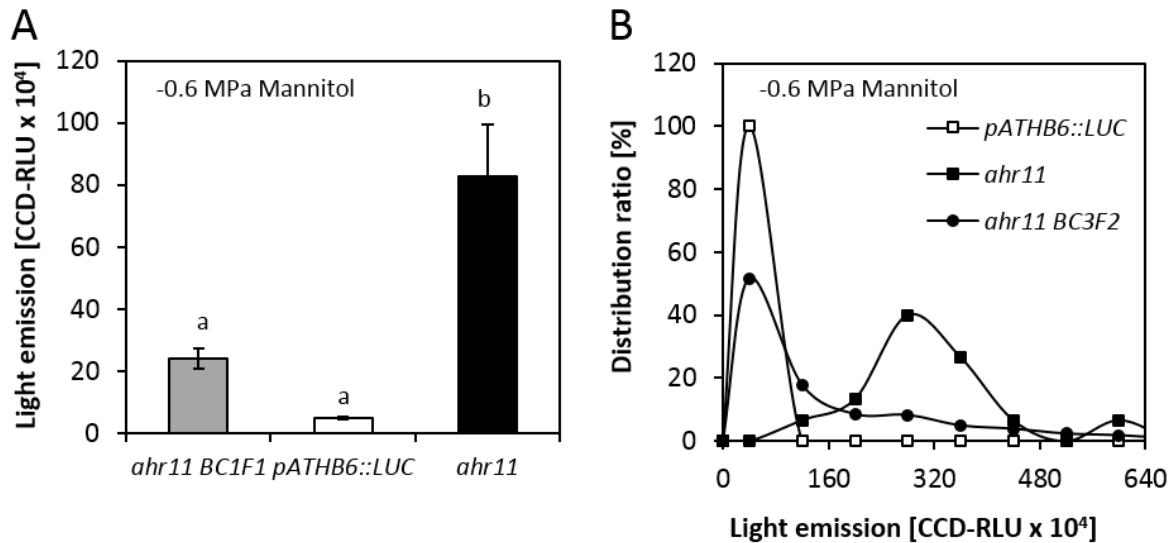


Figure 3-3: **Hypersensitivity of *ahr11* to water deficit stress is a recessive trait**

Original mutant *ahr11* was backcrossed to *pATHB6::LUC* to generate the F₁ generation *ahr11 BC1F1* (1 x backcrossed), which was subsequently amplified for next generation. Successive backcrossing of *ahr11* was performed several times. (A) 4-day-old seedlings of *ahr11 BC1F1* (1 x backcrossed; gray), *pATHB6::LUC* (white) and original *ahr11* (black) were exposed to water deficit stress (-0.6 MPa, mannitol) for 24h. The detection and calculation of luciferase activity of seedlings were performed as indicated in the Figure 3-1 legend. The data are means ± SE (n = 10) and subjected to one-way ANOVA via SPSS 16.0. The bars with similar letters are not significantly different (P > 0.05) according to Least-significant difference (LSD). (B) Light emission distribution of segregating F₂ progenies of *ahr11 BC3F2* (3 x backcrossed; black cycle, n = 387) subjected to water deficit stress (-0.6 MPa, mannitol). The width of each class is set to 80 CCD-RLUx10⁴.

3.2 Map-based cloning and next generation sequencing

Map-based cloning, also called mapping, is a widely used forward genetics approach to isolate genes in different organisms (Chi et al., 2008). The principle of mapping is to narrow down the genetic interval containing a causal mutation by sequentially excluding all other parts in the whole genome (Lukowitz et al., 2000). The major limitation of a mapping project is mapping resolution, which relies on the availability of high density genetic markers and the size of a mapping population. With the data collected in the Cereon Genomics database (Cambridge, MA), comprising most of the single nucleotide polymorphisms (SNPs) and small insertions/deletions (InDels) DNA polymorphisms between Col-0 and *Ler* accessions, the genetic markers required for fine mapping of the *ahr11* mutation are available. In this work, a Col-0 x *Ler* mapping combination was used to genotype the affected gene in ABA-hypersensitive mutant *ahr11*.

3.2.1 Generation of mapping population

A *Ler* x *ahr11* F₂ mapping population was generated by out-crossing *ahr11* (Col-0 background) to the accession Landsberg *erecta* (*Ler*). In F₂ generation, propagated from F₁ plants, luciferase activity was not only controlled by the casual mutation in *ahr11* mutant, but also by the segregation of

pATHB6::LUC ABA-reporter construct. Therefore, only 1/16 out of F₂ population was expected to be homozygous of *ahr11* and *pATHB6::LUC* ABA-reporter construct and selected for next generation. The uniformly intensive light of F₃ seedlings under water deficit stress was scored as the homozygous mutant phenotype in the relevant F₂ individual. As shown in Figure 3-4, homozygous F₃ lines 'F3/1-4-6' and 'F3/4-1-1' homogeneously responded hypersensitively to water deficit stress, whereas a heterozygous line 'F3/1-1-26' displayed a segregating phenotype. The construction of mapping population was the rate-limiting step of map-based cloning. For the first-pass mapping, 17 homozygous individuals were employed in the bulked segregant analysis (Michelmore et al., 1991). Subsequently, it took months to build a mapping population containing 893 homozygous individuals for fine-scale mapping.

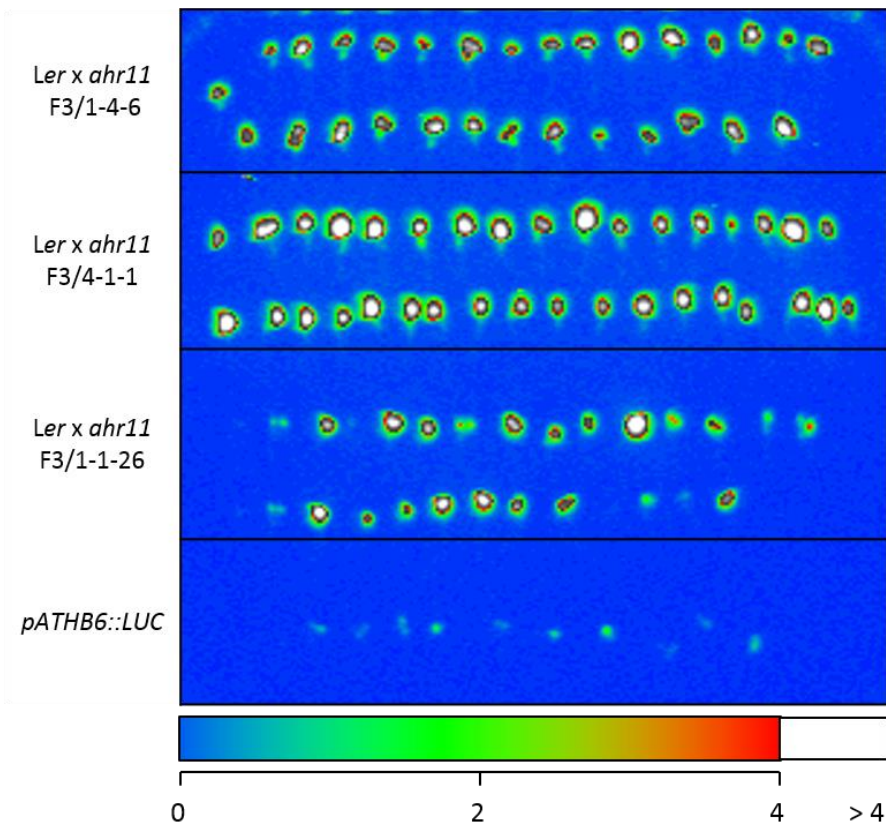


Figure 3-4: Phenotyping of *Ler x ahr11* F₃ progenies

Roots of 4-day-old seedlings of *Ler x ahr11* F₃ progenies were exposed to low water potential (-0.6 MPa, mannitol) for 24 h. The detection of luciferase activity of seedlings was performed as indicated in the Figure 3-1 legend. The false-color spectrums are shown to display the luciferase activity. The false-color scale for the relative light units (CCD-RLU × 10⁴) is provided. Lines *Ler x ahr11* F3/1-4-6 and F3/4-1-1 uniformly responded to water deficit stress in a hypersensitive manner, and are thus considered homozygous for the *ahr11* mutation, whereas an inconsistent response was found in the line F3/1-1-26 which is therefore classified as heterozygous for the *ahr11* mutation. *pATHB6::LUC* seedlings were used as a reference, showing a basic level of light emission under stressed condition. Totally 893 *Ler x ahr11* F₃ homozygous individuals were screened out for fine-scale mapping by this method.

3.2.2 First-pass mapping

Bulked segregant analysis (Michelmore et al., 1991) is an effective way to identify markers which are genetically linked to a certain mutation for reducing the number of PCR reactions necessary to establish linkage. A DNA pool constructed from 17 homozygous F₂ individuals was genotyped with 24 simple sequence length polymorphism (SSLP) markers, spaced evenly every 20 centiMorgan (cM) on the *Arabidopsis thaliana* genome (Figure 3-5A). The DNA pool was homozygous Col-0 genotype at the mutation and therefore mostly Col-0 in the vicinity of mutation, but essentially heterozygous for unlinked markers. As a result, the mutation phenotype of *ahr11* was tightly linked to two markers nga162 and ciw11 on the upper arm of chromosome III as well as two markers cer348 and nga151 on the upper arm of chromosome V (Figure 3-5B).

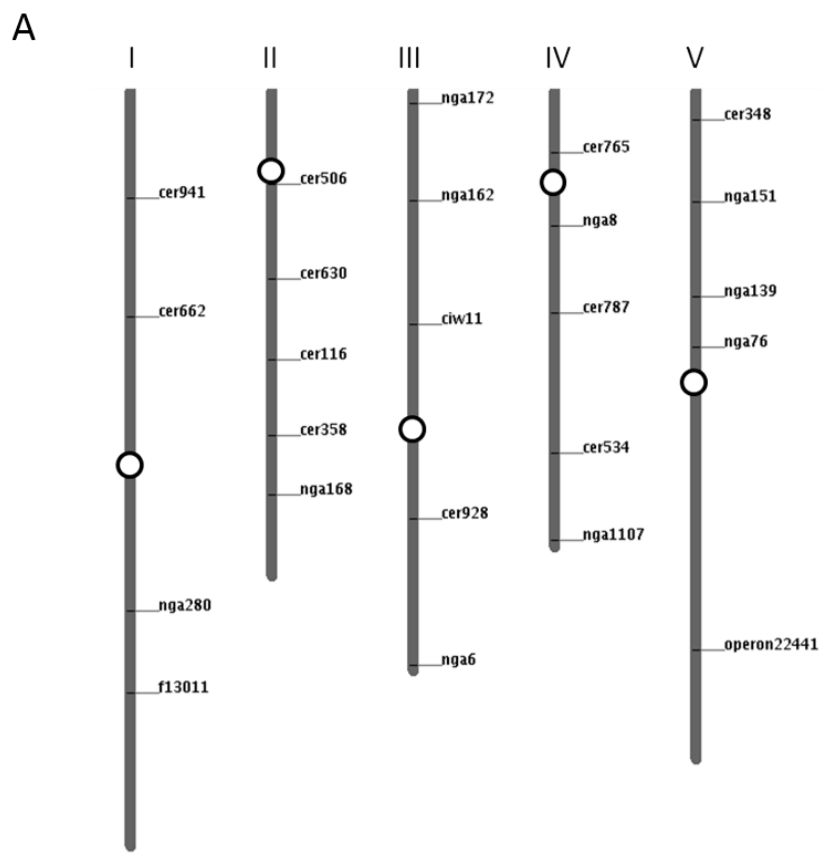


Figure 3-5A: **Schematic representation of first-pass mapping marker set**

The first-pass mapping marker set containing 24 SSLP markers was kindly provided by Dr. Farhah Assaad (TU München). The chromosomes are represented by gray bars with the length corresponding to the physical length. Position of centromeres is marked by open circles. The sequence information of markers is listed in Appendix 5.1.1.

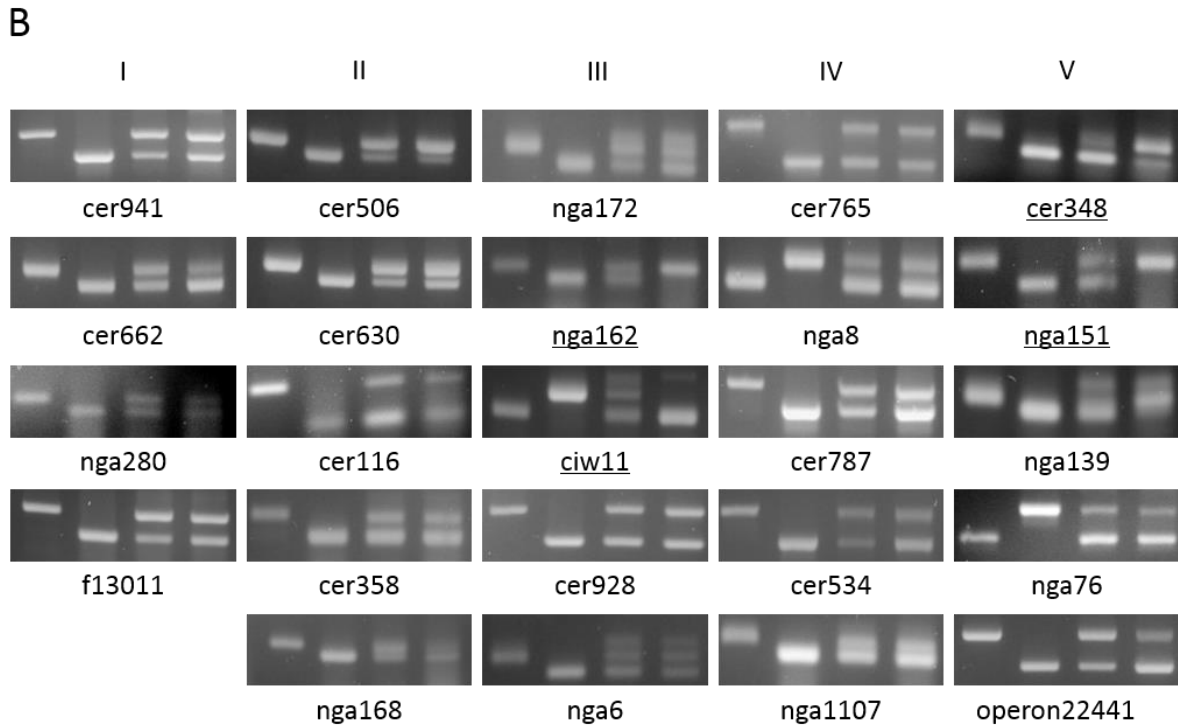


Figure 3-5B: **Bulked segregant analysis of *ahr11* mutant**

The PCR products of each marker were analyzed by agarose gel electrophoresis. The templates for PCR used in each panel are *Col-0*, *Ler*, heterozygous control and the DNA pool of *Ler* x *ahr11* F₂, respectively. The underline indicates the markers with a biased amplification of *Col-0* band which means that these marker loci are linked to the mutation phenotype of *ahr11* in contrast to other loci, where the amplified *Col-0* and *Ler* bands are of approximately the same intensity.

Subsequently, these 17 DNA samples in DNA pool were then examined individually for the respective genotype at the preselected marker loci (Figure 3-6). At the marker *nga151* locus on chromosome V, all 17 individuals were *Col-0* genotype, while at next marker locus, *cer348*, one recombination event happened. In another interesting interval located on chromosome III, there were separately 2 and 3 recombination events in 17 individuals at markers *nga162* and *ciw11* (this region will be discussed detailedly in discussion 4.1). Thus the results of first-pass mapping indicate that the causal mutation of *ahr11* is located on the upper arm of chromosome V and tightly linked to marker *nga151* (Figure 3-7A).

Results

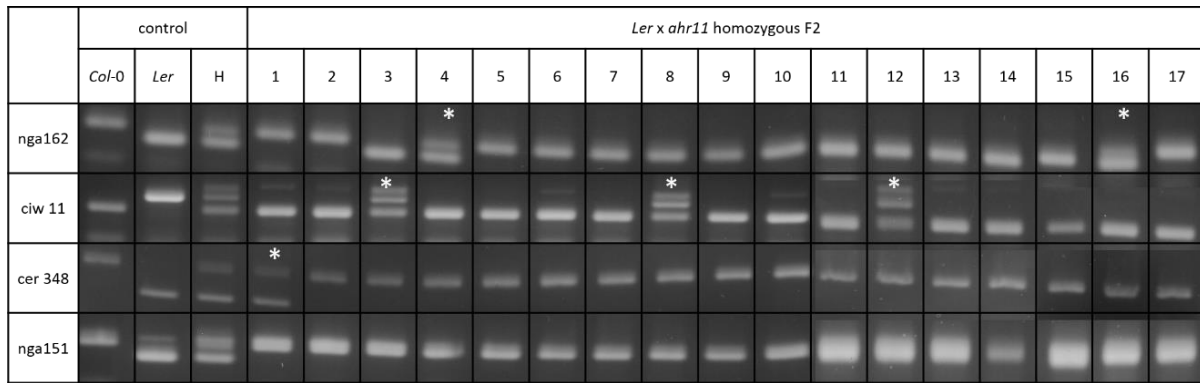


Figure 3-6: **Recombination events of 17 individuals in *Ler x ahr11* F₂ mapping population**

Agarose gel electrophoresis of PCR products of 17 individuals at four interesting markers (nga162, ciw11, cer348 and nga151) is shown. All recombination events are marked with white star. Primer sequences for the ciw11 marker used here are an optimized version of the primers used in the analysis depicted in Figure 3-5.

3.2.3 Fine-scale mapping

Through the first-pass mapping, the causal mutation in *ahr11* was tightly linked to marker nga151. Therefore, additional markers on chromosome V at both proximal and distal sides of nga151 were designed according to the database Cereon Arabidopsis Polymorphism Collection (Cambridge, MA). As shown in Figure 3-7B, at marker nga151, 9 recombination events were observed in 317 individuals. At proximal side, more distant from nga151, more recombination events were identified, and a total of 80 recombinants out of 317 individuals were discovered at the proximal flanking marker cer482 (6.1Mb). At distal side, the number of recombination events was gradually decreased to 0 at marker CA72 (4.24Mb), and then slowly increased to 12 at the distal flanking marker cer477 (3.2Mb). There was no straight forward explanation for this variation in recombination frequency on either side of the initially selected site, but in essence, the recombinants located the mutation distal end of nga151 and close to the marker CA72. Ultimately, all 893 individuals (including the initial 317 samples) were genotyped with additional 7 markers, including CA72, between cer477 and nga151 to narrow down the region of interest (Figure 3-7B), in which 29 recombination events were observed in 28 recombinants (Table 3-1) with the markers ChrV-4.3Mb and ChrV-4.5Mb being closest to the mutation (180 kb apart).

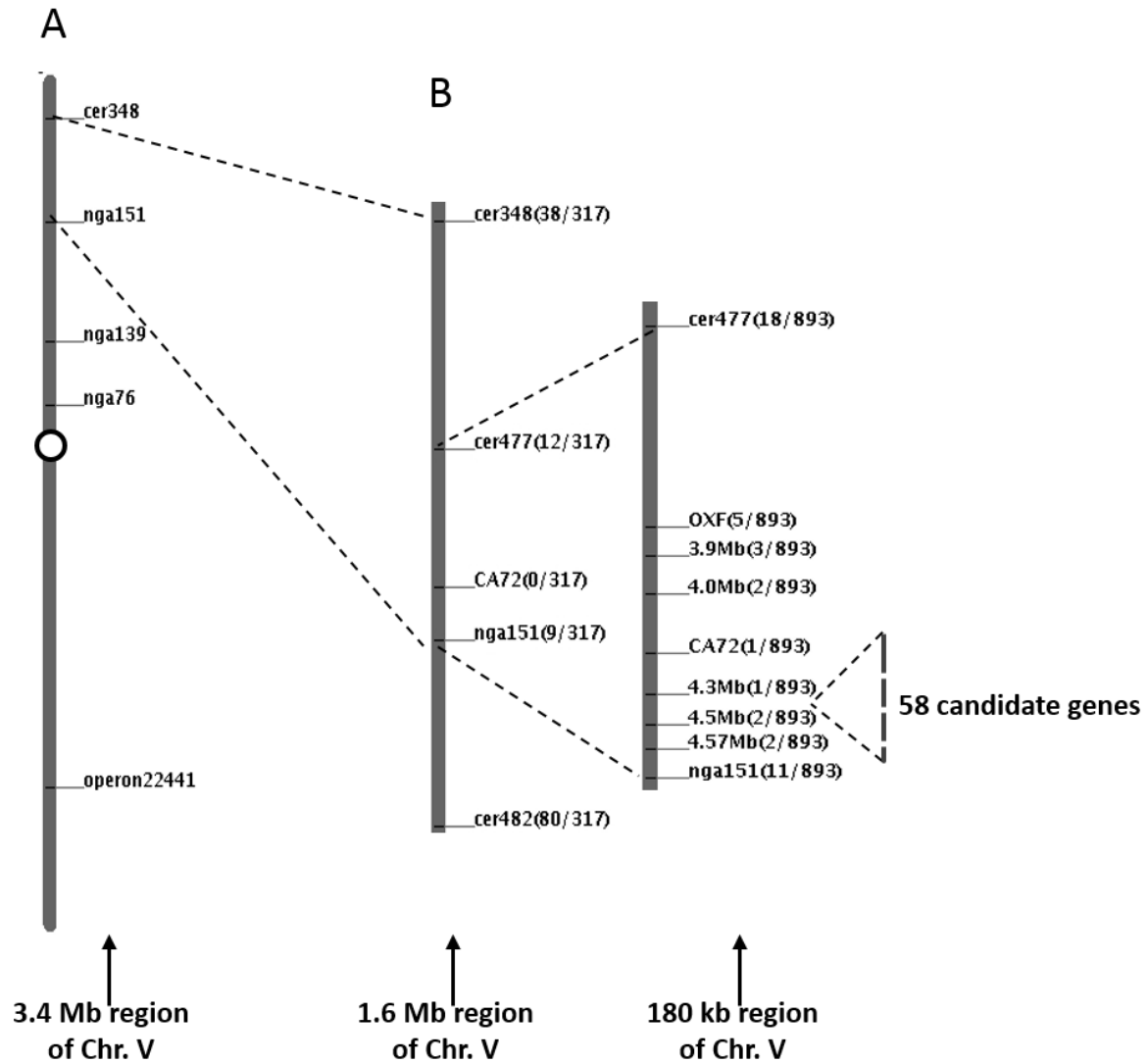


Figure 3-7: Map-based cloning of the *AHR11* gene in *ahr11*

(A) The first-pass mapping of *ahr11* mutation identified flanking markers cer348 and nga151 on chromosome V (3.4 Mb apart). (B) Fine-scale mapping of *ahr11* identified markers Chr. V-4.3Mb and Chr. V-4.5Mb as the closest flanking markers (180 kb apart) based on the available recombinants. The numbers in brackets behind each marker denote the number of recombinants followed by the total number of individuals genotyped. In the region of interest which was finally narrowed down to 180 kb, 58 candidate genes were identified according to the Col-0 genome sequence in TAIR10.

Table 3-1: Genotype of 28 recombinants

Recombinants	Markers on chromosome V									
	cer477	OXF	3.9 Mb	4.0 Mb	CA72	4.3 Mb	←→	4.5 Mb	4.57 Mb	nga151
1	C	C	C	C	C	C		C	C	H
2	C	C	C	C	C	C		C	C	H
3	C	C	C	C	C	C		C	C	H
4	C	C	C	C	C	C		C	C	H
5	C	C	C	C	C	C		C	C	H
6	C	C	C	C	C	C		C	C	H
7	C	C	C	C	C	C		C	C	H
8	C	C	C	C	C	C		C	C	H
9	C	C	C	C	C	C		H	H	H
10	C	C	C	C	C	C		H	H	H
11	H	C	C	C	C	C		C	C	H
12	H	C	C	C	C	C		C	C	C
13	H	C	C	C	C	C		C	C	C
14	H	C	C	C	C	C		C	C	C
15	H	C	C	C	C	C		C	C	C
16	H	C	C	C	C	C		C	C	C
17	H	C	C	C	C	C		C	C	C
18	H	C	C	C	C	C		C	C	C
19	H	C	C	C	C	C		C	C	C
20	H	C	C	C	C	C		C	C	C
21	H	C	C	C	C	C		C	C	C
22	H	C	C	C	C	C		C	C	C
23	H	C	C	C	C	C		C	C	C
24	H	H	H	H	H	H		C	C	C
25	H	H	H	H	C	C		C	C	C
26	H	H	H	C	C	C		C	C	C
27	H	H	C	C	C	C		C	C	C
28	H	H	C	C	C	C		C	C	C

Totally, 29 recombination events were observed in 28 recombinants. The 'C' with green background signifies no recombination (*Col-0* genotype), while the 'H' with yellow background denotes recombination events (heterozygous genotype). There are two recombination events in the 11th recombinant in this table. The red arrow separates the closest flanking markers Chr. V-4.3 Mb and Chr. V-4.5 Mb.

3.2.4 Pre-selection of candidate genes

Markers ChrV-4.3Mb and ChrV-4.5Mb are approximately 180 kb apart. In the *Col-0* genome sequence (TAIR 10), there are 58 genes in this region, of which two genes seemed interesting because they have been reported to be involved in ABA signaling. One candidate is *KEEP ON GOING* (*KEG*; At5g13530), encoding a RING E3 ligase, which has both ubiquitylation and phosphorylation activities and regulates degradation of the transcription factor ABI5 which is activated by ABA signaling (Stone et al., 2006, Liu and Stone, 2010). Three *Arabidopsis* T-DNA insertion mutants (*keg1*, *keg2*, *keg3*; *Col-0* background) exhibited characteristics of post germinative growth arrest and their root growth was extremely sensitive to exogenous ABA (Stone et al., 2006). In contrast, root growth of *ahr11* mutant showed a wild type response to exogenous ABA (described in section 3.4.6). Therefore, we speculated that the *AHR11* is not an allele of *KEG*.

Another candidate gene is *At5g13630* coding the H subunit of Mg-chelatase (CHLH), which is a multifunctional protein involved in chlorophyll synthesis, plastid-to-nucleus retrograde signaling

(Mochizuki et al., 2001) and which has been claimed to be a plastidic-localized ABA-binding protein (ABAR) (Shen et al., 2006, Wu et al., 2009). The ABA-affinity chromatography technique was used to demonstrate that CHLH specifically binds ABA *via* the C-terminus (Shen et al., 2006, Wu et al., 2009, Shang et al., 2010, Du et al., 2012). However, in another ABA binding assay, recombinant CHLH did not bind ABA but specifically affected the ABA-signaling pathway in guard cells (Tsuzuki et al., 2011, Tsuzuki et al., 2013). Meanwhile, the barley CHLH homolog could not function as an ABA receptor (Muller and Hansson, 2009). These contradictory results point out that the natural role of CHLH in ABA signaling is still too early to be concluded. Still, the gene was considered a candidate for the mutation in *ahr11*, and in this project a 6658 bp genomic sequence of *CHLH*, including coding sequence and promoter region, was amplified from *ahr11* by PCR, and then sequenced by single read sequencing. No mutation was detected in *ABAR/CHLH* gene in *ahr11*. Therefore, the mutation of *ahr11* is not in *ABAR/CHLH*.

Although two ABA signaling-related genes, *KEG* and *ABAR/CHLH*, were excluded, the number of candidates was still too large to identify the *AHR11* in reasonable time using a classical approach and therefore, the application of a next generation sequencing (NGS) technique was envisaged.

3.2.5 Next generation sequencing

Considering the automated Sanger sequencing method as a ‘first-generation’ technology, newer whole genome-scale sequencing methods are referred to as next-generation sequencing (NGS). Generation of an enormous volume of detailed genetic information is the major advance offered by NGS (Metzker, 2009). The NGS technology was thus employed to sequence the whole genome of the *ahr11* mutant to obtain information on the mutations located in the mapped region. This information was expected to allow rapid identification of the causal mutation in *ahr11*. The crude sequences obtained by NGS were aligned to the public reference genome from *Arabidopsis thaliana* Col-0 (TAIR10). In the *ahr11* mutant, 172,351,045 reads were obtained covering 99.34% of the reference *Col-0* genome at least 20-fold. The causal mutation of *ahr11* was refined in the 180 kb apart from 4.3 Mb to 4.5 Mb on chromosome V, but for reasons of safety, SNPs in a larger region from 4.0 Mb to 4.5 Mb were examined.

As shown in Figure 3-8 and Table 3-2, 8 exclusively homozygous SNPs were identified in interest region, all of which were C to T transitions: one SNP was in an intergene region between *At5g13170* and *At5g13180*; one SNP was in a promoter region of *At5g13917*; 2 SNPs were located near splicing sites of *At5g12960* and *At5g13130*; and another 4 SNPs were found in 4 gene coding sequences leading to 2 synonymous mutations including *At5g12940* and *At5g13260*, as well as to one amino acid residue exchange in *At5g13930* and one premature termination of *At5g13590*. In the fine-scale mapping process, a definite homozygous individual (the 24th recombinant in Table 3-1) had a recombination event at marker 4.3 Mb. So that 3 SNPs (the 6th, 7th and 8th SNPs in Table 3-2) were extracted as final candidates. For further identification, a new marker 4.48Mb was designed based on the 7th SNP at position 4.48 Mb on Chromosome V. Then 3 recombinants (the 9th, 10th and 24rd in Table 3-1) were analyzed for this marker, and one recombination event was detected in the 9th recombinant, thereby

excluding the 7th and 8th SNP as being causal for the *ahr11* mutation. Finally, the remaining SNP (the 6th in Table 3-2) was found in *At5g13590* encoding a protein with unknown function, where it changed the tryptophan²⁴⁸ to stop-codon, thus generating a truncated protein with 247 amino acid residues.

To sum these results up, based on the results of map-based cloning and NGS, an EMS-induced causal mutation was identified in mutant *ahr11*, which leads to premature termination of gene *At5g13590* with yet unknown function.

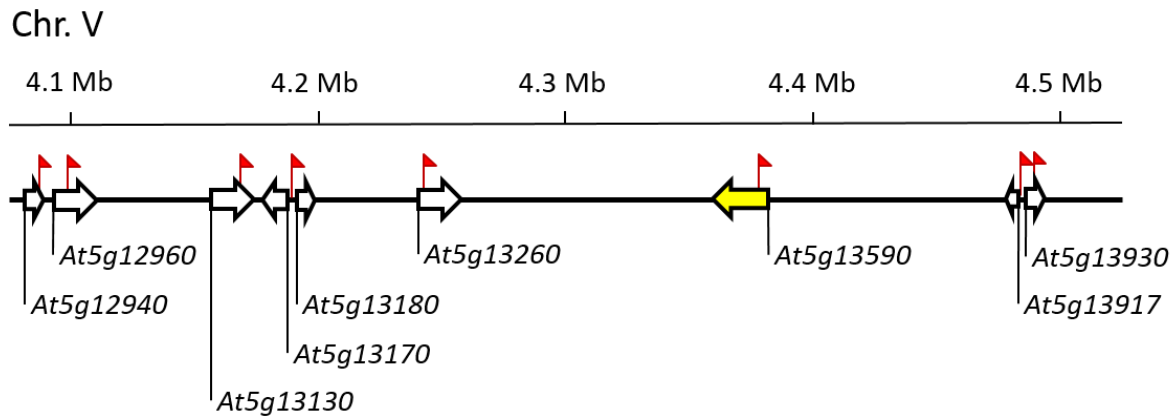


Figure 3-8: SNPs of *ahr11* detected by NGS in interest region on chromosome V

In the 500 kb interest apart (from 4.0 Mb to 4.5 Mb on Chr. V) defined as the region harboring the *ahr11* mutation by map-based cloning, totally 8 SNPs (red flags) were detected from the *ahr11* genome by NGS which was performed by Dr. Tim-Matthias Strom from Helmholtz Center Munich Human Genetic Institute. Arrows indicate the genes disturbed by these SNPs, and the yellow arrow points out the causal mutation candidate *At5g13590* in mutant *ahr11*.

Table3-2: Description of detected SNPs of *ahr11*

Nr.	Position ^a [bp]	Col-0 ^b	<i>ahr11</i> ^c	Description
1	Chr. V 4088510	C	T	<i>At5g12940.1</i> , + ^d , 729C->T, syn ^f , Thr243Thr.
2	Chr. V 4098321	C	T	SNP near splice Site at <i>At5g12960.1</i> , + ^e .
3	Chr. V 4169969	C	T	SNP near splice Site at <i>At5g13130.1</i> ,+.
4	Chr. V 4189735	C	T	interval between <i>At5g13170.1</i> and <i>At5g13180.1</i> .
5	Chr. V 4243556	C	T	<i>At5g13260.1</i> , +, 393C->T, syn, Ser131Ser.
6	Chr. V 4377825	C	T	<i>At5g13590.1</i> , -, 744C->T, non-syn ^g , Trp248Stop.
7	Chr. V 4485672	C	T	promoter of <i>At5g13917.1</i> .
8	Chr. V 4489125	C	T	<i>At5g13930.1</i> , TT4, +, 278C->T, non-syn, Ala93Val.

^a Position of SNP in *Arabidopsis* genome. ^b Reference genome *Arabidopsis thaliana* Col-0 (TAIR10). ^c SNP in *ahr11* genome. ^d Forward strand. ^e Revers strand. ^f Synonymous SNP. ^g Non-synonymous SNP.

3.3 Identification of *AHR11* gene

Arabidopsis gene *At5g13590*, as the candidate of *AHR11*, encodes a protein of 1168 amino acid residues, annotated as a protein with unknown function (<http://www.arabidopsis.org>). The genomic sequence is 3057 bp long and interrupted by 4 introns (79bp, 159bp, 101bp and 84bp long, respectively), and the 5'-UTR and the 3'-UTR sequences are interrupted by an intron, respectively (Figure 3-9). To confirm that the C-to-T transition detected in the second exon of gene *At5g13590* is the cause of *ahr11* phenotype, complementation experiments were performed employing the ectopic expression of wild type *AHR11* both transiently in *ahr11* protoplasts and stably in transgenic plants, as well as the analyses of two T-DNA knockout mutants, $\Delta 476$ (GK-476H03) and N804 (SAIL_88_D02).

AHR11 (*At5g13590*)

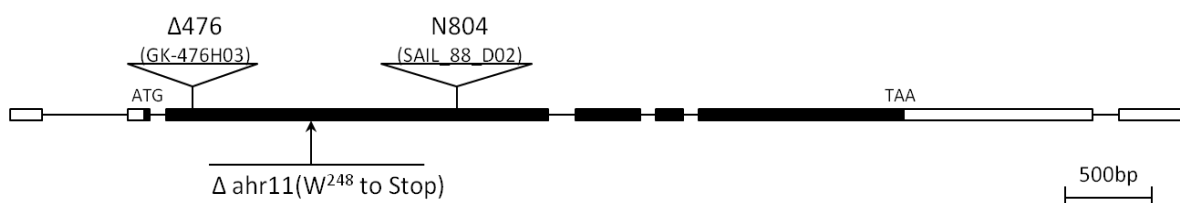


Figure 3-9: Schematic representation of *AHR11* and of changes in *ahr11* mutant alleles

AHR11 gene (*At5g13590*), which encodes a protein with 1168 amino acid residues, is located on reverse strand of chromosome V. White boxes, black boxes and lines represent UTRs, exons and introns, respectively. The EMS-induced mutation present in *ahr11* (W^{248} to Stop) is indicated by the arrow. T-DNA knockout mutants of *AHR11*, $\Delta 476$ (GK-476H03) and N804 (SAIL_88_D02), in which the T-DNA is inserted into the second exon, were obtained from ABRC (<https://abrc.osu.edu>). The scale bar stands for 500 bp.

3.3.1 Ectopic expression in *Arabidopsis thaliana* protoplasts

The protoplast transient gene expression system has become a customary cellular system for analyses of signal transduction (Sheen, 1998, Himmelbach et al., 1998, Yang et al., 2006, Fujii et al., 2009, Ma et al., 2009). The ABA-activated promoters of genes such as *Lti65/RD29B* (Nordin et al., 1993, Yamaguchi-Shinozaki and Shinozaki, 1994), and *RAB18* (Lang and Palva, 1992) are strongly induced by ABA in protoplasts. In this work, the ABA signaling cascade was analyzed by using the *Photinus pyralis* luciferase (LUC) reporter gene driven by the ABA-activated promoter of *RD29B* (*pRD29B::LUC*, #3041) (Christmann et al., 2005). Luciferase oxidizes luciferin to oxyluciferin and this process will release photons which can be sensitively measured by a luminometer. The *p35S::GUS* plasmid (#883) was used as an internal standard to normalize independent transfection of expression efficiency (Yang et al., 2006). Because of the *pATHB6::LUC* ABA-reporter in the *ahr11* genome, the activity of *pATHB6::LUC* construct was firstly pretested in protoplasts. The ABA-induced luciferase activity was not detected in the *ahr11* protoplasts without transfection of the ABA-reporter plasmid *pRD29B::LUC* (Figure 3-10). By contrast, the *ahr11* protoplasts with transfected *pRD29B::LUC* plasmids displayed the hypersensitivity to exogenous ABA by a factor of 63. Therefore, the ABA-induced luciferase activity in protoplasts is not conferred by the genomic *pATHB6::LUC* ABA-reporter, but specifically resulted from the transiently transfected ABA-reporter plasmids *pRD29B::LUC*.

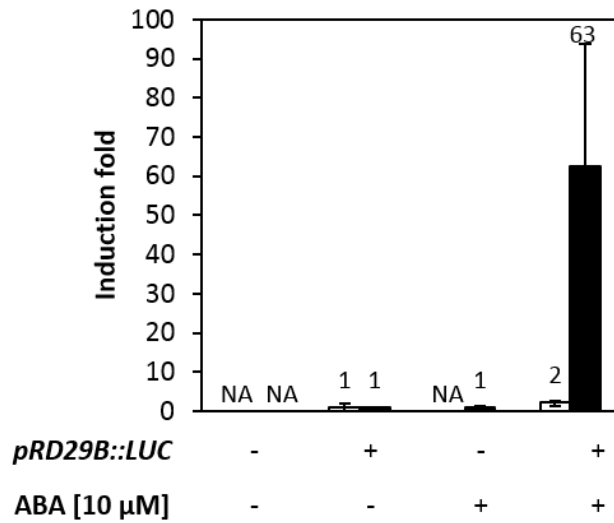


Figure 3-10: The ABA-induced luciferase activity measured in *ahr11* protoplasts specifically results from the ABA-reporter construct *pRD29B::LUC*

The protoplasts of *ahr11* (black) and Col-0 (white) transfected with *pRD29B::LUC* plasmid DNA (#3041; 4 μg) or with an empty vector control (#1337; 4 μg) were incubated in the WIMK incubation solution with or without 10 μM ABA for 16 h. The luciferase activity was detected using luminometer (Flash'n'Glow, BERTHOLD), and total luciferase activity was given as relative luminescence units (RLU) and allowed calculation of RLU/sec. The *p35S::GUS* plasmid DNA (#883; 2 μg) was co-transfected to assess transformation efficiency and to normalize the luciferase activity of single samples. The GUS activity was measured in a microplate reader (Synergy 2, BioTek) and calculated as relative fluorescence units (RFU)/sec. The normalized luciferase activity (LUC/GUS) in absence of ABA was taken as reference and set to 1 (*ahr11*: 4.5×10^4 RLU/RFU; Col-0: 5.8×10^4 RLU/RFU). Data are means \pm SE (n = 2). NA = no activity detected.

Subsequently, the protoplasts isolated from both *ahr11* and wild type Col-0 were transfected with appropriate sets of the ABA-reporter plasmid (*pRD29B::LUC*, #3041) and the internal standard plasmid (*p35S::GUS*, #883), and treated with 0, 0.1, 1, and 10 μM ABA, respectively. As a result, the ABA-dependent luciferase activity of *pRD29B::LUC* in *ahr11* protoplasts was about 3.3-fold up-regulated compared to wild type at 1 μM ABA and about 5.3-fold up-regulated at 10 μM ABA (Figure 3-11A). Then the negative regulator of ABA signaling, ABI2 (Merlot et al., 2001), was co-transfected into the transient expression system. The over-expression of ABI2 significantly inhibited the activation of ABA-dependent reporter genes by ABA in protoplasts of *ahr11* (14-fold) as well as in protoplasts of Col-0 (4-fold) (Figure 3-11B). These results indicate that *ahr11* is hypersensitive to exogenous ABA at the gene expression level, which confirms the previous results from luciferase activity imaging of *ahr11* seedlings (Figure 3-1B).

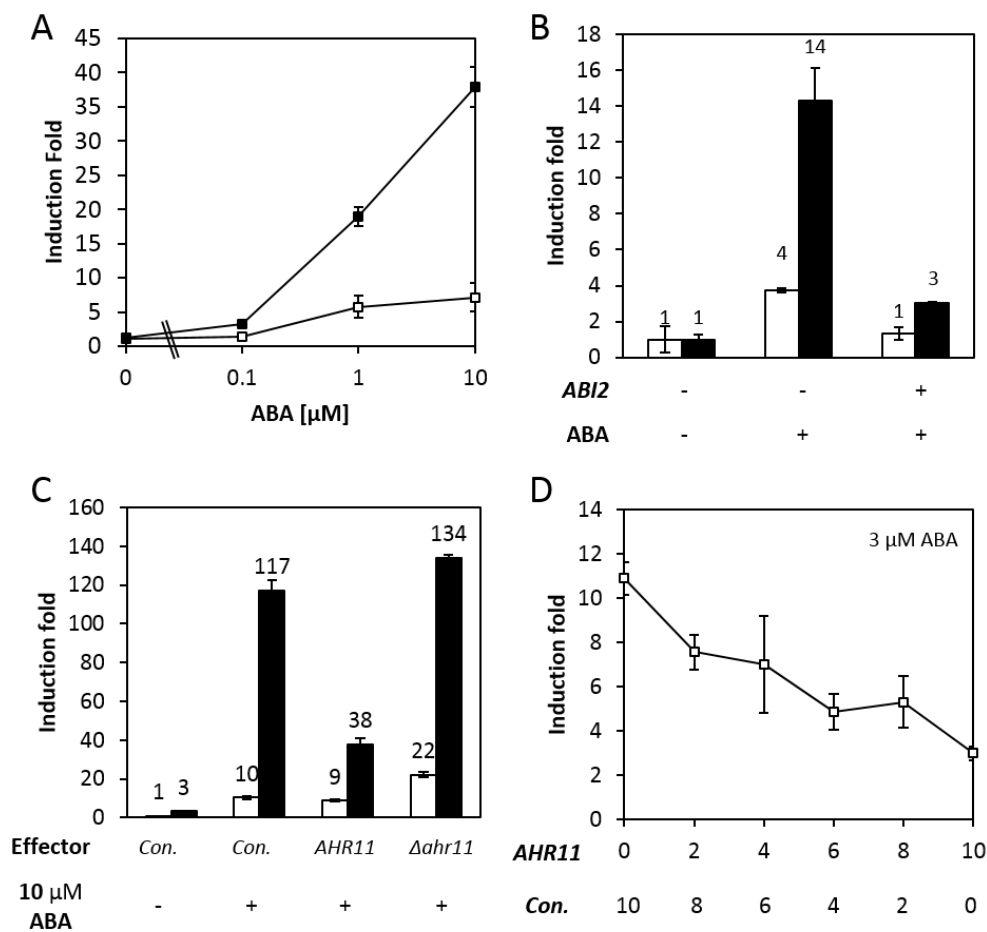


Figure 3-11: The *ahr11* mutant allele confers ABA-hypersensitivity to *Arabidopsis* protoplasts

(A) Induction of the *pRD29B::LUC* reporter by different concentrations of ABA in protoplasts. The *pRD29B::LUC* plasmid (#3041; 4 μ g) was co-transfected with *p35S::GUS* plasmid (#883; 2 μ g) into protoplasts of *ahr11* (black) and Col-0 (white) which were then incubated for 16 h in the presence of different concentrations of ABA. The normalized luciferase activities of *ahr11* and Col-0 protoplasts in absence of exogenous ABA was taken as a reference and set to 1 (*ahr11*: 1.26×10^4 RLU/RFU; Col-0: 1.00×10^4 RLU/RFU). (B) The effect of co-expression of ABI2 on the ABA-responsiveness of *ahr11* (black) and Col-0 (white) protoplasts. The effector plasmid DNA *p35S::ABI2* (#1110; 4 μ g) or control vector (Con., #1337; 4 μ g), were co-transfected with *pRD29B::LUC* (#3041) and *p35S::GUS* (#883) into protoplasts which were then incubated with or without 10 μ M ABA for 16 h. The normalized luciferase activities of *ahr11* and Col-0 protoplasts transfected with empty vector DNA in absence of ABA were 3.4×10^4 RLU/RFU and 1.2×10^4 RLU/RFU, respectively. (C) The effect of co-expression of wild type AHR11 and mutated protein Δ ahr11 on the ABA-responsiveness of *ahr11* (black) and Col-0 (white) protoplasts. As description in (B), the effector plasmids *p35SS1::AHR11* (#4463), *p35SS1:: Δ ahr11* (#4464) or control vector (#1337), were co-transfected. The normalized luciferase activities of Col-0 protoplasts transfected with empty vector DNA in absence of exogenous ABA was taken as a reference and set to 1 (1.75×10^4 RLU/RFU). (D) The dose-dependent inhibition of ABA response by wild type AHR11 in wild type Col-0 protoplasts. The indicated set of effector plasmids *p35SS1::AHR11* (#4463) and control vector (#1337) was co-transfected with *pRD29B::LUC* (#2041) and *p35S::GUS* (#883) into Col-0 (white) protoplasts, which were then incubated with 3 μ M ABA for 16 h. The normalized luciferase activity of Col-0 protoplasts transfected with empty vector DNA in absence of exogenous ABA was taken as a reference and set to 1 (0.6×10^4 RLU/RFU). Data are means \pm SE (n = 3). The experiments were repeated twice with similar results.

To complement the ABA-hypersensitivity of *ahr11* in protoplasts, the full-length coding sequence of *At5g13590* (*AHR11*), as well as the N-terminal truncated coding sequence (Δ *ahr11*) which encoded the same protein length present in the *ahr11* mutant, was cloned from the cDNA of Col-0 and inserted into the construct *pSK-35SS1*. The transient ectopic expression of the wild type *AHR11* efficaciously decreased the ABA-activated hyper luciferase activity in *ahr11* protoplasts by 67% at 10 μ M ABA while only a minor effect was seen in Col-0 (decrease by 13%) (Figure 3-11C). Additionally, in the presence of 3 μ M ABA, 10 μ g *p35SS1::AHR11* plasmid DNA repressed the luciferase activity by a factor of 3.6 (Figure 3-11D). Thus, the inhibition of ABA-induced luciferase activity by wild type *AHR11* displayed a dose-dependent manner in Col-0 protoplasts. By contrast, expression of the truncated protein Δ *ahr11* only marginally affected ABA-dependent luciferase activity in *ahr11* (increase by 14%), whereas the Δ *ahr11* increased the ABA-reporter response of Col-0 protoplasts to 10 μ M ABA by about 100% (Figure 3-11C).

These results illustrate that the protein *AHR11* encoded by the candidate gene *At5g13590* may complement the ABA-hypersensitivity of *ahr11* in protoplasts, and the wild type *AHR11* negatively regulates the ABA-induced gene expression.

3.3.2 Ectopic expression in plants

To further confirm the function of *AHR11* *in vivo*, transgenic plants were generated. Before the cloning of *AHR11*, an intermediate vector *pSK-35SS1::gAHR11-3UTR* was constructed by inserting a genomic fragment (*gAHR11-3'UTR*) into vector *pSK-35SS1*. Then a 6 kb genomic DNA fragment containing parts of *AHR11* was isolated by restriction digest of BAC clone *MSH12* (#4616) containing the *AHR11* gene (*Xma*I and *Bam*HI), and cloned into the intermediate vector *pSK-35SS1::gAHR11-3UTR* to form a new construct containing complete genomic fragment of *At5g13590* (about 8 kb; *pAHR11::AHR11*, #5345), which included 2 kb of the promoter region, 5'-UTR, coding region and 3'-UTR. Afterwards, this fragment was subcloned into the binary vector *pGreen II 1079-Ascl/NotI-hygro* (#5236; *pGII-hygro* for short; modified from binary vector *pGreenII1079*, <http://www.pgreen.ac.uk>), and the resulting *pGII-hygro-pAHR11::AHR11* construct (#5348) was introduced into *ahr11* and *pATHB6::LUC* lines *via* agrobacterium-mediated transformation. In parallel, the enhanced *GFP* (*eGFP*) gene was fused to the C-terminate of *AHR11* to generate the construct *pGII-hygro-pAHR11::AHR11-eGFP* (#5349) which was subsequently transformed into *ahr11* and *pATHB6::LUC* lines respectively.

T₁ transgenic plants were selected according to the hygromycin resistance marker and by subsequent PCR. Hygromycin-resistant T₂ plants with a segregation ratio of approximately 1:3 (death: survival) were selected as transgenic plants with single copy of insertional fragment and transferred into soil for further T₃ homozygous stable transformants screening (Table 3-3).

Table 3-3: The transgenic plants isolation and identification

Transgenic line	Recipient	T-DNA	Number of independent transformants		
			T ₁	T ₂	T ₃
<i>ahr11 pAHR11::AHR11</i>	<i>ahr11</i>	Wild type <i>AHR11</i> under control of its endogenous promoter <i>pAHR11</i>	17	9	6
<i>ahr11 pAHR11::AHR11-eGFP</i>	<i>ahr11</i>	Wild type <i>AHR11</i> fused with <i>eGFP</i> at C-terminal	13	5	4
<i>ahr11 emp</i>	<i>ahr11</i>	Empty vector of <i>pGII-hygro</i>	13	6	6
<i>WT pAHR11::AHR11</i>	<i>pATHB6::LUC</i>	Wild type <i>AHR11</i> under control of its endogenous promoter <i>pAHR11</i>	21	9	8
<i>WT pAHR11::AHR11-eGFP</i>	<i>pATHB6::LUC</i>	Wild type <i>AHR11</i> fused with <i>eGFP</i> at C-terminal	16	9	5
<i>WT emp</i>	<i>pATHB6::LUC</i>	Empty vector of <i>pGII-hygro</i>	35	9	4

The binary constructs *pGII-hygro-pAHR11::AHR11* (#5348), *pGII-hygro-pAHR11::AHR11-eGFP* (#5349) and *pGII-hygro* (#5347) were respectively introduced into *ahr11* and *pATHB6::LUC* lines via agrobacterium-mediated transformation. The first column indicates the name of transformants in this work. The second and the third columns point out the recipient plants and insertional DNA fragments of the transformation respectively. T₁ transformants have one copy of inserted T-DNA. T₂ plants were selected according to the Mendelian Law of segregation to generate homozygous T₃ progenies.

Three homozygous T₃ transgenic lines each representing an independent primary transformation event were selected for further analysis. The ABA-dependent *pATHB6::LUC* reporter response of these transgenic lines was then analyzed by *in vivo*-imaging and compared to the responses in transgenic control lines *WT emp* and *ahr11 emp*, which were transformed with the empty binary construct *pGII-hygro* (#5347) respectively. After 24 h exposed to water deficit stress (-0.6 MPa, mannitol) or 10 μM ABA, the intensity of light emission from *ahr11 emp* seedlings was more than 3 times of light emission from *WT emp* seedlings (Figure 3-12). The *ahr11* transgenic lines transformed with the wild type *AHR11* gene under control of its endogenous promoter *pAHR11* (*ahr11 pAHR11::AHR11*) showed light emission intensities similar to the ones observed from *WT emp* seedlings (Figure 3-12A, B and G). It indicates that the wild type *AHR11* complements the ABA-hypersensitive phenotype of *ahr11* mutant.

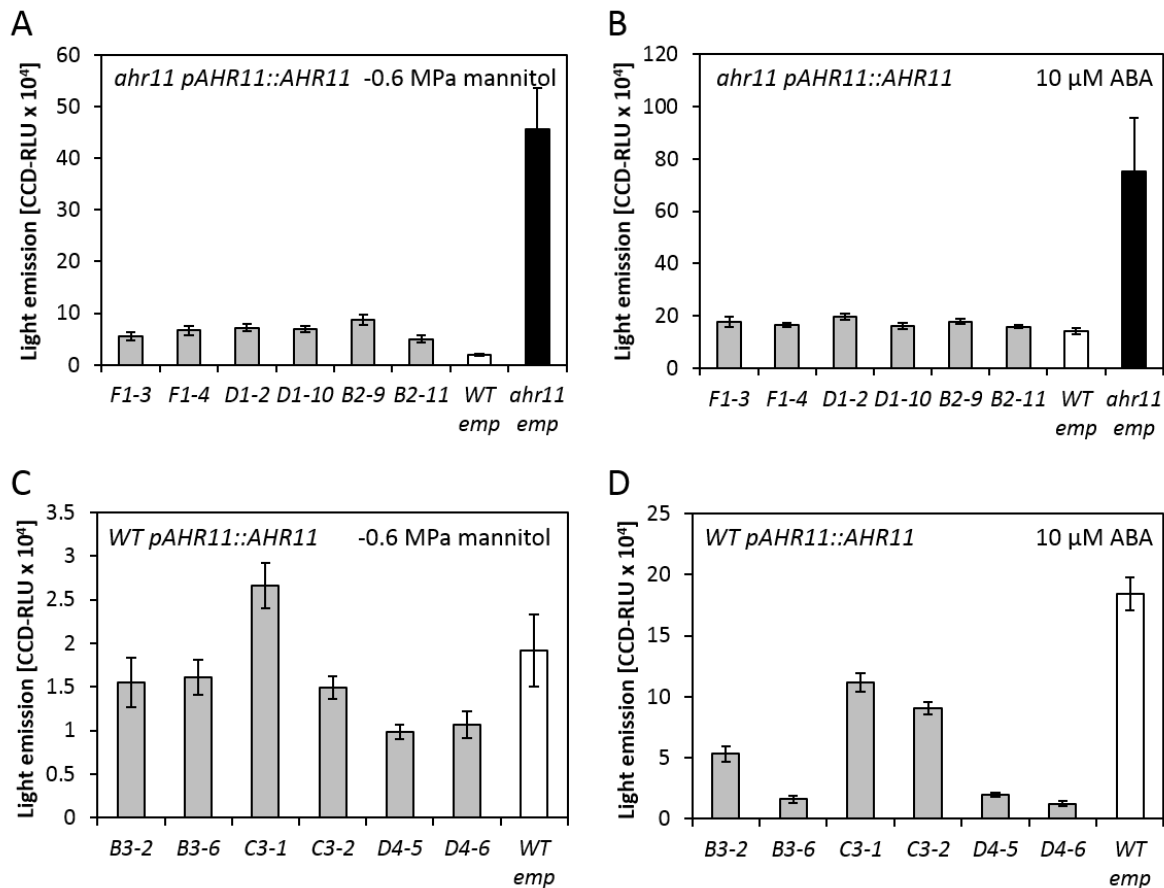


Figure 3-12: **ABA-dependent luciferase activity in response to water deficit stress and ABA of transgenic *ahr11* mutant and wild type *pAtHB6::LUC***

The stress treatments to seedlings, as well as the luciferase activity detection and calculation were performed as indicated in the Figure 3-1 legend. Values are means \pm SE (n = 20). (A) and (B) ABA-reporter responses to water deficit stress (-0.6 MPa, mannitol) and 10 μ M ABA of the independent *ahr11* transgenic lines (*ahr11 pAHR11::AHR11*: F1, D1, and B2) transformed with the wild type *AHR11* under control of its endogenous promoter *pAHR11*, and of the transgenic reference lines *WT emp* and *ahr11 emp*. (C) and (D) ABA-reporter responses to water deficit stress and ABA of the independent wild type transgenic lines (*WT pAHR11::AHR11*: B3, C3, and D4) transformed with the wild type *AHR11* under control of its own promoter *pAHR11*, and of the transgenic reference line *WT emp*.

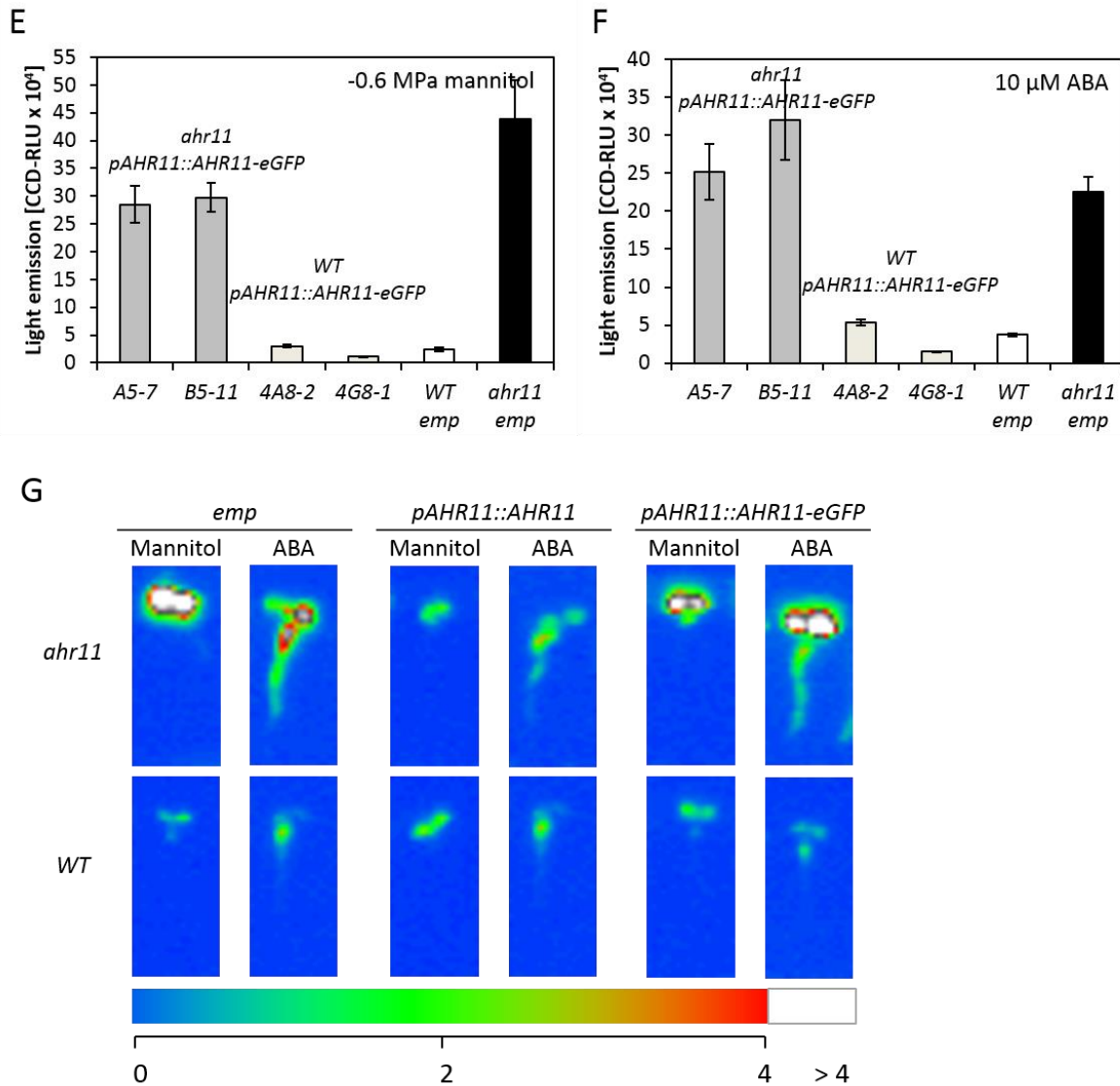


Figure 3-12: **ABA-dependent luciferase activity in response to water deficit stress and ABA of transgenic *ahr11* mutant and wild type *pAtHB6::LUC* (continued)**

(E) and (F) ABA-reporter responses to water deficit stress and ABA of the independent *ahr11* transgenic lines (*ahr11 pAHR11::AHR11-eGFP*: A5 and B5), of the wild type transgenic lines (*WT pAHR11::AHR11-eGFP*: 4A8 and 4G8) transformed with the wild type *AHR11* fused to eGFP under control of its endogenous promoter *pAHR11*, and of the reference lines *WT emp* and *ahr11 emp*. (G) False-color images of typical response from A-F. The color scale for the relative light units (CCD-RLUx10⁴) is provided.

In contrast, expressing a fusion protein between AHR11 and eGFP under control of its endogenous promoter (*pAHR11::AHR11-eGFP*) in *ahr11* did not complement the *ahr11* phenotype (Figure 3-12E, F and G). Moreover, expressing *pAHR11::AHR11* in *pAtHB6::LUC* (*WT pAHR11::AHR11*) reduced the ABA-dependent responses of the wild type reporter lines compatible with a function of AHR11 as a negative regulator in ABA signaling (Figure 3-12C, D and G). With the eGFP fused C-terminally to AHR11, this effect was lost in *WT pAHR11::AHR11-eGFP* transgenic plants (Figure 3-12D, E and G).

The most striking morphological property of mutant *ahr11* is that *ahr11* has shorter diameter of leaf rosette than *pATHB6::LUC* (described in detail in section 3.4.7). When plants were grown in long-day condition for 3 weeks, the transgenic reference lines *ahr11 emp* and *WT emp* displayed the similar morphological phenotypes as their original recipients respectively (Figure 3-13A-B and E-F). These indicate that the transformation of binary construct *pGII-hygro* has no influence on plant morphology. Compared to the original mutant *ahr11* and transgenic reference line *ahr11 emp*, the transgenic *ahr11* plants harboring wild type AHR11 gene under control of its endogenous promoter (*ahr11 pAHR11::AHR11*) significantly enlarged their size of leaf rosettes and were similar to wild type *pATHB6::LUC* and *WT emp* reference line (Figure 3-13C). The eGFP fused AHR11 is not effective in both *ahr11* and WT (Figure 3-13 D and H).

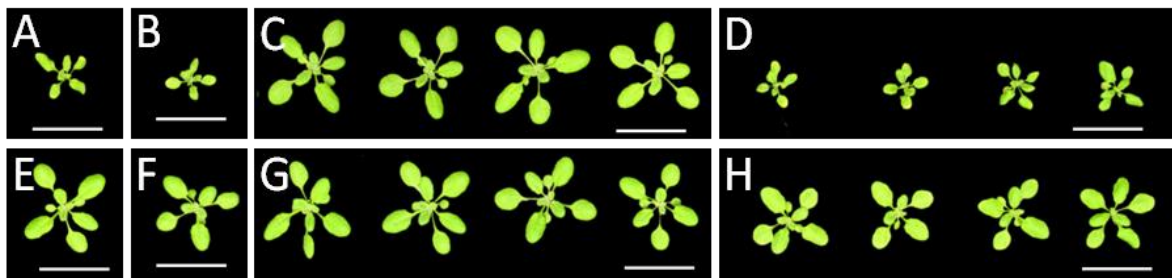


Figure 3-13: Morphological phenotype of transgenic *ahr11* mutant and wild type *pAtHB6::LUC*

The 21-day-old plants were grown in long-day conditions (16 h light/8 h dark) side by side. The photographs were taken with a digital camera (Canon G10, Canon, Japan) controlled by a software (Canon Utilities Remote Capture DC ver. 3.1.0.5). The Scale bar = 20 mm. (A) Original mutant *ahr11*. (B) Transgenic reference *ahr11 emp*. (C) Independent transformants of *ahr11 pAHR11::AHR11*. (D) Independent transformants of *ahr11 pAHR11::AHR11-eGFP*. (E) Wild type (*pATHB6::LUC*). (F) Transgenic reference *WT emp*. (G) Independent transformants of *WT pAHR11::AHR11*. (H) Independent transformants of *WT pAHR11::AHR11-eGFP*.

3.3.3 T-DNA knockout mutants of candidate gene

Two of homozygous T-DNA knockout lines of *AHR11*, $\Delta 476$ (GK-476H03) and N804 (SAIL_88_D02), were selected and analysis for homozygous gene knockout by using appropriate primer combinations (Figure 3-14A-C). As shown in Figure 3-14B and C, $\Delta 476\#1$ and $\#2$, as well as N804 $\#3$, represent homozygous T-DNA insertion for the respective T-DNA mutants. The homozygous T-DNA knockout mutants $\Delta 476$ and N804 were crossed to *pATHB6::LUC* ABA-reporter line to introduce the ABA-reporter construct into T-DNA knockout mutants. The T-DNA knockout lines homozygous for both the respective T-DNA insertion and the ABA-reporter construct were selected for further analysis. Both RT-PCR (Figure 3-14D) and quantitative Real-Time PCR (Figure 3-14E) analyses of *AHR11* expression in two T-DNA knockout mutants, *ahr11* mutant and wild type *pATHB6::LUC* indicate that the insertional T-DNAs successfully knockdown the expression of *AHR11*.

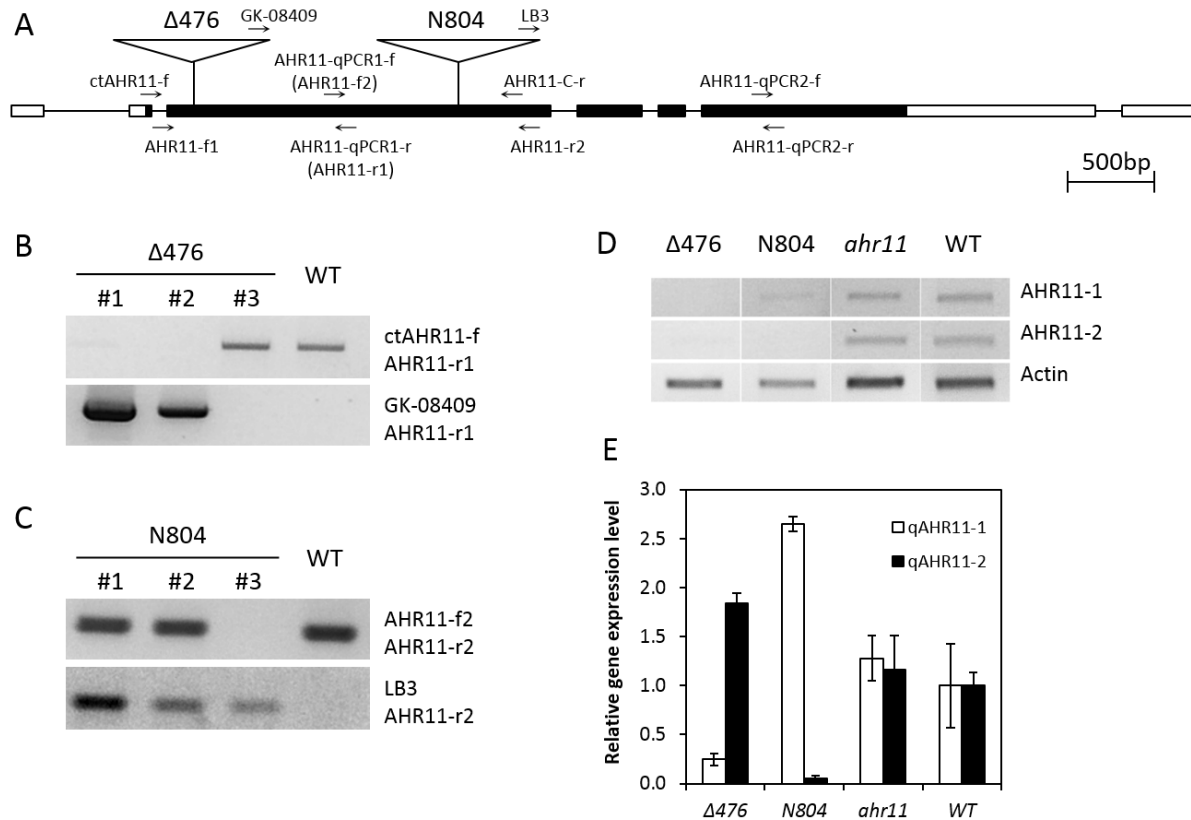


Figure 3-14: Selection and characterization of *AHR11* homozygous T-DNA knockout mutants

(A) Schematic representation of the *AHR11* T-DNA knockout mutants. Positions of the primers used for genetic characterization of T-DNA knockout mutants are indicated. Scale bar = 500 bp. (B) Genetic characterization of T-DNA knockout mutant $\Delta 476$ (GK-476H03). Typical fragment pattern obtained from PCR analysis using primer combinations of ctAHR11-f (#1923), AHR11-r1 (#1924) and GK-08409 (#225). (C) Genetic characterization of T-DNA knockout mutant N804 (SAIL_88_D02). Typical fragment pattern was obtained from PCR analysis using primer combinations of AHR11-f2 (#1925), AHR11-r2 (#1926) and LB3 (#289). (D) The expression level of *AHR11* analyzed using RT-PCR in T-DNA knockout mutants $\Delta 476$ and N804. Total RNA was isolated from shoots of 4-day-old seedlings. The RT-PCR reaction AHR11-1 was performed using primer combination of AHR11-f1 (#1922) and AHR11-r1 (#1924) to analysis the *AHR11* expression in $\Delta 476$, and the RT-PCR reaction AHR11-2 was accomplished using primer combination of AHR11-f2 (#1925) and AHR11-C-r (#1946) to analyze the *AHR11* expression in N804. *Actin* (*At2g37620*) was amplified using primers Actin-f (#108) and Actin-r (#109) as a reference shown at the bottom. (E) The relative expression level of *AHR11* analyzed using Real-Time PCR in T-DNA knockout mutants $\Delta 476$ and N804. Real-time PCR qAHR11-1 was performed using primer combination of AHR11-qPCR1-f (AHR11-f2) and AHR11-qPCR1-r (AHR11-r1), and Real-time PCR qAHR11-2 was performed using primer combination of AHR11-qPCR2-f and AHR11-qPCR2-r. The expression of housekeeping gene *UBC9* (*At4g27960*) was used as a reference. The relative expression level of *AHR11* in WT samples was set to 1. Two biological replicates and three technique replicates were used for each line.

Homozygous T-DNA knockout mutants $\Delta 476$ and N804 harboring *pATHB6::LUC* ABA-reporter construct were exposed to exogenously applied ABA (10 μ M) and to water deficit stress (-0.6 MPa, mannitol), respectively. The seedlings were classified according to their ABA-induced light emission intensity. More than 95% of seedlings of two T-DNA knockout mutants $\Delta 476$ and N804 showed much stronger response to exogenous ABA compared to the *pATHB6::LUC* reporter line and were similar to

ahr11 mutant (Figure 3-15A). However, the water-deficit-stress-induced ABA-reporter response was less pronounced in $\Delta 476$. Exposing to -0.6 MPa mannitol water potential, 42.2% of $\Delta 476$ seedlings and 22.5% of N804 seedlings displayed weak ABA-dependent light emission and were in the range of 0-30 CCD-RLUx10⁴ where all *pATHB6::LUC* seedlings and 8.5% of *ahr11* seedlings were located (Figure 3-15B). These findings demonstrate that the disruption of *At5g13590* leads to hypersensitive *pATHB6::LUC* ABA-reporter response as seen in *ahr11*.

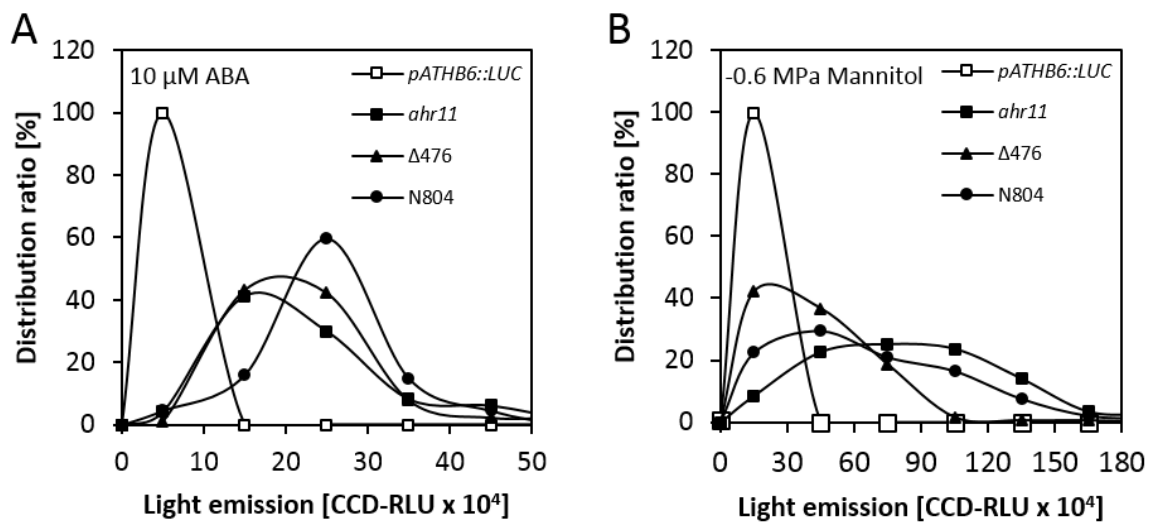


Figure 3-15: **The ABA-induced and water-deficit-induced activation of the ABA-reporter in AHR11 T-DNA knockout mutants harboring the *pATHB6::LUC* ABA-reporter construct**

4-day-old seedlings of *ahr11* (black square), $\Delta 476$ (black triangle), N804 (black round) and *pATHB6::LUC* (white square) were exposed to 10 μ M ABA or to water deficit stress (-0.6 MPa, mannitol) for 24 h. The detection and calculation of ABA-dependent luciferase activity of seedlings were performed as indicated in the Figure 3-1 legend. (A) The distribution of light emission of seedlings treated by ABA. Class interval = 10 CCD-RLUx10⁴; n = 100. (B) The distribution of ABA-dependent light emission of seedlings under water deficit stress. Class interval = 30 CCD-RLUx10⁴; n = 200.

Subsequently, the ABA reporter construct *pRD29B::LUC* (#3041) was transiently expressed in the protoplasts of $\Delta 476$ and N804. After incubation with exogenous ABA, the ABA reporter in T-DNA knockout mutant protoplasts showed hypersensitive induction as in *ahr11* (Figure 3-16). The co-expression of the wild type AHR11 successfully suppressed the ABA reporter induction, whereas the mutated protein Δ ahr11 had almost no effect (Figure 3-16). Accordingly, induction of ABA-dependent gene expression in the *At5g13590* T-DNA knockout mutants is hypersensitive to exogenous ABA and AHR11 is negative regulator of ABA-induced gene expression.

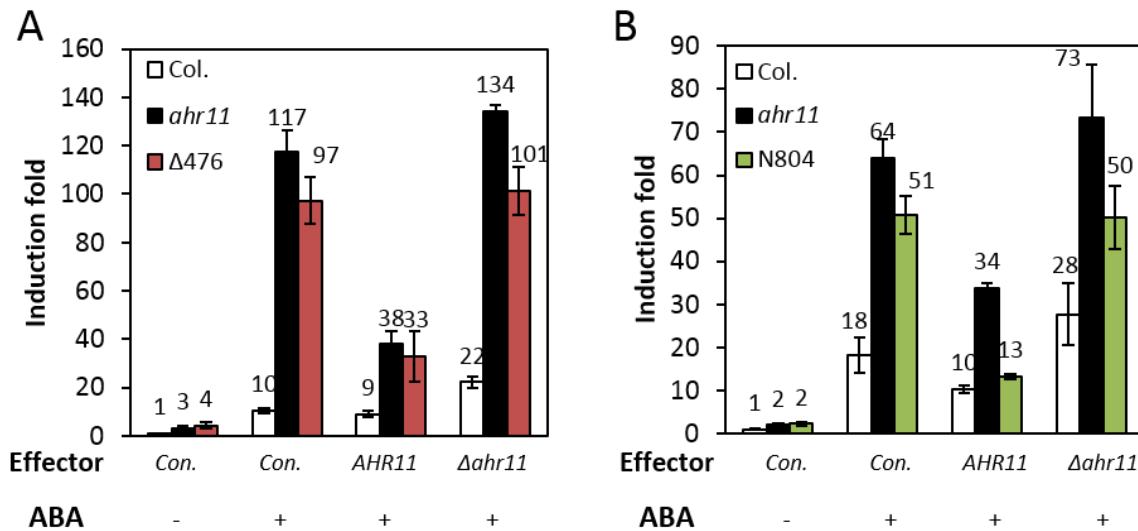


Figure 3-16: Protoplasts of *AHR11* T-DNA knockout mutants show ABA-hypersensitivity which is complemented by the wild type allele

4 μ g of *p35S51::AHR11* (#4463), *p35S51::Δahr11* (#4464) or control vector (Con., #1337), were co-transfected with 4 μ g of *pRD29B::LUC* (#3041) and 2 μ g of *p35S::GUS* (#883) into protoplasts which were then incubated with or without 10 μ M ABA for 16 h. (A) The effect of co-expression of wild type protein (*AHR11*) and mutated protein (Δ *ahr11*) on induction of the *pRD29B::LUC* reporter by 10 μ M ABA in protoplasts of Col-0 (white), *ahr11* (black) and $\Delta 476$ (red) with the normalized reporter response (LUC/GUS) of Col-0 in absence of exogenous ABA taken as a reference (1.75×10^4 RLU/RFU). (B) The effect of co-expression of wild type protein *AHR11* and mutated protein Δ *ahr11* on induction of the *pRD29B::LUC* reporter by 10 μ M ABA in protoplasts of Col-0 (white), *ahr11* (black), and N804 (green) with the normalized reporter response (LUC/GUS) of Col-0 in absence of exogenous ABA taken as a reference (1.3×10^4 RLU/RFU). Values which are indicated above the columns are means \pm SE (n = 3). The experiments were repeated three times to generate similar results.

3.4 Physiological analyses of *ahr11*

The stress phytohormone ABA plays a pivotal role in regulating plant responses to the abiotic stresses including drought, high osmolarity and low temperature but also regulates plant growth and development in the absence of stress (Himmelbach et al., 2003, Christmann et al., 2006, Raghavendra et al., 2010, Finkelstein, 2013). The *ahr11* has been identified as a mutant that shows a hypersensitive ABA reporter response when exposed to water deficit stress in this work. However, this does not necessarily mean that all ABA-regulated physiological processes are affected in this mutant. Therefore, the ABA sensitivity and water deficit resistance in *ahr11* of different physiological processes such as stomatal closure, dormancy, germination, post-germination development, root growth, and flowering was tested and compared to *pAtHB6::LUC*.

3.4.1 Transpiration and leaf temperature under well-watered condition

The stomata aperture determines the transpiration rate from the leaf surface. Since transpiration has a cooling effect, leaf temperature provides a robust indicator of transpiration and reflects phenotypes with altered stomatal behavior (Merlot et al., 2002). Therefore, the transpiration and leaf

temperature of *ahr11* were respectively detected using a gas exchange measuring system (GFS-3000, Heinz Walz) and a thermographic system (VarioCAM high resolution head, InfraTec). Under long-day and well-watered conditions (VWC = 80%), *ahr11* kept a high transpiration rate during day and night (Figure 3-17). Correspondingly, the thermal imaging of *ahr11* and *pATHB6::LUC* displayed a constitutively cool leaf phenotype of *ahr11* plants with leaf temperature being significantly 1°C lower than leaf temperature of *pAtHB6::LUC* (Figure 3-18).

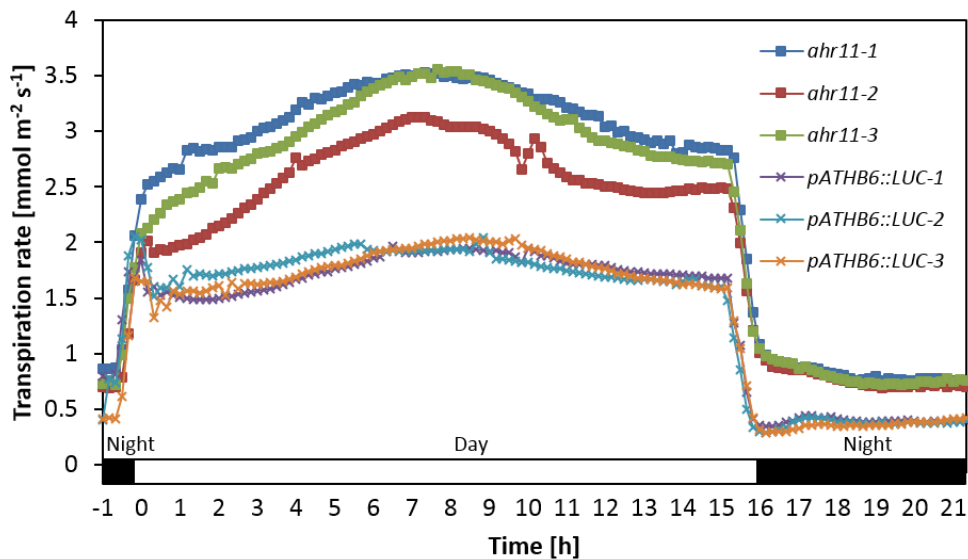


Figure 3-17: **Enhanced transpiration rate of *ahr11* under well-watered conditions**

Arabidopsis plants of *ahr11* (square) and *pATHB6::LUC* (cross) were grown under long-day conditions. The volumetric water content (VWC) of each pot was maintained to 80% by adding additional water every day. The entire aerial portion of 3- to 4-week-old plant was sealed off into a custom designed gas exchange cuvette (ring-chamber, Heinz Walz, Germany). And the long-term transpiration was measured continuously for 24 h using a gas exchange fluorescence system (GFS-3000, Heiz Walz). The plant growth, as well as transpiration measurements, was performed in well-watered and long-day conditions, with cuvette parameters H₂O: 12000 ppm, CO₂: 380 ppm, PPFD: 190 $\mu\text{mol m}^{-2}\text{s}^{-1}$, T: 28.5°C (light) and 22°C (night).

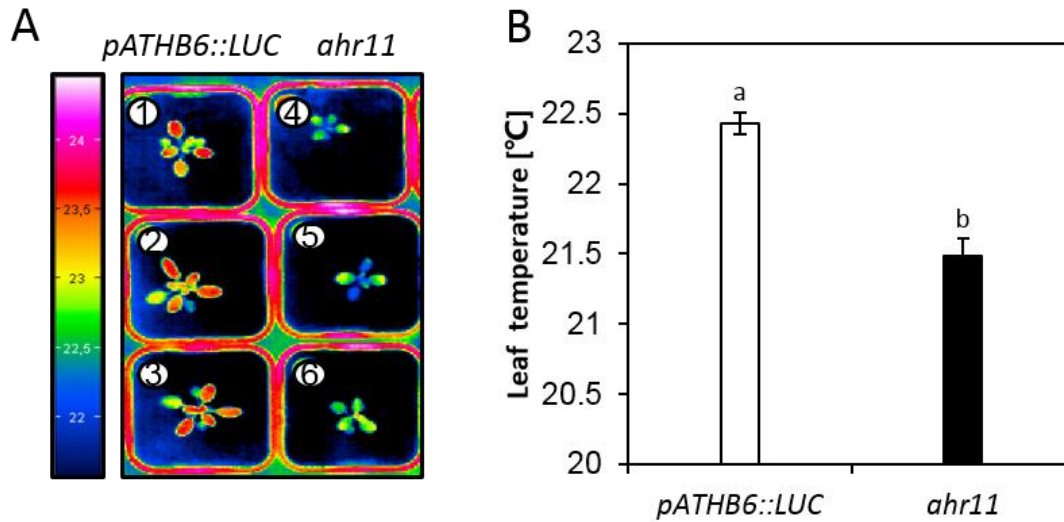


Figure 3-18: **Comparison of leaf temperature of *ahr11* and *pAtHB6::LUC* under well-watered conditions**

Three-week-old *Arabidopsis* plants were grown under the same well-watered and long-day conditions indicated in Figure 3-17 legend. The thermal images were captured using a thermographic system (VarioCAM high resolution head, InfraTec). (A) False-color thermal image of *ahr11* and *pAtHB6::LUC* plants. (B) Quantitative analysis of leaf surface temperature. Data are means \pm SE ($n = 6$). For each plant, ≥ 10 measuring points of leaf surface were used. The data were subjected to one-way ANOVA via SPSS 16.0. The bars with similar letters are not significantly different ($P > 0.05$).

3.4.2 Water loss of detached shoots

To evaluate the low water potential response, water loss of detached shoots or leaves is the easiest experiment (Himmelbach et al., 2002). Subsequently, the whole leaf rosette of *ahr11* was separated from the root and the decline in fresh weight over time was measured. In such experiments, the detached shoots of *ahr11* lost more water than *pAtHB6::LUC* (Figure 3-19). And after a period of 2 h, their fresh weight had declined by 31% while *pAtHB6::LUC* shoots had lost 23% of the initial fresh weight.

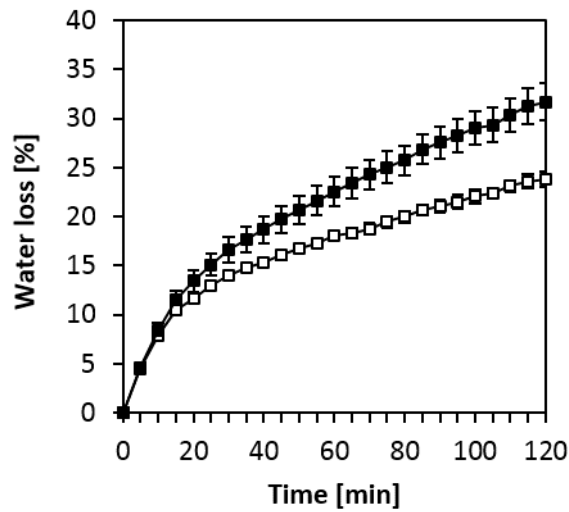


Figure 3-19: Enhanced water loss of detached *ahr11* shoots

The entire rosettes of 3- to 4-week-old plants from *ahr11* (black) and *pATHB6::LUC* (white) were separated from the root and the decline of the fresh weight over time was measured at ambient conditions. Data are mean values \pm SE ($n = 3$).

3.4.3 Stomatal closure and ABA

Balancing CO₂ uptake, which is enhanced by light to boost photosynthesis, and water loss by transpiration is the central function of stomata. Stomatal closure is the earliest water deficit stress response to preserve tissue water potential (Schroeder et al., 2001, Roelfsema and Hedrich, 2005, Verslues et al., 2006, Verslues and Juenger, 2011). On a cellular level, redistribution and enhanced biosynthesis of ABA increases Ca²⁺ concentration in guard cells, inhibits inward-rectifying K⁺ channels and activates both S-type and R-type anion channels (MacRobbie, 1998, Schroeder et al., 2001, Kim et al., 2010b, Wang et al., 2011, Joshi-Saha et al., 2011b). Activation of anion channels depolarizes the guard cell plasma membrane which induces a massive loss of cellular K⁺ *via* outwardly-rectifying K⁺ channels followed by a movement of water out of the cell. The concomitant turgor decline then results in stomatal closure. In this work, the stomatal closure triggered by water deficit or ABA was analyzed by using two methods such as root-inflicted treatment and detached-rosette-leaf-fed treatment.

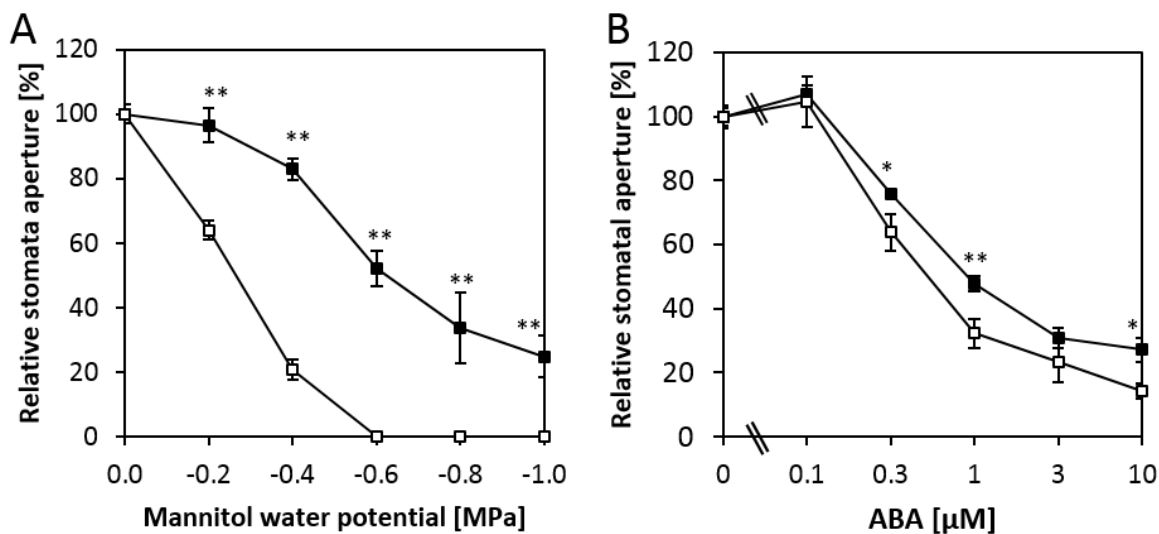


Figure 3-20: The stomatal response of *ahr11* to root-inflicted water deficit and ABA

The 5-day-old seedlings were exposed to MS_{0.5xSuc} medium supplemented with mannitol to adjust medium water potential or with ABA for 24 h. Then the stomata of the abaxial cotyledon surface were directly observed under a microscope. The ratio of width/length of stomatal pore is employed as the functional parameter to reflect stomatal responses to certain treatments. For each condition, more than 100 stomata from 5 seedlings were observed. Data were subjected to one-way ANOVA via SPSS 16.0 (** P < 0.01; * P < 0.05), and normalized by the stomata aperture values of *ahr11* and *pATHB6::LUC* seedlings at control condition. (A) The cotyledon stomatal response of *ahr11* (black) and *pATHB6::LUC* (white) to root-inflicted water deficit stress. Under the control condition (MS_{0.5xSuc} medium, without mannitol), the stomatal aperture of *ahr11* and *pATHB6::LUC* were 0.52 ± 0.05 and 0.48 ± 0.05 , respectively. (B) The cotyledon stomatal response of *ahr11* (black) and *pATHB6::LUC* (white) to ABA. Under the control condition (MS_{0.5xSuc} medium, without ABA), the stomatal aperture values of *ahr11* and *pATHB6::LUC* were 0.47 ± 0.01 and 0.43 ± 0.02 , respectively.

The root-inflicted water deficit has been shown to be sufficient to induce ABA biosynthesis in the shoot and to trigger stomatal closure of *Arabidopsis* (Christmann et al., 2007). Therefore roots of 5-day-old seedlings of *ahr11* and *pATHB6::LUC* were exposed to water deficit stress or exogenous ABA on solid agar medium, and the stomata of the abaxial cotyledon surface were observed under a microscope. The stomata of water-deficit-stressed seedlings of *pATHB6::LUC* were completely closed when the mannitol water potential in the medium was lower than -0.6 MPa, which accorded with the previous reports (Christmann et al., 2007), whereas the stomatal closure was attenuated in stressed seedlings of *ahr11* (Figure 3-20A). However, in the presence of ABA, the stomata of *ahr11* closed similarly as the *pATHB6::LUC* line. Meanwhile, ABA sensitivity of *ahr11* was significant less efficient (P < 0.05) at three ABA concentration conditions (Figure 3-20B). These results indicate that the stomatal response of *ahr11* seedlings is insensitive to water deficit under the experimental condition, and that the exogenous ABA rescues the stomatal closure of *ahr11*.

The ABA-dependent stomatal closure of *ahr11* was further tested using detached rosette leaves exposed to ABA in an incubation solution on which the leaves floated prior measurement of stomatal aperture. The stomata of both *ahr11* and *pATHB6::LUC* were opened by light ($150 \mu\text{mol m}^{-2} \text{s}^{-1}$, 2 h;

Figure 3-21A). Exogenous ABA efficiently triggered the stomatal closure of *ahr11* and *pATHB6::LUC* with stomata of *ahr11* responding abit, but significantly more sensitively to ABA than the *pATHB6::LUC* ($p < 0.01$; Figure 3-21B). Because partial stomatal closure in response to exogenous ABA was observed 4-10 min after ABA application (Siegel et al., 2009), the kinetics of stomatal closure of *ahr11* and *pAHB6::LUC* were studied in response to 10 μM ABA (Figure 3-21C). 5 min after ABA addition, a significant reduction in stomatal aperture of *ahr11* had occurred and after 20 min, an aperture was found which remained more or less constant until the end of the experiment (aperture 180 min: 0.29 ± 0.02 , $n = 30$). In contrast, stomata of *pATHB6::LUC* responded more slowly and the lowest aperture was observed at 180 min after exposure to ABA (aperture 180 min: 0.44 ± 0.02 , $n = 28$).

Ca^{2+} influx is important for stomatal closure in response to ABA and the removal of extracellular Ca^{2+} inhibits the ABA-induced stomatal closure *via* the repression of $[\text{Ca}^{2+}]_i$ oscillation (Klusener et al., 2002, Siegel et al., 2009). Therefore, the rosette leaves of *ahr11* and *pAtHB6::LUC* were exposed to 10 μM ABA under high $[\text{Ca}^{2+}]$ (0.1 mM free Ca^{2+} , buffered by EGTA) and low $[\text{Ca}^{2+}]$ (0 mM free $[\text{Ca}^{2+}]$, buffered by EGTA) conditions (Figure 3-21D). After 5 min exposure to indicated treatments, only minute responses ($P > 0.05$) were found in *pAtHB6::LUC* stomata exposure to ABA both in high and low $[\text{Ca}^{2+}]$ buffer, whereas in the presence of ABA in high $[\text{Ca}^{2+}]$ buffer (' $\text{Ca}^{2+} + \text{ABA}$ ') the stomatal apertures of *ahr11* were reduced to $65.3 \pm 3.8\%$ of the stomata under control condition, while, in low $[\text{Ca}^{2+}]$ buffer, the ABA-induced stomatal closure was attenuated in *ahr11* and stomatal apertures were reduced to $83.4 \pm 3.2\%$.

Taken together, these results indicate that the stomata on cotyledons of *ahr11* are insensitive to root-inflicted water deficit, but the cotyledon stomata of *ahr11* respond similarly to exogenous ABA as wild type at long time exposure (24 h; Figure 3-20B). While the closely kinetics of leaf stomata from *ahr11* are more rapid respond to exogenous ABA than wild type stomata, which is promoted by the presence of Ca^{2+} .

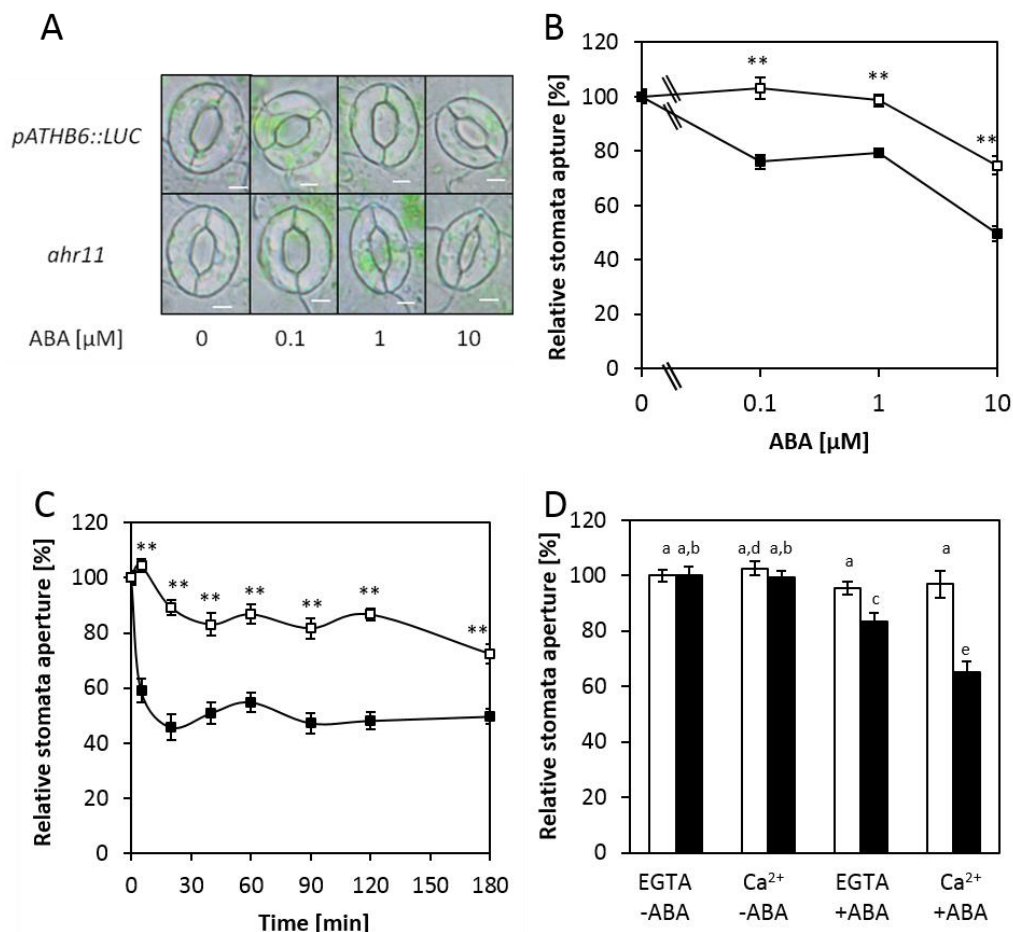


Figure 3-21: Hypersensitive and rapid response to exogenous ABA of detached rosette leaf stomatal closure of *ahr11*

(A)-(C) Rosette leaves cut from 3-week-old plants of *ahr11* (black) and *pATHB6::LUC* (white) were exposed to light ($150 \mu\text{mol m}^{-2} \text{s}^{-1}$) for 2 h floating on incubation solution (KCl 10 mM, CaCl_2 0.2 mM, EGTA 0.1 mM and MES-KOH 10 mM; pH6.15) to open stomata. Then, the incubation solution was replaced by fresh incubation solution supplemented with ABA as indicated and the leaves were exposed to ABA under the same condition. For each condition, about 30 stomata from 2 independent leaves were observed. Data were subjected to one-way ANOVA via SPSS 16.0 (** $P < 0.01$; * $P < 0.05$), and normalized by the stomatal aperture values ($\frac{\text{Width}}{\text{Length}}$) at control condition. (A) Aperture of stomata exposed to different concentrations of exogenous ABA for 2 h. Scale bar = 5 μm . (B) The stomatal response to exogenous ABA for 2 h. Under the control condition (incubation solution, without ABA), the stomatal aperture of *ahr11* and *pATHB6::LUC* were 0.48 ± 0.01 and 0.55 ± 0.02 , respectively. (C) Closely kinetics of stomatal response to 10 μM ABA. Under the control condition (incubation solution, without ABA), the stomatal aperture of *ahr11* and *pATHB6::LUC* were 0.57 ± 0.01 and 0.61 ± 0.01 , respectively. (D) Ca²⁺-dependency of the rapid response of *ahr11* stomata to ABA. The 'Ca²⁺' refers to experiments with 0.1 mM Ca²⁺ buffered by EGTA in the incubation solution (KCl 10 mM, CaCl_2 0.2 mM, EGTA 0.1 mM and MES-KOH 10 mM; pH6.15). The 'EGTA' means experiments with free Ca²⁺-incubation solution where the Ca²⁺ was chelated by EGTA (KCl 10 mM, EGTA 0.1 mM and MES-KOH 10 mM; pH6.15). The stomatal aperture was measured after exposure to buffer with ('+ABA') or without 10 μM ABA ('-ABA') for 5 min. under the control condition (free Ca²⁺-incubation solution, without ABA), the stomatal aperture of *ahr11* and *pATHB6::LUC* were 0.52 ± 0.02 and 0.56 ± 0.01 , respectively. The bars with similar letters are not significantly different ($P > 0.05$) according to Least-significant difference (LSD).

3.4.4 Seed dormancy

Seed dormancy is defined as a status where a viable seed cannot germinate under favorable conditions (Finch-Savage and Leubner-Metzger, 2006, Holdsworth et al., 2008, Bentsink and Koornneef, 2008). ABA produced by the seed during the maturing process induces seed dormancy. The dormancy maintenance of mature seeds during imbibing requires *de novo* ABA biosynthesis (Ali-Rachedi et al., 2004, Lee et al., 2010). Cold stratification in the dark is a routinely employed efficient method to abolish seed dormancy in the lab.

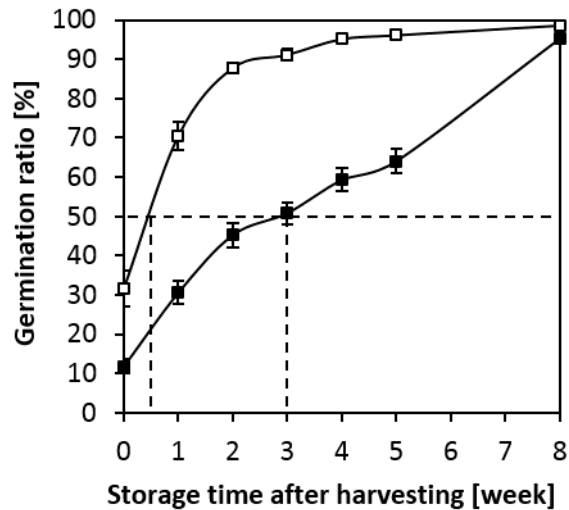


Figure 3-22: The seeds of *ahr11* show an extended dormancy

Germination rates of imbibed seeds of *ahr11* (black) and *pATHB6::LUC* (white) incubated in culture room ($60 \mu\text{mol m}^{-2}\text{s}^{-1}$, 22°C) at different storage time points after seed harvest. Seeds were stored dry between the day of harvest and imbibition. Dotted lines indicate the DSDS₅₀ value, which is defined as the days of seed dry storage (DSDS) required reaching a 50% germination rate. For *ahr11*, the mean germination ratios (\pm SE) were calculated from 8 independent seed batches, while 6 seed batches were used for *pATHB6::LUC*.

Seed dormancy of *ahr11* and *pATHB6::LUC* was analyzed by characterizing their respective germination rates at different time points after harvest. Germination of imbibed seeds incubated under continuous illumination ($60 \mu\text{mol m}^{-2}\text{s}^{-1}$, 22°C) was evaluated in weekly storage intervals until all of seeds had germinated, starting at the harvest date (Figure 3-22). Of freshly harvested seeds $31.6 \pm 4.5\%$ of *pATHB6::LUC* germinated after 7 days incubation, whereas only $11.8 \pm 1.8\%$ of *ahr11* seeds germinated. The Days of Seed Dry Storage (DSDS, after ripening) required reaching a 50% germination rate (DSDS₅₀) was estimated as a parameter of seed dormancy (Alonso-Blanco et al., 2003). The DSDS₅₀ value is influenced by the timing of growth during the growing season and by environmental effects on the mother plants. Thus, for evaluation of DSDS₅₀, all seed batches must be harvested at the same time from plants grown side by side. After 4 weeks of dry storage, about $95.2 \pm 1.4\%$ of imbibed *pATHB6::LUC* seeds germinated, whereas the germination rate of *ahr11* reached to $95.3 \pm 0.8\%$ after 8 weeks of storage. Accordingly, the DSDS₅₀ value of *ahr11* was about 7 folds of *pATHB6::LUC*, being

approximately 21 days and 3 days respectively, in this experiment. Therefore, *ahr11* seeds are much more dormant than *pATHB6::LUC* seeds.

3.4.5 Seed Germination

Germination is defined as the visible emergence of the radicle through surrounding structures (Finch-Savage and Leubner-Metzger, 2006). In *Arabidopsis*, this is a two-stage process with testa rupture followed by endosperm rupture. Germination is controlled by environmental factors such as light, temperature and water status, as well as by the balance between GA and ABA, in which GA promotes seed germination by enhancing degradation of DELLA proteins to favour testa rupture, whereas ABA has an antagonistic effect and inhibits germination *via* the transcriptional regulators ABI3 and ABI5 which repress endosperm rupture.

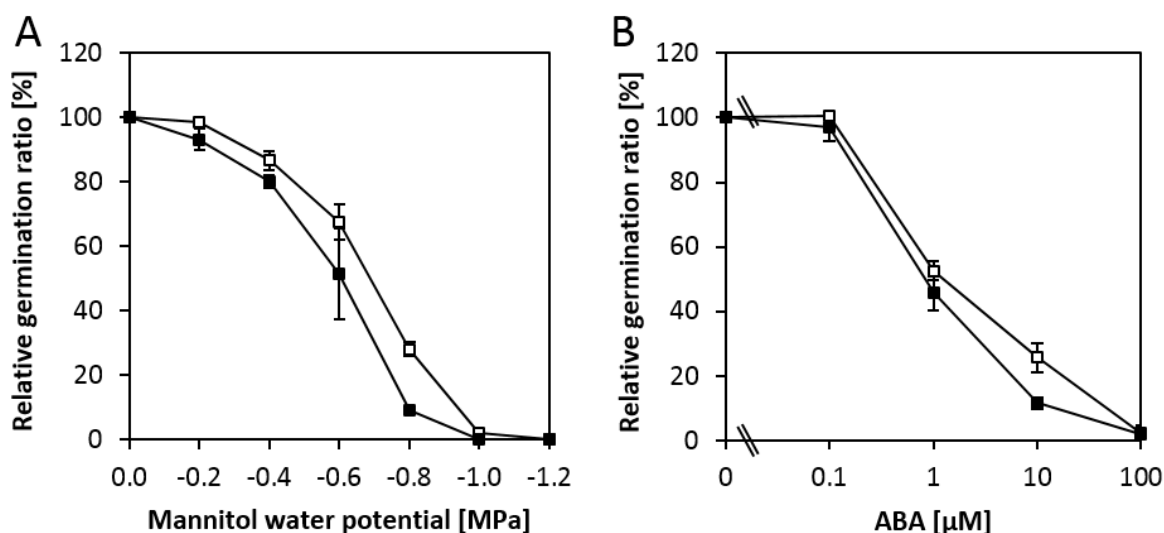


Figure 3-23: **Water deficit stress and exogenous ABA inhibit germination of *ahr11* and *pATHB6::LUC* seeds to a similar extent**

Seeds were sown on MS_{0.5xSuc} medium supplemented with mannitol to modulate low water potential as indicated or with ABA, and were stratified at 4°C in the dark for 2 days. The number of germinated seeds was counted on the 2nd day after transfer to culture room (22°C, light: 60 μ mol m⁻²s⁻¹, constantly). Seeds were scored as germinated when the radicle had visibly emerged through the ruptured testa. Data are means \pm SE (n = 2). Three independent experiments are performed to generate similar results. (A) Inhibition of germination of *ahr11* (black) and *pATHB6::LUC* (white) seeds by water deficit stress in the medium. The germination rate of *ahr11* and *pATHB6::LUC* under control condition (80.8 \pm 0.5% and 99.5 \pm 0.5%, respectively) was taken as a reference and set to 100%. (B) Inhibition of germination of *ahr11* and *pATHB6::LUC* seeds by exogenous ABA. The germination rate of *ahr11* and *pATHB6::LUC* under control condition (75.4 \pm 1.1% and 99.3 \pm 0.7%, respectively) was taken as a reference and set to 100%.

Reduced water availability and exogenous ABA were tested for their effects on germination of imbibed *ahr11* seeds. Under control condition of water deficit stress (MS_{0.5xSuc} without mannitol), 80.8 \pm 0.5% of *ahr11* seeds germinated after 2 days transferred to culture room (22°C, light: 60 μ mol m⁻²s⁻¹, constantly), and 99.5 \pm 0.5% of *pATHB6::LUC* seeds germinated (Figure 3-23A), while under control condition of ABA response (MS_{0.5xSuc} without ABA), the germination rates of *ahr11* and *pATHB6::LUC*

seeds were $75.4 \pm 1.1\%$ and $99.3 \pm 0.7\%$ respectively (Figure 3-23B). These differences could be due to enhanced dormancy of *ahr11* seeds which is still manifest even after several weeks of post-harvest storage and stratification. The germination data were therefore modified for this dormancy effect by setting the germination rate under control conditions to 100%. Considering the relative germination rates, germination of *ahr11* seeds turned out to be as sensitive to ABA and water deficit as wild type seeds, and in both lines, complete inhibition of germination occurred at -1.0 MPa mannitol water potential or 100 μM ABA. These findings indicate that the mutation of AHR11 does not alter the responses to water deficit stress and ABA during germination.

3.4.6 Root growth

Plants adjust root growth when soil water availability decreases. Under moderately water deficit, an increased ABA content in the roots prevents ethylene-induced growth inhibition and maintains root elongation supporting access to non-depleted water resources (Sauter et al., 2001, Sharp and LeNoble, 2002, Sharp, 2002, Sharp et al., 2004, LeNoble et al., 2004, Wilkinson and Davies, 2009). To determine root growth under water deficit conditions, the 4-day-old seedlings of *ahr11* and *pATHB6::LUC* were entirely exposed to low water potential medium for 3 days. The mild water deficit stress (-0.2 MPa, mannitol) promoted root growth of *pATHB6::LUC* seedlings, and an increasing limitation was observed under further reduced mannitol water potential (< -0.6 MPa). In contrast, the root growth of *ahr11* was not stimulated within the range of water potentials tested, and was strongly inhibited with decreasing water potential compared to *pATHB6::LUC* (Figure 3-24A). In the presence of increasing levels of ABA, a stimulation of primary root growth of both *ahr11* and *pAtHB6::LUC* was observed with 0.1 μM and 0.3 μM ABA, while high concentration of ABA (>1 μM) inhibited root growth to a similar degree in both lines (Figure 2-23B; $P > 0.05$). In summary, the primary root growth of *ahr11* is hypersensitive to water deficit, but shows normal sensitivity to exogenous ABA.

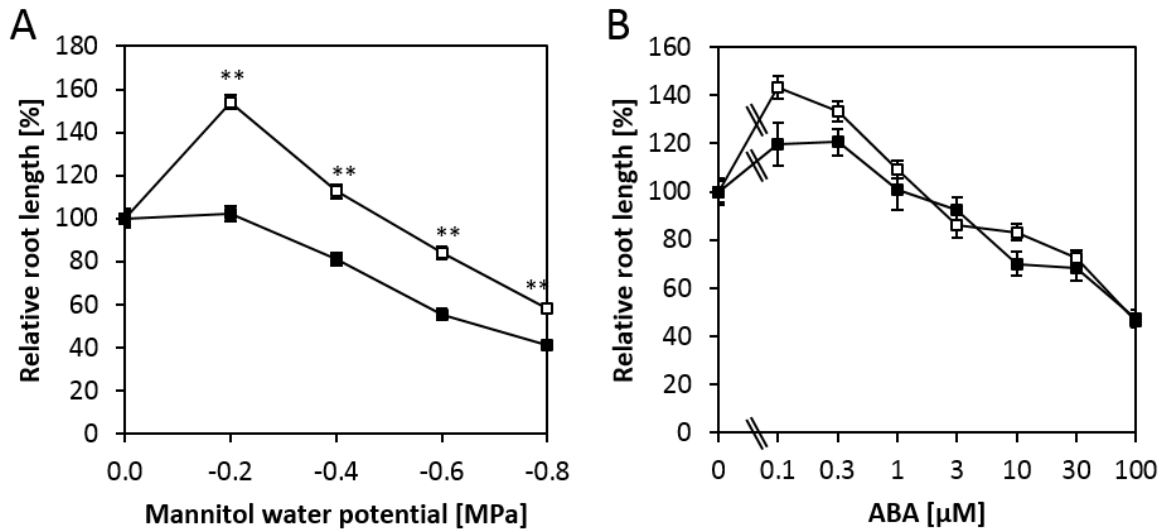


Figure 3-24: **Contrasting sensitivity of *ahr11* root growth to water deficit stress and to exogenous ABA**

The 4-day-old seedlings were entirely exposed to $MS_{0.5xSUC}$ medium supplemented with mannitol to adjust medium water potential or with ABA, and then grown vertically in culture room (22°C, light constant) for 3 days. Then the photographs were taken with a digital camera (Canon G10, Canon, Japan; camera control software: Canon Utilities Remote Capture DC ver. 3.1.0.5), and the root length was measured using an Image J software. The data presented are relative length of root growth (\pm SE; $n = 25$) normalized by the root length of seedlings grown under control conditions. Data were subjected to one-way ANOVA via SPSS 16.0 (** $P < 0.01$; * $P < 0.05$). (A) Response of primary root growth of *ahr11* (black) and *pATHB6::LUC* (white) to a decrease in substrate water potential. The root length of *ahr11* and *pATHB6::LUC* grown under control condition were 8.5 ± 0.4 mm and 7.6 ± 0.3 mm, respectively. (B) Response of primary root growth of *ahr11* (black) and *pATHB6::LUC* (white) to exogenous ABA. The root length of *ahr11* and *pATHB6::LUC* grown under control condition were 9.0 ± 0.5 mm and 8.4 ± 0.4 mm, respectively.

3.4.7 Developmental phenotypes of *ahr11*

The premature translation stop of AHR11 in *ahr11* leads to a series of phenotypic alternations, such as flowering time, number of rosette leaves, inflorescence morphology, chlorophyll content and leaf senescence.

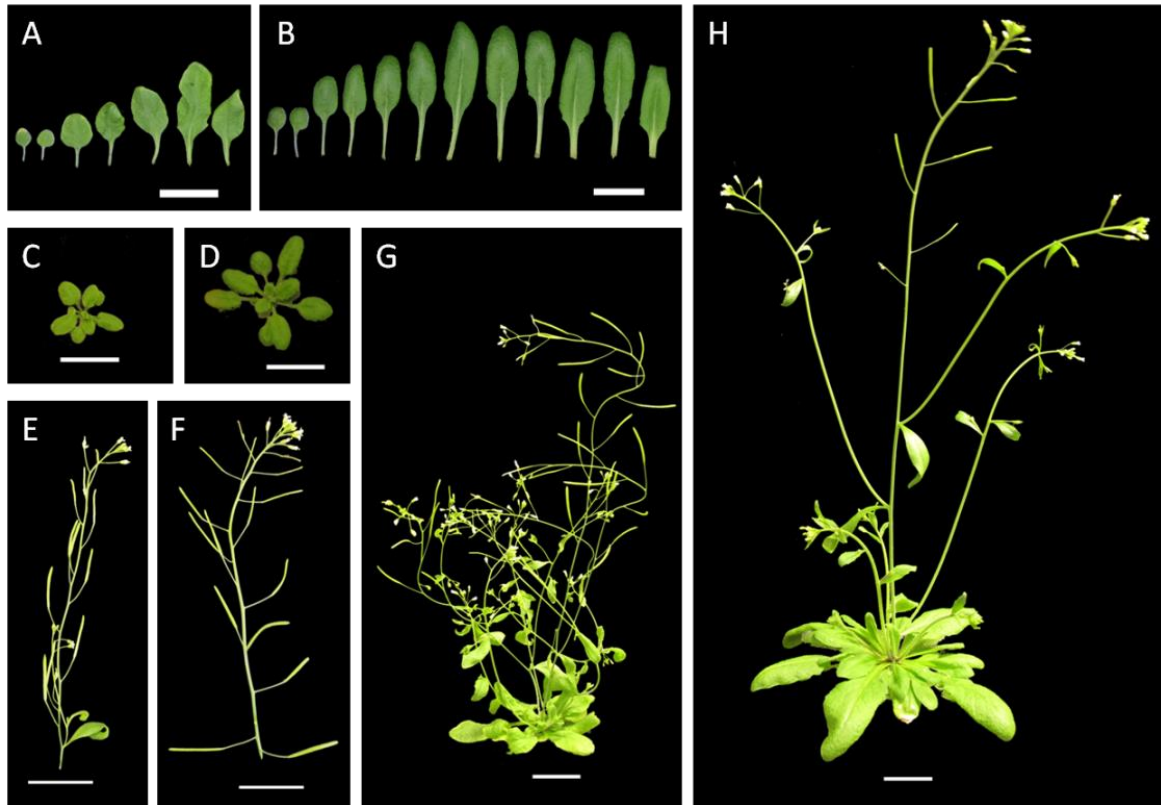


Figure 3-25: Development of *ahr11* compared to *pATHB6::LUC*

(A) and (B) The rosette leaves of 28-day-old *ahr11* mutant and *pATHB6::LUC*. (C) and (D) The 19-day-old plant of *ahr11* mutant and *pATHB6::LUC*. (E) and (F) The inflorescence stem of *ahr11* mutant and *pATHB6::LUC*. (G) and (H) The 34-day-old plant of *ahr11* mutant and *pATHB6::LUC*. All plants were grown under long-day conditions. The photographs were taken with a digital camera (Canon G10, Canon, Japan; camera control software: Canon Utilities Remote Capture DC ver. 3.1.0.5). Scale bar = 20mm.

The morphological phenotype of *ahr11* and wild type *pATHB6::LUC* plants at different development stages are documented in Figure 3-25. At the same developmental stage, *ahr11* has less rosette leaves (Figure 3-25A and B), as well as smaller plant size (Figure 3-25C and D) compared with *pATHB6::LUC*. During reproductive development, siliques of *ahr11* were upright and almost attached to the inflorescence stem (Figure 3-25E), and inflorescences had a bushy appearance due to the weak apical dominance (Figure 3-25G). When plants were grown under long-day conditions, *ahr11* was found to flower earlier than wild type *pATHB6::LUC*. Although in different trials slight variations were seen in the leaf number and plant size, the *ahr11* constantly flowered about 2 days earlier than the *pATHB6::LUC* (Table 3-4).

Table 3-4: Early flowering time of *ahr11* compared to wild type *pATHB6::LUC*

Experiment I				
	Flowering time ^a [days]	Leaf number ^b	Stem length ^c [cm]	leaf length ^d [cm]
<i>pATHB6::LUC</i>	24.4 ± 0.2	10.6 ± 0.1	3.60 ± 0.14	4.17 ± 0.07
<i>ahr11</i>	22.7 ± 0.2	6.5 ± 0.1	2.21 ± 0.08	1.55 ± 0.03
Experiment II				
	Flowering time ^a [days]	Leaf number ^b	Stem length ^c [cm]	leaf length ^d [cm]
<i>pATHB6::LUC</i>	23.9 ± 0.1	9.4 ± 0.1	3.94 ± 0.13	4.21 ± 0.05
<i>ahr11</i>	22.2 ± 0.1	6.4 ± 0.1	3.17 ± 0.10	1.97 ± 0.04

Plants were grown in the same tray under long-day conditions (16 h light/8 h dark). ^a Age of plant when the first flower opened. ^b Number of rosette leaves when the first flower opened. ^c Length of main stem when the first flower opened. ^d Maximum rosette leaf length when the first flower opened. The values presented are mean ± SE (n = 30 in experiment I; n = 54 in experiment II).

Leaf senescence is regarded as a highly plastic trait of plants, which can be induced by a range of different environmental factors including light, nutrient supply, CO₂ concentration and abiotic and biotic stress. Usually the leaf senescence is characterized by a decline in chlorophyll content, the chlorophyll content in seedlings of *ahr11* and *pATHB6::LUC* was therefore measured. The results showed that *ahr11* contains less chlorophyll than *pATHB6::LUC*, which responds to the light green color phenotype of *ahr11* (Figure 3-26). The leaf senescence processes of *ahr11* was slight faster than wild type *pATHB6::LUC* when the plants were grown under long-day conditions. In contrast, under short-day conditions, leaf senescence was accelerated in *ahr11* plants, but was not obviously in *pATHB6::LUC* plants, when plants were 35-day-old (Figure 3-27).

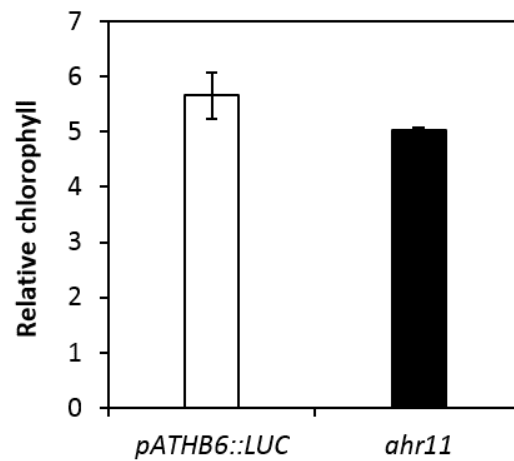


Figure 3-26: Chlorophyll content of *ahr11* and *pATHB6::LUC*

The pigments were extracted from 5-day-old seedlings with methanol, and light absorbance at certain wave lengths, according to Lichtenthaler (1987), was measured with a spectrophotometer to allow calculation of contents of chlorophyll a and b and of total carotinoids. Data are relative content of chlorophyll a + b to total carotinoids (n = 3).

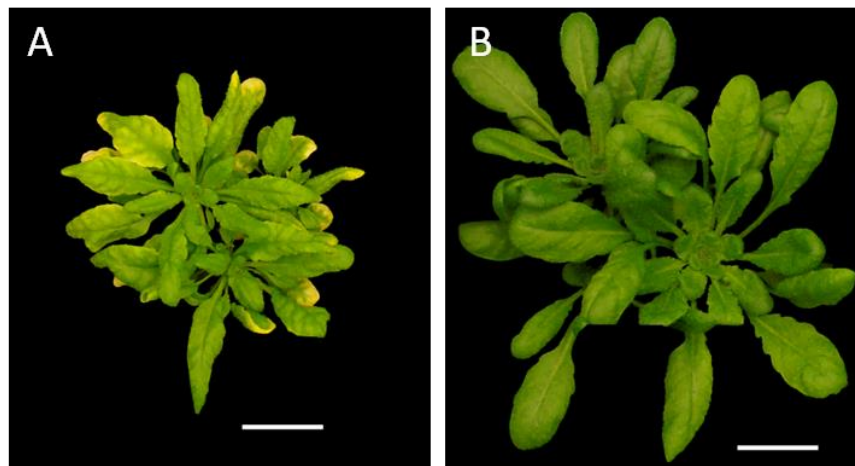


Figure 3-27: Enhanced senescence of *ahr11* compared to *pAtHB6::LUC*

(A) The 35-day-old plants of *ahr11* mutant grown under short-day conditions. (B) The 35-day-old plants of *pATHB6::LUC* grown under short-day conditions. The photographs were taken with a digital camera (DSC-W35, SONY, Japan). Scale bar = 20mm.

3.5 Physiological analyses of *ahr11* mutant in *aba2-1* and *abi1-1* genome background

3.5.1 Crosses of *ahr11* to *aba2-1* and *abi1-1* mutants

In order to further investigate the function of AHR11 in ABA signaling, homozygous *ahr11* was crossed to the ABA-deficit mutant *aba2-1* and to the ABA-insensitive mutant *abi1-1* respectively. Meanwhile, the mutants *aba2-1* and *abi1-1* were crossed to *pATHB6::LUC* reporter line to obtain ABA-reporter construct. The homozygous double mutants *ahr11/aba2-1* and *ahr11/abi1-1*, as well as mutants *aba2-1/pATHB6::LUC* and *abi1-1/pATHB6::LUC*, were selected by appropriate genotyping markers (see Appendix 5.3).

3.5.2 Physiological analyses of double mutants *ahr11/aba2-1* and *ahr11/abi1-1*

Double mutants *ahr11/aba2-1* and *ahr11/abi1-1* were used to analyze the physiological responses to water deficit stress and exogenous ABA. With respect to ABA-induced stomatal closure and ABA-inhibited root elongation, the double mutant *ahr11/aba2-1* displayed insensitivity to water deficit stress and a normal sensitivity to ABA and was similar to single mutant *aba2-1/pATHB6::LUC*, while the double mutant *ahr11/abi1-1* was insensitive to water deficit stress and exogenous ABA as a response manner of single mutant *abi1-1/pATHB6::LUC*. By contrast, specific physiological responses were observed from double mutant *ahr11/abi1-1* during germination.

The seeds of *pATHB6::LUC*, *ahr11*, *aba2-1/pATHB6::LUC* and *abi1-1/pATHB6::LUC* were employed as references in the germination assay of double mutants *ahr11/aba2-1* and *ahr11/abi1-1*. As mentioned above, the *ahr11* mutation does not alter the responses to water deficit stress and ABA during germination. The imbibed seeds of *ahr11/aba2-1* double mutant were insensitive to low water potential as observed for the single mutant *aba2-1/pATHB6::LUC* (relative germination rate: $67.8 \pm 1.4\%$ and $71.3 \pm 3.2\%$, respectively, at -1.0 MPa, mannitol; Figure 3-28A), indicating that ABA biosynthesis is required for the inhibition effect of low water potential on seed germination. On the other hand, severe water deficit stress (-1.0 MPa, mannitol) was not only efficient to inhibit the seed germination of wild type *pATHB6::LUC* and *ahr11* but also of the ABA-insensitive mutant *abi1-1/pATHB6::LUC*, whereas the double mutant *ahr11/abi1-1* was resistant to severe water deficit and maintained a high relative germination rate ($65.7 \pm 3.0\%$ at -1.0 MPa, mannitol; Figure 3-28B). These findings imply that AHR11 and ABI1 additively inhibit seed germination under water deficit stress.

When imbibed seeds were exposed to exogenous ABA, the double mutant *ahr11/aba2-1* and single mutant *aba2-1/pATHB6::LUC* behaved like the wild type *pATHB6::LUC* with strong inhibition of germination occurring in the presence of $1 \mu\text{M}$ ABA (Figure 3-28C). On the other hand, both double mutant *ahr11/abi1-1* and single mutant *abi1-1/pATHB6::LUC* were insensitive to ABA and maintained a high germination rate ($92.4 \pm 3.4\%$ and $76.9 \pm 8.0\%$, respectively, at $1 \mu\text{M}$ ABA; Figure 3-28D). Therefore, the ABA signaling pathway is functional in *ahr11*. However, when high ABA was applied, all of seed germinations were blocked. It implies that the mutated *abi1-1* does not complete block the ABA signaling, but blunts the ABA response.

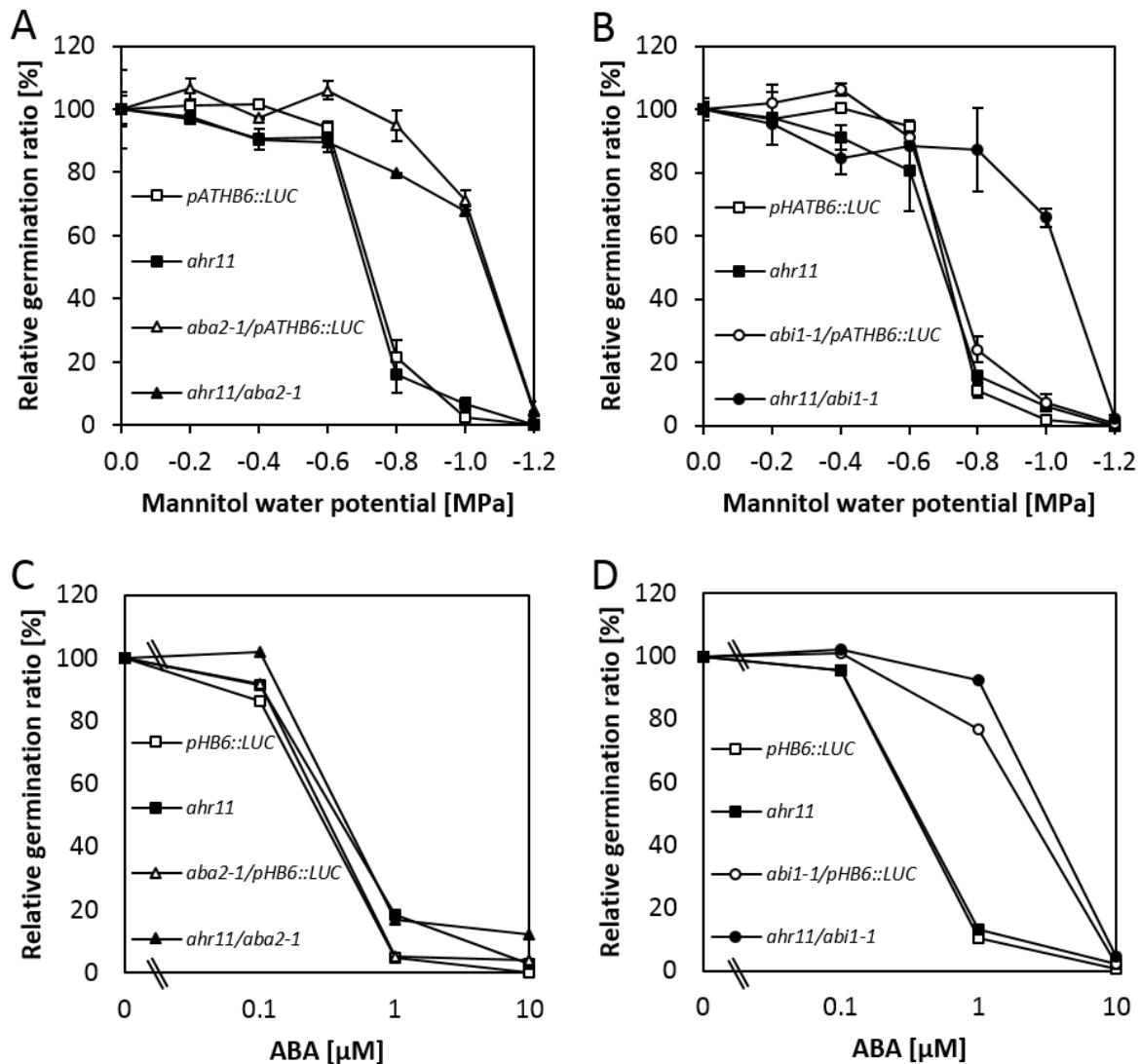


Figure 3-28: Response of germination of ABA-deficient *aba2-1*, ABA-insensitive *abi1-1*, as well as double mutants *ahr11/aba2-1* and *ahr11/abi1-1* to water deficit stress and ABA

(A) Inhibition of germination of *ahr11* (black square), *pATHB6::LUC* (white square), *aba2-1/pATHB6::LUC* (white triangle), and *ahr11/aba2-1* (black triangle) by water deficit stress. Germination rates under the control condition ($MS_{0.5xSuc}$, without mannitol): *ahr11*: $91.0 \pm 5.1\%$, *pATHB6::LUC*: $93.1 \pm 4.2\%$, *aba2-1/pATHB6::LUC*: $76.1 \pm 9.4\%$, and *ahr11/aba2-1*: $97.2 \pm 1.1\%$. (B) Inhibition of germination of *ahr11* (black square), *pHATB6::LUC* (white square), *abi1-1/pATHB6::LUC* (white round), and *ahr11/abi1-1* (black round) by water deficit stress. Germination rates under the control condition: *ahr11*: $91.3 \pm 0.3\%$, *pATHB6::LUC*: $95.2 \pm 3.4\%$, *abi1-1/pATHB6::LUC*: $81.8 \pm 1.3\%$, and *ahr11/abi1-1*: $93.7 \pm 2.2\%$. (C) Inhibition of germination of *ahr11*, *pATHB6::LUC*, *aba2-1/pATHB6::LUC*, and *ahr11/aba2-1* by exogenous ABA. Germination rates under the control condition ($MS_{0.5xSuc}$ without ABA): *ahr11*: $89.6 \pm 0.5\%$, *pATHB6::LUC*: $97.2 \pm 0.7\%$, *aba2-1/pATHB6::LUC*: $98.5 \pm 1.5\%$, *ahr11/aba2-1*: $91.9 \pm 3.9\%$. (D) Inhibition of germination of *ahr11*, *pATHB6::LUC*, *abi1-1/pATHB6::LUC*, and *ahr11/abi1-1* by exogenous ABA. Germination rates under the control condition: *ahr11*: $86.4 \pm 0.0\%$, *pATHB6::LUC*: $94.8 \pm 3.9\%$, *abi1-1/pATHB6::LUC*: $87.5 \pm 0.7\%$, and *ahr11/abi1-1*: $89.9 \pm 3.6\%$. The experiments and calculations were performed as indicated in the Figure 3-23 legend.

3.6 Functional analysis of AHR11

3.6.1 Subcellular localization of wild type AHR11 and of truncated protein Δ ahr11

The subcellular localization of AHR11 was investigated by transient expression in protoplasts. The enhanced green fluorescent protein gene (eGFP) was fused to the N-terminus of the coding sequence (CDS) of wild type AHR11 (*eGFP::AHR11*) and of the CDS of truncated protein Δ ahr11 (*eGFP:: Δ ahr11*) with expression driven by the 35S promoter. When transiently expressed in Col-0 wild type protoplasts, the recombinant truncated protein eGFP:: Δ ahr11 predominantly localized to the nucleus. However, when the construct *35S::eGFP::AHR11* was expressed in protoplasts, no obvious GFP signal could be detected (Figure 3-29).

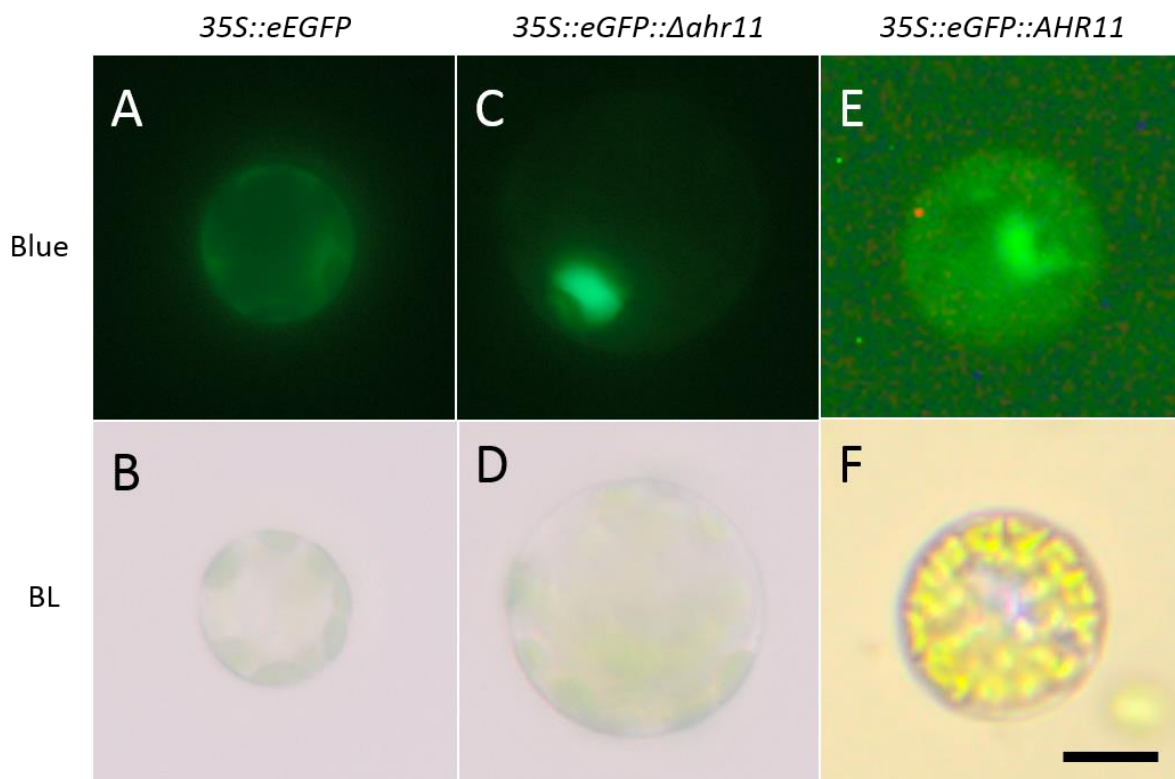


Figure 3-29: **Subcellular localization of eGFP::AHR11 and eGFP:: Δ ahr11 fusion protein in protoplasts**

The eGFP N-terminal fusion proteins (eGFP::AHR11 and eGFP:: Δ ahr11) were expressed in Col-0 protoplasts and their localization observed using fluorescence microscopy (HBO 50 Axioskop, Carl Zeiss). The distribution of eGFP signal, eGFP protein is shown as a control. Blue = Excitation source of eGFP detection at 498 nm. BL = Bright light. Scale bar = 10 μ M.

3.6.2 ABA biosynthesis and distribution under water deficit

Under water deficit stress, ABA is synthesized in the vasculature and subsequently transported into guard cells to trigger the stomata closure (Koiwai et al., 2004, Sirichandra et al., 2009b, Kim et al., 2010b, Bauer et al., 2013). The ABA content of shoots of *ahr11* was measured under root-inflicted water deficit (-0.6 MPa, mannitol). Under non-stress conditions ($MS_{0.5xSuc}$ medium, 0 h and 24 h), the

ABA contents in the shoots of both *ahr11* and *pATHB6::LUC* showed a basal level of about 20-40 ng/g FW (fresh weight). ABA was increased 4 to 5 folds in the water-deficit-stressed shoots of both lines (Figure 3-30A). Since *NCED3* plays a crucial role in increased ABA formation in water deficit response, the transcripts of *NCED3* were analyzed by quantitative real-time PCR in wild type and *ahr11*. Although the transcript abundances of *NCED3* in *ahr11* and wild type seedlings were strongly increased by water deficit stress (factor of 50 and 47, respectively, under 3 h water deficit stress), the difference between these two lines was insignificant (Figure 3-30B). These results suggest that regulation of the water-deficit-induced ABA biosynthesis is similar in *ahr11* and wild type *pATHB6::LUC*. In addition, ABA content of fresh seeds was analyzed. The fresh harvested seeds of *ahr11* contains 491 ng/g FW ABA, which is higher than in wild type seeds (374 ng/g FW) (Figure 3-31).

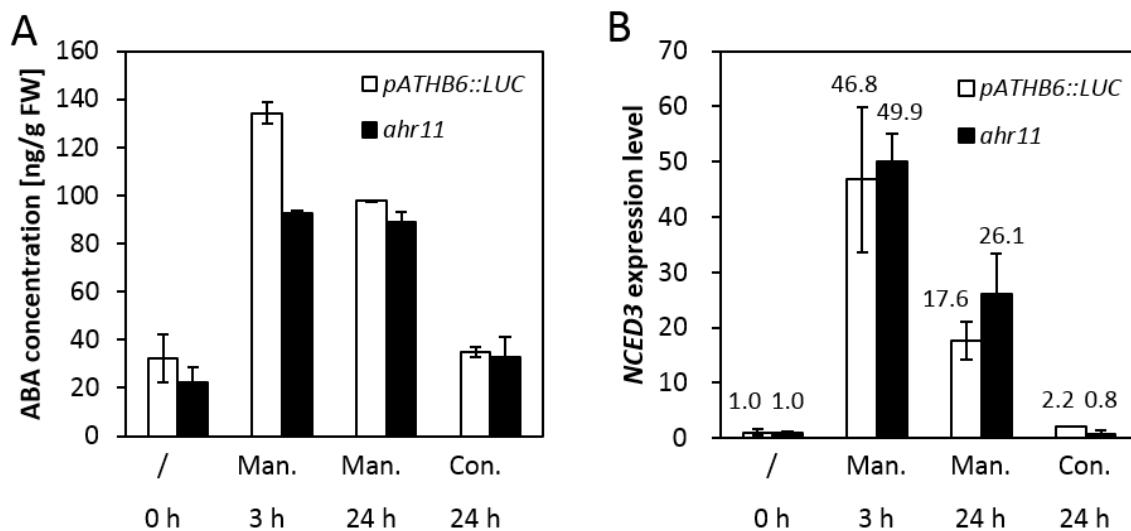


Figure 3-30: The ABA biosynthesis in *ahr11* under water deficit is similar to wild type *pATHB6::LUC*

5-day-old seedlings of *ahr11* (black) and *pATHB6::LUC* (white) were stressed by root-inflicted water deficit (-0.6 MPa, mannitol) for 3 h and 24 h respectively, and the samples under non-stress conditions ($MS_{0.5 \times Suc}$, 0 h and 24 h) were employed as two controls. Shoot materials were collected for ABA quantification and total RNA isolation. (A) ABA content in shoots of *ahr11* and *pATHB6::LUC* under water deficit stress. Gas chromatography mass spectrometry (GC-MS) analysis of ABA quantification was carried out by Prof. Dr. Jutta Ludwig-Müller from the Institut für Botanik of Technische Universität Dresden. Analysis was done with 2 biological replicates and 3 technical replicates for each condition. Data are means \pm SE ($n = 2$). (B) The transcriptional expression level of *NCED3* in the shoots of *ahr11* and *pATHB6::LUC* under water deficit stress. The transcriptional expression level of *NCED3* was analyzed by quantitative real-time PCR (Bio-Rad). And the expression level of the housekeeping gene *UBC9* (*At4g27960*) was used as a reference. Analysis was done with 2 biological replicates and 2 technical replicates for each condition. The number presented above each column signifies the relative expression level of *NCED3* compared to its expression level under control condition (0 h). The data are mean values \pm SE ($n = 2$). Man. = -0.6 MPa mannitol water potential. Con. = non-stressed condition ($MS_{0.5 \times Suc}$).

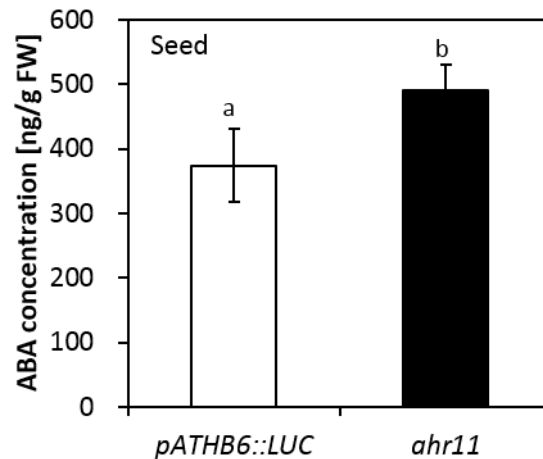


Figure 3-31: **ABA content in fresh seeds of *ahr11* and *pATHB6::LUC***

Fresh harvested seeds of *ahr11* (black) and *pATHB6::LUC* (white) were frozen in liquid nitrogen for GC-MS ABA analysis. Analysis was done with 2 biological replicates and 3 technical replicates for each condition. Data are means \pm SE ($n = 2$) and subjected to one-way ANOVA via SPAA16.0. The bars with different letters are significantly different ($p < 0.05$).

The spatial pattern of ABA activity in *ahr11* was analyzed using the *pATHB6::LUC* ABA-reporter system in seedlings under water deficit (-0.6 MPa, mannitol; 24 h) and exogenous ABA (30 μ M, 24 h). The water-deficit-induced ABA was predominately active in the vascular tissue (Figure3-32A and E), and actively spread to surrounding cells (Figure3-32B and F). In wild type *pATHB6::LUC* seedlings, the stress-induced ABA was active in guard cell to trigger the stomatal closure (Figure3-32F, G and H), whereas the ABA activity was detected outside the guard cells in surrounding epidermic cells in *ahr11* (Figure3-32B, C and D). However, exogenous ABA was imported into guard cells of *ahr11* seedlings as of wild type seedlings (Figure3-33). These results suggest that AHR11 protein regulates ABA translocation.

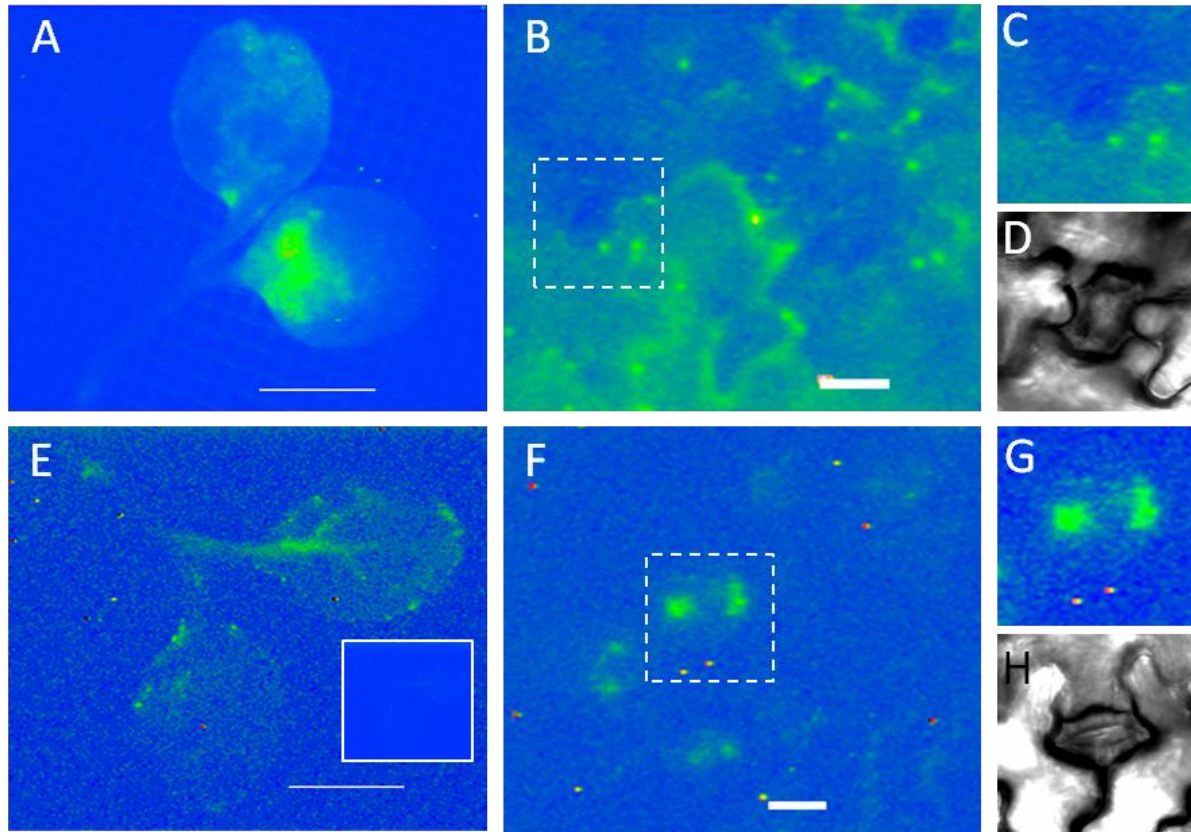


Figure 3-32: **Distribution of water-deficit-induced active ABA in cotyledon of *ahr11* and *pATHB6::LUC***

(A)-(D) 5-day-old seedlings of *ahr11* were exposed to water deficit stress (-0.6 MPa, mannitol) for 24 h. (E)-(H) 5-day-old seedlings of *pATHB6::LUC* were exposed to water deficit stress (-0.6 MPa, mannitol) for 24 h. The ABA-indicative light emission from stressed cotyledon was detected by an intensified CCD camera (ORCAII ERG, Hamamatsu) connected to the inverted microscope (Axiovert 200, Zeiss) with 2.5 X and 20 X magnification of the objectives. The exposure time: 10 min for *ahr11*; 20 min for *pATHB6::LUC*. The luminescence activity is depicted in false-color. The scale of light emission of *pATHB6::LUC* is 2-fold enhanced compared to *ahr11*. The non-enhanced image is shown as the inset in (E). The scale bar = 1 mm in (A) and (E). The scale bar = 20 μ m in (B) and (F). (C)-(D) and (G)-(H) The typical stomata of *ahr11* and *pATHB6::LUC* indicated in the white box in (B) and (F).

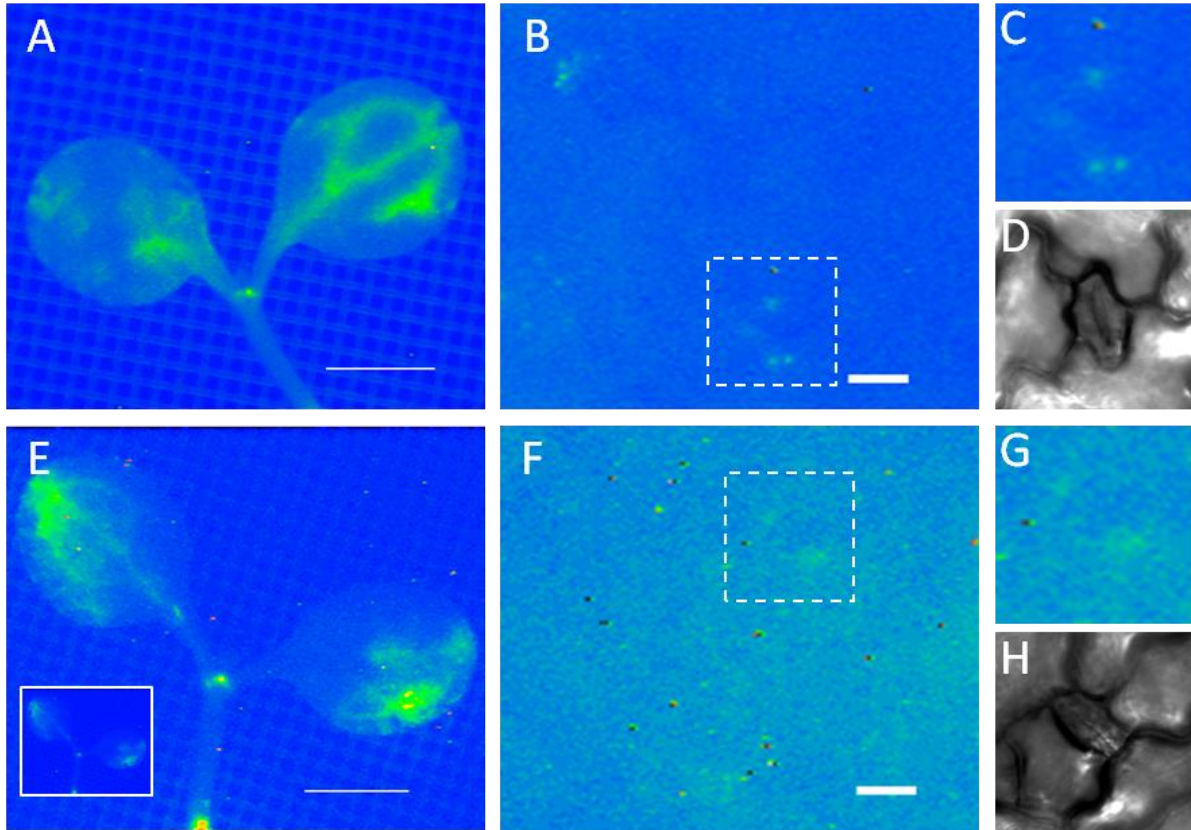


Figure 3-33: **Distribution of exogenous ABA in cotyledon of *ahr11* and *pATHB6::LUC***

(A)-(D) 5-day-old seedlings of *ahr11* were exposed to 30 μ M ABA for 24 h. (E)-(H) 5-day-old seedlings of *pATHB6::LUC* were exposed 30 μ M ABA for 24 h. The detection of ABA-indicative light emission from cotyledon was the same as indicated in Figure 3-32 legend. The exposure time: 10 min for *ahr11*; 30 min for *pATHB6::LUC*. The luminescence activity is depicted in false color. The scale of light emission of *pATHB6::LUC* is 2-fold enhanced compared to *ahr11*. The non-enhanced image is shown as the inset in (E). The scale bar = 1 mm in (A) and (E). The scale bar = 20 μ m in (B) and (F). (C)-(D) and (G)-(H) The typical stomata of *ahr11* and *pATHB6::LUC* indicated in the white box in (B) and (F).

To date, three proteins have been implicated in ABA transport and were characterized as ABA exporter and/or importer in *Arabidopsis thaliana*: ABCG25 (At1g71960), ABCG40 (At1g15520), and AIT1 (At1g69850) (Kang et al., 2010, Kuromori et al., 2010, Kanno et al., 2012). The transcriptional expression of three ABA transporters in the shoot of *ahr11* was detected by quantitative Real-Time PCR. Compared to the expression in wild type *pATHB6::LUC*, the transcripts of ABA importer ABCG40 and AIT1 in *ahr11* was abundantly up-regulated by water deficit stress (Figure 3-34A and C), whereas the ABA exporter ABCG25 were not significantly influenced under the same stress condition in both lines (Figure 3-34B).

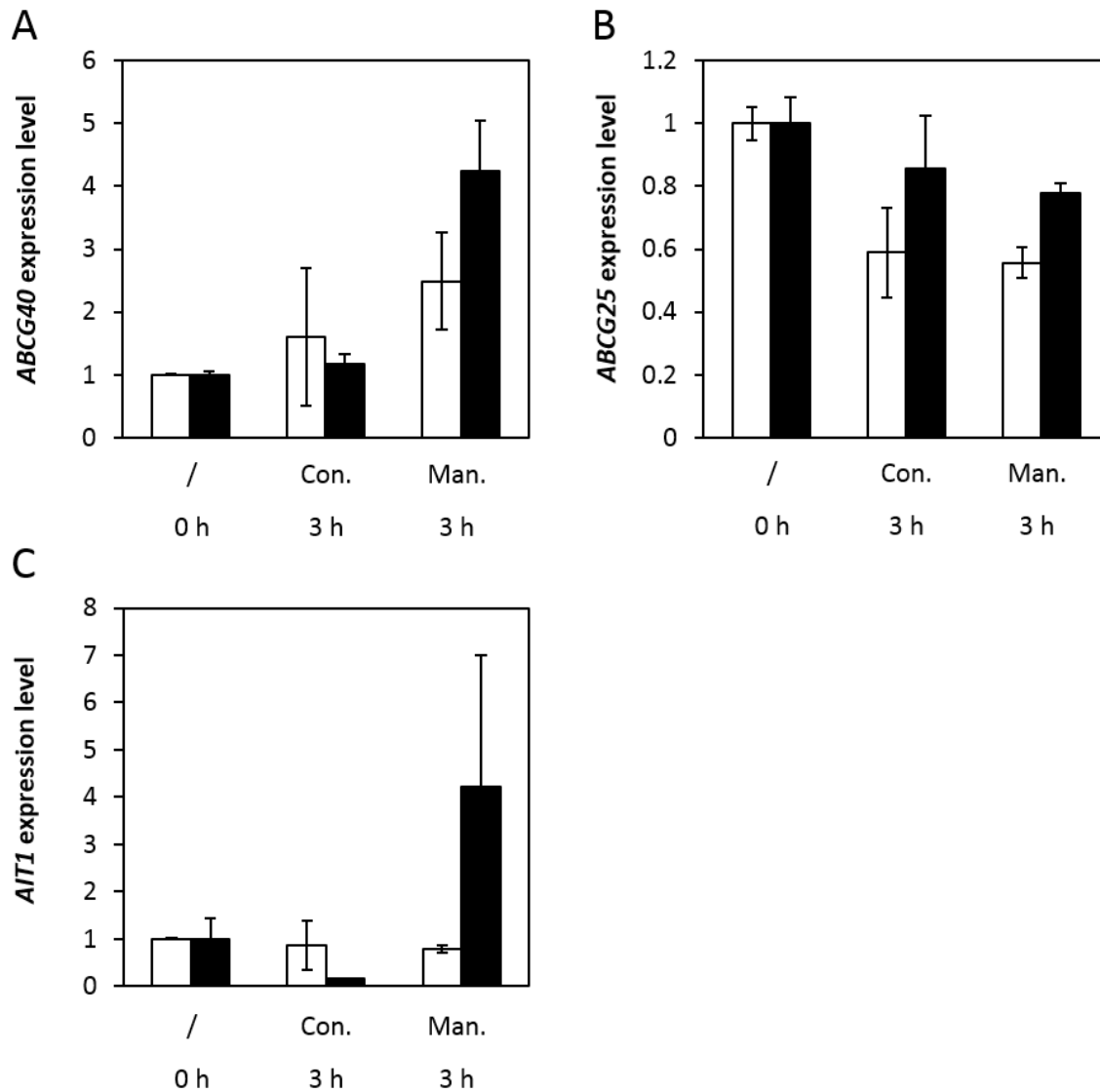


Figure 3-34: **The expression of ABA transporters in *ahr11* under water deficit stress**

15-day-old plants of *ahr11* (black) and *pATHB6::LUC* (white) were stressed by root-inflicted water deficit (-0.6 MPa, mannitol) for 3 h, and the samples under control conditions (MS liquid medium, 0 h and 3 h) were employed as two controls. The RNA isolated from the shoots was applied for quantitative Real-Time PCR. The expression level of the housekeeping gene *UBC9* (*At4g27960*) was used as a reference. Analysis was done with 2 biological replicates and 2 technical replicates for each condition. The data are mean values \pm SE ($n = 2$). (A) Expression level of ABA importer *ABCG40* (*At1g15520*) in the shoots of *ahr11* and *pATHB6::LUC*. (B) Expression level of ABA exporter *ABCG25* (*At1g71960*) in the shoots of *ahr11* and *pATHB6::LUC*. (C) Expression level of ABA importer *AIT1* (*At1g69850*) in the shoots of *ahr11* and *pATHB6::LUC*. Con. = non-stressed condition ($MS_{0.5xSuc}$). Man. = -0.6 MPa mannitol water potential.

3.7 Yeast two-hybrid screen for proteins interacting with AHR11

To decipher the mechanism underlying AHR11-mediated gene regulation, a screening for AHR11-interacting proteins was performed using a high-throughput yeast two-hybrid system (Dreze et al., 2010). An *Arabidopsis thaliana* cDNA library used before to generate an Arabidopsis protein interactome map (*Arabidopsis* Interactome Mapping Consortium, 2011), and kindly donated by Dr. Pascal Braun (TU München), was used as prey and a series of fragmented AHR11 ORFs were used as baits.

3.7.1 Generation of expression plasmids and identification of autoactivators

Firstly, the cDNA of AHR11 was fragmented into 4 regions as represented in Figure 3-35A. The a-region of AHR11 expressed amino acid residues 1-247 representing the same fragment as found in the *ahr11* mutant. Totally, 10 ORF combinations were subcloned into expression vectors *pDEST-AD* (strains: #5125-#5134) and *pDEST-DB* (strains: #5135-#5144) and transformed into yeast strain Y8800 *M AT α* (for AD) and Y8930 *M AT α* (for DB) respectively.

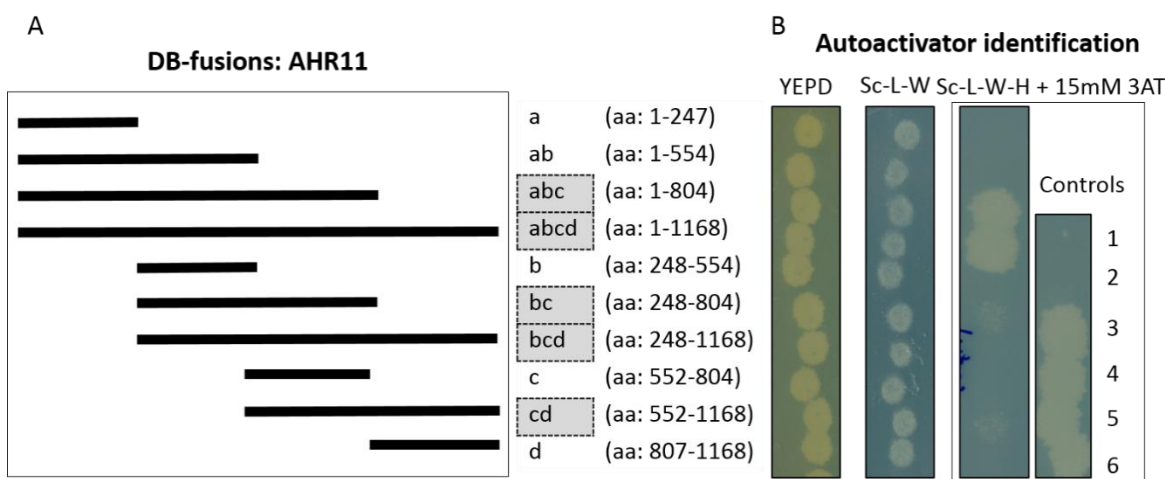


Figure 3-35: Schematic representation of fragmented AHR11 ORFs used as baits in the yeast two-hybrid screen and identification of autoactivators

(A) Ten ORF combinations of AHR11 fused to GAL4 DNA binding domain (BD fusions) are presented schematically. These *pDEST-DB-AHR11* expression vectors were transformed into yeast strain Y8930 *M AT α* . 'a' = premature protein Δ ahr11 in *ahr11* mutant. (B) Autoactivator identification of DB-fusion collections. 10 DB-AHR11 yeast strains were mated with yeast strain containing AD-empty vector on YEPD medium for 14-18 h. Then the diploid yeast strains were selected on Sc-L-W medium. The growth phenotype of diploid yeast strains on His selective medium (Sc-L-W-H + 15 mM 3AT) is the criterion for selection of autoactivators. The controls (1-6) indicate the interaction grade: 1. None, background; 2. Weak (control for CHX control plates); 3. Moderately strong; 4. Very strong; 5. Strong; 6. Strong (control for CHX plates). The DB-AHR11s indicated in the gray box were identified as autoactivators.

Before screening, generation of artifacts in the yeast-two-hybrid system must be avoided as much as possible. The identification of autoactivators was accomplished in diploid yeast strains by mating DB-AHR11s yeast strains with yeast strain containing *AD-empty* vector on YEPD medium. Diploid yeast

strains were replicated on Sc-L-W selection medium and Sc-L-W-H + 15 mM 3AT His-phenotype medium. The diploid yeasts with *BD-AHR11-abc* and *BD-AHR11-abcd* (Figure 3-35A) showed a strong growth phenotype on His-phenotype medium compared with the 'no interaction' Y2H control (control 1; Figure 3-35B). Therefore, these two strains were definitely autoactivators and were removed from the collection of DB-AHR11s. In addition, other three diploid yeasts harboring *DB-AHR11-bc*, *-bcd* and *-cd* displayed weak autoactivation phenotype, but were still included into DB-AHR11s collection. As a result, totally 8 different DB-AHR11s were employed for further screening for interacting proteins.

3.7.2 Yeast-two-hybrid screen and verification of putative interactions

Eight DB-AHR11s yeast strains harboring *DB-AHR11-a*, *-ab*, *-b*, *-bc*, *-bcd*, *-c*, *-cd*, and *-d* vectors, respectively, were used as bait to mate with AD pools consisting the AD-cDNA library expressing yeast clones. The positive clones were selected for His and Ade auxotrophy on selection medium. Through the screening of 59 AD pools (containing about 11000 cDNAs), 75 interacting candidates were selected by growth phenotyping and sequence analysis, which were listed in Appendix 5.4. For verification of interactions, all of these 75 yeast strains harboring AD-fusions of interacting candidates were mated with 8 DB-AHR11s yeast strains respectively. The growth phenotype of diploid yeast strains on selection medium was used to verify the candidate interaction pairs in yeast. Slight growth of diploids on the CHX control medium (second and forth columns in Figure 3-36) was considered to be the result of autoactivation. Therefore, and as anticipated from the initial results (Figure 3-35B), all interacting pairs of DB-AHR11-bc, bcd and cd were considered as autoactivators and excluded from further growth phenotype scoring. With growth evaluation on both the selective -His and -Ade medium, finally 7 independent AHR11-interacting candidates were identified in the yeast-two-hybrid screening (Figure 3-36) and subsequently grouped into three groups according to the interacting region of AHR11 and interacting intensity (Figure 3-37).

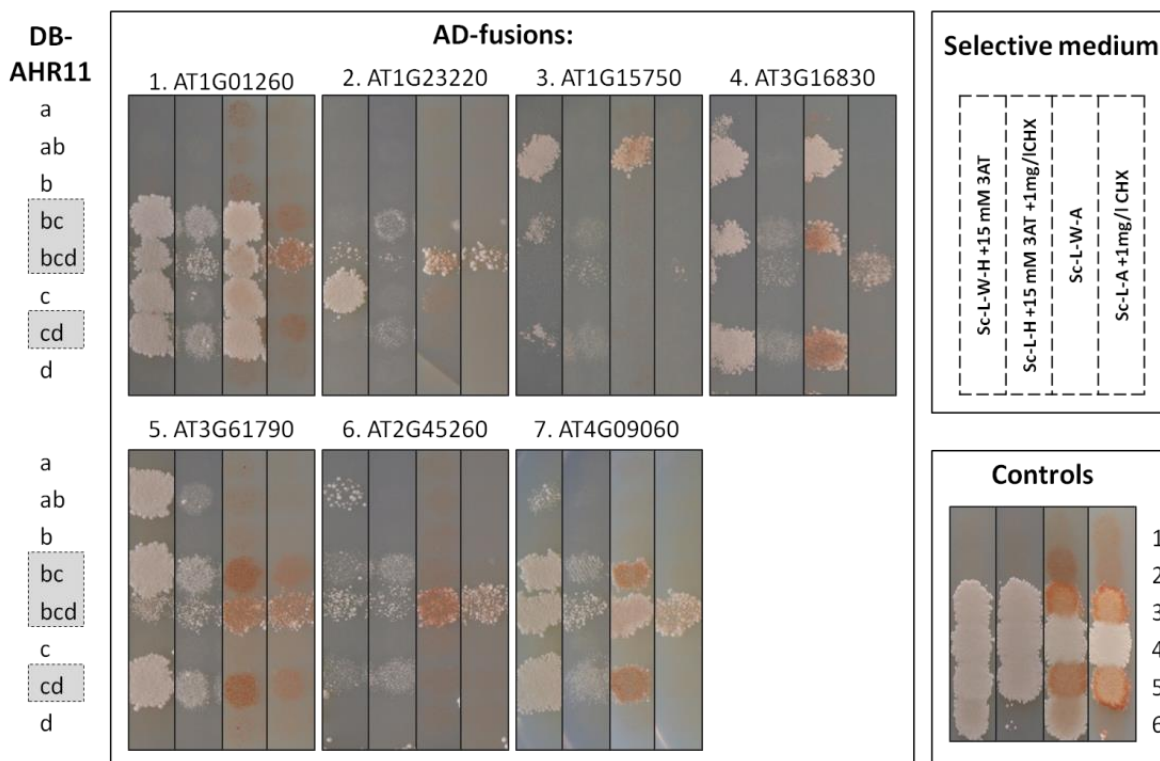


Figure 3-36: Interaction between fragmented AHR11 and candidate proteins in Y2H

All 75 interacting candidates AD-fusion yeast strains were mated with 8 DB-AHR11s yeast strains respectively on YEPD medium, and then the growth phenotype of diploids was scored on four phenotyping plates after 3 days incubation at 30°C. The interacting pairs which conferred slight growth on the CHX control plates was considered as autoactivator. The growth of diploids was evaluated on the selective -His and/or -Ade plates using the six controls described in Figure 3-34 as a reference. The four phenotyping plates are (from left to right; see section 2.16.7 for more details on composition of the mediums): Sc-L-W-H + 15 mM 3AT (His auxotrophy), Sc-L-H + 15 mM 3AT + 1 mg/l CHX (CHX control plate for -His), Sc-L-W-A (Ade auxotrophy), and Sc-L-A + 1 mg/l CHX (CHX control plate for -Ade). Three independent verification analyses were performed. The AHR11-ORFs indicated in the gray box were identified as autoactivators, which had to be excluded from subsequent growth phenotype scoring.

DB-	AD-					
	Group I		Group II			Group III
Fragmented AHR11 	AT1G01260	AT1G23220	AT1G15750	AT3G16830	AT3G61790	AT2G45260 AT4G09060
			+++	+++	+++	+ +
	+++	+++				

Figure 3-37: **Grouping of AHR11-interacting candidates**

The growth phenotype of diploid yeast strains on His- and Ade-selection medium was used to verify the interaction pairs. Grouping of interacting candidates was performed according to the interacting region on AHR11 as well as protein-protein interacting intensity. +++ Strong interaction; + Weak interaction.

3.7.3 Analysis of potential interacting candidates

The potential interacting partners of AHR11 include known and unknown proteins (Table 3-5). Of the known proteins, JAM2 (Jasmonate-associated MYC2-like 2; At1g01260) belongs to a bHLH-type transcription factor family, containing 3 homologs (JAM1, 2 and 3), which display high similarity to MYC2 (Sasaki-Sekimoto et al., 2013). TPL (TOPLESS; At1g15750) and TPR2 (TOPLESS-related 2; At3g16830) are members of the TOPLESS corepressor family, which contains 5 members (TPL and TPL-related 1 to 4) in *Arabidopsis thaliana* (Long et al., 2006). TPL/TPRs act as general repressors of gene transcription in plants, which directly or indirectly repress the expression of downstream target genes involved in a large range of processes, such as meristem maintenance, leaf shape development, circadian transcription, auxin signaling, jasmonate signaling and defense responses (Causier et al., 2012).

The *At1g23220* encodes a member of dynein light chain (DLC) type 1 protein family in *Arabidopsis thaliana*. In animal cells homologous DLC proteins are components of the dynein and mosin V motor complex involved in microtubule-based processes (King and Patel-King, 1995, Dick et al., 1996, Liang et al., 1999, Day et al., 2004). However, the cellular function of plant DLCs is little known. The AT3G61790 protein containing a RING-finger domain and a sina (seven in absentia)-domain is predicted to have ubiquitin-protein ligase activity and involved in ubiquitin-dependent protein degradation.

In addition, two proteins with unknown function were found encoded by *At2g45260* and *At4g09060*, respectively. The AT2G45260 protein has a conserved region DUF641 (Domain of unknown function)

found in a number of plant proteins with unknown function. No known domains are found in the AT4G09060 protein sequence nor is further specific information available concerning this gene.

Table 3-5: List of candidate proteins interacting with AHR11 in yeast

Group	Locus ID	Gene description	References
I	AT1G01260	JAM2; Negative regulator of JA responses	Sasaki-Sekimoto et al., 2013, Nakata and Ohme-Takagi, 2013
	AT1G23220	DLC type 1; Dynein light chain type 1 family protein	
II	AT1G15750	TOPLESS; involved in transcriptional repression	Causier et al., 2012, Causier et al., 2011
	AT3G16830	TPR2; TOPLESS-RELATED 2	Pauwels et al., 2010, Long et al., 2006
	AT3G61790	Protein with RING-finger and sina-domains	
III	AT2G45260	Plant protein of unknown function (DUF641)	
	AT4G09060	unknown protein	

4. Discussions

The molecular network of water deficit response is a highly orchestrated, complex signaling network recruiting different signaling pathways (Chinnusamy et al., 2004, Ahuja et al., 2010, Gollmack et al., 2014), in which the central role of ABA signaling has been well established (Cutler et al., 2010, Fujii and Zhu, 2012). Transcriptomic studies have identified types of transcription factors (TFs) regulating drought-responsive gene transcription, such as bZIP, AP2/ERF, NAC, bHLH, ZF, MYB and WRKYs (Tran et al., 2007a, Nakashima et al., 2009b). In contrast of ABA-induced bZIP-TF ABFs/AREBs, the drought-induced AP2-TF DREB2A/CBF3 ABA-independently regulates the expression of many drought-responsive genes by recognizing a DRE *cis*-element presenting in promoter region of these genes (Liu et al., 1998, Sakuma et al., 2006). However, the expression of *DREB2A* is ABA dependent for the ABRE *cis*-elements in its promoter (Kim et al., 2011b). Therefore, the ABA-independent water deficit response signaling pathway is still much less clear, compared with the prosperous research on the ABA-dependent pathway. Subsequently, the identity of new components responsible for the water deficit response is one of the most important issues in plant stress biology. In this work, a novel signaling element, the protein AHR11 was identified by a forward genetic approach and characterized as a negative regulator of ABA-dependent water deficit signaling pathway. Isolation of interacting partners of AHR11 in a yeast two-hybrid screen allowed proposing a possible molecular mechanism by which AHR11 represses target genes through recruiting of members of the TPL/TPRs corepressor family.

4.1 Identification of AHR11 using a forward genetic approach

Phenotype-based forward genetic approach is the most frequently used method to link phenotypes to genomic elements (Alonso-Blanco et al., 2005). The robust detection of a reliable phenotype is the decisive factor for successful forward genetic identification (Lukowitz et al., 2000, Jander et al., 2002, Peters et al., 2003). In our laboratory, a transgenic *Arabidopsis thaliana* ABA-reporter line *pATHB6::LUC* was generated and characterized as being well suited to monitor the accumulation and distribution of physiologically active ABA *in vivo* (Christmann et al., 2005, Christmann et al., 2007). When supplied with the luciferase substrate luciferin, seedlings of the ABA-reporter line *pATHB6::LUC* emit light in response to water deficit stress or to exogenous application of ABA. From an EMS-mutagenized population of this *pATHB6::LUC* ABA-reporter line the mutant *ahr11* was isolated based on a hypersensitive response to water deficit stress and exogenous ABA (Figure 3-1 and Figure 3-2). Using map-based cloning and next generation sequencing (NGS), hypersensitivity was assigned to a lesion in a gene *AHR11* (*At5g13590*) located on the chromosome V with unknown function.

The biggest advantage of map-based cloning is that this process may be performed without prior assumptions on the gene identity, and that any genomic element affecting the phenotype of interest could be found (Jander et al., 2002). In this work, the intensified ABA-dependent bioluminescence of the mutant *ahr11* under water deficit stress involves at least two loci including the causal mutation as

well as the transformed chimeric gene construct *pATHB6::LUC*. In the first-pass mapping, the bulked segregant analysis of *ahr11* indicated two interesting regions flanked by two molecular markers, respectively (Figure 3-5B). One region on chromosome V was proven to harbor the mutation of *AHR11* in this work while the second region located on chromosome III was simultaneously highlighted in a parallel map-based cloning approach targeting a different mutation (Cao et al., unpublished). Thus it was likely that the ABA-reporter construct *pATHB6::LUC* is inserted in the region on chromosome III flanked by markers *nga162* and *ciw11*, which was subsequently confirmed by NGS analysis. Sequence information of the region flanked by *nga162* and *ciw11* illustrated that the ABA-reporter construct *pATHB6::LUC* is inserted into the promoter region of *MYB15* gene (*At3g23250*), which is a member of the R2R3 factor gene family, and encodes a transcriptional factor involved in ABA and osmotic stress responses (Agarwal et al., 2006, Ding et al., 2009). Since the ABA-reporter line behaves like wild type *Arabidopsis thaliana* Col-0 in all ABA-dependent physiological processes routinely assayed in our laboratory, there is no indication to date that the insertion of the ABA-reporter construct has any effect on ABA-signaling.

For the fine-scale mapping, it has been suggested that using a mapping population of 3,000 to 4,000 plants results in mapping of the gene of interest to a genomic region of less than 4 kb size with a high probability (Jander et al., 2002), while the application of NGS efficiently and precisely releases high-resolution genotype information which allows reducing the mapping population size and shortening the mapping schedule (Schneeberger et al., 2009, Austin et al., 2011). In this work, a mapping population comprising 893 homozygous individuals allowed to narrow down the region of interest to 180 kb on chromosome V. NGS revealed a limited number of mutations in this region with only one exerting a non-synonymous change in a coding region (Figure 3-8 and Table 3-2). Therefore the combination of map-based cloning and NGS greatly facilitated the process to identifying the gene *At5g13590* as *AHR11*.

Following identification of *AHR11*, verification of the lesion in *AHR11* being responsible for the *ahr11* phenotype was performed using three approaches. (I) Ectopic expression of wild type *AHR11* which rescued the ABA-hypersensitive responses of *ahr11* in protoplasts (Figure 3-11C). (II) Generation of transgenic *ahr11 pAHR11::AHR11* mutant plants in which wild type ABA-sensitivity and wild type water-deficit-sensitivity were restored (Figure 3-12A and B). (III) Knockout mutants of *AHR11*, $\Delta 476$ and N804, were ABA-hypersensitive and displayed the same response pattern to water deficit and ABA as *ahr11* (Figure 3-15). The ectopic expression of *AHR11* could restore ABA sensitivity in protoplasts isolated from knockout mutants (Figure 3-16). Taken together the results clearly proof *At5g13590* as being *AHR11*. Although the transgenic complementation mutant *ahr11 pAHR11::AHR11* resembled wild type morphology with bigger rosettes and more explanate leaves than found in *ahr11* (Figure 3-13C), the reversion of morphology was still not complete, suggesting a dosage-dependent effect of the AHR11 protein. A parallel attempt to complement the mutant phenotype by stable expression of an AHR11-eGFP fusion protein in *ahr11*, transformed with the *pAHR11::AHR11-eGFP* construct, failed to reduce the hypersensitivity to water deficit as well as to ABA seen in *ahr11* (Figure 3-13D). The possible reason is that the eGFP protein interferes with the function of AHR11 when fused

to it C-terminally. Since impaired function of AHR11 may be accompanied by mislocalization of the fusion protein, new transgenic plants expressing N-terminally fused eGFP-AHR11 in the *ahr11* background must be generated to detect the localization of functional AHR11 protein in the future.

4.2 Function of AHR11 in plants

4.2.1 AHR11 protein

AHR11 (*At5g13590*) is a single copy gene located on chromosome V in *Arabidopsis thaliana*, which encodes a 129-kD protein (1168 aa) with unknown function (<http://www.arabidopsis.org>). The protein sequence similarity analysis performed by using BLINK (BLAST Link) at NCBI (National Center for Biotechnology Information) indicated that 247 proteins sharing similar sequence with AHR11 were detected in 126 species, including bacteria, fungi, plants and metazoans (Figure 4-1), and a C-terminal region (from 800 to 1168) is conserved across these species. The genomes of bacteria (e.g. *Arthrobacter sp.*) or of fungi (e.g. *Aspergillus ruler*) have one or two copies of genes encoding the conserved region, while in metazoans and plants the number of similar proteins ranges from single copy up to multiple copies, but do not largely diversify (Figure 4-2).

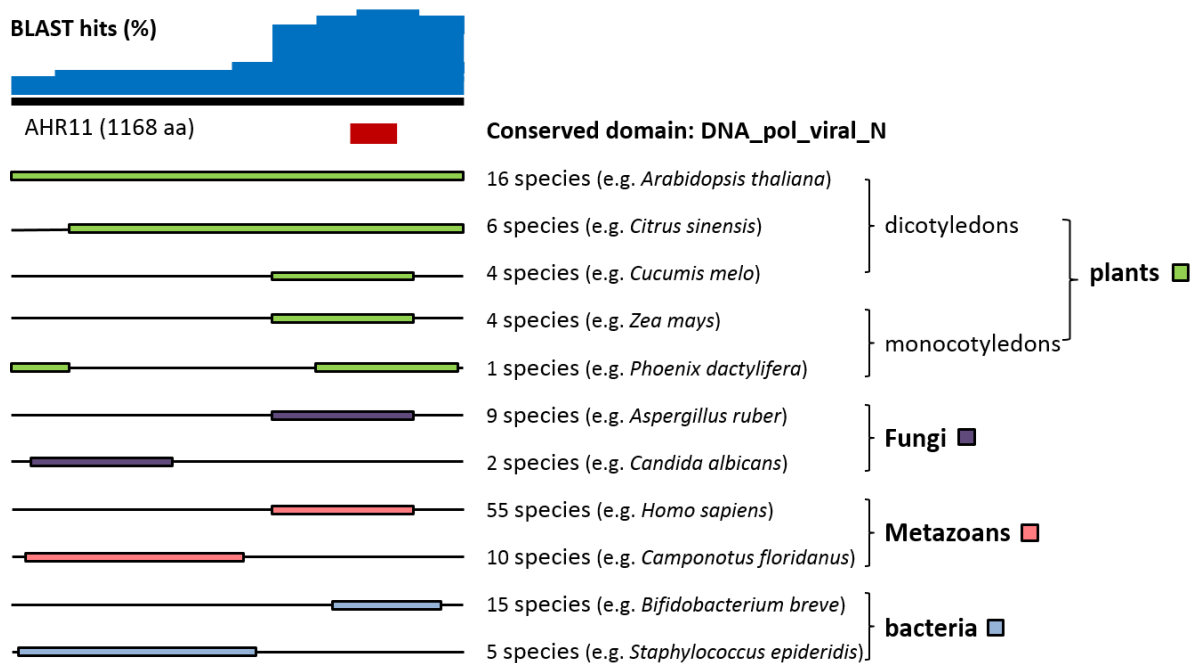


Figure 4-1: Similarity analysis of AHR11 protein in the kingdom

Similar protein sequences of AHR11 in the kingdom were found by a BLAST search against the protein non-redundant database by using BLINK at NCBI. The percentage of BLAST hits is presented as blue-box on the top. The colored column indicates the typical location of conserved region in each species to AHR11 protein. Conserved domain DNA_pol_viral_N is displayed in red bar. Modified from on-line BLINK of AHR11 protein.

According to NCBI-CDD database (National Center for Biotechnology Information-Conserved domain database), a conserved domain DNA_pol_viral_N (DNA-polymerase N-Terminal domain of virus; accession: cl02825) was found in this C-terminal conserved region (aa: 848-995), having been

identified in superfamily member of pfam00242, which contains a number of DNA polymerase from viruses such as Hepatitis B virus (HBV) (Grethe et al., 2000, Huy et al., 2004), woodchuck hepatitis virus 7 (Cohen et al., 1988) and wood chuck monkey hepatitis B virus (Lanford et al., 2003). It is already known that the DNA polymerase N-terminal domain of P protein in duck HBV (DHBV) is composed of a hepadnavirus-specific terminal protein domain (TP), which was identified as a (-)-DNA linker, and a highly variable spacer domain. Together with the C-terminal polymerase/reverse transcriptase (RT) domain, the P protein primes reverse transcription during virus replication (Bartenschlager and Schaller, 1988, Beck and Nassal, 2007). Compared to C-terminal region, the N-terminal region of AHR11 is less conserved. Only several proteins of bacteria (e.g. *Staphylococcus epideridis*), of fungi (e.g. *Candida albicans*) and of metazoans (e.g. *Camponotus floridanus*) display similarity to the N-terminal region of AHR11 (Figure 4-1), which are predicted as histone demethylase, otogelin-like proteins, or mucin-like proteins. The full length protein of AHR11 is highly conserved in dicotyledons, but not in monocotyledons. Therefore, it seems like that the C-terminal region of AHR11 might have a function of DNA binding, and has been preserved in the course of evolution, and that a new function domain is combined to the N-terminus of conserved domain in dicots radiation.

To research the biological function of N-terminal region of AHR11, the peptide alignment among orthologs of AHR11 and function domain predictions were performed. As shown in Figure 4-3, a highly conserved region (²³⁵NRE(S/T)NWDLNTTMDV(A)WE²⁴⁹) is present in AHR11 orthologs from 7 dicotyledons. This conserved region might be preserved during evolution for some undiscovered functions. The W²⁴⁸-to-STOP mutation in *ahr11* mutant occurs at the C-terminal side of this region. According to the common sequence LxLxL (Ohta et al., 2001, Kagale and Rozwadowski, 2010), where 'x' is represented by any amino acid residue, two ethylene response factor-associated amphiphilic repression (EAR) motifs are found in the N-terminal region of AHR11 (²⁰⁸LNL²¹² and ³¹⁴LSLGL³¹⁸, respectively, Figure 4-4). EAR-motif is the most analyzed form of transcriptional repression motif, generally found in transcriptional regulators known to function as negative regulators (Kagale and Rozwadowski, 2010). Therefore, AHR11 is predicted as a novel EAR-repressor to regulate gene transcription.

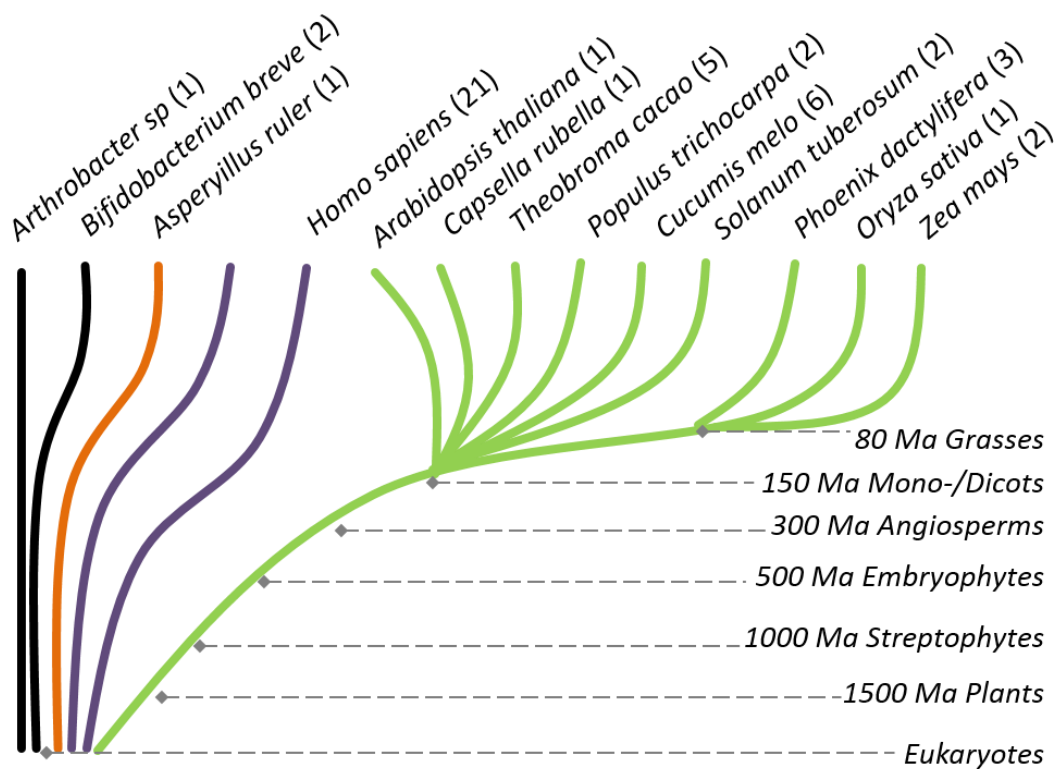


Figure 4-2: **Schematic evolutionary tree representing AHR11 radiation**

The estimated evolutionary timescale of plant diversification is indicated by dashed lines and given in million years [Ma] (Pires and Dolan, 2012). The organisms representing different kingdoms in the tree are: *Arthrobacter sp.* and *Bifidobacterium breve*, Bacteria (brown); *Aspergillus ruler*, Fungi (sand); *Drosophila melanogaster* and *Homo sapiens*, Metazoans (purple); the dicots *Arabidopsis thaliana*, *Capsella rubella*, *Theobroma cacao*, *Populus trichocarpa*, *Cucumis melo*, *Solanum tuberosum*; and the monocots *Phoenix dactylifera*, *Oryza sativa*, *Zea mays* (green). The numbers in parentheses represent the number of genes with the C-terminal conserved region of AHR11 in the corresponding species.

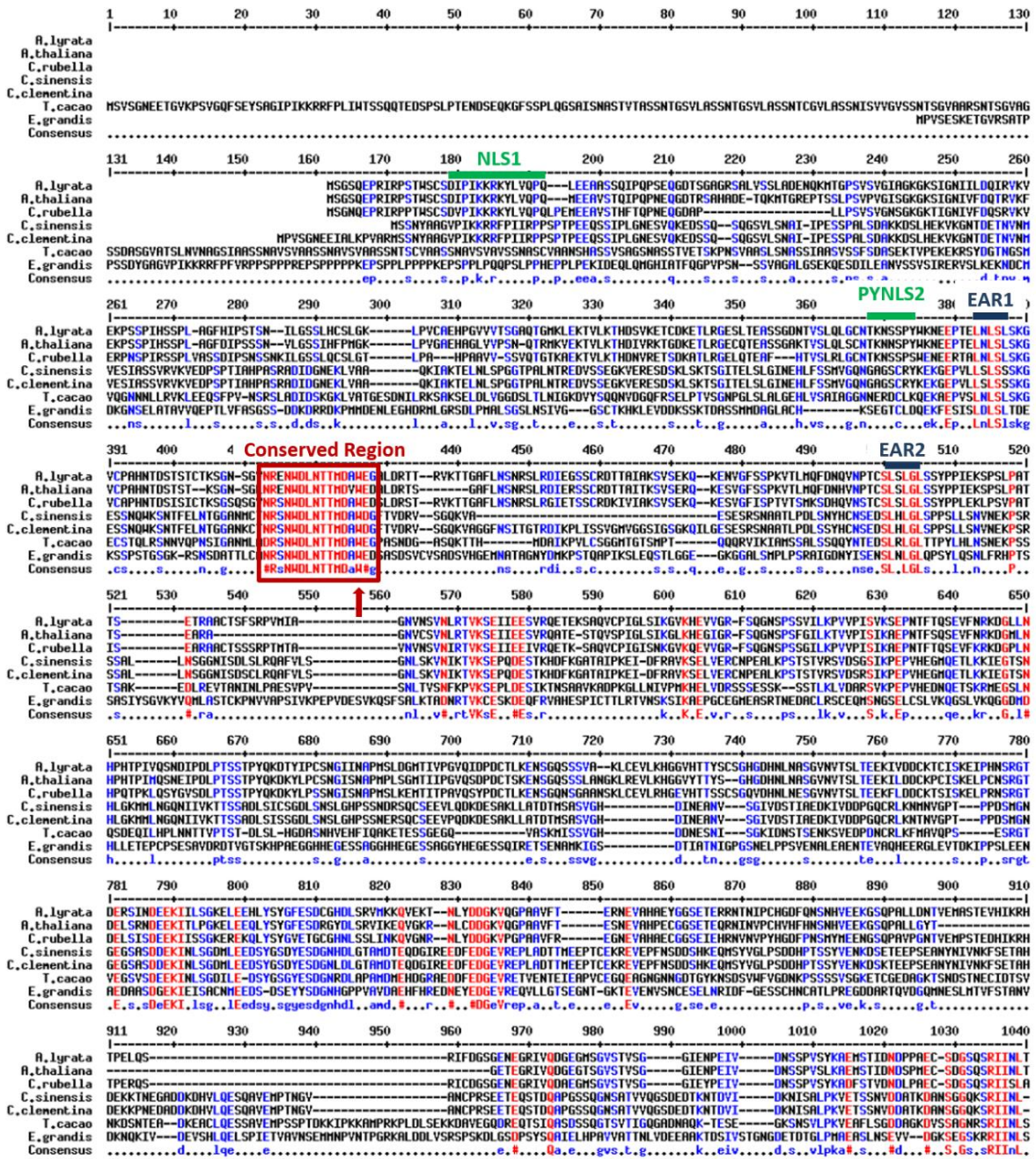


Figure 4-3: Alignment of amino acid sequences of AHR11 orthologs from different species

The amino acid sequence alignment of AHR11 orthologs from 7 species was performed using the online tool MultAlin (<http://multalin.toulouse.inra.fr/multalin/>). The consensus sequence is presented in the bottom line in which the red color signifies the conserved amino acid residues with high consensus value (90%) and the blue color indicates the low conserved amino acid residues with low consensus value (50%). The typical domains of AHR11 are indicated: NLSs (green), EAR-motifs (blue), N-terminal conserved region (red) and C-terminal domain DNA_pol_vial_N (purple). The red arrow points out the W²⁴⁸-to-Stop mutation in *ahr11*.

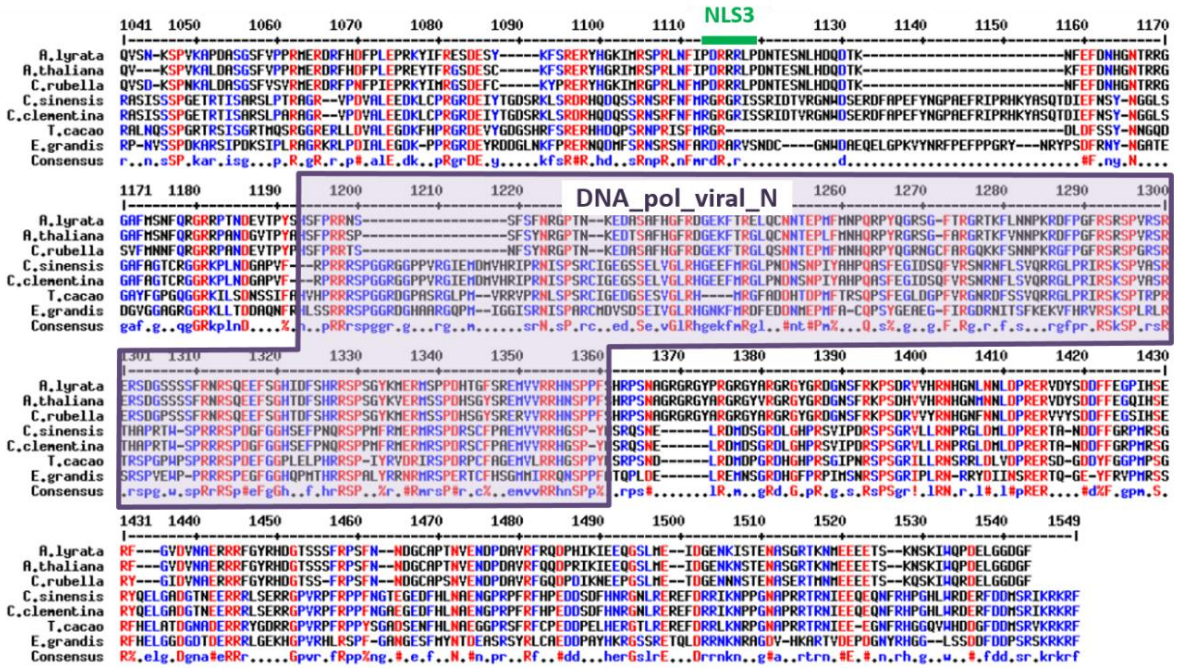


Figure 4-3: Alignment of amino acid sequences of AHR11 orthologs from different species (continued)

In addition, AHR11 is predicted to localize to the nucleus by SubCellular Proteomic Database SUBA3 (Tanz et al., 2013) but was also detected in the *Arabidopsis* plasmodesmal proteome (Fernandez-Calvino et al., 2011). Nuclear localization signal (NLS) is consensus sequence of the nucleus-localized proteins and is recognized by import receptors termed karyopherins or importins. As shown in Figure 4-2, three putative NLSs of AHR11 are respectively defined as NLS1 (¹⁸DIPIKKRKYLVQ²⁹), PYNLS2 (¹⁹⁴KNNSPY¹⁹⁹), and NLS3 (⁷⁹³PDRRRLLP⁷⁹⁹). Based on the conventional sequence similarity search (WoLF PSORT, <http://wolffpsort.org/>), NLS1 and NLS3 were predicted to be required for nuclear importing in WoLF PSORT (Horton et al., 2007), while in cNLS Mapper program (<http://nls-mapper.iab.keio.ac.jp>) only the NLS1 was announced as a functional nuclear localization sequence being specific to the importin α/β pathway (Kosugi et al., 2009). PYNLS2 was defined as a karyopherin-recognized NLS termed the PY-NLS for its crucial amino acid residues PY at the C-terminus in yeast (Lange et al., 2008). While only weak GFP signal was detected from eGFP-fused AHR11 protein in protoplast system, the truncated version Δ ahr11, which contains two predicted NLSs (NLS1 and PYNLS2), predominantly localized to nucleus when fused to eGFP (Figure 3-29). Therefore, NLS1 and/or PYNLS2 are probably also sufficient to target AHR11 into the nucleus. However, the localization of wild type AHR11 still needs to be confirmed.

In summary, the C-terminal domain DNA_pol_viral_N of AHR11 is preserved among AHR11 orthologs and predicted a DNA-binding domain, where another N-terminal region with unknown function is highly conserved in dicot AHR11 orthologs. The combination between N-terminal and C-terminal domains is a specific event in the course of dicots evolution. The NLSs lead to a possibility to import AHR11 into nucleus, and EAR-motifs imply AHR11 as an EAR-repressor of gene transcription repression.



Figure 4-4: Conserved domains of the AHR11 protein

The conserved region of AHR11 orthologs is presented in red color. The red arrow points out the W²⁴⁸-to-Stop mutation in *ahr11* mutant. The nuclear localization signals (NLSs) and EAR-motifs are indicated using green color and blue color, respectively. Three NLSs were predicted using different software and the sequences published by Lange et al. (2008): NLS1: ¹⁸DIPIKRRKYLVQ²⁹ according to WoLF PSORT (<http://wolffpsort.org/>) and cNLS Mapper (<http://nls-mapper.iab.keio.ac.jp>); PYNLS2: ¹⁹⁴KNNSPY¹⁹⁹ according to Lange et al. (2008); and NLS3: ⁷⁹³PDRRRLP⁷⁹⁹ according to WoLF PSORT (<http://wolffpsort.org/>). The EAR-motifs (EAR1: ²⁰⁸LNLSL²¹² and EAR2: ³¹⁴LSLGL³¹⁸) represent EAR-motifs characterized by the sequence of LxLxL (Kagale and Rozwadowski, 2010). In the truncated Δ ahr11 protein, only NLS1, PYNLS2 and EAR1 are present.

4.2.2 AHR11 negatively regulates ABA-induced gene expression

Both the *ahr11* mutant where only a premature translated AHR11 (Δ ahr11) may be present and its T-DNA knockout alleles Δ 476 and N804 displayed a hypersensitive activation of the ABA-reporter construct *pATHB6::LUC* in response to water deficit stress and to exogenous ABA. In order to test the possibility that the hypersensitivity represents a *pAtHB6::LUC*-specific effect, the induction of another ABA-specific construct *pRD29B::LUC* by exogenous ABA was analyzed in protoplasts. *RD29B* is a dehydration- and ABA-inducible gene that contains two ABA-responsive elements (ABREs) in its promoter region (Uno et al., 2000). In protoplast system, the *pATHB6::LUC* ABA-reporter construct present in the genome of *ahr11* is not activated by ABA (Figure 3-10). One explanation seems to be the crucial role of the turgor pressure from cell wall for the activation of the *pATHB6::LUC* ABA-reporter construct. Therefore, the ABA-induced luciferase activity measured in protoplasts harboring the *pATHB6::LUC* constructs specifically results from the transfected *pRD29B::LUC* construct. Compared to Col-0 protoplasts, the *pRD29B::LUC* construct expression was more intensively induced

by exogenous ABA in protoplasts of *ahr11* (Figure 3-11A) and of T-DNA knockout lines (Figure 3-16), while transient ectopic expression of wild type *AHR11* in Col-0 protoplasts inhibited luciferase expression in the presence ABA by a factor of 3.6 (Figure 3-11D). Transient expression of *ABI2*, which encodes a negative regulator of ABA signaling, was sufficient to repress the activation of *pRD29B::LUC* by ABA in *ahr11* protoplasts (Figure 3-11B). These results indicate that *AHR11* functions as a negative regulator of ABA signaling pathway and analysis of *pATHB6::LUC* lines transformed with a *pAHR11::AHR11* constructs supports this view (Figure 3-12D).

4.2.3 Physiological function of *AHR11* under water deficit

Although *AHR11* negatively regulates ABA-induced gene expression, *ahr11* mutant did not always respond hypersensitively to ABA in the ABA-regulated physiological processes. The cotyledon stomata of *ahr11* were defective to close in their response to water deficit (Figure 3-20A) and the wild type response could be restored by applying ABA exogenously (Figure 3-20B). Further analyses of transpiration under well-watered long-day conditions and water loss from detached shoots, also indicate that the regulation of stomatal aperture is impaired in *ahr11*. *Ahr11* seeds display the unaltered, wild type-like sensitivity to ABA and to restricted water availability in germination (Figure 3-23), while the primary root elongation of *ahr11* seedlings was strongly inhibited by water deficit stress (Figure 3-24A). These results indicate that physiological responses to water deficit rather than responses to ABA are impaired in *ahr11* suggesting that the *AHR11* protein might function to affect both water deficit signaling upstream of the ABA perception and ABA-dependent gene expression.

4.2.3.1 *AHR11* affects ABA redistribution under water deficit stress

ABA biosynthetic enzymes including *ABA2/SDR1* (Cheng et al., 2002), *NCED3* (Barrero et al., 2006, Endo et al., 2008, Hao et al., 2009), and *AAO3* (Koiwai et al., 2004) are confined to vascular tissues, as well as guard cells (Bauer et al., 2013). Water deficit-induced ABA is biosynthesized in plant vasculature tissues, and subsequently redistributed to cells outside the vasculature including probably guard cells (Boursiac et al., 2013). Therefore, the local level of active ABA in plants depends not only on the rate of stress-induced biosynthetic ABA formation, but also on ABA translocation. The analysis of ABA content of the stressed *ahr11* shoots (Figure 3-30A) revealed that the shoot ABA biosynthesis is induced by water deficit in the *ahr11* mutant to a degree also observed in wild type shoot, and *NCED3* transcript abundance exhibited a corresponding increase (Figure 3-30B). The hypersensitive ABA-reporter response in *ahr11* can thus not be explained by an increase in bulk leaf ABA levels while an affected ABA translocation from the synthesis sites to the perception sites cannot be ruled out. Figure 4-5 demonstrates the translocation of ABA facilitated by ABA transporters: ABA-exporter *ABCG25*, as well as ABA-importers *ABCG40* and *AIT1/NRT1.2* (Kuromori and Shinozaki, 2010, Kuromori et al., 2010, Kang et al., 2010, Kanno et al., 2012, Boursiac et al., 2013).

ABCG25 was identified as an ABA-exporter at ABA biosynthesis site, belonging to the WBC (white-brown complex) group of ABCG transporter subfamily (Kuromori and Shinozaki, 2010, Kang et al., 2010). The *ABCG25* over-expressing plants have a high leaf temperature phenotype compatible with

increased delivery of ABA to sites of perception (Kang et al., 2010). Under water deficit stress, ABA is synthesized in vascular parenchyma cells where the ABA-exporter ABCG25 then manages transport of ABA into the bundle sheath cell apoplast area outside the stele which is continuous with the mesophyll and epidermal cell apoplast (Kuromori et al., 2010, Shatil-Cohen et al., 2011), and where ABA is distributed passively with the flow of water directed to the sites of transpiration. Subsequently, ABA influx into guard cells is facilitated by ABA-importer ABCG40 to trigger stomatal closure (Kuromori and Shinozaki, 2010). ABCG40 belongs to the PDR (Pleiotropic drug resistance) group of ABCG transporter subfamily, and is detectable in many tissues but preferentially expressed in guard cells and targeted to the plasma membrane there (Kang et al., 2010). *atabcg40* knockout mutants are insensitive to ABA with respect to stomatal closure. And the expression of ABA-inducible genes is delayed in the *atabcg40* mutant indicating that ABCG40 is important for rapid ABA-mediated stress responses (Kang et al., 2010). In addition, AIT1/NRT1.2 was identified recently and shown to be an ABA-importer located in the vascular tissues (Kanno et al., 2012). The *ait1* mutant showed a decreased ABA response in dormancy, and decreased stomatal closure. Thus the possible function of AIT1/NRT1.2 is to retrieve excess ABA from the apoplast into bundle sheath cells to maintain the ABA pool size at the site of biosynthesis and also to facilitate ABA influx into guard cells (Kanno et al., 2012).

In *ahr11* mutant, the shoot expression of ABA-importers (both *ABCG40* and *AIT1/NRT1.2*) were strongly increased by water deficit stress, compared to the expression extent in wild type, while the expression of ABA-exporter was down-regulated by water deficit stress but undistinguishable between *ahr11* and wild type (Figure 3-34). ABA *in vivo*-imaging revealed that ABA action was not detectable in cotyledon guard cells under water deficit, while mesophyll cells and epidermal cells responded strongly (Figure 3-32). This finding could explain the observed insensitivity of *ahr11* stomata to water deficit and the hypersensitive response of ABA-reporter. Because of the high expression of ABA-transporters in *ahr11* under water deficit stress, it is now suggested that the AHR11 represses transcription of ABA-transporters to prevent ABA uptake thereby ensuring that sufficient ABA arrives at the guard cells. Although the same amount of ABA is synthesized in shoot of *ahr11* and wild type, ABA is predominantly taken up and not released by mesophyll and epidermal cells in *ahr11* causing enhanced activation of the ABA-reporter. A concomitant ABA deficit in guard cells impairs the response of stomata to water deficit. However, when ABA was supplied exogenously, enough ABA is available to the apoplast surrounding stomata guard cells to allow *ahr11* guard cells to take up sufficient hormone to initiate stomatal closure. The faster ABA-induced stomatal closure in *ahr11* (Figure 3-21C) suggests the enhanced hormone uptake or increased hormone response in *ahr11*. This might be interpreted such that AHR11 exerts an inhibitory effect on expression of ABA-transporters including guard cells. Accordingly, *ahr11* guard cells might have an enhanced capacity to take up ABA which, however, does not compensate the effect of enhanced ABA retrieval from the apoplast on its way from the vasculature to the guard cells.

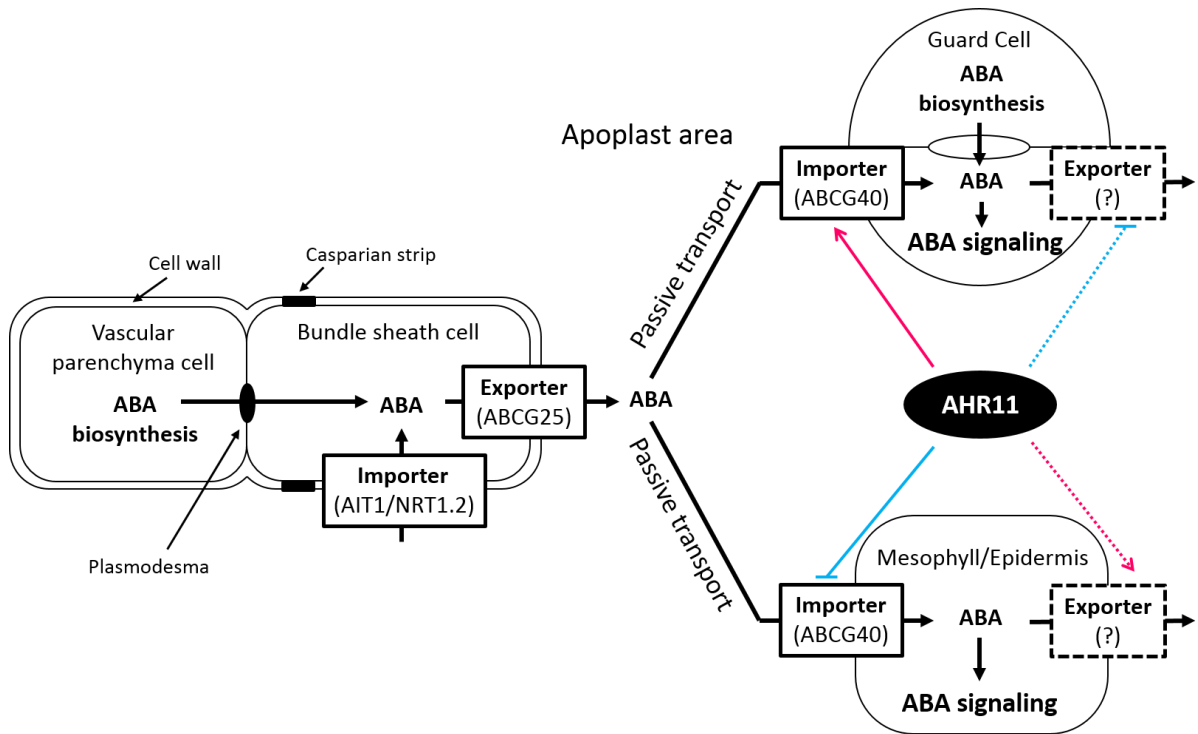


Figure 4-5: Schematic view of hypothetical function of AHR11 in ABA intercellular transmission

ABA is synthesized in vascular parenchyma cells, as well as guard cells. ABCG25 functions as an ABA-exporter at ABA biosynthesis site (Kuromori and Shinozaki, 2010, Kang et al., 2010). The ABA is transmitted into the bundle sheath cells and released into the apoplast outside the stele, then imported by ABA-importer ABCG40 into guard cells and mesophyll cells/epidermis (Kuromori and Shinozaki, 2010). AIT1/NRT1.2 ensures ABA remaining in vascular tissue (Kanno et al., 2012). In addition, the potential ABA-exporters might manage ABA export from guard cells and mesophyll cells. The hypothetical role of AHR11 is to affect ABA translocation by regulating the expression of ABA-transporters. The mutation of AHR11 in *ahr11* mutant leads to the dislocation of ABA under water deficit stress.

It was reported recently that guard cells may autonomously synthesize ABA to promote stomatal closure (Bauer et al., 2013). However, the ABA response appeared not to be significantly triggered in *ahr11* guard cells under our experimental conditions given a limited degree of reporter activation and an impaired response of stomata to restricted water availability. These findings would be interpreted that the guard cell-synthesized ABA in *ahr11* is not sufficient for closure or exported from guard cells by unidentified ABA-exporters. Since the discovery of ABCG25 and ABCG40, the ABCG group members of ABC transporter family are strong candidates for ABA transporters. Several ABCG proteins have also been reported to be involved in drought and salt tolerance, e.g. ABCG36 (Kim et al., 2010a) and ABCG22 (Kuromori et al., 2011), but the substrates transported by them have not been determined. Therefore, these results imply the existence of the undiscovered ABA-transporters, which might be positively and/or negatively regulated by AHR11 in mesophyll cells and/or guard cells. I would speculate here that the expression of guard cell-specific ABA-exporter(s) is repressed by AHR11, and released in *ahr11* mutant.

Further important physiological processes regulated by ABA translocation are preventing of premature germination during seed development (Kanno et al., 2010) and initiation and maintenance of dormancy during seed maturation and imbibition (Ali-Rachedi et al., 2004, Lee et al., 2010). A seed coat bedding assay has proven the maternal ABA translocation from dormant seed coat to non-dormant embryo to keep dormancy (Lee et al., 2010, Lee and Lopez-Molina, 2013). The ABA-transporter mutants or over-expressing lines displayed normal ABA-involved germination phenotypes (Kanno et al., 2012, Kuromori et al., 2010). In this work, fresh *ahr11* seeds were found to contain higher concentrations of ABA than wild type (Figure 3-31), and displayed a deep dormant phenotype (Figure 3-22). According to data from the Arabidopsis eFP Browser (Winter et al., 2007, Bassel et al., 2008), *AHR11* is relatively lowly expressed in immature seeds but highly expressed in dry seeds (Figure 4-6 and Figure 4-7) and is degraded after imbibition in water (Figure 4-8), which is faster than the parallel degradation of *ABI5* (Figure 4-8).

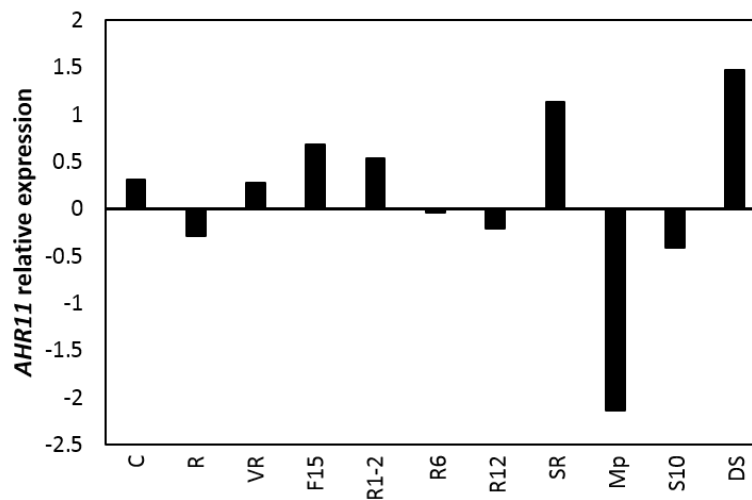


Figure 4-6: Expression pattern of *AHR11* during *Arabidopsis thaliana* Col-0 plant development

The log₂ ratio of *AHR11* expression compared to reference gene *UBC9* (*At4g27960*) in different developmental tissues was obtained from the eFP Browser website (http://bar.utoronto.ca/efp_arabidopsis/cgi-bin/efpWeb.cgi; Winter et al., 2007, Bassel et al., 2008,). RNA was isolated from samples in indicated conditions and analyzed on the ATH1 GeneChip. C = Cotyledon; R = Root; VP = Vegetative rosette; F15 = Flower stage 15; R1-2 = Rosette leaf 1+2; R6 = Rosette leaf 6; R12 = Rosette leaf 12; SR= Senescing rosette leaf; MP = Mature pollen; S10 = Seed stage 10; DS = Dry seed.

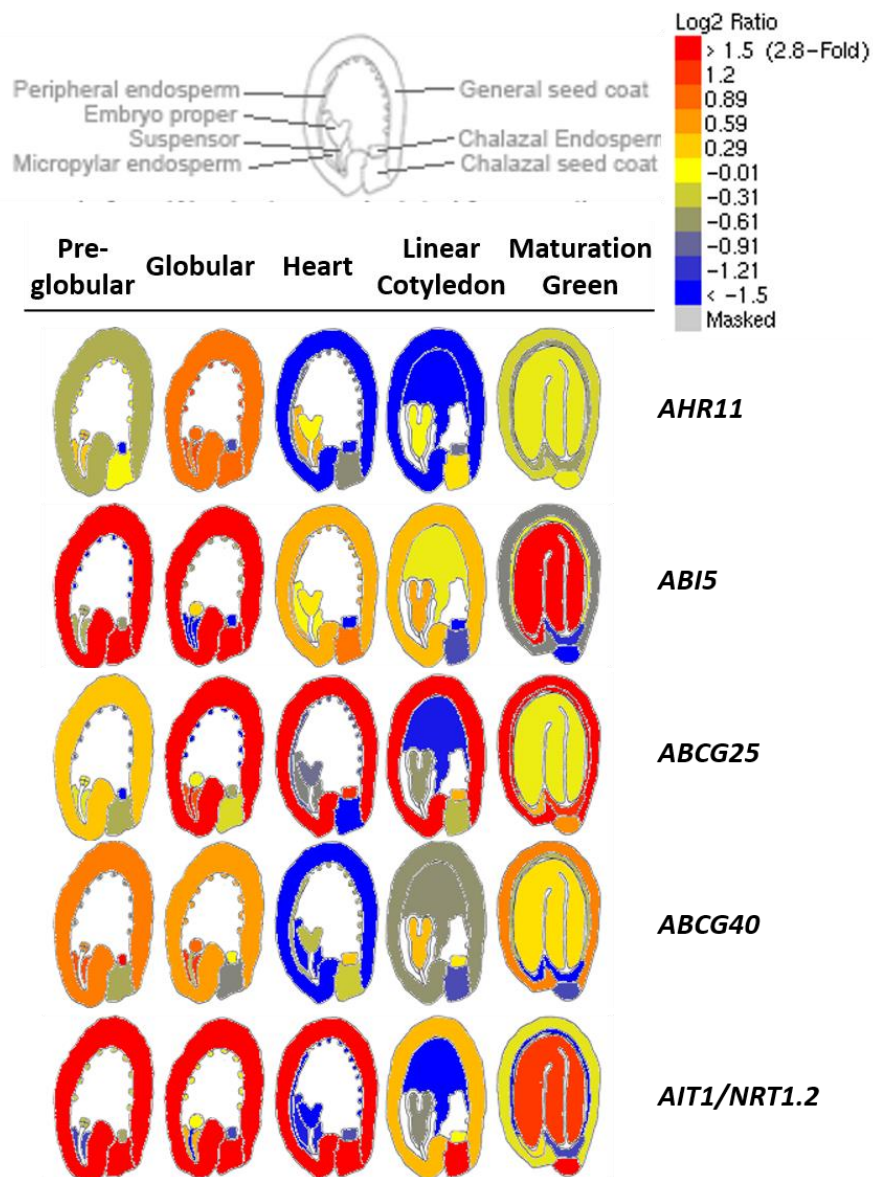


Figure 4-7: Gene expression pattern during seed development

False-color image indicates the relative expression level of *AHR11*, *ABI5*, *ABCG25*, *ABCG40* and *AIT1/NRT1.2* compared to reference gene *UBC9* (At4g27960) during seed development, modified from the output of eFP Browser search (http://bar.utoronto.ca/efp_arabidopsis/cgi-bin/efpWeb.cgi; Winter et al., 2007, Bassel et al., 2008). The signal threshold (log₂) is set to 1.5.

The expression pattern of ABA-transporters was also analyzed. During seed development *ABCG40* is lowly expressed, while *ABCG25* starts accumulation in seed coat from globular stage till seed maturation (Figure 4-7). *AIT1/NRT1.2* is expressed in seed coat at early stage of seed development and highly accumulate in embryo of matured seed, sharing similar expression pattern with *ABI5* (Figure 4-7). *AHR11* accumulates when seeds are after-ripened and in dry seeds (Figure 4-8), where ABA-transporters are low expressed. While expressions of *ABCG25* and *ABCG40* are depressed after imbibition, *AIT1/NRT1.2* is slightly increased, accompanied by degradation of *AHR11* and *ABI5* (Figure

4-8). Therefore, it seems like that ABCG25 acts to export ABA from seed coat, while AIT1/NRT1.2 functions to import ABA into embryo to initiate dormancy at late stage of seed development, and ABCG40 has minor function in this process. Because of the important role of ABA transport for seed development, low expression of AHR11 during seed development would help to induce ABA-transporters to manage ABA transport. Accordingly, high expression of ABA-transporters in *ahr11* leads to an excess of ABA in *ahr11* embryo generating a deep dormant phenotype. However, this model is of course speculative and requires further experimental evidence with respect to ABA-transporters expression and ABA transport during seed development and imbibition.

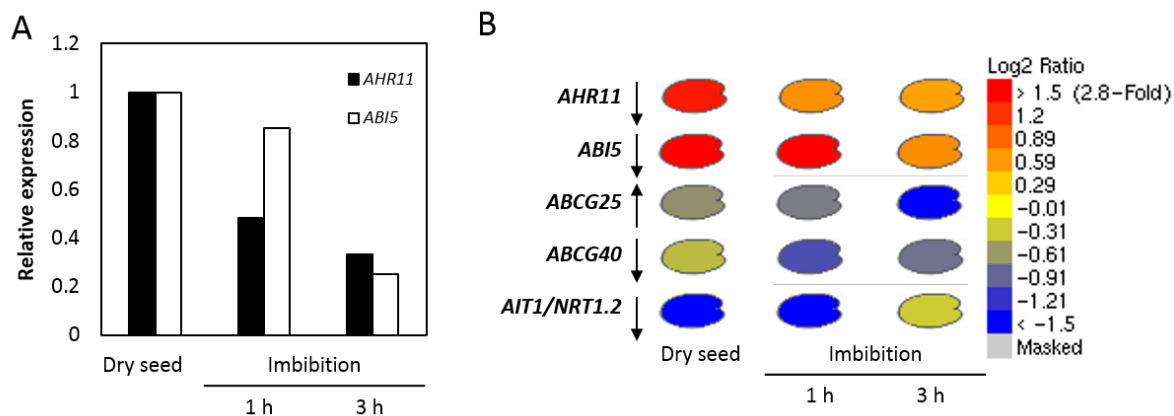


Figure 4-8: **Gene expression pattern during imbibition**

Relative expression value of target genes compared to reference gene *UBC9* (*At4g27960*) is obtained from eFP Browser website (http://bar.utoronto.ca/efp_arabidopsis/cgi-bin/efpWeb.cgi; Winter et al., 2007, Bassel et al., 2008). Seeds for germination were after-ripened 2-4 months and not stratified. RNA was isolated from samples in indicated conditions and analyzed on the ATH1 GeneChip. (A) Relative expression of *AHR11* (black) and *ABI5* (white) in Col-0 seeds during imbibition. The log₂ values of *AHR11* and *ABI5* in dry seed are 1.35 and 2.66, respectively, and set to 1. (B) Expression pattern of *AHR11*, *ABI5*, *ABCG25*, *ABCG40* and *AIT1/NRT1.2* during Col-0 seed imbibition indicated in false-color image. Signal threshold (log₂) is set to 1.5.

4.2.3.2 AHR11 functions in the *aba2-1* and *abi1-1* background

The function of AHR11 in ABA signaling was further studied by crossing *ahr11* to the ABA-deficient mutant *aba2-1* and to the ABA-insensitive mutant *abi1-1*, respectively. *aba2-1* is ABA-deficient due to a lesion in the ABA biosynthesis enzyme ABA2/SDR1 (Leon-Kloosterziel et al., 1996), and is therefore ABA-insensitive to water deficit, while the ABA signaling pathway is undisturbed in *aba2-1* allowing the mutant to respond to exogenous ABA. Analysis of germination under water stress conditions of the double mutant *ahr11/aba2-1* verified that the enhanced water deficit sensitivity observed in *ahr11* is dependent on ABA biosynthesis, supporting a role of AHR11 downstream of ABA biosynthesis. *abi1-1*, is a dominant ABA-insensitive mutant with a single amino acid exchange in ABI1 (Koornneef et al., 1984, Leung et al., 1994, Meyer et al., 1994). The mutation impairs the interaction between *abi1-1* and RCARs (Santiago et al., 2009a, Ma et al., 2009) and *abi1-1* mutant is therefore dominantly insensitive to the hormone signal. In our experimental conditions, 1 μM ABA was sufficient to inhibit

germination of wild type *pATHB6::LUC* and *ahr11* single mutant, not of *abi1-1/pATHB6::LUC* mutant, but 10 μ M ABA is successfully block the seed germination of *abi1-1/pATHB6::LUC* (Figure 3-28D). It implies that *abi1-1* is not fully blocking the ABA response, but shifting the ABA sensitivity to a high concentration. Therefore, the water deficit-inhibited germination on *abi1-1/pATHB6::LUC* (Figure 3-28B) might be also managed by the ABA-dependent pathway. However, the double mutant *ahr11/abi1-1* displayed a high germination rate under severe water deficit stress (65.7% under -1.0 MPa, Figure3-28B), providing strong evidence that AHR11 and ABI1 additively inhibit seed germination under water deficit stress. However, the molecular mechanism of AHR11 in this pathway is still unclear.

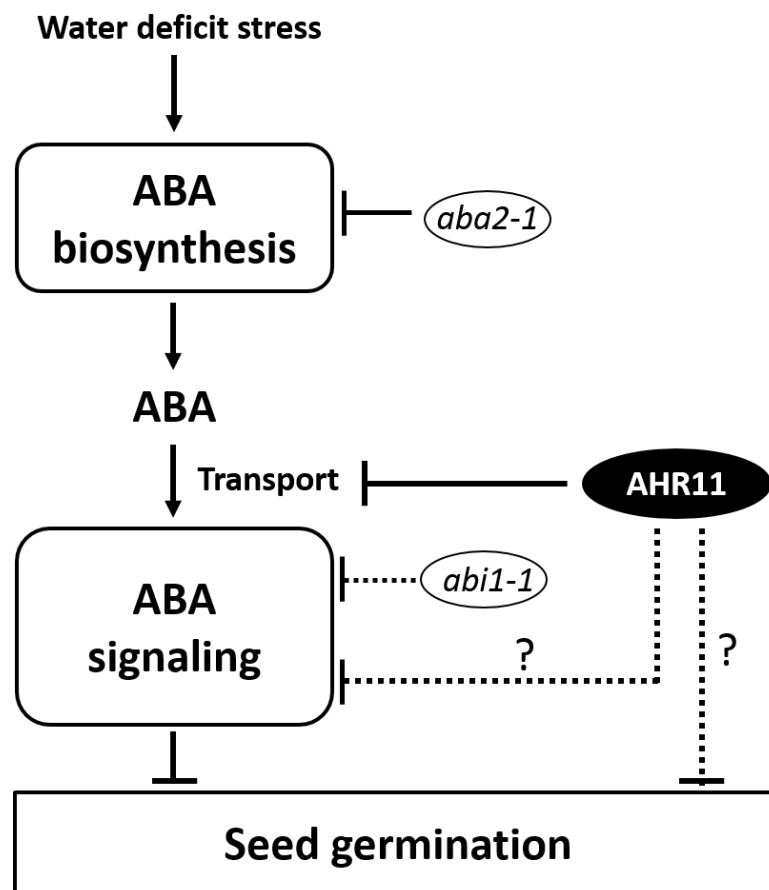


Figure 4-9: Hypothetical function of AHR11 in germination under water deficit stress

ABA biosynthesis is initiated by water deficit stress, and ABA subsequently actively transported intercellularly, activating the core ABA signaling pathway to inhibit seed germination. ABA-deficient mutant *aba2-1* blocks ABA biosynthesis and the ABA-dependent germination inhibition. ABA-insensitive mutant *abi1-1* inhibits ABA response signaling, but does not fully block this pathway. AHR11 acts as a negative regulator to repress active ABA transport, resulting in germination inhibition under water deficit stress. *ahr11* mutant enhances ABA transport, but additively contributes to the *abi1-1* effect in promoting germination under water deficit stress. The connection between AHR11 and ABA signaling is still unclear, and direct germination inhibition by AHR11 cannot be excluded.

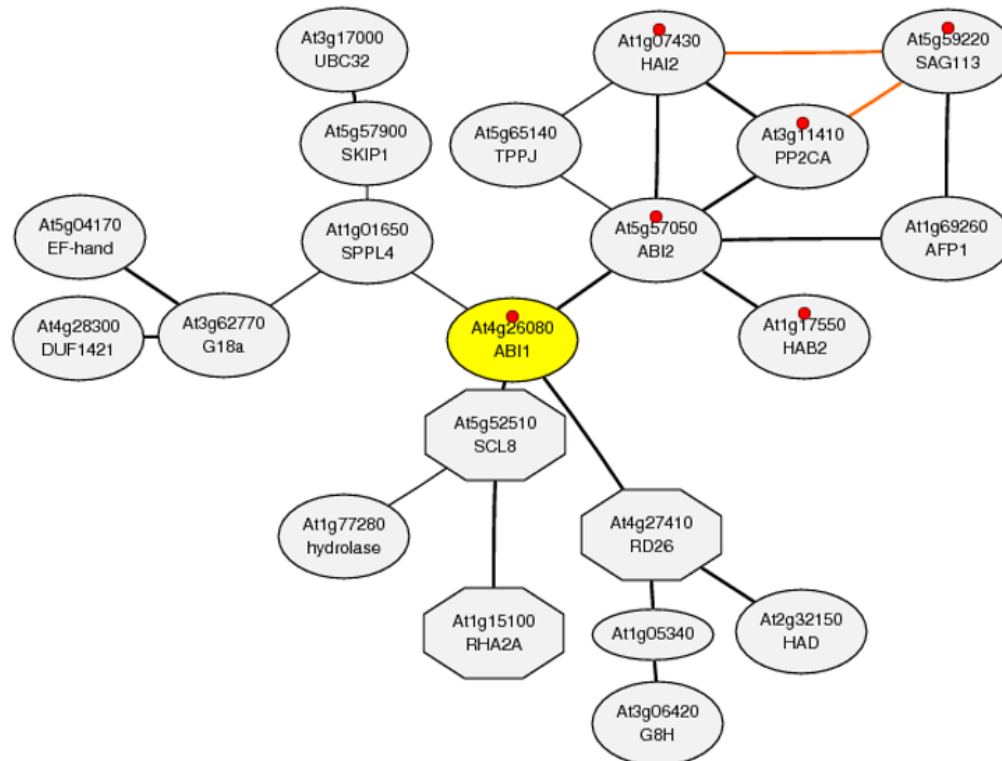
4.3 AHR11 as a component of a regulatory network

The output of water deficit signal transduction is dependent on the respective contribution of positive and negative regulators which are part of a protein-protein interaction network. In order to understand how AHR11 is integrated into this network, a yeast two-hybrid interactome screen was performed for AHR11-interacting partners.

4.3.1 Network of genes co-regulated with AHR11

Online tool ATTED-II ver.7.1 (<http://atted.jp>) is a database that provides co-regulated gene relationships based primarily on co-expression microarray data (Obayashi et al., 2009). Using information on *cis*-elements in promoters of co-expressed genes, co-regulation of genes is predicted. As a result of the ATTED-II database search, a network of genes with a high probability of being co-regulated with *AHR11* (Figure 4-11), as well as *ABI1* (Figure 4-12) for comparison, was obtained.

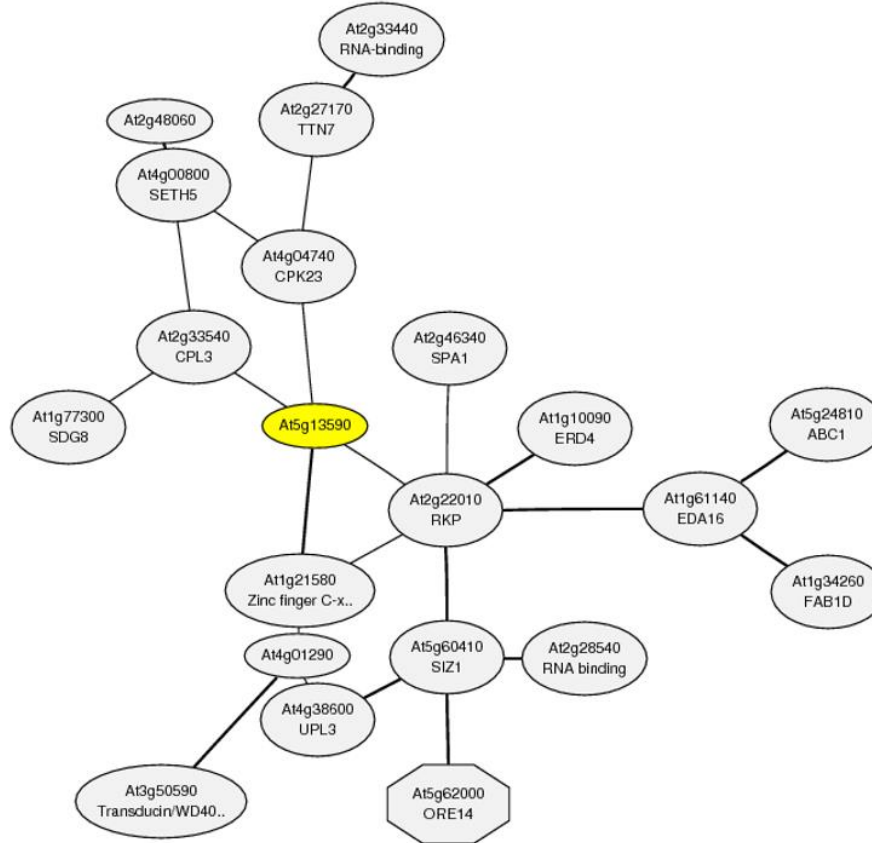
The clade A PP2C, ABI1, has been characterized as coreceptor of RCAR ABA receptors, negatively regulating ABA signaling pathway (Fuchs et al., 2012). *ABI1* locates in the center of the co-regulated gene network (figure 4-10), being surrounded by some related genes, in which five members of clade A PP2Cs are highlighted by red points, including *ABI2*, *SAG113*, *PP2CA*, *HAI2* and *HAB2*, and other important proteins are also involved, e.g. transcription factors including NAC TF *RD26* (MR 4.6) and homeodomain protein *HB7* (MR 5.7). Therefore, the co-regulated gene network efficiently indicates related-genes with similar function or with syntropic regulation. In the co-regulated gene network of *AHR11* (Figure 4-11), four genes with the highest co-regulation probability are directly connected to *AHR11*, including *At1g21580*, *RKP* (Related to KPC1 protein; *At2g22010*), *CPL3* (C-terminal domain phosphatase-like 3; *At2g33540*), and *CPK23* (Calcium dependent protein kinase 23; *At4g04740*).



Rank	MR ^a	Locus	Gene annotation
1	1.7	At5g57050	Protein phosphatase 2C family protein (ABI2)
2	4.6	At4g27410	NAC transcriptional regulator (RD26)
3	4.6	At5g52510	SCARECROW-like 8 (SCL8)
4	4.7	At5g59220	highly ABA-induced PP2C gene 1 (SAG113)
5	5.5	At3g11410	protein phosphatase 2CA (PP2CA)
6	5.7	At2g46680	homeobox 7 (HB-7)
7	6	At1g07430	highly ABA-induced PP2C gene 2 (HAI2)
8	7.4	At1g17550	homology to ABI2 (HAB2)
9	7.8	At3g14440	nine-cis-epoxycarotenoid dioxygenase 3 (STO1)
10	8.5	At1g52890	NAC domain containing protein 19 (NAC019)

Figure 4-10: **ABI1** as part of a network of putatively co-regulated genes

ABI1 (*At4g26080*) is highlighted as a central component of a network of co-expressed genes which was constructed using ATTED-II ver.7.1 (<http://atted.jp>). Octagon-shape nodes represent transcription factors. Connection lines indicate the mutual rank value (MR^a value), which is the geometrically average value of two correlation ranks as a measure of gene co-expression. Bold connection lines: MR < 5; normal lines: MR < 30; thin lines: MR > 30. List of ten genes with the highest co-regulation probability are listed at the bottom.



Rank	MR ^a	Locus	Gene annotation
1	2.8	At1g21580	CCCH type Zinc finger family protein
2	6.6	At2g22010	RING E3 ubiquitin ligase related to KPC1 (RKP)
3	8.8	At2g33540	C-terminal domain phosphatase-like 3 (CPL3)
4	11.7	At4g04740	Calcium-dependent protein kinase 23 (CPK23)
5	12.2	At2g28540	RNA binding (RRM/RBD/RNP motifs) family protein
6	13.3	At5g04560	HhH-GPD base excision DNA repair family protein (DME)
7	17.9	At5g46470	Disease resistance protein (TIR-NBS-LRR class) family (RPS 6)
8	20.8	At2g37840	Protein kinase super-family protein
9	21.2	At2g20050	Protein serine/threonine phosphatase; cAMP-dependent protein kinase regulator
10	21.3	At5g62000	Auxin response factor 2 (ARF2)

Figure 4-11: **AHR11** as part of a network of putatively co-regulated genes

AHR11 (At5g13590) is highlighted as a central component of a network of co-expressed genes which was constructed using ATTED-II ver.7.1 (<http://atted.jp>). Octagon-shape nodes represent transcription factors. Connection lines indicate the mutual rank value (MR^a value), which is the geometrically average value of two correlation ranks as a measure of gene co-expression. Bold connection lines: MR < 5; normal lines: MR < 30; thin lines: MR > 30. List of ten genes with the highest co-regulation probability are listed at the bottom.

The gene with the highest probability of being co-regulated with *AHR11*, *At1g21580*, encodes a member of the CCCH-type Zinc finger protein family. Proteins of this family contain 1 to 6 tandem zinc-binding motifs characterized by three cysteines followed by one histidine and are proposed to be RNA-binding proteins with regulatory functions in mRNA processing (Wang et al., 2008a), thereby playing important regulatory roles in diverse biological processes in plants (Li et al., 2001, Cheng et al., 2003, Sunkar and Zhu, 2004, Borsani et al., 2005, Kong et al., 2006, Lee et al., 2006a, Sun et al., 2007, Kim et al., 2008, Wang et al., 2008b, Guo et al., 2009, Deng et al., 2011). The CCCH-type zinc finger protein SOMNUS, for instance, is involved in light-dependent modulation of expression of ABA and GA metabolic genes thereby playing a role in regulation of seed germination (Kim et al., 2008), and two related zinc finger proteins AtSZF1 and AtSZF2 negatively regulate salt stress responses (Sun et al., 2007).

The RING-type E3 ubiquitin ligase *RKP* is a homolog of the human cell cycle regulator *KPC1*. In *Arabidopsis*, *RKP* is induced by the C4 protein from *Beet severe curly top virus* (BSCTV) during virus infection and regulates the host cell cycle by degrading the cyclin-dependent kinase inhibitor KRP1/ICK1 (Ren et al., 2008, Lai et al., 2009).

CPL3 encodes a RNA polymerase II (RNAP II) CTD phosphatase-like protein which plays a role in modulating RNAP II phosphorylation status during osmotic stress and thereby negatively regulates ABA responses (Koiwa et al., 2002, Bang et al., 2006). The core component of RNAP II not only catalyzes mRNA synthesis, but also regulates RNA processing including capping, splicing, and polyadenylation (Hirose and Manley, 2000). The activity of RNAP II is dependent on the phosphorylation status of the CTD domain, which is regulated by both CTD kinases and phosphatases (Palancade and Bensaude, 2003). Therefore, *At1g21580* and *CPL3* might point to a function of *AHR11* in regulation of mRNA synthesis, processing and degradation.

The calcium-dependent protein kinase CPK23 has been demonstrated to be involved in responses to drought and salt stresses (Ma and Wu, 2007). The *cpk23* mutant exhibits decreased stomatal aperture and a slowed-down water loss together with enhanced tolerance to drought and salt stresses (Ma and Wu, 2007). In guard cells, CPK23 action is relieved from ABI1 inhibition in the presence of ABA by inactivation of ABA in the RCAR-ABA-ABI1 receptor complex and subsequently results in phosphorylation and activation of SLAC1 at resting cytosolic Ca²⁺ concentrations, whereas its homolog CPK21 regulates SLAC1 activity in a calcium-dependent way (Geiger et al., 2010). Given the impaired stomatal regulation observed in *ahr11*, co-regulation of CPK23 and *AHR11* might reflect a functional connection of the two proteins in water deficit stress signaling.

4.3.2 Yeast two-hybrid interactome screen for interacting partners of *AHR11*

Since the yeast two-hybrid (Y2H) system was established (Fields and Song, 1989), it became one of the most efficient and popular tools for protein-protein interaction assays and recently, an improved high-throughput binary interactome mapping pipeline based on the Y2H system was used to generate a protein-protein interaction map for the interactome network of the plant *Arabidopsis thaliana* containing about 6200 highly reliable interaction between about 2700 proteins (*Arabidopsis*

Interactome Mapping Consortium, 2011). Recently, AHR11 was published as an interacting candidate of AtCSP3 (COLD SHOCK DOMAIN PROTEIN 3; At2g17870) in a classic Y2H screen (Sasaki et al., 2013). AtCSP3, sharing the cold shock domain (CSD) with bacterial cold shock proteins (CSDs), acts as a RNA chaperone to regulate freezing tolerance in *Arabidopsis thaliana* (Kim et al., 2009). However, the interaction between AtCSP3 and AHR11 could not be confirmed *in planta* (Sasaki et al., 2013).

To decipher the mechanism underlying AHR11-mediated gene regulation, interactome analysis of AHR11 using a high-throughput Y2H screen (Dreze et al., 2010) was performed. Because the full-length DNA binding domain (DB)-AHR11 fusion protein strongly activated the transcription of Y2H reporter genes irrespective of the presence of any activation domain (AD)-fusion protein (Figure 3-35), the AHR11 protein was fragmented in order to screen for interacting candidates. However, the fragmentation of AHR11 still could not prevent entirely autoactivation. We found that the combinations of AHR11 fragments containing the c-region (aa: 552-804) always exhibited autoactivation, except the c-region alone. It implies that the c-region might be important, but not sufficient, for transcription activation. Subsequently, AHR11 fragments were shown to interact with seven proteins, which were then classified into three groups according to their interaction region of AHR11, as well as the interaction intensity (Figure 3-37 and Figure 4-12). Group I includes JAM2 (Jasmonate-associated MYC2-like 2; AT1G01260) and dynein light chain (DLC) type 1 protein (AT1G23220), which display a strong interaction with the c-region (aa: 552-804) of AHR11 protein. Group II includes TPL (TOPLESS; AT1G15750), TPR2 (TOPLESS-related 2; AT3G16830), and SINAT-like protein (AT3G61790), which strongly bind the ab-region (aa: 1-554) of AHR11. Group III encompasses AT2G45260 and AT4G09060, two proteins with unknown function showing weak interaction with the ab-region (aa: 1-554). The interaction between AHR11 and AtCSP3 could not be detected in our screen, because AtCSP3 is not present in the library.

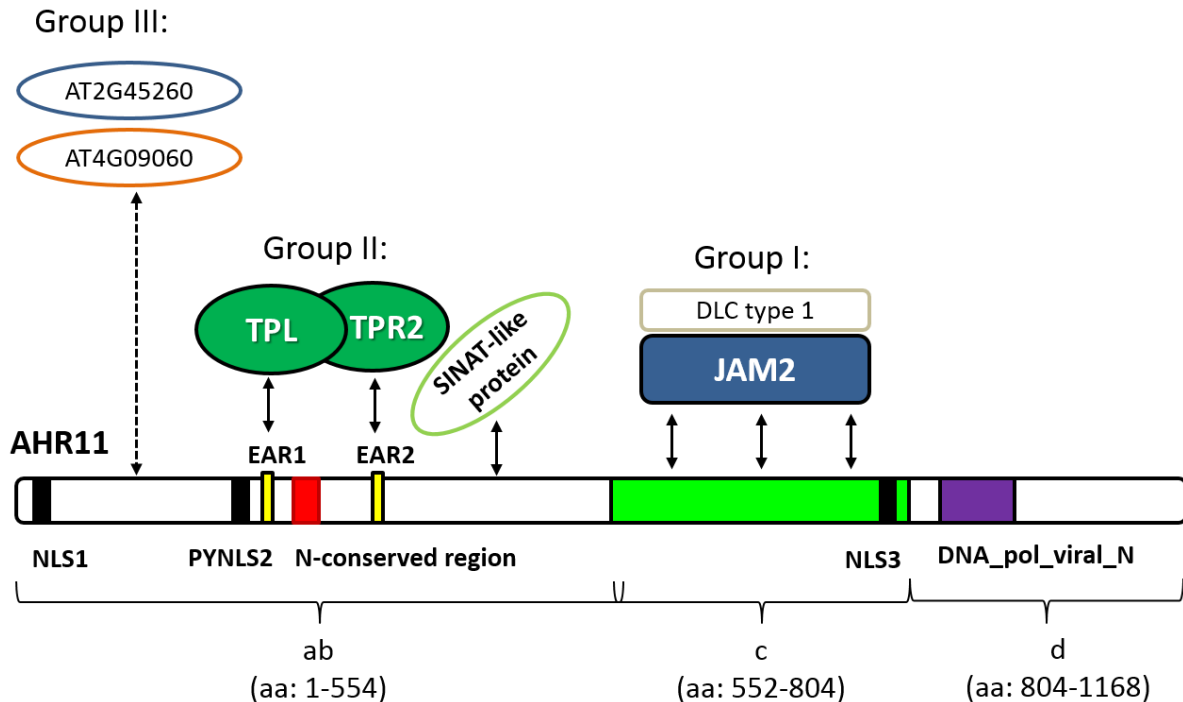


Figure 4-12: **Protein-protein interactions of AHR11**

AHR11 protein is presented as a white bar, and its predicted conserved domains are indicated by colored boxes, including NLSs (black), EAR-motifs (yellow), N-terminal conserved region (red), and C-terminal DNA_pol_viral_N domain (purple). Group I members of AHR11-interacting proteins, including JAM2 (AT1G01260) and DLC type 1 (AT1G23220), strongly interact with the c-region (aa: 552-804, green) of AHR11. Group II contains two proteins of TOPLESS/TPR protein family, TPL (AT1G15750) and TPR2 (AT3G16830), which are known to interact with EAR-motif, as well as a SINAT-like protein (AT3G61790) with predicted ubiquitin-protein E3 ligase activity. AHR11-interacting proteins of Group III, AT2G45260 and AT4G09060, show weak interaction with the ab-region (aa: 1-504) of AHR11. Solid arrow and dashed arrow indicate the strong interaction and weak interaction, respectively, in yeast.

4.3.2.1 JAM2 is a transcription factor in JA signaling and ABA signaling

JAM2, together with its homologs JAM1 and JAM3, has been identified as a jasmonate-associated MYC2-like transcription factor that negatively regulate jasmonic acid (JA) signaling (Sasaki-Sekimoto et al., 2013, Nakata and Ohme-Takagi, 2013, Nakata et al., 2013), in which the master regulator MYC2 (AT1G32640) positively regulates insect defense *via* the VSP2 pathway, while negatively regulates pathogen defense *via* the PDF1.2 pathway (Lorenzo et al., 2004, Kazan and Manners, 2013). Both MYC2 and JAMs belong to bHLH-TF family, sharing the C-terminal bHLH-domain, which is required for binding to specific *cis*-element G-box (CACGTG) and TF dimerization (Toledo-Ortiz et al., 2003, Heim et al., 2003). MYC2 contains an acidic region in amino-terminal domain (MYC_N), which is important for transcription activation (Nakata et al., 2013) (Figure 4-13A). The expression of JAMs is dependent on MYC2, while the expression of MYC2 is less regulated by JAMs. Therefore, MYC2 is functioning upstream of the JAMs, and the MYC2-induced JAMs and MYC2 competitively bind to G-box (CACGTG)

to regulate the expression of their common target genes, such as *VSP2*, *ANAC019* and *PAP1* in JA signaling (Sasaki-Sekimoto et al., 2013, Kazan and Manners, 2013) (Figure 4-13C).

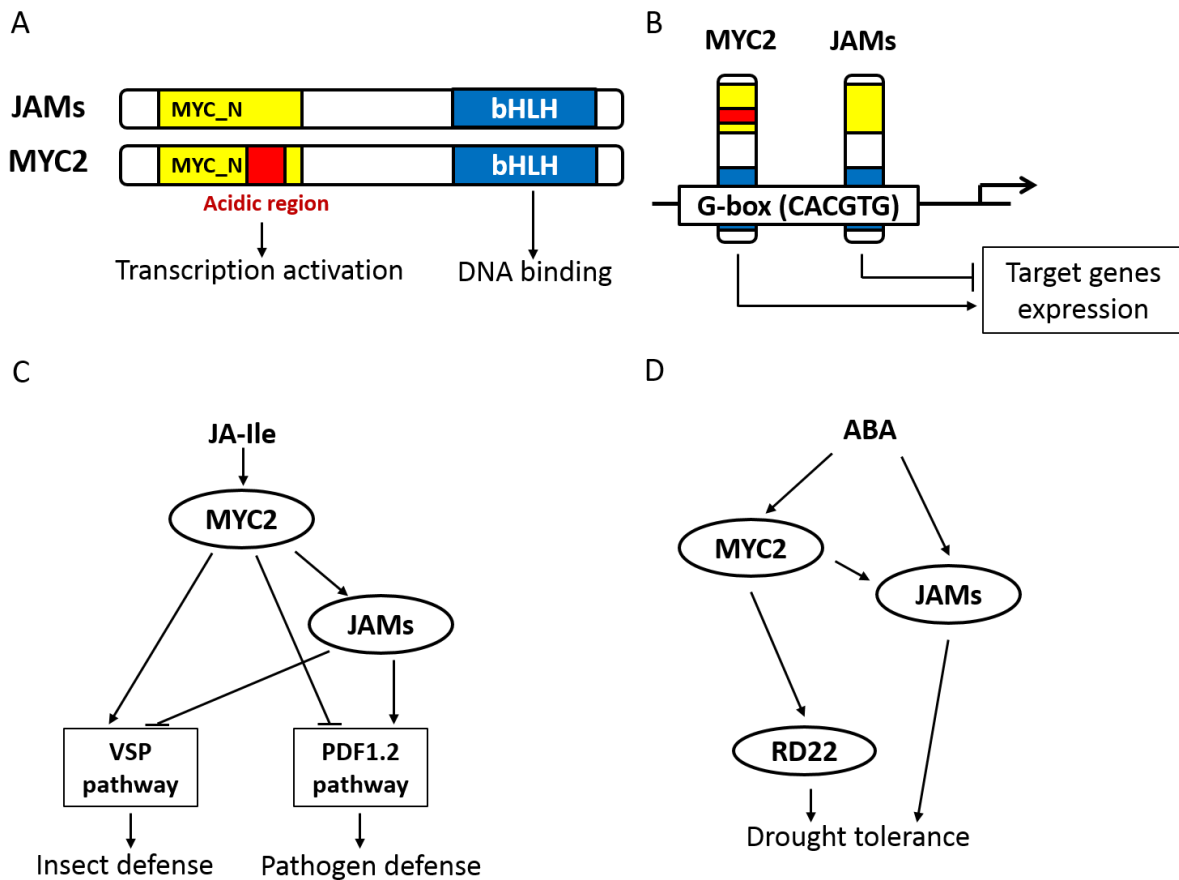


Figure 4-13: functions of MYC2 and JAMs in JA signaling and osmotic response

(A) bHLH-TFs MYC2 and JAMs (JAM1, JAM2 and JAM3) share the C-terminal conserved domain bHLH (blue) for DNA binding, but MYC2 has a specific acidic region (red) for transcription activation in MYC_N domain (yellow). (B) MYC2 and JAMs competitively binds to G-box (CACGTG) to activate and repress target genes expression, respectively. (C) MYC2 and JAMs antagonistically regulate JA signaling in insect and pathogen defense. (D) Both MYC2 and JAMs enhanced drought tolerance *via* ABA-dependent signaling pathway. Expression of *RD22* is activated by MYC2 (Abe et al., 1997, Abe et al., 2003), but not JAM1 (Li et al., 2007).

In addition, MYC2 has initially been characterized as a positive regulator of ABA-inducible genes under osmotic stress (Figure 4-13D), and functions cooperatively with MYB2 in transcriptional activation of *RD22*, a gene responsive to dehydration stress (Abe et al., 1997, Abe et al., 2003). Meanwhile, JAM1 was also named AIB (ABA-inducible bHLH transcription factor) for its positive regulation in response to ABA (Li et al., 2007). Correspondingly, ABA insensitivity was observed in the knockdown mutant *aib*, whereas JAM1/AIB over-expressing lines were hypersensitive to ABA in post-germination developments (Li et al., 2007). The MYC2-binding G-box (CACGTG) (Toledo-Ortiz et al., 2003, Heim et al., 2003) is also present in one type of ABA-responsive element G-box-like ABRE (G/ABRE: CACGTGGC), which is normally found in ABA/stress-inducible promoters, and is targeted by AREBs/ABFs/ABI5 (Choi et al., 2000). Therefore, it seems possible that bHLH-TFs, such as MYC2 and JAMs, compete with bZIP-

TFs, such as AREBs/ABFs/ABI5, for the G/ABRE binding sites to regulate target genes expression. As discussed in JA signaling, MYC2 is a transcriptional activator, but JAMs are a repressor, which might be caused by the presence/absence of the N-terminal acidic region. In ABA signaling, the regulation mechanism seems more indirect. Although the promoter region of *RD22* does not contain any ABREs, the dehydration-induced *RD22* expression is also activated by MYC2 *via* its G-box (Iwasaki et al., 1995), but not by JAM1 (Li et al., 2007). The target specificity of MYC2 and JAMs in ABA signaling is still unclear. In this work, the interaction between JAM2 and c-region (aa: 542-804) of AHR11 was found in yeast. Combination with the negative regulatory role of AHR11, we could speculate that AHR11 repress JAM2-targeted gene expression. However, it is still a matter of speculation whether AHR11 might have a general function as a regulator of activities of bHLH-TFs. It is necessary to analyze the molecular function of the interaction between AHR11 and JAM2, as well as other JAMs and MYC2 in future.

4.3.2.2 TPL/TPRs corepressor complex regulate general transcription repression

In this work, AHR11 has been identified as a novel EAR-motif protein, containing two predicted EAR-motifs: EAR1 in the a-region (aa: 1-247) and EAR2 in the b-region (aa: 248-544) (Figure 4-4). In addition, a conserved region (aa: 235-249) with unknown function is present between these two EAR-motifs. It is already known that EAR-motif proteins repress gene transcription *via* recruiting TOPLESS and TOPLESS-related transcriptional corepressors to target genes (Kagale et al., 2010). In yeast, the ab-region (aa: 1-544) of AHR11 strongly interacted with TPL (TOPLESS; AT1G15750) and TPR2 (TOPLESS-related 2; AT3G16830), while the a-region (aa: 1-247) or b-region (aa: 248-544) containing a single EAR-motif was impaired binding either TPL or TPR2. These results could imply that a single EAR-motif is not sufficient for AHR11 to recruit TPL/TPRs, which can be proved by inactivation of a EAR-motif in the ab-region. The EAR-motif surrounding sequence such as N-conserved region might also contribute to TPL/TPRs recruitment.

TPL and TPR2 belong to the TOPLESS co-repressor family (TPL/TPRs), and were initially identified as transcriptional corepressors that negatively regulate apical embryonic fate in *Arabidopsis* (Long et al., 2006). The C-terminal to lissencephaly homology (CTLH) domain of TPL directly binds to the EAR-motif located in the domain I of IAA12/BDL (Emes and Ponting, 2001, Szemenyei et al., 2008). The TPL-interactome analysis revealed that TPL/TPR corepressors predominantly interact directly with specific transcription factors (Causier et al., 2011). Many of which were previously implicated in transcriptional repression as EAR-repressors involved in diverse processes, including growth and development, hormone responses, and stress responses (Kieffer et al., 2006, Long et al., 2006, Takase et al., 2007, Szemenyei et al., 2008, Pauwels et al., 2010, Causier et al., 2011, Wang et al., 2012a, Krogan et al., 2012, Tao et al., 2013). Therefore, TPL/TPRs manage a common transcriptional repression mechanism, which has been unraveled in detail in several hormone responses pathways including auxin signaling (Szemenyei et al., 2008) and JA signaling (Pauwels et al., 2010). In auxin signaling (Figure 4-14), auxin response TFs (ARFs) recognize auxin-responsive *cis*-element (ARE: TGTCTC) to activate target gene expression (Ulmasov et al., 1997). The EAR-repressors of AUX/IAA

family couple the TPL/TPRs transcriptional corepressor complex to ARFs, subsequently TPL/TPRs repress auxin-induced transcription probably *via* the HISTONE DEACETYLASE 19 (HDA19) (Szemenyei et al., 2008). Similar transcriptional repression has also been found in JA signaling (Figure 4-15). JASMONATE-ZIM DOMAIN (JAZ) proteins, which play a central repressive role in JA signaling, binds to the JAZ interaction domain (JID) at the N-terminal region of MYC2. If the JAZs contain the aforementioned EAR-motif, also bind to TPL/TPRs (Shyu et al., 2012), thereby recruiting the TPL/TPRs co-repressors, putatively together with HDA19, to repress MYC2 target genes expression (Pauwels and Goossens, 2011, Niu et al., 2011, Fernandez-Calvo et al., 2011, Shyu et al., 2012, Kazan and Manners, 2013). The Non-EAR-motif JAZ proteins may cooperate with the EAR-motif adaptor protein NINJA (Novel interactor of JAZ) to recruit TPL/TPRs (Pauwels et al., 2010). When auxin or JA (JA-Ile) are present, the receptor complex TIR1-auxin-AUX/IAA or COI1-JA-Ile-JAZ initiates the ubiquitylation and degradation of the EAR-repressors AUX/IAA or JAZ by the proteasome pathway to release transcriptions from repression by TPL/TPRs.

Interestingly, the ABI5-binding proteins (AFPs) share three conserved domains with the adaptor protein NINJA (Lopez-Molina et al., 2003, Garcia et al., 2008) and also carry the EAR-motif to interact with TPL/TPRs (Pauwels et al., 2010). Therefore, AFPs likely function as EAR-repressor adaptor proteins to inhibit ABI5 target genes transcription in ABA signaling by recruiting the transcriptional repressors TPL/TPRs.

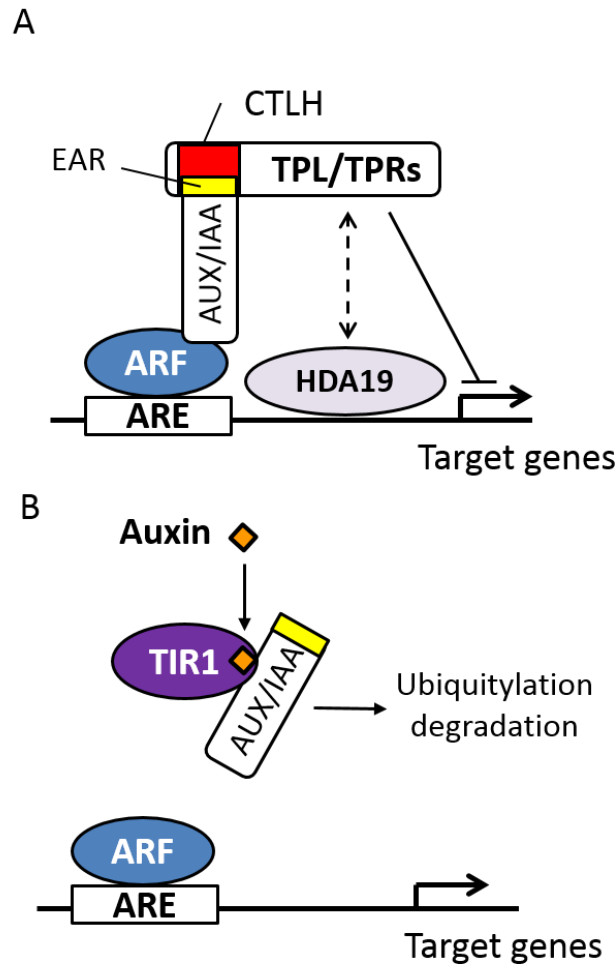


Figure 4-14: Model of Auxin-regulated transcription

(A) Auxin response TFs (ARFs) bind to auxin response *cis*-element (ARE: TGTCTC) to activate target gene expression in auxin signaling (Ulmasov et al., 1997). EAR-repressor proteins AUX/IAAs interact with both ARFs and TPL/TPRs, and TPL/TPRs, putatively together with the HISTONE DEACETYLASE 19 (HDA19), are thereby recruited to inhibit the expression of ARF target genes (Szemenyei et al., 2008). (B) In the presence of auxin, degradation of AUX/IAAs is initiated by binding of the hormone to TIR1 *via* ubiquitylation and subsequent degradation, resulting in target genes expression (Teale et al., 2006). Modified from Szemenyei et al (2008) and Woodward et al (2005). EAR: EAR-motif (LxLxL or DLNxxP, where x may represent any amino acid residue). CTLH: C-terminal to lissencephaly homology domain.

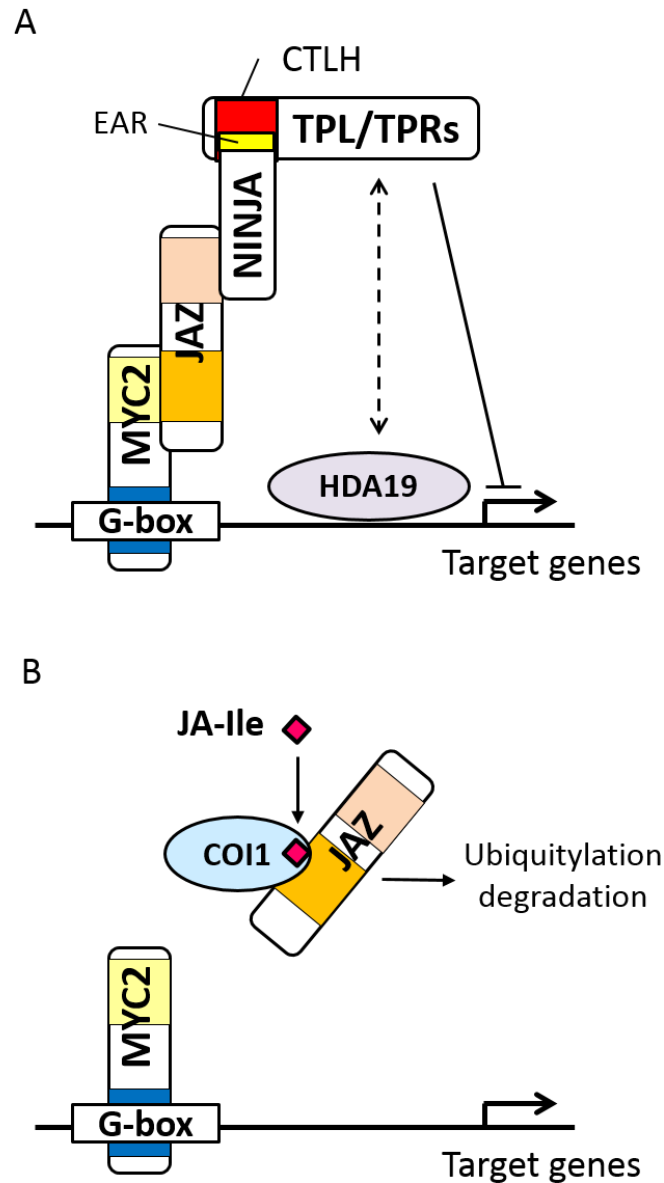


Figure 4-15: **Model of JA-regulated transcription**

(A) bHLH TF MYC2 recognizes a specific *cis*-element G-box (CACGTG), regulating target genes expression in JA signaling (Toledo-Ortiz et al., 2003, Heim et al., 2003). The TPL/TPRs corepressor complex, probably as well as HDA19, are targeted to MYC2 to repress transcription by an EAR-repressor adaptor complex JAZs-NINJA in which JAZs bind to MYC2, and NINJA connects to TPL/TPRs *via* EAR-motif (Kazan and Manners, 2013). (B) When active JA (JA-Ile) is present, the COI1-JA-Ile-JAZ co-receptor complex triggers ubiquitylation and thus degradation of JAZs, resulting in activation of target genes transcription (Pauwels et al., 2010). EAR: EAR-motif (LxLxL or DLNxxP, where x may represent any amino acid residue). CTLH: C-terminal to lissencephaly homology domain.

4.3.2.3 RING-finger E3 ligase mediates AHR11 degradation

In Y2H screen, the ab-region (aa: 1-544) of AHR11 strongly interacted with a RING-finger E3 ligase SINAT-like protein (AT3G61790; Figure 4-12) and these data might point to proteasome-mediated protein degradation as the underlying regulatory principle controlling AHR11 protein levels. The SINAT-like protein contains two zinc finger domains of different types: one shows a RING-type profile and is located between amino acids 62 and 102; the second has a SEVEN IN ABSENTIA HOMOLOG (SIAH)-type profile and is located between amino acids 177 and 305. The SIAH-type domain was firstly found in the *Drosophila* SINA (SEVEN IN ABSENTIA) protein (Carthew and Rubin, 1990). The combination of RING-type zinc finger and SIAH-type zinc finger in SINAT-like protein is also conserved in SINA, as well as its mammalian homologs SIAHs (Hu et al., 1997) and plant homologs SINATs (Xie et al., 2002, Welsch et al., 2007). All SINA proteins have ubiquitin protein E3 ligase activity to mediate the ubiquitylation of substrate proteins to promote their degradation. In the *Drosophila* eye SINA initiates Ttk88 degradation to regulate the specification of R7 cell fate (Carthew and Rubin, 1990). *Homo sapiens* SIAH1 and SIAH2 interact with and degrade nonreceptor tyrosine kinase ACK1 (Activated Cdc42-associated kinase 1) to regulate cell transformation (Buchwald et al., 2012). In plant, SINAT5 targets NAC1 for ubiquitin-mediated protein proteolysis to down-regulate auxin signaling (Xie et al., 2002), and SINAT2 regulates the protein level of AP2-TF AtRAP2.2 in *Arabidopsis* (Welsch et al., 2007).

As discussed above, in the presence of hormones, the EAR-repressor adaptor proteins are degraded *via* ubiquitin protein ligases, such as the F-box E3 ligases TIR1 in auxin signaling (Dharmasiri et al., 2005) and COI1 in JA signaling (Yan et al., 2009), releasing target genes expression from TPL/TPRs-mediated transcription repression. Therefore, it is speculated that the SINAT-like protein (AT3G61790) functions as an E3 ligase to initiate the ubiquitylation degradation of AHR11 during stress.

4.3.2.4 Model of AHR11 function as a transcriptional repressor

AHR11 has been characterized in this work as a negative regulator of response to water deficit stress, especially involved in ABA/stress-induced gene transcription. According to its interaction with both bHLH-TF JAM2 and TPL/TPRs transcriptional corepressors in yeast, the novel EAR-protein AHR11 is proposed to function as an adaptor protein, recruiting the TPL/TPRs corepressor complex to inhibit transcription of JAM2-regulated genes (Figure 4-7A). In the *ahr11* mutant, the C-terminal truncated protein Δ ahr11 is impaired to interact with either JAM2 or TPL/TPRs, allowing a constitutive transcription of JAM2 target genes. Although several target genes of JAM2 in JA signaling have been found such as *VSP2*, *PAP1*, *ANAC019* and *ERF1* (Sasaki-Sekimoto et al., 2013), the target genes of JAM2 in water deficit and ABA signaling is still unclear (Li et al., 2007). As discussed in section 4.2.3.2, the transcript level of the ABA-importer *ABCG40* is significantly higher in *ahr11* shoot after exposure to water deficit stress. The *cis*-element analysis of *ABCG40* promoter reveals the presence of 11 G-box elements which might be recognized by JAM2 in the upstream region (1635 bp) of *ABCG40*, in addition to one ABRE and several CE elements which are responsible for ABA responsive regulation. Therefore, *ABCG40* seems to be a potential target gene of AHR11 and JAM2.

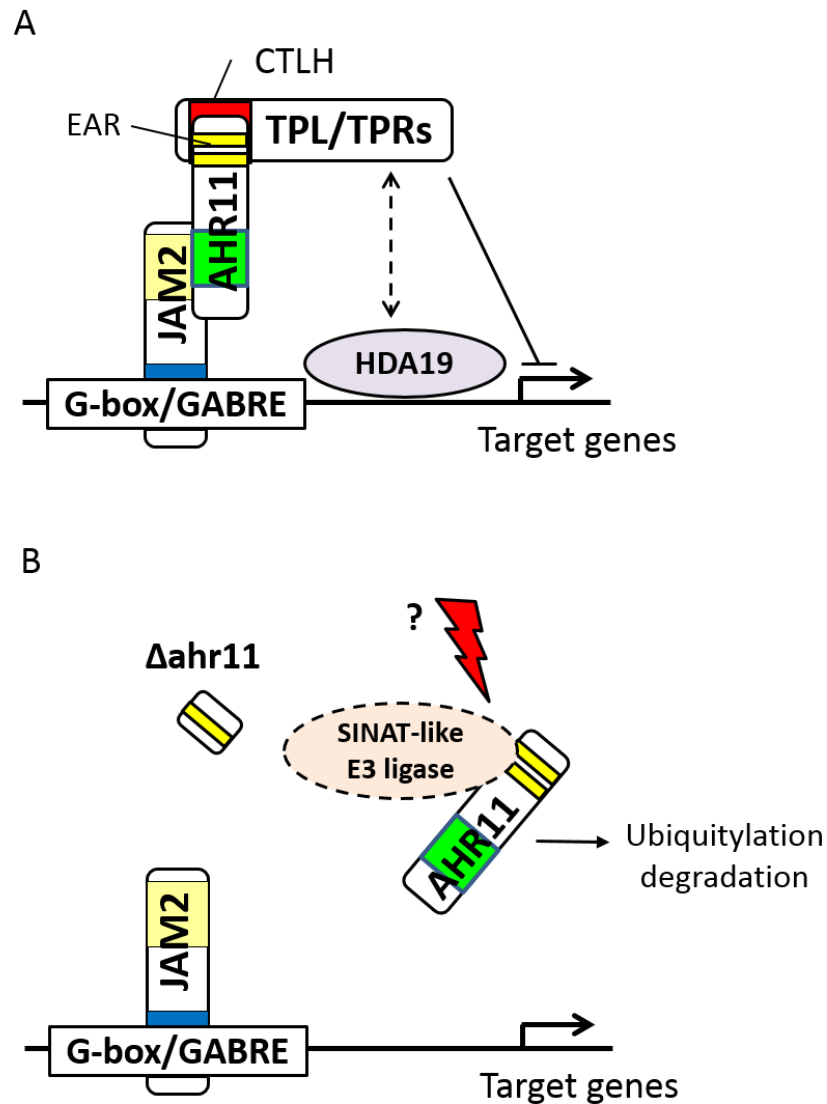


Figure 4-16: **Hypothetical model of AHR11-regulated transcription**

(A) bHLH-TF JAM2 binds to G-box (CACGTG) and G-box-like ABRE (G/ABRE: CACGTGGC) to regulate target genes expression. The EAR-repressor protein AHR11 interacts with both JAM2 through c-region (aa: 542-804, green)) and corepressors complex TPL/TPRs *via* EAR-motifs (EAR1²⁰⁸ and EAR2³¹⁴, yellow). Thus, AHR11 acts as an adaptor protein to recruit TPL/TPRs inhibiting the transcription of JAM2 target genes. (B) In the *ahr11* mutant, the mutated protein Δ ahr11 is impaired to bind to either JAM2 or TPL/TPRs, and the target genes thus are constitutively released from transcriptional repression. Compared to auxin signaling (Figure 4-14) and JA signaling (Figure 4-15), ubiquitylation-mediated degradation of AHR11 might result in initiation of JAM2 target gene expression. A SINAT-like protein (AT3G61790) has been predicted as a protein ubiquitin E3 ligase, and is supposed here to be involved in ubiquitylation-mediated degradation of AHR11.

Similar to auxin signaling (Figure 4-14) and JA signaling (Figure 4-15), the transcriptional repression adaptor protein AHR11 is presumably susceptible to ubiquitin-mediated degradation as inferred from the observation that it interacts with the RING-finger E3 ligase SINAT-like protein (AT3G61790). Additionally, the RING-type E3 ligase RKP co-regulated with AHR11 might reflect a role of AHR11 level regulation. In the *ahr11* mutant, the mutated protein Δ ahr11 is impaired to bind to either JAM2 or TPL/TPRs, and the JAM2-regulated genes thus are constitutively released from transcriptional repression. The subsequent genome-wide transcription analysis of water deficit-stressed *ahr11* would uncover the target genes of JAM2, as well as of AHR11, in water deficit response.

Although the high-throughput Y2H screen used in this work is a reliable tool which recently has been employed successfully in several studies (Yu et al., 2008, Braun, 2012, Braun et al., 2013), protein-protein interaction between AHR11 and its interacting partners still need to be confirmed *in planta*, e.g. by using bimolecular fluorescence complementation (BiFC) in protoplasts (Bhat et al., 2006).

4.4 Multiple functions of AHR11 in development and non-ABA hormone signaling pathways

Although the mutant *ahr11* shows an altered response in several ABA-regulated physiological processes, *ahr11* also displays specifically phenotypic alternations such as early flowering (Table 3-4), less rosette leaves (Figure 3-25), and reduced apical dominance (Figure 3-25). Thus, AHR11 presumably has multiple regulatory functions in plant development and non-ABA hormone signaling pathways. Due to the dual function of the AHR11-interacting protein JAM2 in ABA and JA signaling, AHR11 is supposed to also be involved in JA signaling by suppressing the expression of JAM2 target genes. Both JAMs and MYC2 are positive regulators of ABA signaling (Abe et al., 1997, Abe et al., 2003, Li et al., 2007), but antagonistically regulate JA signaling (Sasaki-Sekimoto et al., 2013, Kazan and Manners, 2013). How AHR11 is involved as a regulatory element in both signaling pathways, perhaps representing a node of crosstalk of ABA and JA signaling needs further investigation.

The transition from vegetative growth to flowering is an important developmental process in plants. This switch is regulated by several pathways including the photoperiod response pathway, the autonomous pathway and GA signaling (Mouradov et al., 2002). In the floral transition process, ABA seems to play a minor role, acting as a floral repressor while GA plays a dominant role in promoting the transition to reproductive development (Domagalska et al., 2010). Since *ahr11* shows an early flowering phenotype under long day conditions and develops less rosette leaves compared to wild type (*pATHB6::LUC*) plants (Table 3-4), AHR11 might be also involved in the cross talk between ABA and GA signaling during transition to flowering.

During the reproductive developmental stage, *ahr11* plants exhibit reduced apical dominance with respect to inflorescence branching (Figure 3-25). It is already known that the shoot architecture is largely regulated by three classes of hormone: auxin, cytokinin (CK) and strigolactone (SL) (Ferguson and Beveridge, 2009). Typically, the young leaves synthesize auxin at the tip of the main shoot to inhibit branching (Booker et al., 2003). The hormones CK and SL both are up-regulated by auxin, and

move into the axillary buds (Dun et al., 2009) to antagonistically promote or inhibit lateral branching (Davies et al., 1966, Gomez-Roldan et al., 2008, Umehara et al., 2008). Probably SL also influences CK levels. Many SL mutants display an abnormal CK level in xylem sap (Foo et al., 2007). SL promotes shoot branching by triggering rapid depletion of auxin efflux protein PIN1 from the plasma membrane (Balla et al., 2012, Shinohara et al., 2013, Koltai, 2014, Young et al., 2014). In addition, the lateral bud outgrowth is also inhibited by ABA *via* an auxin-independent manner (Cline and Oh, 2006). These imply that AHR11 not only regulates stress responses but also modulates aspects of plant growth development by affecting the cross talk between ABA and other hormonal and developmental cues.

5. Appendix

5.1 Oligo nucleotides used in this work

5.1.1 Primers for mapping

Table 5-1: Maker set of first-pass mapping

Chr.	Position [Mb]	Marker	Type	Annealing T [°C]	Forward primer (5'->3')	Reverse primer (5'->3')
I	4.51	cer 941	SSLP	55.0	aactcaaccatcaacaatg	ccataaagaaccaccggaatt
	9.20	cer 662	SSLP	51.0	acaatcatgtatcgatgagaaa	aattcgaaaaacctccacgaa
	16.20	nga 280	SSLP	57.3	ctgatctcacggaacaatagtc	ggctccataaaaagtgcacc
	24.00	f 13011	SSLP	55.0	agtgattggatgggtcggtag	tggttttggtagttcigct
II	3.97	cer 506	SSLP	54.0	ctcatcgcggttttagcaaat	tgggcaagctgttgaata
	7.72	cer 630	SSLP	61.0	gagatggtagtttggcgccicgggtc	actggctatcgcgtgtctttgatcgc
	10.93	cer 1116	SSLP	58.0	tcaacctgacccgctttatttcgg	gaatcagatactgtcgcacatcaagg
	14.00	cer 358	SSLP	50.0	aactggttggtttaagaataa	aaccaacgatcccttttga
16.30	nga 168	SSLP	55.0	tcgtctactgcacatgcgcg	ggagacatgatataggagcctcg	
III	0.80	nga 172	SSLP	55.0	catccgaatgccatgttc	agctgcttccttatagcgtcc
	4.60	nga 162	SSLP	55.0	catcaattgcatctgaggg	ctctgctacttttctctcgg
	9.50	ciw11_rp	SSLP	58.0	ccgtggaaaggagaacaactctctag	cagatgaccttttagaaactttgcag
	9.80	ciw 11	SSLP	52.0	ccccgagttgaggtatt	gaagaaattcctaaagcattc
17.30	cer 928	SSLP	63.4	tcactgataaggacaagttctt	agtttctgcaggaggagaaacctc	
23.00	nga 6	SSLP	56.0	tggatttctctctctctac	atggagaagcttacactgatc	
IV	2.70	cer 765	SSLP	56.3	ggatgcttggtaaaagctctcagcc	ctcgtcttcttttcggcttctcc
	5.60	nga 8	SSLP	55.0	tggcttctgtttataaacatcc	gagggcaaatcttttatttcgg
	9.10	cer 787	SSLP	56.3	aggatccaaacggctcgtctcag	fggggttcttcccaagattccccctc
	14.60	cer 534	SSLP	56.3	gcccagaggagaagagcaactagc	tgggaattcatgagagaataatfgggac
18.10	nga 1107	SSLP	50.0	gcgaaaaaacaaaaatcca	cgacgaatcgacagaatttagg	
V	1.40	cer 348	SSLP	56.3	ggaaaaaatgaaatgaaagaacgagag	aaacatgaaagaaatcttggagcgaag
	4.70	nga 151	SSLP	55.2	cagctaaaaagcagagatagatg	gttttgggaagtttgcctgg
	8.40	nga 139	SSLP	57.9	ggtttcttctactatccagg	agagctaccagatccgatgg
	10.40	nga 76	SSLP	57.3	aggcatgggagacatttag	ggagaaaaatgtcactctccacc
22.40	operon	SSLP	62.4	cttgggatcttctctcc	ccggtgagcatcaaaagtcc	

Table 5-2: Maker set of fine-scale mapping

Position [Mb]	Marker	Type	Col [bp]	Ler [bp]	Note	Annealing T [°C]	Forward primer (5'→3')	Revers primer (5'→3')
ChrV-1.40	cer 348	SSLP	185	100	/	56.3	ggaaaacaatgaaattgaaagaacagagag	aaacatgaaagagaatctttggagcgaag
ChrV-3.20	cer 477	SSLP	71	40	/	58.0	tcagttcaaccttattctt	tcatgacgaaaccgggttct
ChrV-3.84	OXF	CAPS	600	461+139	EcoRV	54.0	tgccccctttaaatttggtggt	tcacgcaataaataatgttggga
ChrV-3.93	3.9Mb	CAPS	243+182	425	DraI	60.0	gacgatgtaagttggggaaccaca	gttgatccaagaatgatgcaagggc
ChrV-4.00	4.0Mb	SSLP	249	269	/	58.0	tgtataccagtcagtggttgcatggg	ctaggttttttacgcaggacatgtttcc
ChrV-4.24	CAT72	SSLP	124	110	/	57.0	cccagttcaaccgaccac	aatcccagtaaccacaacacaca
ChrV-4.32	4.3Mb	SSLP	377	349	/	54.0	cataagatatgtcaitttggttgag	gaaacaacttcatatgtgaaagctc
ChrV-4.48	4.48Mb	SNP	585	585	Sequencing	53.0	gtaacgtctctcgaaacaactggag	catcggataacgigtatagactag
ChrV-4.50	4.5Mb	CAPS	287+218	505	NdeI	60.0	atgaccctagggttcatgttaggttc	gttcctcgtcctgaaatgtagatgctc
ChrV-4.57	4.57Mb	CAPS	127 + 142	269	Fnu4HI	58.0	gaattccaigtgtataggacagg	gcatacgcgcttctctgttccac
ChrV-4.70	nga151	SSLP	157	123	/	55.2	tgccccattttgtcttctc	gttatggagtttcttagggcaag
ChrV-5.34	5.3Mb	CAPS	368	180 + 188	BamHI	60°C	tcgacgcttctgtagcagggaatc	ccaatggaagccagtttcttagctc
ChrV-6.10	cer 482	SSLP	80	40	/	60.0	ggttccttcttcaaatga	gtaacgcagcttcatccagc
ChrV-8.40	nga139	SSLP	174	132	/	57.9	ggtttcgtttcactatccagg	agagctaccagatccgatgg
ChrV-13.68	nga76	SSLP	220	300	/	57.3	aggcatgggagacatttaccg	ggagaaaaatgtcactctccacc
ChrV-22.40	operon2 2441	SSLP	370	260	/	62.4	ctttggcatcttctctccc	ccggttagcatcaagctc

5.1.2 Primers for Cloning and genotyping

Table 5-3: Uniform primers

#	Primer	Nucleotide-Sequence (5'->3')	Purpose
225	GK_08409	ATATTGACCATCATACTCATTGC	Genotyping of GABI-Kat T-DNA mutant
289	LB3	TAGCATCTGAATTCATAACCAATCT CGATACA	Genotyping of SAIL T-DNA mutant
856	T3-f	AATTAACCCCTCACTAAAGGG	Sequencing for pSK vector.
1915	p35S-end-f	CTCTCTACAAATCTATCTCTCTC	Sequencing for the insertion after 35S1 promoter.
1916	pDEST-AD	CGCGTTTGGAACTACTACAGGG	Sequencing for pDEST-AD vector.
1917	pDEST-DB	GGCTTCAGTGGAGACTGATATGCCT C	Sequencing for pDEST-DB vector.
1918	pDEST-Term	GGAGACTTGACCAACCTCTGGCG	Sequencing for pDEST-AD vector and pDEST-DB vector.
1919	pENTR-seq-r	GTAACATCAGAGATTTTGGACAC	Sequencing for pENTR vector.
1920	LacZ-ins-f	GACCATGATTACGCCAAGCTCG	86bp to Ascl, Sequencing for Binary vector and transgenic plants.
1921	LacZ-ins-r	GATTAAGTTGGGTAACGCCAGG	192bp to Ascl, Sequencing for Binary vector and transgenic plants.

Table 5-4: Specific primers

#	Primer	Nucleotide-Sequence (5'->3')	Purpose
108	Actin-f	TGGGATGACATGGAGAAGAT	RT-PCR
109	Actin-r	ATACCAATCATAGATGGCTGG	RT-PCR
216	abi1_XhoI_for	AATTCCTCGAGGGAAGTATCTCCGG C	Genotyping of <i>abi1-1</i>
219	abi1_XhoI_rev	GTACTCGAGTCAGTTCAAGGGTTTGC	Genotyping of <i>abi1-1</i>
554	aba2- 1_DeCAPS_f	GTTTTGGCTAGCGATGACTCGCGGT ACTTAA	Genotyping of <i>aba2-1</i>
555	aba2- 1_DeCAPS_r	AGACATGATAAATTGGCGGACAATA AAC	Genotyping of <i>aba2-1</i>
1922	AHR11-f1	CCGGAATTCATGTCTGGAAGCCAAG AGCCTAG	<i>AHR11</i> (<i>At5g13590</i>) cloning (EcoRI)
1923	ctAHR11-f	ctATGTCTGGAAGCCAAGAGCCTAG	<i>AHR11</i> sequencing
1924	AHR11-r1	ATCCTACACTTTCCTTCTGTC	<i>AHR11</i> sequencing
1925	AHR11-f2	CTAGATCGCACAAAGTGGTGC	<i>AHR11</i> sequencing
1926	AHR11-r2	CCTCTAGCTCCTTACCAGGT	<i>AHR11</i> sequencing
1927	AHR11-f3	CGAAAGAACTCCCTTGTAAATC	<i>AHR11</i> sequencing
1928	AHR11-r3	ATTTAACCTTGGGCTTCTCATAATC	<i>AHR11</i> sequencing
1929	AHR11-f4	TGCTTCAGGCAGCTTTGTG	<i>AHR11</i> sequencing
1930	AHR11-r4	GAAGATCTTTAAAAACCATCACCACC GAGCT	<i>AHR11</i> cloning (BglII)
1931	AHR11-nonstop- r4	GCGTCGACGCAAAACCATCACCACC GAGCT	<i>AHR11</i> cloning (Sall)
1932	Δ ahr11-r	GAAGATCTTCAAACATCCATGGTAGT ATTCAAATC	Δ ahr11 cloning (BglII)

1933	Δ ahr11-nonstop-r	GCGTCGACGCAACATCCATGGTAGT ATTCAAATC	<i>Δahr11</i> cloning (Sall)
1934	ahr11-CAPS-f	AAATTGGGATTTGAATACTACCATGG ATGTCTG	Genotyping of <i>ahr11</i> (+ AHR11-r1)
1935	pAHR11-f	G <u>GACTAGT</u> GGAGAACCAGATTCCT AGAAC	Promoter of <i>AHR11</i> cloning (SpeI)
1936	pAHR11-r	CGG <u>GATCC</u> ACTCTGCAGCAGCAACTT TGC	Promoter of <i>AHR11</i> cloning (BamHI)
1937	pAHR11-seq1-r	CCAATCTCACTACCTGAAGGAACC	<i>pAHR11</i> sequencing
1938	pAHR11-seq2-f	CCTTATGGAGATGGAAGCTTTTCG	<i>pAHR11</i> sequencing
1039	pAHR11-seq3-r	GACCAGTCAAATATCTCCTAC	<i>pAHR11</i> sequencing
1940	AHR11-5UTR-f	CC <u>CCCGGG</u> GTTGCTGCTGCAGAGT TGTG	<i>AHR11-5'UTR</i> cloning (XmaI)
1941	AHR11-5UTR-r	CGG <u>GATCC</u> TAGTTGAACCTCGAGGG TCCT	<i>AHR11-5'UTR</i> cloning (BamHI)
1942	AHR11-3UTR-r	GCGTCGACGAATTGGAGCCCAACTA CTTGC	<i>AHR11-3'UTR</i> cloning (Sall)
1943	AHR11-A-f	GCGTCGACATGTCTGGAAGCCAAGA GCC	Subcloning of <i>AHR11</i> for Y2H (Sall)
1944	AHR11-B-r	CCGGAATTCTCAAACATCCATGGTAG TATTCAAATC	Subcloning of <i>AHR11</i> for Y2H (EcoRI)
1945	AHR11-B-f	GCGTCGACTGGGAAGATGCTCTAGA TCGC	Subcloning of <i>AHR11</i> for Y2H (Sall)
1946	AHR11-C-r	CCGGAATTCTCAAGTCCACGAGAAT TACAAGGG	Subcloning of <i>AHR11</i> for Y2H (EcoRI)
1947	AHR11-C-f	GCGTCGACCGTGGAACTGATGAACT TTCCAG	Subcloning of <i>AHR11</i> for Y2H (Sall)
1948	AHR11-D-r	CCGGAATTCTCAGCTTTCTGTGTTAT CAGGTAATCTC	Subcloning of <i>AHR11</i> for Y2H (EcoRI)
1949	AHR11-D-f	GCGTCGACAATCTGCATGACCAGGA CAC	Subcloning of <i>AHR11</i> for Y2H (Sall)
1950	AHR11-E-r	CCGGAATTCTTAAAAACCATCACCAC CGAGC	Subcloning of <i>AHR11</i> for Y2H (EcoRI)
1620	HB6LUC-Pos-f	GGCTAGCAAAACCTTAACTAAACCC	Genotyping of the insertional <i>pATHB6::LUC</i> ABA-reporter construct in the genome of <i>Arabidopsis</i>
1621	HB6LUC-Pos-r	GCAACTACTGTTTGGGCTTTGAG	Genotyping of the insertional <i>pATHB6::LUC</i> ABA-reporter construct in the genome of <i>Arabidopsis</i>
1622	HB6LUC-InsChk-r	GTTCCGATTTAGTGCTTTACGGC	Genotyping of the insertional <i>pATHB6::LUC</i> ABA-reporter construct in the genome of <i>Arabidopsis</i>
1786	AIB-f	GCGTCGACATGAATATGAGTGATTT AGGTTGGG	<i>AIB/JAM1</i> (<i>At2g46510</i>) cloning (Sall)
1787	AIB-r	CCGGAATTCTTATATATCACCAGAGA CCTGTG	<i>AIB/JAM1</i> cloning (EcoRI)
1788	AIB.1-SpeI-f	G <u>GACTAGT</u> ATGAATATGAGTGATTT AGGTTGGG	<i>AIB/JAM1</i> cloning (SpeI)
1789	AIB-nostop-r	GCGTCGACAGTATATCACCAGAGAC CTGTG	<i>AIB/JAM1</i> cloning (Sall)
1784	AIB-f2	GACTGGAGGGATTCACAAGC	<i>AIB/JAM1</i> sequencing
1785	AIB-r2	CTTCCCAACTTTGAGGAGTG	<i>AIB/JAM1</i> sequencing

1779	bHLH13-f	TCCCCCGGGATGAATATTGGTCGCC TAGTGTGG	<i>JAM2</i> (<i>At1g01260</i>) cloning (XmaI)
1780	bHLH13-r	GCGTCGACCTATCTACCTGATGATGT TCTTG	<i>JAM2</i> cloning (Sall)
1783	bHLH13-nostop-r	GCGTCGACAGTCTACCTGATGATGTT CTTGACTG	<i>JAM2</i> cloning (Sall)
1781	bHLH13-r2	CTCTTGGGAGCTCTATCATCC	<i>JAM2</i> sequencing
1782	bHLH13-f2	CAACAACCACCGCAACAGCAAC	<i>JAM2</i> sequencing
1777	bHLH13-check-f	CCATGACATAATCTAAGGGGTTTTTC	Genotyping of <i>JAM2</i> T-DNA knockout mutant
1778	bHLH13-check-r	CCAACAGAAAATGAGGAATTGAG	Genotyping of <i>JAM2</i> T-DNA knockout mutant
1790	MYC2-f	TCCCCCGGGATGACTGATTACCGGC TACAAC	<i>MYC2</i> (<i>At1g32640</i>) cloning (XmaI)
1791	MYC2-r	AACTGCAGTTAACCGATTTTTGAAAT C	<i>MYC2</i> cloning (PstI)
1792	MYC2-nostop-r	CCGCTCGAGGTACCGATTTTTGAAAT C	<i>MYC2</i> cloning (XhoI)
1800	TOPLESS-f	TCCCCCGGGATGTCTTCTTAGTA GAGA	<i>TPL</i> (<i>At1g15750</i>) cloning (XmaI)
1801	TOPLESS-r	GCGTCGACTCATCTCTGAGGCTGATC AG	<i>TPL</i> cloning (Sall)
1802	TOPLESS-f2	CCCACATCCAGCTGTCTCAGC	<i>TPL</i> sequencing
1803	TOPLESS-f3	GGGACGAGTAAAGATGGAGAG	<i>TPL</i> sequencing
1804	TOPLESS-r3	GCACAACACCTAGAGAACGC	<i>TPL</i> sequencing
1805	TOPLESS-r2	GAATCGTGCTATCATCCATCCC	<i>TPL</i> sequencing
1806	TPL-nostop-r	GCGTCGACAGTCTCTGAGGCTGATC AG	<i>TPL</i> cloning (Sall)
1796	tpl1-1-f	GAACTCCTCCAATAATGCTTC	Genotyping of <i>TPL</i> T-DNA knockout mutant
1797	tpl1-1-r	GCAGGGTCTGTTAATTGGATGG	Genotyping of <i>TPL</i> T-DNA knockout mutant
1798	tpl1-2-f	GTTGAGTGGAATGAAAGCGAAGG	Genotyping of <i>TPL</i> T-DNA knockout mutant
1799	tpl1-2-f	GGAGAGAGCCTTCTTGTTG	Genotyping of <i>TPL</i> T-DNA knockout mutant
1811	TPR2-f	TCCCCCGGGATGTCGTCTTTGAGCA GAGAG	<i>TPR2</i> (<i>At3g16830</i>) cloning (XmaI)
1812	TPR2-r	GCGTCGACTTACCTTTGAATCTGATC CGAACTTG	<i>TPR2</i> cloning (Sall)
1813	TPR2-f2	CAATCTAATCCTGCTCCGGC	<i>TPR2</i> sequencing
1814	TPR2-f3	CGTCGAGTGAATGAGAGTGAAG	<i>TPR2</i> sequencing
1815	TPR2-r3	CAGCTGATTTCTCTAAAGCC	<i>TPR2</i> sequencing
1816	TPR2-r2	GAGTCCTCCATCCCGATTGC	<i>TPR2</i> sequencing
1817	TPR2-nostop-r	GCGTCGACCAGCCTTTGAATCTGATC CGAACTTG	<i>TPR2</i> cloning (Sall)
1807	tpr2-1-f	CTTAATGTTGCTTTGCGACG	Genotyping of <i>TPR2</i> T-DNA knockout mutant
1808	tpr2-1-r	CAGATTCCTTGAACTTCTCCTC	Genotyping of <i>TPR2</i> T-DNA knockout mutant
1809	tpr2-2-f	CTTTGAAGGACAGAGGCAC	Genotyping of <i>TPR2</i> T-DNA knockout mutant
1810	tpr2-2-r	CTTCCATCAAGAGCGGTTGAG	Genotyping of <i>TPR2</i> T-DNA knockout mutant

1826	RING/Ubox-f	TCCCCCGGGATGGATTTGGATAGC ATGGACTG	<i>At3g61790</i> cloning (XmaI)
1827	RING/Ubox-r	GCGTCGACTCAAGACAAGTTTGGGA TACAAGC	<i>At3g61790</i> cloning (Sall)
1828	RING/Ubox-nostop-r	GCGTCGACAGAGACAAGTTTGGGAT ACAAGCTCC	<i>At3g61790</i> cloning (Sall)
1793	DLCT1-f	TCCCCCGGGATGGAAGGAGTTGAG CTAGAATTAG	<i>At1g23220</i> cloning (XmaI)
1794	DLCT1-r	GCGTCGACTCATTTTTGTACTAACGG CTCCACG	<i>At1g23220</i> cloning (Sall)
1795	DLCT1-nostop-r	GCGTCGACAGTTTTTGTACTAACGGC TCCACGG	<i>At1g23220</i> cloning (Sall)
1822	<i>At2g45260</i> -f	TCCCCCGGGATGCTACCAAGTGGG TTGAAAG	<i>At2g45260</i> cloning (XmaI)
1823	<i>At2g45260</i> -r	GCGTCGACTCACTCAAGGACCTTCAC ACC	<i>At2g45260</i> cloning (Sall)
1824	<i>At2g45260</i> -nostop-r	GCGTCGACCAGCTCAAGGACCTTCA CACCAG	<i>At2g45260</i> cloning (Sall)
1825	<i>At2g45260m</i> -r	GTCTTCAACAACTCTGTCTGC	Genotyping of <i>At2g45260</i> T-DNA knockout mutant
1834	<i>At4g09060</i> -f	CCCCCGGGATGCGGAGCGAGAGA ATTGATTC	<i>At4g09060</i> cloning (XmaI)
1835	<i>At4g09060</i> -r	GCGTCGACTCAATTGTTTCATCTT AGAATC	<i>At4g09060</i> cloning (Sall)
1836	<i>At4g09060</i> -nostop-r	GCGTCGACGCATTGTTTCATCTTA GAATCTGG	<i>At4g09060</i> cloning (Sall)

5.1.3 Primers for Real Time-PCR

Table 5-5: Primers for Real-Time PCR

Primer	Nucleotide-Sequence (5'->3')	Gene
TIP41L-qPCR1-f	GTGAAAAGTGTGGAGAGAAGCAA	<i>At4g34270</i> (Czechowski et al 2005)
TIP41L-qPCR1-r	TCAACTGGATACCCTTCGCA	<i>At4g34270</i> (Czechowski et al 2005)
UBC9-qPCR1-f	TCACAATTTCCAAGGTGCTGC	<i>At4g27960</i> (Czechowski et al 2005)
UBC9-qPCR1-r	TCATCTGGGTTTGGATCCGT	<i>At4g27960</i> (Czechowski et al 2005)
AHR11-qPCR1-f	CTAGATCGCACAAAGTGGTGC	<i>At5g13590</i> (same as AHR11-f2)
AHR11-qPCR1-r	ATCCTACACTTCTCTGTCTGC	<i>At5g13590</i> (same as AHR11-r1)
AHR11-qPCR2-f	GGTCGAGGTTATGGAAGAGATGG	<i>At5g13590</i>
AHR11-qPCR2-r	GGATCCAAGTTATTCATGTTTCCATGG	<i>At5g13590</i>
RD29A-qPCR1-f	CAACACACACCAGCAGCAC	<i>At5g52310</i>
RD29A-qPCR1-r	TCATGCTCATTGCTTTGTCC	<i>At5g52310</i>
RD29B-qPCR1-f	AGCAAGCAGAAGAACCAATCA	<i>At5g52300</i>
RD29B-qPCR1-r	CTTGATGCTCCCTTCTCA	<i>At5g52300</i>
RD22-qPCR1-f	TTAACACCGGAGCGTTATTG	<i>At5g25610</i>
RD22-qPCR1-r	TCCGCCTTACTACTTGGGA	<i>At5g25610</i>
RAB18-qPCR1-f	ACTGAAGGCTTTGGAAGTGG	<i>At5g66400</i>
RAB18-qPCR1-r	TCCTCCCTCCTTGCCATC	<i>At5g66400</i>

ERD1-qPCR1-f	GACTGCCATTGCTGAAGGAC	<i>At5g51070</i>
ERD1-qPCR1-r	CTCCAGCTCTCCCCTTTCTT	<i>At5g51070</i>
HB6-qPCR1-f	TTCAGTGGGTGGTCTCATCTC	<i>At2g22430</i>
HB6-qPCR1-r	CACCGTATCTCCTCGGACTC	<i>At2g22430</i>
NCED3-qPCR1-f	ATGGCTTCTTTACGGCAACGGC	<i>At3g14440</i>
NCED3-qPCR1-r	GCTACAATAACTCAAGTCGGAGC	<i>At3g14440</i>
GFP-qPCR1-f	CGTAAACGGCCACAAGTTCAG	<i>eGFP</i>
GFP-qPCR1-r	GTGGTGCAGATGAACTTCAGG	<i>eGFP</i>
G40-qPCR1-f	CACCAAGCGAGTAATAGTATGAG	<i>At1g15520</i>
G40-qPCR1-r	GCTTCTTCATCGTCTTCTTCTC	<i>At1g15520</i>
G40-qPCR2-f	CTGCTAGAGAGGCTCATCAAAG	<i>At1g15520</i>
G40-qPCR2-r	GTTTCCAGAGGAGTTTCTCATGCTC	<i>At1g15520</i>
G25-qPCR1-f	GTCAGATTTCATCTCCTCGTC	<i>At1g71960</i>
G25-qPCR1-r	GAACTTGAGGGTGATTGGGAAAC	<i>At1g71960</i>
G25-qPCR2-f	CTACAATCGTGACCGTGACAATG	<i>At1g71960</i>
G25-qPCR2-r	CTTTGTTGACGTAGTAACCACCG	<i>At1g71960</i>
AIT1-qPCR1-f	TCGTGCGATAGTCCACATG	<i>At1g69850</i> (Kanno, Y. et al. 2012)
AIT1-qPCR1-r	GGTACAACCCACGAATAGCA	<i>At1g69850</i> (Kanno, Y. et al. 2012)

5.2 Strains used in this work

#	Organism	Strain	Vector/Plasmid	Resistance
425	EC	DH5 α	<i>pSK Ascl</i>	Amp
625	AT	GV3101	<i>pMP90/pSOUP</i>	Rif/Gent/Tet
883	EC	DH5 α	<i>pSK 35SΩGUS</i>	Amp
1110	EC	DH5 α	<i>pBI221 35S::ABI2</i>	Amp
1238	EC	DH5 α	<i>pSPYCE-35S/pUC-SPYCE</i>	Amp
1240	EC	DH5 α	<i>pSPYNE-35S/pUC-SPYNE</i>	Amp
1246	EC	DH5 α	<i>PEZS-CL (EGFP)</i>	Amp
1337	EC	DH5 α	<i>pSK delta (HincII - SmaI)</i>	Amp
2970	EC	DH5 α	empty strain for competent cells	
3041	EC	DH5 α	<i>pSK_pRD29B::LUC new</i>	Amp
3331	Y	AH109	empty strain for competent cells	
3333	EC	DH5 α	empty strain for competent cells	
3340	EC	XL1 blue	empty strain for competent cells	Tet
4065	EC	DH5 α	<i>pSK 35S empty MCS Ter</i>	Amp
4344	EC	DH5 α	<i>pSK-35s-CHC1</i>	Amp
4463	EC	XL1 blue	<i>pSK 35S RRSC26*</i>	Amp
4464	EC	XL1 blue	<i>pSK 35S rrsc26</i>	Amp
4465	EC	DH5 α	<i>pEZS EGFP rrsc26</i>	Amp
4466	EC	DH5 α	<i>pART27 Ascl 35S rrsc26</i>	Kan
4467	AT	GV3101	<i>pART27 Ascl 35S rrsc26</i>	kan/Rif
4554	EC	DH5 α	<i>pGY-35S::rrsc26-EGFP</i>	Amp
4555	EC	DH5 α	<i>PGAD424-rrsc26</i>	Amp
4556	EC	DH5 α	<i>pBridge-rrsc26</i>	Amp
4557	EC	DH5 α	<i>pART27 Ascl-35S::EGFP-rrsc26</i>	Kan
4558	AT	GV3101	<i>pART27 Ascl-35S::EGFP-rrsc26</i>	kan/Rif

Appendix

4581	EC	DH5α	<i>pEZS-35S-EGFP::RRSC26</i>	Amp
4582	EC	DH5α	<i>PGY-35S::RRSC26-EGFP</i>	Amp
4583	EC	DH5α	<i>pGAD424-RRSC26</i>	Amp
4584	EC	DH5α	<i>pBridge-RRSC26</i>	Amp
4585	EC	DH5α	<i>pBI Ascl Bar-RRSC26</i>	Kan
4586	AT	GV3101	<i>pBI Ascl Bar-RRSC26</i>	kan/Rif
4615	EC	DH10B	<i>T6l14(BAC)</i>	Cam
4616	EC	NS3529	<i>MISH12(BAC)</i>	Kan (25µg/ml)
4619	EC	DH5α	<i>pEZS-NLS1-EGFP</i>	Amp
4620	EC	DH5α	<i>pEZS-NLS2-EGFP</i>	Amp
4621	EC	DH5α	<i>pEZS-PYNLS-EGFP</i>	Amp
4622	EC	DH5α	<i>pNIGEL18</i>	Amp
4623	Y	AH109	<i>pBridge-RRSC26</i>	-Trp
4624	Y	AH109	<i>pBridge-rrsc26</i>	-Trp
4625	Y	AH109	<i>pGAD424-RRSC26</i>	-Leu
4626	Y	AH109	<i>PGAD424-rrsc26</i>	-Leu
5115	EC	DH5α	<i>pENTR1A_AHR11_a</i>	Kan
5116	EC	DH5α	<i>pENTR1A_AHR11_ab</i>	Kan
5117	EC	DH5α	<i>pENTR1A_AHR11_abc</i>	Kan
5118	EC	DH5α	<i>pENTR1A_AHR11_abcd</i>	Kan
5119	EC	DH5α	<i>pENTR1A_AHR11_b</i>	Kan
5120	EC	DH5α	<i>pENTR1A_AHR11_bc</i>	Kan
5121	EC	DH5α	<i>pENTR1A_AHR11_bcd</i>	Kan
5122	EC	DH5α	<i>pENTR1A_AHR11_c</i>	Kan
5123	EC	DH5α	<i>pENTR1A_AHR11_cd</i>	Kan
5124	EC	DH5α	<i>pENTR1A_AHR11_d</i>	Kan
5125	EC	XL1blue	<i>pDESTAD_AHR11_a</i>	Amp
5126	EC	XL1blue	<i>pDESTAD_AHR11_ab</i>	Amp
5127	EC	XL1blue	<i>pDESTAD_AHR11_abc</i>	Amp
5128	EC	XL1blue	<i>pDESTAD_AHR11_abcd</i>	Amp
5129	EC	XL1blue	<i>pDESTAD_AHR11_b</i>	Amp
5130	EC	XL1blue	<i>pDESTAD_AHR11_bc</i>	Amp
5131	EC	XL1blue	<i>pDESTAD_AHR11_bcd</i>	Amp
5132	EC	XL1blue	<i>pDESTAD_AHR11_c</i>	Amp
5133	EC	XL1blue	<i>pDESTAD_AHR11_cd</i>	Amp
5134	EC	XL1blue	<i>pDESTAD_AHR11_d</i>	Amp
5135	EC	XL1blue	<i>pDESTDB_AHR11_a</i>	Amp
5136	EC	XL1blue	<i>pDESTDB_AHR11_ab</i>	Amp
5137	EC	XL1blue	<i>pDESTDB_AHR11_abc</i>	Amp
5138	EC	XL1blue	<i>pDESTDB_AHR11_abcd</i>	Amp
5139	EC	XL1blue	<i>pDESTDB_AHR11_b</i>	Amp
5140	EC	XL1blue	<i>pDESTDB_AHR11_bc</i>	Amp
5141	EC	XL1blue	<i>pDESTDB_AHR11_bcd</i>	Amp
5142	EC	XL1blue	<i>pDESTDB_AHR11_c</i>	Amp
5143	EC	XL1blue	<i>pDESTDB_AHR11_cd</i>	Amp
5144	EC	XL1blue	<i>pDESTDB_AHR11_d</i>	Amp
5236	EC	XL1Blue	<i>pGreenII0179 Ascl Hygromycin</i>	Kan
5345	EC	DH5α	<i>psk-Ascl-endgAHR11</i>	Amp
5346	EC	DH5α	<i>psk-Ascl-endgAHR11-EGFP</i>	Amp
5347	EC	DH5α	<i>pGreenII1079-Ascl-Hygro-emp</i>	Kan
5348	EC	DH5α	<i>pGreenII1079-Ascl-Hygro-endgAHR11</i>	Kan
5349	EC	DH5α	<i>pGreenII1079-Ascl-Hygro-endgAHR11-EGFP</i>	Kan
5350	AT	GV 3101 pMP90/pSOUP	<i>pGreenII1079-Ascl-Hygro-emp</i>	kan/Rif/Gent

5351	AT	GV 3101 pMP90/pSOUP	<i>pGreenII1079-Ascl-Hygro-endgAHR11</i>	kan/Rif/Gent
5352	AT	GV 3101 pMP90/pSOUP	<i>pGreenII1079-Ascl-Hygro-endgAHR11-EGFP</i>	kan/Rif/Gent
5353	EC	DH5 α	<i>psk-Ascl-35S-AHR11-p90-GFP</i>	Amp
5354	EC	DH5 α	<i>psk-Ascl-35S-AHR11-p600-GFP</i>	Amp
5355	EC	DH5 α	<i>psk-Ascl-35S-gAHR11-3UTR</i>	Amp
5356	EC	DH5 α	<i>psk-Ascl-35S-gAHR11</i>	Amp
5357	EC	DH5 α	<i>psk-Ascl-pAHR11</i>	Amp
5358	EC	DH5 α	<i>psk-Ascl-pAHR11-5UTR</i>	Amp
5359	EC	DH5 α	<i>psk-Ascl-pAHR11-LUC</i>	Amp
5360	EC	DH5 α	<i>psk-Ascl-pAHR11-5UTR-LUC</i>	Amp
5621	EC	DH5 α	<i>pENTR-AIB</i>	kan
5622	EC	DH5 α	<i>pENTR-AIB.2</i>	kan
5624	EC		<i>pDESTAD</i>	Amp
5625	EC		<i>pDESTDB</i>	Amp
5627	EC	DH5 α	<i>pGreenII1079-Ascl-Hygro-35s-AHR11-CDS</i>	kan
5628	EC	DH5 α	<i>pGreenII1079-Ascl-Hygro-35s-gAHR11-3UTR</i>	kan
5629	EC	DH5 α	<i>pGreenII1079-Ascl-Hygro-35s-delta-ahr11</i>	kan
5630	AT	GV 3101 pMP90/pSOUP	<i>pGreenII1079-Ascl-Hygro-35s-AHR11-CDS</i>	kan/Rif/Gent
5631	AT	GV 3101 pMP90/pSOUP	<i>pGreenII1079-Ascl-Hygro-35s-gAHR11-3UTR</i>	kan/Rif/Gent
5632	AT	GV 3101 pMP90/pSOUP	<i>pGreenII1079-Ascl-Hygro-35s-delta-ahr11</i>	kan/Rif/Gent
5854	EC	DH5 α	<i>pSK-Ascl-35S-MYC2</i>	Amp
5855	EC	DH5 α	<i>pSK-Ascl-35S-bHLH13</i>	Amp
5856	EC	DH5 α	<i>pSK-Ascl-35S-DLCT1</i>	Amp
5890	EC	DH5 α	<i>psk-Ascl-35S-RING</i>	Amp
5891	EC	DH5 α	<i>psk-Ascl-35S-AIB.1</i>	Amp
5892	EC	DH5 α	<i>psk-Ascl-35S-AIB.2</i>	Amp

*RRSC26 is the old lab-working name of *AHR11* (At5g13590).

5.3 Genotyping of mutants and transformants of *Arabidopsis thaliana*

5.3.1 EMS-induced mutant *ahr11*

According to the EMS-induced C-to-T mutation in *AHR11* gene (*At5g13590*), the novel EMS-mutant *ahr11* was genotyped by using designed CAPS-marker (primers: #1931 + #1924). The polymerase chain reaction (PCR: annealing temperature 53°C) was performed basically. The DNA fragment amplified from *ahr11* mutant has one restriction site (DdeI: 5'-C[^]TNAG-3') and is digested into two fragments 138 bp and 32 bp, whereas the DNA fragment amplified from wild type genomic DNA has no restriction site (Figure 5-1). The products were separated by 2% (w/v) agarose gel electrophoresis after digestion by restriction enzyme DdeI (NEB).

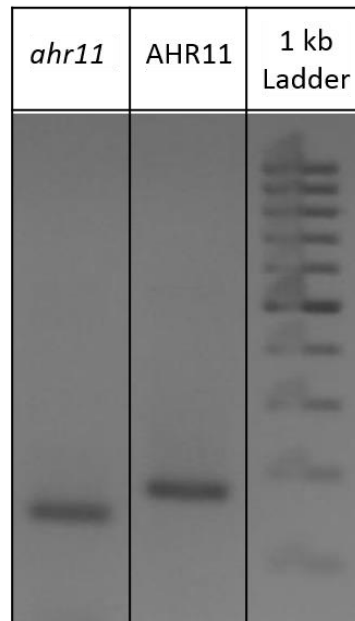


Figure 5-1: **Genotyping of EMS-induced mutant *ahr11***

Genomic DNA was isolated from seedlings of mutant *ahr11* and wild type *pATHB6::LUC*. The CAPS-marker: AHR11-CAPS-f + AHR11-r1 (sequence information in Appendix 5.1.2) were employed to select homozygous *ahr11* mutant. After the amplification from *ahr11* and *pATHB6::LUC*, the DNA fragments were digested by the restriction enzyme DdeI (NEB), resulting in two fragments 138 bp and 32 bp (only the big fragment was visible in gel electrophoresis) in *ahr11*, as well as 170 bp fragment in wild type. The 1 kb DNA ladder was used in 2% (w/v) agarose gel electrophoresis.

5.3.2 ABA-reporter line *pATHB6::LUC*

The *pATHB6::LUC* ABA-reporter construct was inserted into the promoter region of *MYB15* (*At3g23250*) in the genome of *Arabidopsis thaliana* Col-0, monitoring the active ABA *in vivo* (Christmann et al., 2005). Therefore, three primers were designed to select the homozygous ABA-reporter line *pATHB6::LUC*, of which the primers HB6LUC-Pos-f (#1620) and HB6LUC-Pos-r (#1621) are located up- and down-stream of the construct insertion point (8.308 Mb on Chromosome III), respectively, and the primer HB6LUC-InsChk-r (#1622) is on the insertional *pATHB6::LUC* construct. The primer sequence information is listed in Appendix 5.1.2. As shown in Figure 5-2, a 550 bp genomic DNA fragment was amplified from wild type Col-0 using the primer combination (#1620 + #1621; annealing temperature 55°C), and a 700 bp DNA fragment containing part of insertion construct was amplified from the homozygous ABA-reporter line *pATHB6::LUC* using the primer combination (#1620 + #1622; annealing temperature 55°C). The PCR products were separated by 1% (w/v) agarose gel electrophoresis.

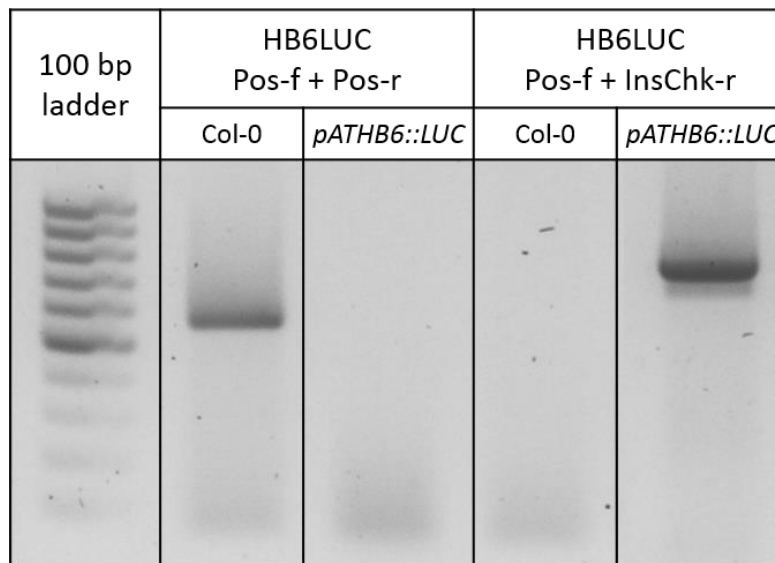


Figure 5-2: **Genotyping of ABA-reporter line *pATHB6::LUC* harboring the *pATHB6::LUC* ABA-reporter construct**

Genomic DNA was isolated from seedlings of Col-0 and ABA-reporter line *pATHB6::LUC*. Two PCR reactions were performed following the indicated primer combinations (sequence information in Appendix 5.1.2), and the products were analyzed by using 1% (w/v) agarose gel electrophoresis. The 100 bp ladder was employed in the gel analysis.

5.3.3 ABA-deficient mutant *aba2-1*

The ABA-deficient mutant *aba2-1* was isolated by selection for germinating seeds on the GA inhibitor paclobutrazol (Leon-Kloosterziel et al., 1996). For the osmotic stress resistance phenotype resulted from the Ser²⁶²-to-Asn substitution in ABA2, the *aba2-1* was preselected on high sucrose medium (MS medium with 0.3 M sucrose). As a result, only the seeds of homozygous *aba2-1* mutant survived on low water potential medium. Furthermore, a designed CAPS marker (primers: #554 + #555) was used to recheck the genotype of *aba2-1* lines. The PCR reaction (annealing temperature 56°C) was performed basically. The DNA fragment amplified from wild type has one restriction site (AflIII: 5'-C[^]TTAAG-3') and is digested into two fragments 124 bp and 32 bp, whereas the DNA fragment amplified from *aba2-1* mutant is 156 bp and has no restriction site (Figure 5-3). The products were separated by 2% (w/v) agarose gel electrophoresis after digestion by restriction enzyme AflIII (NEB).

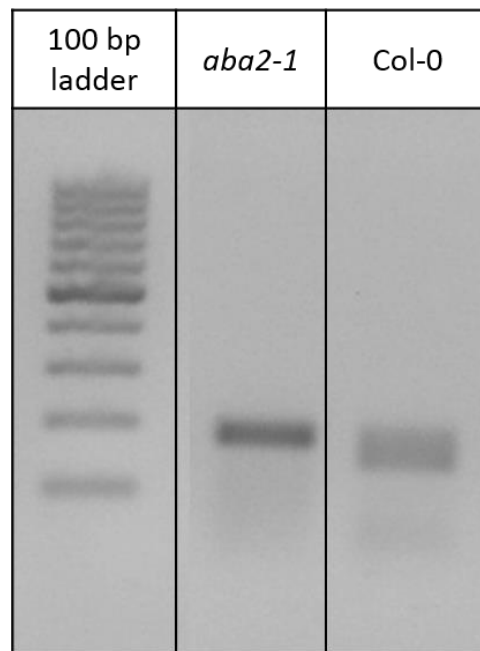


Figure 5-3: **Genotyping of ABA-deficient mutant *aba2-1***

Genomic DNA was isolated from seedlings of mutant *aba2-1* and wild type Col-0. The deCAPS-marker of *aba2-1* locus (primers: #554 + #555; sequence information in Appedix 5.1.2) was employed to select homozygous *aba2-1*. After the amplification from *aba2-1* and wild type Col-0, the DNA fragments were digested by the restriction enzyme AflIII (NEB), resulting in two fragments 124 bp and 32 bp (only the big fragment was visible in gel electrophoresis) in Col-0, as well as 156 bp fragment in *aba2-1*. The 100 bp DNA ladder was used in 2% (w/v) agarose gel electrophoresis.

5.3.4 ABA-insensitive mutant *abi1-1*

The *abi1-1* mutant is (semi)dominantly insensitive to ABA (Koornneef et al., 1984). The converting Gly¹⁸⁰-to-Asp of ABI1 in *abi1-1* was selected using CAPS marker (primers: #216 + #219). The PCR reaction (annealing temperature 54°C) was performed basically. The DNA fragment amplified from wild type has one restriction site (NcoI: 5'-C[^]CATGG-3') and is digested into two fragments 1081 bp and 536 bp, whereas the DNA fragment amplified from *abi1-1* mutant is 1617 bp and has no restriction site (Figure 5-4). The products were separated by 1% (w/v) agarose gel electrophoresis after digestion by restriction enzyme NcoI (NEB).

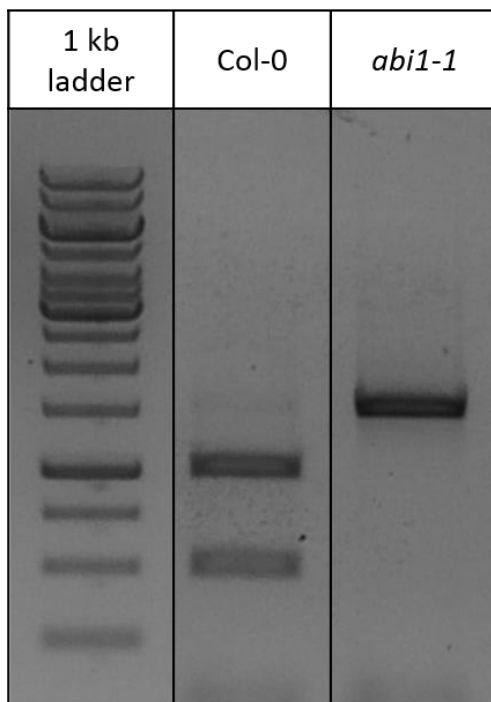


Figure 5-4: Genotyping of ABA-deficient mutant *abi1-1*

Genomic DNA was isolated from seedlings of mutant *abi1-1* and wild type Col-0. The CAPS-marker of *abi1-1* locus (primers: #216 + #219; sequence information in Appedix 5.1.2) was employed to select homozygous *abi1-1*. After the amplification from *abi1-1* and wild type Col-0, the DNA fragments were digested by the restriction enzyme NcoI (NEB), resulting in two fragments 1081 bp and 536 bp in Col-0, as well as 1617 bp fragment in *abi1-1*. The 1 kb DNA ladder was used in 1% (w/v) agarose gel electrophoresis.

5.4 AHR11-interacting candidates in yeast two-hybrid screen

AT1G01260	AT2G07696	AT2G37090	AT3G49310	AT4G25660	AT5G22210
AT1G06460	AT2G17570	AT2G37240	AT3G53020	AT4G27650	AT5G24360
AT1G08710	AT2G18670	AT2G45260	AT3G55700	AT4G27880	AT5G38410
AT1G13540	AT2G21080	AT2G45680	AT3G58680	AT4G29780	AT5G38420
AT1G15750	AT2G21820	AT2G47920	AT3G61790	AT4G31240	AT5G38430
AT1G22920	AT2G23290	AT3G01090	AT3G61930	AT4G31340	AT5G42180
AT1G23220	AT2G23420	AT3G06035	AT4G01920	AT4G33320	AT5G42480
AT1G29920	AT2G26100	AT3G06640	AT4G03415	AT4G34080	AT5G47890
AT1G58470	AT2G28660	AT3G09880	AT4G09060	AT4G36250	AT5G57900
AT1G71230	AT2G30930	AT3G13672	AT4G16146	AT5G01720	AT5G58960
AT1G72150	AT2G31060	AT3G16830	AT4G20170	AT5G09770	
AT1G76850	AT2G32600	AT3G25800	AT4G20870	AT5G18460	
AT2G05230	AT2G33860	AT3G26030	AT4G22710	AT5G19690	

6. References

- Abe, H., Urao, T., Ito, T., Seki, M., Shinozaki, K. & Yamaguchi-Shinozaki, K. (2003). Arabidopsis AtMYC2 (bHLH) and AtMYB2 (MYB) function as transcriptional activators in abscisic acid signaling. *Plant Cell*, Vol. 15, No. 1, pp. 63-78.
- Abe, H., Yamaguchi-Shinozaki, K., Urao, T., Iwasaki, T., Hosokawa, D. & Shinozaki, K. (1997). Role of arabidopsis MYC and MYB homologs in drought- and abscisic acid-regulated gene expression. *Plant Cell*, Vol. 9, No. 10, pp. 1859-68.
- Abebe, T., Melmaiee, K., Berg, V. & Wise, R.P. (2009). Drought response in the spikes of barley: gene expression in the lemma, palea, awn, and seed. *Funct Integr Genomics*, Vol. 10, No. 2, pp. 191-205.
- Abel, S. & Theologis, A. (1994). Transient transformation of Arabidopsis leaf protoplasts: a versatile experimental system to study gene expression. *Plant J*, Vol. 5, No. 3, pp. 421-7.
- Ache, P., Bauer, H., Kollist, H., Al-Rasheid, K.A., Lautner, S., Hartung, W. & Hedrich, R. (2010). Stomatal action directly feeds back on leaf turgor: new insights into the regulation of the plant water status from non-invasive pressure probe measurements. *Plant J*, Vol. 62, No. 6, pp. 1072-82.
- Agarwal, M., Hao, Y., Kapoor, A., Dong, C.H., Fujii, H., Zheng, X. & Zhu, J.K. (2006). A R2R3 type MYB transcription factor is involved in the cold regulation of CBF genes and in acquired freezing tolerance. *J Biol Chem*, Vol. 281, No. 49, pp. 37636-45.
- Ahuja, I., de Vos, R.C., Bones, A.M. & Hall, R.D. (2010). Plant molecular stress responses face climate change. *Trends Plant Sci*, Vol. 15, No. 12, pp. 664-74.
- Akhtar, M., Jaiswal, A., Taj, G., Jaiswal, J.P., Qureshi, M.I. & Singh, N.K. (2012). DREB1/CBF transcription factors: their structure, function and role in abiotic stress tolerance in plants. *J Genet*, Vol. 91, No. 3, pp. 385-95.
- Alcazar, R., Bitrian, M., Bartels, D., Koncz, C., Altabella, T. & Tiburcio, A.F. (2011). Polyamine metabolic canalization in response to drought stress in Arabidopsis and the resurrection plant *Craterostigma plantagineum*. *Plant Signal Behav*, Vol. 6, No. 2, pp. 243-50.
- Ali-Rachedi, S., Bouinot, D., Wagner, M.H., Bonnet, M., Sotta, B., Grappin, P. & Jullien, M. (2004). Changes in endogenous abscisic acid levels during dormancy release and maintenance of mature seeds: studies with the Cape Verde Islands ecotype, the dormant model of Arabidopsis thaliana. *Planta*, Vol. 219, No. 3, pp. 479-88.
- Allan, A.C., Fricker, M.D., Ward, J.L., Beale, M.H. & Trewavas, A.J. (1994). Two Transduction Pathways Mediate Rapid Effects of Abscisic Acid in Commelina Guard Cells. *Plant Cell*, Vol. 6, No. 9, pp. 1319-1328.
- Alonso-Blanco, C., Bentsink, L., Hanhart, C.J., Blankestijn-de Vries, H. & Koornneef, M. (2003). Analysis of natural allelic variation at seed dormancy loci of Arabidopsis thaliana. *Genetics*, Vol. 164, No. 2, pp. 711-29.
- Alonso-Blanco, C., Mendez-Vigo, B. & Koornneef, M. (2005). From phenotypic to molecular polymorphisms involved in naturally occurring variation of plant development. *Int J Dev Biol*, Vol. 49, No. 5-6, pp. 717-32.
- Aprile, A., Mastrangelo, A.M., De Leonardis, A.M., Galiba, G., Roncaglia, E., Ferrari, F., De Bellis, L., Turchi, L., Giuliano, G. & Cattivelli, L. (2009). Transcriptional profiling in response to terminal drought stress reveals differential responses along the wheat genome. *BMC Genomics*, Vol. 10, pp. 279.
- Aravind, L. & Ponting, C.P. (1999). The cytoplasmic helical linker domain of receptor histidine kinase and methyl-accepting proteins is common to many prokaryotic signalling proteins. *FEMS Microbiol Lett*, Vol. 176, No. 1, pp. 111-6.

References

- Arnadottir, J. & Chalfie, M. (2010). Eukaryotic mechanosensitive channels. *Annu Rev Biophys*, Vol. 39, pp. 111-37.
- Asano, T., Hayashi, N., Kikuchi, S. & Ohsugi, R. (2012). CDPK-mediated abiotic stress signaling. *Plant Signal Behav*, Vol. 7, No. 7, pp. 817-21.
- Audran, C., Borel, C., Frey, A., Sotta, B., Meyer, C., Simonneau, T. & Marion-Poll, A. (1998). Expression studies of the zeaxanthin epoxidase gene in *Nicotiana glauca*. *Plant Physiol*, Vol. 118, No. 3, pp. 1021-8.
- Austin, R.S., Vidaurre, D., Stamatiou, G., Breit, R., Provart, N.J., Bonetta, D., Zhang, J., Fung, P., Gong, Y., Wang, P.W., McCourt, P. & Guttman, D.S. (2011). Next-generation mapping of Arabidopsis genes. *Plant J*, Vol. 67, No. 4, pp. 715-25.
- Bai, L., Zhang, G., Zhou, Y., Zhang, Z., Wang, W., Du, Y., Wu, Z. & Song, C.P. (2009a). Plasma membrane-associated proline-rich extensin-like receptor kinase 4, a novel regulator of Ca signalling, is required for abscisic acid responses in *Arabidopsis thaliana*. *Plant J*, Vol. 60, No. 2, pp. 314-27.
- Bai, L., Zhou, Y. & Song, C.P. (2009b). *Arabidopsis* proline-rich extensin-like receptor kinase 4 modulates the early event toward abscisic acid response in root tip growth. *Plant Signal Behav*, Vol. 4, No. 11, pp. 1075-7.
- Balla, J., Kalousek, P., Reinohl, V., Friml, J. & Prochazka, S. (2012). Competitive canalization of PIN-dependent auxin flow from axillary buds controls pea bud outgrowth. *Plant J*, Vol. 65, No. 4, pp. 571-7.
- Bang, W., Kim, S., Ueda, A., Vikram, M., Yun, D., Bressan, R.A., Hasegawa, P.M., Bahk, J. & Koiwa, H. (2006). *Arabidopsis* carboxyl-terminal domain phosphatase-like isoforms share common catalytic and interaction domains but have distinct in planta functions. *Plant Physiol*, Vol. 142, No. 2, pp. 586-94.
- Barrero, J.M., Rodriguez, P.L., Quesada, V., Piqueras, P., Ponce, M.R. & Micol, J.L. (2006). Both abscisic acid (ABA)-dependent and ABA-independent pathways govern the induction of NCED3, AAO3 and ABA1 in response to salt stress. *Plant Cell Environ*, Vol. 29, No. 10, pp. 2000-8.
- Bartels, D. (2005). Desiccation Tolerance Studied in the Resurrection Plant *Craterostigma plantagineum*. *Integr Comp Biol*, Vol. 45, No. 5, pp. 696-701.
- Bartenschlager, R. & Schaller, H. (1988). The amino-terminal domain of the hepadnaviral P-gene encodes the terminal protein (genome-linked protein) believed to prime reverse transcription. *EMBO J*, Vol. 7, No. 13, pp. 4185-92.
- Bassel, G.W., Fung, P., Chow, T.F., Foong, J.A., Provart, N.J. & Cutler, S.R. (2008). Elucidating the germination transcriptional program using small molecules. *Plant Physiol*, Vol. 147, No. 1, pp. 143-55.
- Batistic, O. & Kudla, J. (2004). Integration and channeling of calcium signaling through the CBL calcium sensor/CIPK protein kinase network. *Planta*, Vol. 219, No. 6, pp. 915-24.
- Bauer, H., Ache, P., Lautner, S., Fromm, J., Hartung, W., Al-Rasheid, K.A., Sonnewald, S., Sonnewald, U., Kneitz, S., Lachmann, N., Mendel, R.R., Bittner, F., Hetherington, A.M. & Hedrich, R. (2013). The stomatal response to reduced relative humidity requires guard cell-autonomous ABA synthesis. *Curr Biol*, Vol. 23, No. 1, pp. 53-7.
- Becerra, C., Jahrmann, T., Puigdomenech, P. & Vicient, C.M. (2004). Ankyrin repeat-containing proteins in *Arabidopsis*: characterization of a novel and abundant group of genes coding ankyrin-transmembrane proteins. *Gene*, Vol. 340, No. 1, pp. 111-21.
- Beck, J. & Nassal, M. (2007). Hepatitis B virus replication. *World J Gastroenterol*, Vol. 13, No. 1, pp. 48-64.
- Belin, C., de Franco, P.O., Bourbousse, C., Chaignepain, S., Schmitter, J.M., Vavasseur, A., Giraudat, J., Barbier-Brygoo, H. & Thomine, S. (2006). Identification of features regulating OST1 kinase activity and OST1 function in guard cells. *Plant Physiol*, Vol. 141, No. 4, pp. 1316-27.
- Bentsink, L. & Koornneef, M. (2008). Seed dormancy and germination. *Arabidopsis Book*, Vol. 6, pp. e0119.

- Bhaskara, G.B., Nguyen, T.T. & Verslues, P.E. (2012). Unique drought resistance functions of the highly ABA-induced clade A protein phosphatase 2Cs. *Plant Physiol*, Vol. 160, No. 1, pp. 379-95.
- Bhat, R.A., Lahaye, T. & Panstruga, R. (2006). The visible touch: in planta visualization of protein-protein interactions by fluorophore-based methods. *Plant Methods*, Vol. 2, pp. 12.
- Boguslawski, G. (1992). PBS2, a yeast gene encoding a putative protein kinase, interacts with the RAS2 pathway and affects osmotic sensitivity of *Saccharomyces cerevisiae*. *J Gen Microbiol*, Vol. 138, No. 11, pp. 2425-32.
- Boisson-Dernier, A., Kessler, S.A. & Grossniklaus, U. (2011). The walls have ears: the role of plant CrRLK1Ls in sensing and transducing extracellular signals. *J Exp Bot*, Vol. 62, No. 5, pp. 1581-91.
- Booker, J., Chatfield, S. & Leyser, O. (2003). Auxin acts in xylem-associated or medullary cells to mediate apical dominance. *Plant Cell*, Vol. 15, No. 2, pp. 495-507.
- Borsani, O., Zhu, J., Verslues, P.E., Sunkar, R. & Zhu, J.K. (2005). Endogenous siRNAs derived from a pair of natural cis-antisense transcripts regulate salt tolerance in *Arabidopsis*. *Cell*, Vol. 123, No. 7, pp. 1279-91.
- Bossi, F., Cordoba, E., Dupre, P., Mendoza, M.S., Roman, C.S. & Leon, P. (2009). The *Arabidopsis* ABA-INSENSITIVE (ABI) 4 factor acts as a central transcription activator of the expression of its own gene, and for the induction of ABI5 and SBE2.2 genes during sugar signaling. *Plant J*, Vol. 59, No. 3, pp. 359-74.
- Boudsocq, M., Barbier-Brygoo, H. & Lauriere, C. (2004). Identification of nine sucrose nonfermenting 1-related protein kinases 2 activated by hyperosmotic and saline stresses in *Arabidopsis thaliana*. *J Biol Chem*, Vol. 279, No. 40, pp. 41758-66.
- Boursiac, Y., Leran, S., Corratge-Faillie, C., Gojon, A., Krouk, G. & Lacombe, B. (2013). ABA transport and transporters. *Trends Plant Sci*, Vol. 18, No. 6, pp. 325-33.
- Boyer, J.S. & Kramer, P.J. (1995). *Measuring the water status of plants and soils*, San Diego, Calif.: Academic Press, p. x, 178 p.
- Brandt, B., Brodsky, D.E., Xue, S., Negi, J., Iba, K., Kangasjarvi, J., Ghassemian, M., Stephan, A.B., Hu, H. & Schroeder, J.I. (2012). Reconstitution of abscisic acid activation of SLAC1 anion channel by CPK6 and OST1 kinases and branched ABI1 PP2C phosphatase action. *Proc Natl Acad Sci U S A*, Vol. 109, No. 26, pp. 10593-8.
- Braun, P. (2012). Interactome mapping for analysis of complex phenotypes: insights from benchmarking binary interaction assays. *Proteomics*, Vol. 12, No. 10, pp. 1499-518.
- Braun, P., Aubourg, S., Van Leene, J., De Jaeger, G. & Lurin, C. (2013). Plant protein interactomes. *Annu Rev Plant Biol*, Vol. 64, pp. 161-87.
- Bray, E.A. (2002). Classification of genes differentially expressed during water-deficit stress in *Arabidopsis thaliana*: an analysis using microarray and differential expression data. *Ann Bot*, Vol. 89 Spec No, pp. 803-11.
- Bray, E.A. & Zeevaart, J.A. (1985). The Compartmentation of Abscisic Acid and beta-d-Glucopyranosyl Abscisate in Mesophyll Cells. *Plant Physiol*, Vol. 79, No. 3, pp. 719-22.
- Brewster, J.L., de Valoir, T., Dwyer, N.D., Winter, E. & Gustin, M.C. (1993). An osmosensing signal transduction pathway in yeast. *Science*, Vol. 259, No. 5102, pp. 1760-3.
- Buchanan-Wollaston, V., Page, T., Harrison, E., Breeze, E., Lim, P.O., Nam, H.G., Lin, J.F., Wu, S.H., Swidzinski, J., Ishizaki, K. & Leaver, C.J. (2005). Comparative transcriptome analysis reveals significant differences in gene expression and signalling pathways between developmental and dark/starvation-induced senescence in *Arabidopsis*. *Plant J*, Vol. 42, No. 4, pp. 567-85.

References

- Buchwald, M., Pietschmann, K., Brand, P., Gunther, A., Mahajan, N.P., Heinzl, T. & Kramer, O.H. (2012). SIAH ubiquitin ligases target the nonreceptor tyrosine kinase ACK1 for ubiquitylation and proteasomal degradation. *Oncogene*, Vol. 32, No. 41, pp. 4913-20.
- Bugos, R.C., Hieber, A.D. & Yamamoto, H.Y. (1998). Xanthophyll cycle enzymes are members of the lipocalin family, the first identified from plants. *J Biol Chem*, Vol. 273, No. 25, pp. 15321-4.
- Burla, B., Pfrunder, S., Nagy, R., Francisco, R.M., Lee, Y. & Martinoia, E. (2013). Vacuolar transport of abscisic acid glucosyl ester is mediated by ATP-binding cassette and proton-antiport mechanisms in Arabidopsis. *Plant Physiol*, Vol. 163, No. 3, pp. 1446-58.
- Burza, A.M., Pekala, I., Sikora, J., Siedlecki, P., Malagocki, P., Bucholc, M., Koper, L., Zielenkiewicz, P., Dadlez, M. & Dobrowolska, G. (2006). Nicotiana tabacum osmotic stress-activated kinase is regulated by phosphorylation on Ser-154 and Ser-158 in the kinase activation loop. *J Biol Chem*, Vol. 281, No. 45, pp. 34299-311.
- Cao, F.Y., Yoshioka, K. & Desveaux, D. (2011). The roles of ABA in plant-pathogen interactions. *J Plant Res*, Vol. 124, No. 4, pp. 489-99.
- Carthew, R.W. & Rubin, G.M. (1990). seven in absentia, a gene required for specification of R7 cell fate in the Drosophila eye. *Cell*, Vol. 63, No. 3, pp. 561-77.
- Causier, B., Ashworth, M., Guo, W. & Davies, B. (2011). The TOPLESS interactome: a framework for gene repression in Arabidopsis. *Plant Physiol*, Vol. 158, No. 1, pp. 423-38.
- Causier, B., Lloyd, J., Stevens, L. & Davies, B. (2012). TOPLESS co-repressor interactions and their evolutionary conservation in plants. *Plant Signal Behav*, Vol. 7, No. 3, pp. 325-8.
- Chalfie, M. & Au, M. (1989). Genetic control of differentiation of the Caenorhabditis elegans touch receptor neurons. *Science*, Vol. 243, No. 4894 Pt 1, pp. 1027-33.
- Chen, C.C., Liang, C.S., Kao, A.L. & Yang, C.C. (2009). HHP1 is involved in osmotic stress sensitivity in Arabidopsis. *J Exp Bot*, Vol. 60, No. 6, pp. 1589-604.
- Chen, C.C., Liang, C.S., Kao, A.L. & Yang, C.C. (2010a). HHP1, a novel signalling component in the cross-talk between the cold and osmotic signalling pathways in Arabidopsis. *J Exp Bot*, Vol. 61, No. 12, pp. 3305-20.
- Chen, H., Lai, Z., Shi, J., Xiao, Y., Chen, Z. & Xu, X. (2010b). Roles of arabidopsis WRKY18, WRKY40 and WRKY60 transcription factors in plant responses to abscisic acid and abiotic stress. *BMC Plant Biol*, Vol. 10, pp. 281.
- Cheng, W.H., Endo, A., Zhou, L., Penney, J., Chen, H.C., Arroyo, A., Leon, P., Nambara, E., Asami, T., Seo, M., Koshiba, T. & Sheen, J. (2002). A unique short-chain dehydrogenase/reductase in Arabidopsis glucose signaling and abscisic acid biosynthesis and functions. *Plant Cell*, Vol. 14, No. 11, pp. 2723-43.
- Cheng, Y., Kato, N., Wang, W., Li, J. & Chen, X. (2003). Two RNA binding proteins, HEN4 and HUA1, act in the processing of AGAMOUS pre-mRNA in Arabidopsis thaliana. *Dev Cell*, Vol. 4, No. 1, pp. 53-66.
- Cheong, Y.H., Kim, K.N., Pandey, G.K., Gupta, R., Grant, J.J. & Luan, S. (2003). CBL1, a calcium sensor that differentially regulates salt, drought, and cold responses in Arabidopsis. *Plant Cell*, Vol. 15, No. 8, pp. 1833-45.
- Cheong, Y.H., Pandey, G.K., Grant, J.J., Batistic, O., Li, L., Kim, B.G., Lee, S.C., Kudla, J. & Luan, S. (2007). Two calcineurin B-like calcium sensors, interacting with protein kinase CIPK23, regulate leaf transpiration and root potassium uptake in Arabidopsis. *Plant J*, Vol. 52, No. 2, pp. 223-39.
- Chi, X.F., Lou, X.Y. & Shu, Q.Y. (2008). Progressive fine mapping in experimental populations: an improved strategy toward positional cloning. *J Theor Biol*, Vol. 253, No. 4, pp. 817-23.

- Chinnusamy, V., Schumaker, K. & Zhu, J.K. (2004). Molecular genetic perspectives on cross-talk and specificity in abiotic stress signalling in plants. *J Exp Bot*, Vol. 55, No. 395, pp. 225-36.
- Choi, H., Hong, J., Ha, J., Kang, J. & Kim, S.Y. (2000). ABFs, a family of ABA-responsive element binding factors. *J Biol Chem*, Vol. 275, No. 3, pp. 1723-30.
- Choi, H.I., Park, H.J., Park, J.H., Kim, S., Im, M.Y., Seo, H.H., Kim, Y.W., Hwang, I. & Kim, S.Y. (2005). Arabidopsis calcium-dependent protein kinase AtCPK32 interacts with ABF4, a transcriptional regulator of abscisic acid-responsive gene expression, and modulates its activity. *Plant Physiol*, Vol. 139, No. 4, pp. 1750-61.
- Chooback, L. & West, A.H. (2003). Co-crystallization of the yeast phosphorelay protein YPD1 with the SLN1 response-regulator domain and preliminary X-ray diffraction analysis. *Acta Crystallogr D Biol Crystallogr*, Vol. 59, No. Pt 5, pp. 927-9.
- Choudhury, A. & Lahiri, A. (2010). Comparative analysis of abscisic acid-regulated transcriptomes in Arabidopsis. *Plant Biol (Stuttg)*, Vol. 13, No. 1, pp. 28-35.
- Choudhury, S., Panda, P., Sahoo, L. & Panda, S.K. (2013). Reactive oxygen species signaling in plants under abiotic stress. *Plant Signal Behav*, Vol. 8, No. 4, pp. e23681.
- Christmann, A. & Grill, E. (2009). Are GTGs ABA's biggest fans? *Cell*, Vol. 136, No. 1, pp. 21-3.
- Christmann, A., Grill, E. & Huang, J. (2013). Hydraulic signals in long-distance signaling. *Curr Opin Plant Biol*, Vol. 16, No. 3, pp. 293-300.
- Christmann, A., Hoffmann, T., Teplova, I., Grill, E. & Muller, A. (2005). Generation of active pools of abscisic acid revealed by in vivo imaging of water-stressed Arabidopsis. *Plant Physiol*, Vol. 137, No. 1, pp. 209-19.
- Christmann, A., Moes, D., Himmelbach, A., Yang, Y., Tang, Y. & Grill, E. (2006). Integration of abscisic acid signalling into plant responses. *Plant Biol (Stuttg)*, Vol. 8, No. 3, pp. 314-25.
- Christmann, A., Weiler, E.W., Steudle, E. & Grill, E. (2007). A hydraulic signal in root-to-shoot signalling of water shortage. *Plant J*, Vol. 52, No. 1, pp. 167-74.
- Cline, M.G. & Oh, C. (2006). A reappraisal of the role of abscisic acid and its interaction with auxin in apical dominance. *Ann Bot*, Vol. 98, No. 4, pp. 891-7.
- Cohen, J.I., Miller, R.H., Rosenblum, B., Denniston, K., Gerin, J.L. & Purcell, R.H. (1988). Sequence comparison of woodchuck hepatitis virus replicative forms shows conservation of the genome. *Virology*, Vol. 162, No. 1, pp. 12-20.
- Colcombet, J. & Hirt, H. (2008). Arabidopsis MAPKs: a complex signalling network involved in multiple biological processes. *Biochem J*, Vol. 413, No. 2, pp. 217-26.
- Cosgrove, D.J. & Hedrich, R. (1991). Stretch-activated chloride, potassium, and calcium channels coexisting in plasma membranes of guard cells of *Vicia faba* L. *Planta*, Vol. 186, No. 1, pp. 143-53.
- Cutler, A.J. & Krochko, J.E. (1999). Formation and breakdown of ABA. *Trends Plant Sci*, Vol. 4, No. 12, pp. 472-478.
- Cutler, S.R., Rodriguez, P.L., Finkelstein, R.R. & Abrams, S.R. (2010). Abscisic acid: emergence of a core signaling network. *Annu Rev Plant Biol*, Vol. 61, pp. 651-79.
- Czechowski, T., Stitt, M., Altmann, T., Udvardi, M.K. & Scheible, W.R. (2005). Genome-wide identification and testing of superior reference genes for transcript normalization in Arabidopsis. *Plant Physiol*, Vol. 139, No. 1, pp. 5-17.
- D'Angelo, C., Weinl, S., Batistic, O., Pandey, G.K., Cheong, Y.H., Schultke, S., Albrecht, V., Ehlert, B., Schulz, B., Harter, K., Luan, S., Bock, R. & Kudla, J. (2006). Alternative complex formation of the Ca-regulated protein kinase CIPK1 controls abscisic acid-dependent and independent stress responses in Arabidopsis. *Plant J*, Vol. 48, No. 6, pp. 857-72.

References

- Das, R. & Pandey, G.K. (2010). Expressional analysis and role of calcium regulated kinases in abiotic stress signaling. *Curr Genomics*, Vol. 11, No. 1, pp. 2-13.
- Davies, C.R., Seth, A.K. & Wareing, P.F. (1966). Auxin and kinetin interaction in apical dominance. *Science*, Vol. 151, No. 3709, pp. 468-9.
- Day, C.L., Puthalakath, H., Skea, G., Strasser, A., Barsukov, I., Lian, L.Y., Huang, D.C. & Hinds, M.G. (2004). Localization of dynein light chains 1 and 2 and their pro-apoptotic ligands. *Biochem J*, Vol. 377, No. Pt 3, pp. 597-605.
- Deng, H., Liu, H., Li, X., Xiao, J. & Wang, S. (2011). A CCCH-type zinc finger nucleic acid-binding protein quantitatively confers resistance against rice bacterial blight disease. *Plant Physiol*, Vol. 158, No. 2, pp. 876-89.
- Desikan, R., Neill, S.J. & Hancock, J.T. (2000). Hydrogen peroxide-induced gene expression in *Arabidopsis thaliana*. *Free Radic Biol Med*, Vol. 28, No. 5, pp. 773-8.
- Desikan, R., S, A.H.-M., Hancock, J.T. & Neill, S.J. (2001). Regulation of the *Arabidopsis* transcriptome by oxidative stress. *Plant Physiol*, Vol. 127, No. 1, pp. 159-72.
- Dharmasiri, N., Dharmasiri, S. & Estelle, M. (2005). The F-box protein TIR1 is an auxin receptor. *Nature*, Vol. 435, No. 7041, pp. 441-5.
- Dick, T., Ray, K., Salz, H.K. & Chia, W. (1996). Cytoplasmic dynein (*ddlc1*) mutations cause morphogenetic defects and apoptotic cell death in *Drosophila melanogaster*. *Mol Cell Biol*, Vol. 16, No. 5, pp. 1966-77.
- Dietz, K.J., Sauter, A., Wichert, K., Messdaghi, D. & Hartung, W. (2000). Extracellular beta-glucosidase activity in barley involved in the hydrolysis of ABA glucose conjugate in leaves. *J Exp Bot*, Vol. 51, No. 346, pp. 937-44.
- Ding, J.P. & Pickard, B.G. (1993). Modulation of mechanosensitive calcium-selective cation channels by temperature. *Plant J*, Vol. 3, No. 5, pp. 713-20.
- Ding, Z., Li, S., An, X., Liu, X., Qin, H. & Wang, D. (2009). Transgenic expression of MYB15 confers enhanced sensitivity to abscisic acid and improved drought tolerance in *Arabidopsis thaliana*. *J Genet Genomics*, Vol. 36, No. 1, pp. 17-29.
- Domagalska, M.A., Sarnowska, E., Nagy, F. & Davis, S.J. (2010). Genetic analyses of interactions among gibberellin, abscisic acid, and brassinosteroids in the control of flowering time in *Arabidopsis thaliana*. *PLoS One*, Vol. 5, No. 11, pp. e14012.
- Dortay, H., Mehnert, N., Burkle, L., Schmulling, T. & Heyl, A. (2006). Analysis of protein interactions within the cytokinin-signaling pathway of *Arabidopsis thaliana*. *FEBS J*, Vol. 273, No. 20, pp. 4631-44.
- Drerup, M.M., Schlucking, K., Hashimoto, K., Manishankar, P., Steinhorst, L., Kuchitsu, K. & Kudla, J. (2013). The Calcineurin B-like calcium sensors CBL1 and CBL9 together with their interacting protein kinase CIPK26 regulate the *Arabidopsis* NADPH oxidase RBOHF. *Mol Plant*, Vol. 6, No. 2, pp. 559-69.
- Dreze, M., Monachello, D., Lurin, C., Cusick, M.E., Hill, D.E., Vidal, M. & Braun, P. (2010). High-quality binary interactome mapping. *Methods Enzymol*, Vol. 470, pp. 281-315.
- Droillard, M., Boudsocq, M., Barbier-Brygoo, H. & Lauriere, C. (2002). Different protein kinase families are activated by osmotic stresses in *Arabidopsis thaliana* cell suspensions. Involvement of the MAP kinases AtMPK3 and AtMPK6. *FEBS Lett*, Vol. 527, No. 1-3, pp. 43-50.
- Droillard, M.J., Boudsocq, M., Barbier-Brygoo, H. & Lauriere, C. (2004). Involvement of MPK4 in osmotic stress response pathways in cell suspensions and plantlets of *Arabidopsis thaliana*: activation by hypoosmolarity and negative role in hyperosmolarity tolerance. *FEBS Lett*, Vol. 574, No. 1-3, pp. 42-8.

- Droillard, M.J., Thibivilliers, S., Cazale, A.C., Barbier-Brygoo, H. & Lauriere, C. (2000). Protein kinases induced by osmotic stresses and elicitor molecules in tobacco cell suspensions: two crossroad MAP kinases and one osmoregulation-specific protein kinase. *FEBS Lett*, Vol. 474, No. 2-3, pp. 217-22.
- Du, S.Y., Zhang, X.F., Lu, Z., Xin, Q., Wu, Z., Jiang, T., Lu, Y., Wang, X.F. & Zhang, D.P. (2012). Roles of the different components of magnesium chelatase in abscisic acid signal transduction. *Plant Mol Biol*, Vol. 80, No. 4-5, pp. 519-37.
- Dubos, C., Stracke, R., Grotewold, E., Weisshaar, B., Martin, C. & Lepiniec, L. (2010). MYB transcription factors in Arabidopsis. *Trends Plant Sci*, Vol. 15, No. 10, pp. 573-81.
- Dun, E.A., Brewer, P.B. & Beveridge, C.A. (2009). Strigolactones: discovery of the elusive shoot branching hormone. *Trends Plant Sci*, Vol. 14, No. 7, pp. 364-72.
- Dupeux, F., Santiago, J., Betz, K., Twycross, J., Park, S.Y., Rodriguez, L., Gonzalez-Guzman, M., Jensen, M.R., Krasnogor, N., Blackledge, M., Holdsworth, M., Cutler, S.R., Rodriguez, P.L. & Marquez, J.A. (2011). A thermodynamic switch modulates abscisic acid receptor sensitivity. *EMBO J*, Vol. 30, No. 20, pp. 4171-84.
- Dupres, V., Alsteens, D., Wilk, S., Hansen, B., Heinisch, J.J. & Dufrene, Y.F. (2009). The yeast Wsc1 cell surface sensor behaves like a nanospring in vivo. *Nat Chem Biol*, Vol. 5, No. 11, pp. 857-62.
- Dure, L., 3rd, Greenway, S.C. & Galau, G.A. (1981). Developmental biochemistry of cottonseed embryogenesis and germination: changing messenger ribonucleic acid populations as shown by in vitro and in vivo protein synthesis. *Biochemistry*, Vol. 20, No. 14, pp. 4162-8.
- Dutta, R. & Robinson, K.R. (2004). Identification and characterization of stretch-activated ion channels in pollen protoplasts. *Plant Physiol*, Vol. 135, No. 3, pp. 1398-406.
- Elhiti, M. & Stasolla, C. (2009). Structure and function of homodomain-leucine zipper (HD-Zip) proteins. *Plant Signal Behav*, Vol. 4, No. 2, pp. 86-8.
- Emes, R.D. & Ponting, C.P. (2001). A new sequence motif linking lissencephaly, Treacher Collins and oral-facial-digital type 1 syndromes, microtubule dynamics and cell migration. *Hum Mol Genet*, Vol. 10, No. 24, pp. 2813-20.
- Endo, A., Sawada, Y., Takahashi, H., Okamoto, M., Ikegami, K., Koiwai, H., Seo, M., Toyomasu, T., Mitsuhashi, W., Shinozaki, K., Nakazono, M., Kamiya, Y., Koshihara, T. & Nambara, E. (2008). Drought induction of Arabidopsis 9-cis-epoxycarotenoid dioxygenase occurs in vascular parenchyma cells. *Plant Physiol*, Vol. 147, No. 4, pp. 1984-93.
- Falke, L.C., Edwards, K.L., Pickard, B.G. & Mislner, S. (1988). A stretch-activated anion channel in tobacco protoplasts. *FEBS Lett*, Vol. 237, No. 1-2, pp. 141-4.
- Fan, L., Linker, R., Gepstein, S., Tanimoto, E., Yamamoto, R. & Neumann, P.M. (2006). Progressive inhibition by water deficit of cell wall extensibility and growth along the elongation zone of maize roots is related to increased lignin metabolism and progressive stelar accumulation of wall phenolics. *Plant Physiol*, Vol. 140, No. 2, pp. 603-12.
- Fan, L. & Neumann, P.M. (2004). The spatially variable inhibition by water deficit of maize root growth correlates with altered profiles of proton flux and cell wall pH. *Plant Physiol*, Vol. 135, No. 4, pp. 2291-300.
- Ferguson, B.J. & Beveridge, C.A. (2009). Roles for auxin, cytokinin, and strigolactone in regulating shoot branching. *Plant Physiol*, Vol. 149, No. 4, pp. 1929-44.
- Fernandez-Calvino, L., Faulkner, C., Walshaw, J., Saalbach, G., Bayer, E., Benitez-Alfonso, Y. & Maule, A. (2011). Arabidopsis plasmodesmal proteome. *PLoS One*, Vol. 6, No. 4, pp. e18880.
- Fernandez-Calvo, P., Chini, A., Fernandez-Barbero, G., Chico, J.M., Gimenez-Ibanez, S., Geerinck, J., Eeckhout, D., Schweizer, F., Godoy, M., Franco-Zorrilla, J.M., Pauwels, L., Witters, E., Puga, M.I., Paz-Ares, J., Goossens, A., Reymond, P., De Jaeger, G. & Solano, R. (2011). The Arabidopsis bHLH transcription

References

- factors MYC3 and MYC4 are targets of JAZ repressors and act additively with MYC2 in the activation of jasmonate responses. *Plant Cell*, Vol. 23, No. 2, pp. 701-15.
- Fields, S. & Song, O. (1989). A novel genetic system to detect protein-protein interactions. *Nature*, Vol. 340, No. 6230, pp. 245-6.
- Finch-Savage, W.E. & Leubner-Metzger, G. (2006). Seed dormancy and the control of germination. *New Phytol*, Vol. 171, No. 3, pp. 501-23.
- Finkelstein, R. (2013). Abscisic Acid synthesis and response. *Arabidopsis Book*, Vol. 11, pp. e0166.
- Finkelstein, R.R., Gampala, S.S. & Rock, C.D. (2002). Abscisic acid signaling in seeds and seedlings. *Plant Cell*, Vol. 14 Suppl, pp. S15-45.
- Finkelstein, R.R. & Lynch, T.J. (2000). The Arabidopsis abscisic acid response gene ABI5 encodes a basic leucine zipper transcription factor. *Plant Cell*, Vol. 12, No. 4, pp. 599-609.
- Finkelstein, R.R., Wang, M.L., Lynch, T.J., Rao, S. & Goodman, H.M. (1998). The Arabidopsis abscisic acid response locus ABI4 encodes an APETALA 2 domain protein. *Plant Cell*, Vol. 10, No. 6, pp. 1043-54.
- Flexas, J., Bota, J., Loreto, F., Cornic, G. & Sharkey, T.D. (2004). Diffusive and metabolic limitations to photosynthesis under drought and salinity in C(3) plants. *Plant Biol (Stuttg)*, Vol. 6, No. 3, pp. 269-79.
- Foo, E., Morris, S.E., Parmenter, K., Young, N., Wang, H., Jones, A., Rameau, C., Turnbull, C.G. & Beveridge, C.A. (2007). Feedback regulation of xylem cytokinin content is conserved in pea and Arabidopsis. *Plant Physiol*, Vol. 143, No. 3, pp. 1418-28.
- Foreman, J., Demidchik, V., Bothwell, J.H., Mylona, P., Miedema, H., Torres, M.A., Linstead, P., Costa, S., Brownlee, C., Jones, J.D., Davies, J.M. & Dolan, L. (2003). Reactive oxygen species produced by NADPH oxidase regulate plant cell growth. *Nature*, Vol. 422, No. 6930, pp. 442-6.
- Forst, S., Comeau, D., Norioka, S. & Inouye, M. (1987). Localization and membrane topology of EnvZ, a protein involved in osmoregulation of OmpF and OmpC in Escherichia coli. *J Biol Chem*, Vol. 262, No. 34, pp. 16433-8.
- Fuchs, S., Grill, E., Meskiene, I. & Schweighofer, A. (2012). Type 2C protein phosphatases in plants. *FEBS J*, Vol. 280, No. 2, pp. 681-93.
- Fuchs, S., Tischer, S.V., Wunschel, C., Christmann, A. & Grill, E. (2014). Abscisic acid sensor RCAR7/PYL13, specific regulator of protein phosphatase coreceptors. *Proc Natl Acad Sci U S A*.
- Fujii, H., Chinnusamy, V., Rodrigues, A., Rubio, S., Antoni, R., Park, S.Y., Cutler, S.R., Sheen, J., Rodriguez, P.L. & Zhu, J.K. (2009). In vitro reconstitution of an abscisic acid signalling pathway. *Nature*, Vol. 462, No. 7273, pp. 660-4.
- Fujii, H., Verslues, P.E. & Zhu, J.K. (2007). Identification of two protein kinases required for abscisic acid regulation of seed germination, root growth, and gene expression in Arabidopsis. *Plant Cell*, Vol. 19, No. 2, pp. 485-94.
- Fujii, H., Verslues, P.E. & Zhu, J.K. (2011). Arabidopsis decuple mutant reveals the importance of SnRK2 kinases in osmotic stress responses in vivo. *Proc Natl Acad Sci U S A*, Vol. 108, No. 4, pp. 1717-22.
- Fujii, H. & Zhu, J.K. (2009). Arabidopsis mutant deficient in 3 abscisic acid-activated protein kinases reveals critical roles in growth, reproduction, and stress. *Proc Natl Acad Sci U S A*, Vol. 106, No. 20, pp. 8380-5.
- Fujii, H. & Zhu, J.K. (2012). Osmotic stress signaling via protein kinases. *Cell Mol Life Sci*, Vol. 69, No. 19, pp. 3165-73.
- Fujita, M., Fujita, Y., Noutoshi, Y., Takahashi, F., Narusaka, Y., Yamaguchi-Shinozaki, K. & Shinozaki, K. (2006). Crosstalk between abiotic and biotic stress responses: a current view from the points of convergence in the stress signaling networks. *Curr Opin Plant Biol*, Vol. 9, No. 4, pp. 436-42.

- Fujita, Y., Fujita, M., Satoh, R., Maruyama, K., Parvez, M.M., Seki, M., Hiratsu, K., Ohme-Takagi, M., Shinozaki, K. & Yamaguchi-Shinozaki, K. (2005). AREB1 is a transcription activator of novel ABRE-dependent ABA signaling that enhances drought stress tolerance in Arabidopsis. *Plant Cell*, Vol. 17, No. 12, pp. 3470-88.
- Fujita, Y., Nakashima, K., Yoshida, T., Katagiri, T., Kidokoro, S., Kanamori, N., Umezawa, T., Fujita, M., Maruyama, K., Ishiyama, K., Kobayashi, M., Nakasone, S., Yamada, K., Ito, T., Shinozaki, K. & Yamaguchi-Shinozaki, K. (2009). Three SnRK2 protein kinases are the main positive regulators of abscisic acid signaling in response to water stress in Arabidopsis. *Plant Cell Physiol*, Vol. 50, No. 12, pp. 2123-32.
- Fujita, Y., Yoshida, T. & Yamaguchi-Shinozaki, K. (2012). Pivotal role of the AREB/ABF-SnRK2 pathway in ABRE-mediated transcription in response to osmotic stress in plants. *Physiol Plant*, Vol. 147, No. 1, pp. 15-27.
- Furihata, T., Maruyama, K., Fujita, Y., Umezawa, T., Yoshida, R., Shinozaki, K. & Yamaguchi-Shinozaki, K. (2006). Abscisic acid-dependent multisite phosphorylation regulates the activity of a transcription activator AREB1. *Proc Natl Acad Sci U S A*, Vol. 103, No. 6, pp. 1988-93.
- Furuichi, T., Iida, H., Sokabe, M. & Tatsumi, H. (2012). Expression of Arabidopsis MCA1 enhanced mechanosensitive channel activity in the *Xenopus laevis* oocyte plasma membrane. *Plant Signal Behav*, Vol. 7, No. 8, pp. 1022-6.
- Gaff, D.F. (1971). Desiccation-tolerant flowering plants in southern Africa. *Science*, Vol. 174, No. 4013, pp. 1033-4.
- Gao, Y., Zeng, Q., Guo, J., Cheng, J., Ellis, B.E. & Chen, J.G. (2007). Genetic characterization reveals no role for the reported ABA receptor, GCR2, in ABA control of seed germination and early seedling development in Arabidopsis. *Plant J*, Vol. 52, No. 6, pp. 1001-13.
- Garcia, M.E., Lynch, T., Peeters, J., Snowden, C. & Finkelstein, R. (2008). A small plant-specific protein family of ABI five binding proteins (AFPs) regulates stress response in germinating Arabidopsis seeds and seedlings. *Plant Mol Biol*, Vol. 67, No. 6, pp. 643-58.
- Garcia, P., Tajadura, V., Garcia, I. & Sanchez, Y. (2006). Role of Rho GTPases and Rho-GEFs in the regulation of cell shape and integrity in fission yeast. *Yeast*, Vol. 23, No. 13, pp. 1031-43.
- Geiger, D., Maierhofer, T., Al-Rasheid, K.A., Scherzer, S., Mumm, P., Liese, A., Ache, P., Wellmann, C., Marten, I., Grill, E., Romeis, T. & Hedrich, R. (2011). Stomatal closure by fast abscisic acid signaling is mediated by the guard cell anion channel SLAH3 and the receptor RCAR1. *Sci Signal*, Vol. 4, No. 173, pp. ra32.
- Geiger, D., Scherzer, S., Mumm, P., Marten, I., Ache, P., Matschi, S., Liese, A., Wellmann, C., Al-Rasheid, K.A., Grill, E., Romeis, T. & Hedrich, R. (2010). Guard cell anion channel SLAC1 is regulated by CDPK protein kinases with distinct Ca²⁺ affinities. *Proc Natl Acad Sci U S A*, Vol. 107, No. 17, pp. 8023-8.
- Geiger, D., Scherzer, S., Mumm, P., Stange, A., Marten, I., Bauer, H., Ache, P., Matschi, S., Liese, A., Al-Rasheid, K.A., Romeis, T. & Hedrich, R. (2009). Activity of guard cell anion channel SLAC1 is controlled by drought-stress signaling kinase-phosphatase pair. *Proc Natl Acad Sci U S A*, Vol. 106, No. 50, pp. 21425-30.
- Gietz, R.D. & Woods, R.A. (2002). Transformation of yeast by lithium acetate/single-stranded carrier DNA/polyethylene glycol method. *Methods Enzymol*, Vol. 350, pp. 87-96.
- Gil, P.M., Gurovich, L., Schaffer, B., Alcayaga, J., Rey, S. & Iturriaga, R. (2008). Root to leaf electrical signaling in avocado in response to light and soil water content. *J Plant Physiol*, Vol. 165, No. 10, pp. 1070-8.
- Giraudat, J., Hauge, B.M., Valon, C., Smalle, J., Parcy, F. & Goodman, H.M. (1992). Isolation of the Arabidopsis ABI3 gene by positional cloning. *Plant Cell*, Vol. 4, No. 10, pp. 1251-61.
- Gleeson, T., Wada, Y., Bierkens, M.F. & van Beek, L.P. (2012). Water balance of global aquifers revealed by groundwater footprint. *Nature*, Vol. 488, No. 7410, pp. 197-200.

References

- Golldack, D., Li, C., Mohan, H. & Probst, N. (2014). Tolerance to drought and salt stress in plants: Unraveling the signaling networks. *Front Plant Sci*, Vol. 5, pp. 151.
- Gomez-Roldan, V., Fermas, S., Brewer, P.B., Puech-Pages, V., Dun, E.A., Pillot, J.P., Letisse, F., Matusova, R., Danoun, S., Portais, J.C., Bouwmeester, H., Becard, G., Beveridge, C.A., Rameau, C. & Rochange, S.F. (2008). Strigolactone inhibition of shoot branching. *Nature*, Vol. 455, No. 7210, pp. 189-94.
- Gouget, A., Senchou, V., Govers, F., Sanson, A., Barre, A., Rouge, P., Pont-Lezica, R. & Canut, H. (2006). Lectin receptor kinases participate in protein-protein interactions to mediate plasma membrane-cell wall adhesions in Arabidopsis. *Plant Physiol*, Vol. 140, No. 1, pp. 81-90.
- Grams, T.E., Koziolok, C., Lautner, S., Matyssek, R. & Fromm, J. (2007). Distinct roles of electric and hydraulic signals on the reaction of leaf gas exchange upon re-irrigation in *Zea mays* L. *Plant Cell Environ*, Vol. 30, No. 1, pp. 79-84.
- Grant, J.J., Yun, B.W. & Loake, G.J. (2000). Oxidative burst and cognate redox signalling reported by luciferase imaging: identification of a signal network that functions independently of ethylene, SA and Me-JA but is dependent on MAPKK activity. *Plant J*, Vol. 24, No. 5, pp. 569-82.
- Grethe, S., Heckel, J.O., Rietschel, W. & Hufert, F.T. (2000). Molecular epidemiology of hepatitis B virus variants in nonhuman primates. *J Virol*, Vol. 74, No. 11, pp. 5377-81.
- Gultinan, M.J., Marcotte, W.R., Jr. & Quatrano, R.S. (1990). A plant leucine zipper protein that recognizes an abscisic acid response element. *Science*, Vol. 250, No. 4978, pp. 267-71.
- Guo, Y. & Gan, S.S. (2012). Convergence and divergence in gene expression profiles induced by leaf senescence and 27 senescence-promoting hormonal, pathological and environmental stress treatments. *Plant Cell Environ*, Vol. 35, No. 3, pp. 644-55.
- Guo, Y., Xiong, L., Song, C.P., Gong, D., Halfter, U. & Zhu, J.K. (2002). A calcium sensor and its interacting protein kinase are global regulators of abscisic acid signaling in Arabidopsis. *Dev Cell*, Vol. 3, No. 2, pp. 233-44.
- Guo, Y.H., Yu, Y.P., Wang, D., Wu, C.A., Yang, G.D., Huang, J.G. & Zheng, C.C. (2009). GhZFP1, a novel CCCH-type zinc finger protein from cotton, enhances salt stress tolerance and fungal disease resistance in transgenic tobacco by interacting with GZIRD21A and GZIPR5. *New Phytol*, Vol. 183, No. 1, pp. 62-75.
- Hao, G.P., Wu, Z.Y., Chen, M.S., Cao, M.Q., Pelletier, G., Huang, C.L. & Yang, Q. (2004). [ATHK1 gene regulates signal transduction of osmotic stress in Arabidopsis thaliana]. *Zhi Wu Sheng Li Yu Fen Zi Sheng Wu Xue Xue Bao*, Vol. 30, No. 5, pp. 553-60.
- Hao, G.P., Zhang, X.H., Wang, Y.Q., Wu, Z.Y. & Huang, C.L. (2009). Nucleotide variation in the NCED3 region of Arabidopsis thaliana and its association study with abscisic acid content under drought stress. *J Integr Plant Biol*, Vol. 51, No. 2, pp. 175-83.
- Hao, Q., Yin, P., Li, W., Wang, L., Yan, C., Lin, Z., Wu, J.Z., Wang, J., Yan, S.F. & Yan, N. (2011). The molecular basis of ABA-independent inhibition of PP2Cs by a subclass of PYL proteins. *Mol Cell*, Vol. 42, No. 5, pp. 662-72.
- Harmon, A.C., Gribskov, M. & Harper, J.F. (2000). CDPKs - a kinase for every Ca²⁺ signal? *Trends Plant Sci*, Vol. 5, No. 4, pp. 154-9.
- Harrison, S.J., Mott, E.K., Parsley, K., Aspinall, S., Gray, J.C. & Cottage, A. (2006). A rapid and robust method of identifying transformed Arabidopsis thaliana seedlings following floral dip transformation. *Plant Methods*, Vol. 2, pp. 19.
- Haswell, E.S. & Meyerowitz, E.M. (2006). MscS-like proteins control plastid size and shape in Arabidopsis thaliana. *Curr Biol*, Vol. 16, No. 1, pp. 1-11.
- Haswell, E.S., Peyronnet, R., Barbier-Brygoo, H., Meyerowitz, E.M. & Frachisse, J.M. (2008). Two MscS homologs provide mechanosensitive channel activities in the Arabidopsis root. *Curr Biol*, Vol. 18, No. 10, pp. 730-4.

- Haswell, E.S., Phillips, R. & Rees, D.C. (2011). Mechanosensitive channels: what can they do and how do they do it? *Structure*, Vol. 19, No. 10, pp. 1356-69.
- Hayano-Kanashiro, C., Calderon-Vazquez, C., Ibarra-Laclette, E., Herrera-Estrella, L. & Simpson, J. (2009). Analysis of gene expression and physiological responses in three Mexican maize landraces under drought stress and recovery irrigation. *PLoS One*, Vol. 4, No. 10, pp. e7531.
- Hayat, S., Hayat, Q., Alyemeni, M.N., Wani, A.S., Pichtel, J. & Ahmad, A. (2012). Role of proline under changing environments: a review. *Plant Signal Behav*, Vol. 7, No. 11, pp. 1456-66.
- Head, C.G., Tardy, A. & Kenney, L.J. (1998). Relative binding affinities of OmpR and OmpR-phosphate at the ompF and ompC regulatory sites. *J Mol Biol*, Vol. 281, No. 5, pp. 857-70.
- Heim, M.A., Jakoby, M., Werber, M., Martin, C., Weisshaar, B. & Bailey, P.C. (2003). The basic helix-loop-helix transcription factor family in plants: a genome-wide study of protein structure and functional diversity. *Mol Biol Evol*, Vol. 20, No. 5, pp. 735-47.
- Hellens, R.P., Edwards, E.A., Leyland, N.R., Bean, S. & Mullineaux, P.M. (2000). pGreen: a versatile and flexible binary Ti vector for Agrobacterium-mediated plant transformation. *Plant Mol Biol*, Vol. 42, No. 6, pp. 819-32.
- Hetherington, A.M. & Woodward, F.I. (2003). The role of stomata in sensing and driving environmental change. *Nature*, Vol. 424, No. 6951, pp. 901-8.
- Himmelbach, A., Hoffmann, T., Leube, M., Hohener, B. & Grill, E. (2002). Homeodomain protein ATHB6 is a target of the protein phosphatase ABI1 and regulates hormone responses in Arabidopsis. *EMBO J*, Vol. 21, No. 12, pp. 3029-38.
- Himmelbach, A., Iten, M. & Grill, E. (1998). Signalling of abscisic acid to regulate plant growth. *Philos Trans R Soc Lond B Biol Sci*, Vol. 353, No. 1374, pp. 1439-44.
- Himmelbach, A., Yang, Y. & Grill, E. (2003). Relay and control of abscisic acid signaling. *Curr Opin Plant Biol*, Vol. 6, No. 5, pp. 470-9.
- Hirose, Y. & Manley, J.L. (2000). RNA polymerase II and the integration of nuclear events. *Genes Dev*, Vol. 14, No. 12, pp. 1415-29.
- Hobo, T., Asada, M., Kowiyama, Y. & Hattori, T. (1999). ACGT-containing abscisic acid response element (ABRE) and coupling element 3 (CE3) are functionally equivalent. *Plant J*, Vol. 19, No. 6, pp. 679-89.
- Holbrook, N.M., Shashidhar, V.R., James, R.A. & Munns, R. (2002). Stomatal control in tomato with ABA-deficient roots: response of grafted plants to soil drying. *J Exp Bot*, Vol. 53, No. 373, pp. 1503-14.
- Holdsworth, M.J., Bentsink, L. & Soppe, W.J. (2008). Molecular networks regulating Arabidopsis seed maturation, after-ripening, dormancy and germination. *New Phytol*, Vol. 179, No. 1, pp. 33-54.
- Horton, P., Park, K.J., Obayashi, T., Fujita, N., Harada, H., Adams-Collier, C.J. & Nakai, K. (2007). WoLF PSORT: protein localization predictor. *Nucleic Acids Res*, Vol. 35, No. Web Server issue, pp. W585-7.
- Hou, X., Li, L., Peng, Z., Wei, B., Tang, S., Ding, M., Liu, J., Zhang, F., Zhao, Y., Gu, H. & Qu, L.J. (2010). A platform of high-density INDEL/CAPS markers for map-based cloning in Arabidopsis. *Plant J*, Vol. 63, No. 5, pp. 880-8.
- Howard, J. & Bechstetdt, S. (2004). Hypothesis: a helix of ankyrin repeats of the NOMPC-TRP ion channel is the gating spring of mechanoreceptors. *Curr Biol*, Vol. 14, No. 6, pp. R224-6.
- Hsiao, T.C. & Xu, L.K. (2000). Sensitivity of growth of roots versus leaves to water stress: biophysical analysis and relation to water transport. *J Exp Bot*, Vol. 51, No. 350, pp. 1595-616.
- Hu, G., Chung, Y.L., Glover, T., Valentine, V., Look, A.T. & Fearon, E.R. (1997). Characterization of human homologs of the Drosophila seven in absentia (sina) gene. *Genomics*, Vol. 46, No. 1, pp. 103-11.

References

- Huai, J., Wang, M., He, J., Zheng, J., Dong, Z., Lv, H., Zhao, J. & Wang, G. (2008). Cloning and characterization of the SnRK2 gene family from *Zea mays*. *Plant Cell Rep*, Vol. 27, No. 12, pp. 1861-8.
- Huang, G.T., Ma, S.L., Bai, L.P., Zhang, L., Ma, H., Jia, P., Liu, J., Zhong, M. & Guo, Z.F. (2011). Signal transduction during cold, salt, and drought stresses in plants. *Mol Biol Rep*, Vol. 39, No. 2, pp. 969-87.
- Huang, N.C., Liu, K.H., Lo, H.J. & Tsay, Y.F. (1999). Cloning and functional characterization of an Arabidopsis nitrate transporter gene that encodes a constitutive component of low-affinity uptake. *Plant Cell*, Vol. 11, No. 8, pp. 1381-92.
- Hummel, I., Pantin, F., Sulpice, R., Piques, M., Rolland, G., Dauzat, M., Christophe, A., Pervent, M., Bouteille, M., Stitt, M., Gibon, Y. & Muller, B. (2010). Arabidopsis plants acclimate to water deficit at low cost through changes of carbon usage: an integrated perspective using growth, metabolite, enzyme, and gene expression analysis. *Plant Physiol*, Vol. 154, No. 1, pp. 357-72.
- Hundertmark, M. & Hinch, D.K. (2008). LEA (late embryogenesis abundant) proteins and their encoding genes in Arabidopsis thaliana. *BMC Genomics*, Vol. 9, pp. 118.
- Hutchison, C.E., Li, J., Argueso, C., Gonzalez, M., Lee, E., Lewis, M.W., Maxwell, B.B., Perdue, T.D., Schaller, G.E., Alonso, J.M., Ecker, J.R. & Kieber, J.J. (2006). The Arabidopsis histidine phosphotransfer proteins are redundant positive regulators of cytokinin signaling. *Plant Cell*, Vol. 18, No. 11, pp. 3073-87.
- Hutzler, F., Gerstl, R., Lommel, M. & Strahl, S. (2008). Protein N-glycosylation determines functionality of the Saccharomyces cerevisiae cell wall integrity sensor Mid2p. *Mol Microbiol*, Vol. 68, No. 6, pp. 1438-49.
- Huy, T.T., Ushijima, H., Quang, V.X., Win, K.M., Luengrojanakul, P., Kikuchi, K., Sata, T. & Abe, K. (2004). Genotype C of hepatitis B virus can be classified into at least two subgroups. *J Gen Virol*, Vol. 85, No. Pt 2, pp. 283-92.
- Ichimura, K., Mizoguchi, T., Yoshida, R., Yuasa, T. & Shinozaki, K. (2000). Various abiotic stresses rapidly activate Arabidopsis MAP kinases ATMPK4 and ATMPK6. *Plant J*, Vol. 24, No. 5, pp. 655-65.
- Ichimura, K., Shinozaki, K., Tena, G., Sheen, J., Henry, Y., Champion, A., Kreis, M., Zhang, S., Hirt, H., Wilson, C., Heberle-Bors, E., Ellis, B., Morris, P., Innes, R., Ecker, J., Scheel, D., Klessig, D., Machida, Y., Mundy, J., Ohashi, Y. & Walker, J. (2002). Mitogen-activated protein kinase cascades in plants: a new nomenclature. *Trends Plant Sci*, Vol. 7, No. 7, pp. 301-8.
- Iida, H., Nakamura, H., Ono, T., Okumura, M.S. & Anraku, Y. (1994). MID1, a novel Saccharomyces cerevisiae gene encoding a plasma membrane protein, is required for Ca²⁺ influx and mating. *Mol Cell Biol*, Vol. 14, No. 12, pp. 8259-71.
- Imamura, A., Hanaki, N., Nakamura, A., Suzuki, T., Taniguchi, M., Kiba, T., Ueguchi, C., Sugiyama, T. & Mizuno, T. (1999). Cloning and characterization of Arabidopsis thaliana response regulators implicated in His-Asp phosphorelay signal transduction. *Plant Cell Physiol*, Vol. 40, No. 7, pp. 733-42.
- Imamura, T., Higuchi, A. & Takahashi, H. (2013). Dehydrins are highly expressed in overwintering buds and enhance drought and freezing tolerance in *Gentiana triflora*. *Plant Sci*, Vol. 213, pp. 55-66.
- Imes, D., Mumm, P., Bohm, J., Al-Rasheid, K.A., Marten, I., Geiger, D. & Hedrich, R. (2013). Open Stomata Kinase OST1 controls R-type anion channel QUAC1 in Arabidopsis guard cells. *Plant J*.
- Iordachescu, M. & Imai, R. (2008). Trehalose biosynthesis in response to abiotic stresses. *J Integr Plant Biol*, Vol. 50, No. 10, pp. 1223-9.
- Iuchi, S., Kobayashi, M., Yamaguchi-Shinozaki, K. & Shinozaki, K. (2000). A stress-inducible gene for 9-cis-epoxycarotenoid dioxygenase involved in abscisic acid biosynthesis under water stress in drought-tolerant cowpea. *Plant Physiol*, Vol. 123, No. 2, pp. 553-62.
- Iwasaki, T., Yamaguchi-Shinozaki, K. & Shinozaki, K. (1995). Identification of a cis-regulatory region of a gene in Arabidopsis thaliana whose induction by dehydration is mediated by abscisic acid and requires protein synthesis. *Mol Gen Genet*, Vol. 247, No. 4, pp. 391-8.

- James, P., Halladay, J. & Craig, E.A. (1996). Genomic libraries and a host strain designed for highly efficient two-hybrid selection in yeast. *Genetics*, Vol. 144, No. 4, pp. 1425-36.
- Jammes, F., Yang, X., Xiao, S. & Kwak, J.M. (2011). Two Arabidopsis guard cell-preferential MAPK genes, MPK9 and MPK12, function in biotic stress response. *Plant Signal Behav*, Vol. 6, No. 11.
- Jander, G. (2006). Gene identification and cloning by molecular marker mapping. *Methods Mol Biol*, Vol. 323, pp. 115-26.
- Jander, G., Norris, S.R., Rounsley, S.D., Bush, D.F., Levin, I.M. & Last, R.L. (2002). Arabidopsis map-based cloning in the post-genome era. *Plant Physiol*, Vol. 129, No. 2, pp. 440-50.
- Janiak-Spens, F., Sparling, J.M., Gurfinkel, M. & West, A.H. (1999). Differential stabilities of phosphorylated response regulator domains reflect functional roles of the yeast osmoregulatory SLN1 and SSK1 proteins. *J Bacteriol*, Vol. 181, No. 2, pp. 411-7.
- Jeannette, E., Rona, J.P., Bardat, F., Cornel, D., Sotta, B. & Miginiac, E. (1999). Induction of RAB18 gene expression and activation of K⁺ outward rectifying channels depend on an extracellular perception of ABA in Arabidopsis thaliana suspension cells. *Plant J*, Vol. 18, No. 1, pp. 13-22.
- Jensen, G.S. & Haswell, E.S. (2012). Functional analysis of conserved motifs in the mechanosensitive channel homolog MscS-Like2 from Arabidopsis thaliana. *PLoS One*, Vol. 7, No. 6, pp. e40336.
- Jensen, M.K., Hagedorn, P.H., de Torres-Zabala, M., Grant, M.R., Rung, J.H., Collinge, D.B. & Lyngkjaer, M.F. (2008). Transcriptional regulation by an NAC (NAM-ATAF1,2-CUC2) transcription factor attenuates ABA signalling for efficient basal defence towards Blumeria graminis f. sp. hordei in Arabidopsis. *Plant J*, Vol. 56, No. 6, pp. 867-80.
- Jensen, M.K., Lindemose, S., de Masi, F., Reimer, J.J., Nielsen, M., Perera, V., Workman, C.T., Turck, F., Grant, M.R., Mundy, J., Petersen, M. & Skriver, K. (2013). ATAF1 transcription factor directly regulates abscisic acid biosynthetic gene NCED3 in Arabidopsis thaliana. *FEBS Open Bio*, Vol. 3, pp. 321-7.
- Ji, H., Pardo, J.M., Batelli, G., Van Oosten, M.J., Bressan, R.A. & Li, X. (2013). The Salt Overly Sensitive (SOS) pathway: established and emerging roles. *Mol Plant*, Vol. 6, No. 2, pp. 275-86.
- Jiang, Y. & Deyholos, M.K. (2009). Functional characterization of Arabidopsis NaCl-inducible WRKY25 and WRKY33 transcription factors in abiotic stresses. *Plant Mol Biol*, Vol. 69, No. 1-2, pp. 91-105.
- Jiang, Y., Liang, G. & Yu, D. (2012). Activated expression of WRKY57 confers drought tolerance in Arabidopsis. *Mol Plant*, Vol. 5, No. 6, pp. 1375-88.
- Jogaiah, S., Govind, S.R. & Tran, L.S. (2012). Systems biology-based approaches toward understanding drought tolerance in food crops. *Crit Rev Biotechnol*, Vol. 33, No. 1, pp. 23-39.
- Johnson, R.R., Wagner, R.L., Verhey, S.D. & Walker-Simmons, M.K. (2002). The abscisic acid-responsive kinase PKABA1 interacts with a seed-specific abscisic acid response element-binding factor, TaABF, and phosphorylates TaABF peptide sequences. *Plant Physiol*, Vol. 130, No. 2, pp. 837-46.
- Johnston, C.A., Temple, B.R., Chen, J.G., Gao, Y., Moriyama, E.N., Jones, A.M., Siderovski, D.P. & Willard, F.S. (2007). Comment on "A G protein coupled receptor is a plasma membrane receptor for the plant hormone abscisic acid". *Science*, Vol. 318, No. 5852, pp. 914; author reply 914.
- Joshi-Saha, A., Valon, C. & Leung, J. (2011a). Abscisic acid signal off the STARting block. *Mol Plant*, Vol. 4, No. 4, pp. 562-80.
- Joshi-Saha, A., Valon, C. & Leung, J. (2011b). A brand new START: abscisic acid perception and transduction in the guard cell. *Sci Signal*, Vol. 4, No. 201, pp. re4.
- Kagale, S., Links, M.G. & Rozwadowski, K. (2010). Genome-wide analysis of ethylene-responsive element binding factor-associated amphiphilic repression motif-containing transcriptional regulators in Arabidopsis. *Plant Physiol*, Vol. 152, No. 3, pp. 1109-34.

References

- Kagale, S. & Rozwadowski, K. (2010). EAR motif-mediated transcriptional repression in plants: an underlying mechanism for epigenetic regulation of gene expression. *Epigenetics*, Vol. 6, No. 2, pp. 141-6.
- Kang, J., Hwang, J.U., Lee, M., Kim, Y.Y., Assmann, S.M., Martinoia, E. & Lee, Y. (2010). PDR-type ABC transporter mediates cellular uptake of the phytohormone abscisic acid. *Proc Natl Acad Sci U S A*, Vol. 107, No. 5, pp. 2355-60.
- Kang, J., Park, J., Choi, H., Burla, B., Kretschmar, T., Lee, Y. & Martinoia, E. (2012). Plant ABC Transporters. *Arabidopsis Book*, Vol. 9, pp. e0153.
- Kang, J.Y., Choi, H.I., Im, M.Y. & Kim, S.Y. (2002). Arabidopsis basic leucine zipper proteins that mediate stress-responsive abscisic acid signaling. *Plant Cell*, Vol. 14, No. 2, pp. 343-57.
- Kanno, Y., Hanada, A., Chiba, Y., Ichikawa, T., Nakazawa, M., Matsui, M., Koshiba, T., Kamiya, Y. & Seo, M. (2012). Identification of an abscisic acid transporter by functional screening using the receptor complex as a sensor. *Proc Natl Acad Sci U S A*, Vol. 109, No. 24, pp. 9653-8.
- Kanno, Y., Jikumaru, Y., Hanada, A., Nambara, E., Abrams, S.R., Kamiya, Y. & Seo, M. (2010). Comprehensive hormone profiling in developing Arabidopsis seeds: examination of the site of ABA biosynthesis, ABA transport and hormone interactions. *Plant Cell Physiol*, Vol. 51, No. 12, pp. 1988-2001.
- Kanzaki, M., Nagasawa, M., Kojima, I., Sato, C., Naruse, K., Sokabe, M. & Iida, H. (1999). Molecular identification of a eukaryotic, stretch-activated nonselective cation channel. *Science*, Vol. 285, No. 5429, pp. 882-6.
- Kar, R.K. (2011). Plant responses to water stress: Role of reactive oxygen species. *Plant Signal Behav*, Vol. 6, No. 11.
- Karimi, M., Depicker, A. & Hilson, P. (2007). Recombinational cloning with plant gateway vectors. *Plant Physiol*, Vol. 145, No. 4, pp. 1144-54.
- Kazan, K. & Manners, J.M. (2013). MYC2: The Master in Action. *Mol Plant*, Vol. 6, No. 3, pp. 686-703.
- Kieffer, M., Stern, Y., Cook, H., Clerici, E., Maulbetsch, C., Laux, T. & Davies, B. (2006). Analysis of the transcription factor WUSCHEL and its functional homologue in Antirrhinum reveals a potential mechanism for their roles in meristem maintenance. *Plant Cell*, Vol. 18, No. 3, pp. 560-73.
- Kiegerl, S., Cardinale, F., Siligan, C., Gross, A., Baudouin, E., Liwosz, A., Eklof, S., Till, S., Bogre, L., Hirt, H. & Meskiene, I. (2000). SIMKK, a mitogen-activated protein kinase (MAPK) kinase, is a specific activator of the salt stress-induced MAPK, SIMK. *Plant Cell*, Vol. 12, No. 11, pp. 2247-58.
- Kim, D.H., Yamaguchi, S., Lim, S., Oh, E., Park, J., Hanada, A., Kamiya, Y. & Choi, G. (2008). SOMNUS, a CCCH-type zinc finger protein in Arabidopsis, negatively regulates light-dependent seed germination downstream of PIL5. *Plant Cell*, Vol. 20, No. 5, pp. 1260-77.
- Kim, D.Y., Jin, J.Y., Alejandro, S., Martinoia, E. & Lee, Y. (2010a). Overexpression of AtABCG36 improves drought and salt stress resistance in Arabidopsis. *Physiol Plant*, Vol. 139, No. 2, pp. 170-80.
- Kim, J.M., Woo, D.H., Kim, S.H., Lee, S.Y., Park, H.Y., Seok, H.Y., Chung, W.S. & Moon, Y.H. (2011a). Arabidopsis MCKK20 is involved in osmotic stress response via regulation of MPK6 activity. *Plant Cell Rep*, Vol. 31, No. 1, pp. 217-24.
- Kim, J.S., Mizoi, J., Yoshida, T., Fujita, Y., Nakajima, J., Ohori, T., Todaka, D., Nakashima, K., Hirayama, T., Shinozaki, K. & Yamaguchi-Shinozaki, K. (2011b). An ABRE promoter sequence is involved in osmotic stress-responsive expression of the DREB2A gene, which encodes a transcription factor regulating drought-inducible genes in Arabidopsis. *Plant Cell Physiol*, Vol. 52, No. 12, pp. 2136-46.
- Kim, M.H., Sasaki, K. & Imai, R. (2009). Cold shock domain protein 3 regulates freezing tolerance in Arabidopsis thaliana. *J Biol Chem*, Vol. 284, No. 35, pp. 23454-60.

- Kim, S., Kang, J.Y., Cho, D.I., Park, J.H. & Kim, S.Y. (2004). ABF2, an ABRE-binding bZIP factor, is an essential component of glucose signaling and its overexpression affects multiple stress tolerance. *Plant J*, Vol. 40, No. 1, pp. 75-87.
- Kim, T.H., Bohmer, M., Hu, H., Nishimura, N. & Schroeder, J.I. (2010b). Guard cell signal transduction network: advances in understanding abscisic acid, CO₂, and Ca²⁺ signaling. *Annu Rev Plant Biol*, Vol. 61, pp. 561-91.
- King, S.M. & Patel-King, R.S. (1995). The M(r) = 8,000 and 11,000 outer arm dynein light chains from *Chlamydomonas* flagella have cytoplasmic homologues. *J Biol Chem*, Vol. 270, No. 19, pp. 11445-52.
- King, S.T. & Kenney, L.J. (2007). Application of fluorescence resonance energy transfer to examine EnvZ/OmpR interactions. *Methods Enzymol*, Vol. 422, pp. 352-60.
- Kloda, A. & Martinac, B. (2002). Mechanosensitive channels of bacteria and archaea share a common ancestral origin. *Eur Biophys J*, Vol. 31, No. 1, pp. 14-25.
- Klusener, B., Young, J.J., Murata, Y., Allen, G.J., Mori, I.C., Hugouvieux, V. & Schroeder, J.I. (2002). Convergence of calcium signaling pathways of pathogenic elicitors and abscisic acid in *Arabidopsis* guard cells. *Plant Physiol*, Vol. 130, No. 4, pp. 2152-63.
- Knepper, C., Savory, E.A. & Day, B. (2011). *Arabidopsis* NDR1 is an integrin-like protein with a role in fluid loss and plasma membrane-cell wall adhesion. *Plant Physiol*, Vol. 156, No. 1, pp. 286-300.
- Knight, H., Trewavas, A.J. & Knight, M.R. (1997). Calcium signalling in *Arabidopsis thaliana* responding to drought and salinity. *Plant J*, Vol. 12, No. 5, pp. 1067-78.
- Kobayashi, Y., Murata, M., Minami, H., Yamamoto, S., Kagaya, Y., Hobo, T., Yamamoto, A. & Hattori, T. (2005). Abscisic acid-activated SNRK2 protein kinases function in the gene-regulation pathway of ABA signal transduction by phosphorylating ABA response element-binding factors. *Plant J*, Vol. 44, No. 6, pp. 939-49.
- Kobayashi, Y., Yamamoto, S., Minami, H., Kagaya, Y. & Hattori, T. (2004). Differential activation of the rice sucrose nonfermenting1-related protein kinase2 family by hyperosmotic stress and abscisic acid. *Plant Cell*, Vol. 16, No. 5, pp. 1163-77.
- Kogan, F. (1997). Global drought watch from space. *Bull Am Meteorol Soc*, Vol. 78, pp. 621-636.
- Kohorn, B.D. & Kohorn, S.L. (2012). The cell wall-associated kinases, WAKs, as pectin receptors. *Front Plant Sci*, Vol. 3, pp. 88.
- Koiwa, H., Barb, A.W., Xiong, L., Li, F., McCully, M.G., Lee, B.H., Sokolchik, I., Zhu, J., Gong, Z., Reddy, M., Sharkhuu, A., Manabe, Y., Yokoi, S., Zhu, J.K., Bressan, R.A. & Hasegawa, P.M. (2002). C-terminal domain phosphatase-like family members (AtCPLs) differentially regulate *Arabidopsis thaliana* abiotic stress signaling, growth, and development. *Proc Natl Acad Sci U S A*, Vol. 99, No. 16, pp. 10893-8.
- Koiwai, H., Nakaminami, K., Seo, M., Mitsuhashi, W., Toyomasu, T. & Koshiba, T. (2004). Tissue-specific localization of an abscisic acid biosynthetic enzyme, AAO3, in *Arabidopsis*. *Plant Physiol*, Vol. 134, No. 4, pp. 1697-707.
- Koltai, H. (2014). Receptors, repressors, PINs: a playground for strigolactone signaling. *Trends Plant Sci*.
- Kolukisaoglu, U., Weinl, S., Blazevic, D., Batistic, O. & Kudla, J. (2004). Calcium sensors and their interacting protein kinases: genomics of the *Arabidopsis* and rice CBL-CIPK signaling networks. *Plant Physiol*, Vol. 134, No. 1, pp. 43-58.
- Kong, Z., Li, M., Yang, W., Xu, W. & Xue, Y. (2006). A novel nuclear-localized CCCH-type zinc finger protein, OsDOS, is involved in delaying leaf senescence in rice. *Plant Physiol*, Vol. 141, No. 4, pp. 1376-88.
- Koornneef, M., Bentsink, L. & Hilhorst, H. (2002). Seed dormancy and germination. *Curr Opin Plant Biol*, Vol. 5, No. 1, pp. 33-6.

References

- Koornneef, M., Jorna, M.L., Brinkhorst-van der Swan, D.L. & Karssen, C.M. (1982). The isolation of abscisic acid (ABA) deficient mutants by selection of induced revertants in non-germinating gibberellin sensitive lines of *Arabidopsis thaliana* (L.) heynh. *Theor Appl Genet*, Vol. 61, No. 4, pp. 385-93.
- Koornneef, M., Reuling, G. & Karssen, C.M. (1984). The isolation and characterisation of abscisic acid-insensitive mutants of *Arabidopsis thaliana*. *Physiol Plant* Vol. 61, pp. 377-383.
- Kosugi, S., Hasebe, M., Matsumura, N., Takashima, H., Miyamoto-Sato, E., Tomita, M. & Yanagawa, H. (2009). Six classes of nuclear localization signals specific to different binding grooves of importin alpha. *J Biol Chem*, Vol. 284, No. 1, pp. 478-85.
- Kotak, S., Vierling, E., Baumlein, H. & von Koskull-Doring, P. (2007). A novel transcriptional cascade regulating expression of heat stress proteins during seed development of *Arabidopsis*. *Plant Cell*, Vol. 19, No. 1, pp. 182-95.
- Kovtun, Y., Chiu, W.L., Tena, G. & Sheen, J. (2000). Functional analysis of oxidative stress-activated mitogen-activated protein kinase cascade in plants. *Proc Natl Acad Sci U S A*, Vol. 97, No. 6, pp. 2940-5.
- Kramer, P.J. & Boyer, J.S. (1995). *Water relations of plants and soils*, San Diego: Academic Press, p. xv, 495 p.
- Krogan, N.T., Hogan, K. & Long, J.A. (2012). APETALA2 negatively regulates multiple floral organ identity genes in *Arabidopsis* by recruiting the co-repressor TOPLESS and the histone deacetylase HDA19. *Development*, Vol. 139, No. 22, pp. 4180-90.
- Kuhn, J.M., Boisson-Dernier, A., Dizon, M.B., Maktabi, M.H. & Schroeder, J.I. (2006). The protein phosphatase AtPP2CA negatively regulates abscisic acid signal transduction in *Arabidopsis*, and effects of abh1 on AtPP2CA mRNA. *Plant Physiol*, Vol. 140, No. 1, pp. 127-39.
- Kulik, A., Wawer, I., Krzywinska, E., Bucholc, M. & Dobrowolska, G. (2011). SnRK2 protein kinases--key regulators of plant response to abiotic stresses. *OMICS*, Vol. 15, No. 12, pp. 859-72.
- Kumar, M.N., Jane, W.N. & Verslues, P.E. (2013). Role of the putative osmosensor *Arabidopsis* histidine kinase1 in dehydration avoidance and low-water-potential response. *Plant Physiol*, Vol. 161, No. 2, pp. 942-53.
- Kuromori, T., Miyaji, T., Yabuuchi, H., Shimizu, H., Sugimoto, E., Kamiya, A., Moriyama, Y. & Shinozaki, K. (2010). ABC transporter AtABCG25 is involved in abscisic acid transport and responses. *Proc Natl Acad Sci U S A*, Vol. 107, No. 5, pp. 2361-6.
- Kuromori, T. & Shinozaki, K. (2010). ABA transport factors found in *Arabidopsis* ABC transporters. *Plant Signal Behav*, Vol. 5, No. 9, pp. 1124-6.
- Kuromori, T., Sugimoto, E. & Shinozaki, K. (2011). *Arabidopsis* mutants of AtABCG22, an ABC transporter gene, increase water transpiration and drought susceptibility. *Plant J*, Vol. 67, No. 5, pp. 885-94.
- Kushiro, T., Okamoto, M., Nakabayashi, K., Yamagishi, K., Kitamura, S., Asami, T., Hirai, N., Koshihara, T., Kamiya, Y. & Nambara, E. (2004). The *Arabidopsis* cytochrome P450 CYP707A encodes ABA 8'-hydroxylases: key enzymes in ABA catabolism. *EMBO J*, Vol. 23, No. 7, pp. 1647-56.
- Kushwaha, H.R., Singla-Pareek, S.L. & Pareek, A. (2013). Putative osmosensor - OsHK3b - a histidine kinase protein from rice shows high structural conservation with its ortholog AtHK1 from *Arabidopsis*. *J Biomol Struct Dyn*.
- Kwak, J.M., Mori, I.C., Pei, Z.M., Leonhardt, N., Torres, M.A., Dangel, J.L., Bloom, R.E., Bodde, S., Jones, J.D. & Schroeder, J.I. (2003). NADPH oxidase AtrbohD and AtrbohF genes function in ROS-dependent ABA signaling in *Arabidopsis*. *EMBO J*, Vol. 22, No. 11, pp. 2623-33.
- Kwak, J.M., Murata, Y., Baizabal-Aguirre, V.M., Merrill, J., Wang, M., Kemper, A., Hawke, S.D., Tallman, G. & Schroeder, J.I. (2001). Dominant negative guard cell K⁺ channel mutants reduce inward-rectifying K⁺ currents and light-induced stomatal opening in *Arabidopsis*. *Plant Physiol*, Vol. 127, No. 2, pp. 473-85.

- Lai, J., Chen, H., Teng, K., Zhao, Q., Zhang, Z., Li, Y., Liang, L., Xia, R., Wu, Y., Guo, H. & Xie, Q. (2009). RKP, a RING finger E3 ligase induced by BSCTV C4 protein, affects geminivirus infection by regulation of the plant cell cycle. *Plant J*, Vol. 57, No. 5, pp. 905-17.
- Lan, W.Z., Lee, S.C., Che, Y.F., Jiang, Y.Q. & Luan, S. (2011). Mechanistic analysis of AKT1 regulation by the CBL-CIPK-PP2CA interactions. *Mol Plant*, Vol. 4, No. 3, pp. 527-36.
- Lanford, R.E., Chavez, D., Barrera, A. & Brasky, K.M. (2003). An infectious clone of woolly monkey hepatitis B virus. *J Virol*, Vol. 77, No. 14, pp. 7814-9.
- Lang, F. (2007). Mechanisms and significance of cell volume regulation. *J Am Coll Nutr*, Vol. 26, No. 5 Suppl, pp. 613S-623S.
- Lang, V. & Palva, E.T. (1992). The expression of a rab-related gene, rab18, is induced by abscisic acid during the cold acclimation process of *Arabidopsis thaliana* (L.) Heynh. *Plant Mol Biol*, Vol. 20, No. 5, pp. 951-62.
- Lange, A., Mills, R.E., Devine, S.E. & Corbett, A.H. (2008). A PY-NLS nuclear targeting signal is required for nuclear localization and function of the *Saccharomyces cerevisiae* mRNA-binding protein Hrp1. *J Biol Chem*, Vol. 283, No. 19, pp. 12926-34.
- Le, D.T., Nishiyama, R., Watanabe, Y., Tanaka, M., Seki, M., Ham le, H., Yamaguchi-Shinozaki, K., Shinozaki, K. & Tran, L.S. (2012). Differential gene expression in soybean leaf tissues at late developmental stages under drought stress revealed by genome-wide transcriptome analysis. *PLoS One*, Vol. 7, No. 11, pp. e49522.
- Lebaudy, A., Pascaud, F., Very, A.A., Alcon, C., Dreyer, I., Thibaud, J.B. & Lacombe, B. (2009). Preferential KAT1-KAT2 heteromerization determines inward K⁺ current properties in *Arabidopsis* guard cells. *J Biol Chem*, Vol. 285, No. 9, pp. 6265-74.
- Lee, B.H., Kapoor, A., Zhu, J. & Zhu, J.K. (2006a). STABILIZED1, a stress-upregulated nuclear protein, is required for pre-mRNA splicing, mRNA turnover, and stress tolerance in *Arabidopsis*. *Plant Cell*, Vol. 18, No. 7, pp. 1736-49.
- Lee, G., Abdi, K., Jiang, Y., Michaely, P., Bennett, V. & Marszalek, P.E. (2006b). Nanospring behaviour of ankyrin repeats. *Nature*, Vol. 440, No. 7081, pp. 246-9.
- Lee, K.H., Piao, H.L., Kim, H.Y., Choi, S.M., Jiang, F., Hartung, W., Hwang, I., Kwak, J.M. & Lee, I.J. (2006c). Activation of glucosidase via stress-induced polymerization rapidly increases active pools of abscisic acid. *Cell*, Vol. 126, No. 6, pp. 1109-20.
- Lee, K.P. & Lopez-Molina, L. (2013). A seed coat bedding assay to genetically explore in vitro how the endosperm controls seed germination in *Arabidopsis thaliana*. *J Vis Exp*, No. 81, pp. e50732.
- Lee, K.P., Piskurewicz, U., Tureckova, V., Strnad, M. & Lopez-Molina, L. (2010). A seed coat bedding assay shows that RGL2-dependent release of abscisic acid by the endosperm controls embryo growth in *Arabidopsis* dormant seeds. *Proc Natl Acad Sci U S A*, Vol. 107, No. 44, pp. 19108-13.
- Lee, S.C., Lan, W., Buchanan, B.B. & Luan, S. (2009). A protein kinase-phosphatase pair interacts with an ion channel to regulate ABA signaling in plant guard cells. *Proc Natl Acad Sci U S A*, Vol. 106, No. 50, pp. 21419-24.
- Lee, S.C., Lim, C.W., Lan, W., He, K. & Luan, S. (2012). ABA signaling in guard cells entails a dynamic protein-protein interaction relay from the PYL-RCAR family receptors to ion channels. *Mol Plant*, Vol. 6, No. 2, pp. 528-38.
- Lefebvre, V., North, H., Frey, A., Sotta, B., Seo, M., Okamoto, M., Nambara, E. & Marion-Poll, A. (2006). Functional analysis of *Arabidopsis* NCED6 and NCED9 genes indicates that ABA synthesized in the endosperm is involved in the induction of seed dormancy. *Plant J*, Vol. 45, No. 3, pp. 309-19.
- Legate, K.R., Wickstrom, S.A. & Fassler, R. (2009). Genetic and cell biological analysis of integrin outside-in signaling. *Genes Dev*, Vol. 23, No. 4, pp. 397-418.

References

- LeNoble, M.E., Spollen, W.G. & Sharp, R.E. (2004). Maintenance of shoot growth by endogenous ABA: genetic assessment of the involvement of ethylene suppression. *J Exp Bot*, Vol. 55, No. 395, pp. 237-45.
- Leon-Kloosterziel, K.M., Gil, M.A., Ruijs, G.J., Jacobsen, S.E., Olszewski, N.E., Schwartz, S.H., Zeevaart, J.A. & Koornneef, M. (1996). Isolation and characterization of abscisic acid-deficient Arabidopsis mutants at two new loci. *Plant J*, Vol. 10, No. 4, pp. 655-61.
- Leube, M.P., Grill, E. & Amrhein, N. (1998). ABI1 of Arabidopsis is a protein serine/threonine phosphatase highly regulated by the proton and magnesium ion concentration. *FEBS Lett*, Vol. 424, No. 1-2, pp. 100-4.
- Leung, J., Bouvier-Durand, M., Morris, P.C., Guerrier, D., Chefdor, F. & Giraudat, J. (1994). Arabidopsis ABA response gene ABI1: features of a calcium-modulated protein phosphatase. *Science*, Vol. 264, No. 5164, pp. 1448-52.
- Leung, J., Merlot, S. & Giraudat, J. (1997). The Arabidopsis ABSCISIC ACID-INSENSITIVE2 (ABI2) and ABI1 genes encode homologous protein phosphatases 2C involved in abscisic acid signal transduction. *Plant Cell*, Vol. 9, No. 5, pp. 759-71.
- Levin, D.E. (2005). Cell wall integrity signaling in *Saccharomyces cerevisiae*. *Microbiol Mol Biol Rev*, Vol. 69, No. 2, pp. 262-91.
- Levin, D.E. (2011). Regulation of cell wall biogenesis in *Saccharomyces cerevisiae*: the cell wall integrity signaling pathway. *Genetics*, Vol. 189, No. 4, pp. 1145-75.
- Levina, N., Totemeyer, S., Stokes, N.R., Louis, P., Jones, M.A. & Booth, I.R. (1999). Protection of *Escherichia coli* cells against extreme turgor by activation of MscS and MscL mechanosensitive channels: identification of genes required for MscS activity. *EMBO J*, Vol. 18, No. 7, pp. 1730-7.
- Levitt, J. (1972). *Responses of plants to environmental stresses*, New York,: Academic Press, p. xii, 697 p.
- Li, H., Sun, J., Xu, Y., Jiang, H., Wu, X. & Li, C. (2007). The bHLH-type transcription factor AtAIB positively regulates ABA response in Arabidopsis. *Plant Mol Biol*, Vol. 65, No. 5, pp. 655-65.
- Li, J., Jia, D. & Chen, X. (2001). HUA1, a regulator of stamen and carpel identities in Arabidopsis, codes for a nuclear RNA binding protein. *Plant Cell*, Vol. 13, No. 10, pp. 2269-81.
- Li, J., Wang, X.Q., Watson, M.B. & Assmann, S.M. (2000). Regulation of abscisic acid-induced stomatal closure and anion channels by guard cell AAPK kinase. *Science*, Vol. 287, No. 5451, pp. 300-3.
- Li, L., Kim, B.G., Cheong, Y.H., Pandey, G.K. & Luan, S. (2006). A Ca²⁺ signaling pathway regulates a K⁺ channel for low-K response in Arabidopsis. *Proc Natl Acad Sci U S A*, Vol. 103, No. 33, pp. 12625-30.
- Li, S., Fu, Q., Chen, L., Huang, W. & Yu, D. (2011). Arabidopsis thaliana WRKY25, WRKY26, and WRKY33 coordinate induction of plant thermotolerance. *Planta*, Vol. 233, No. 6, pp. 1237-52.
- Li, W., Wang, L., Sheng, X., Yan, C., Zhou, R., Hang, J., Yin, P. & Yan, N. (2013). Molecular basis for the selective and ABA-independent inhibition of PP2CA by PYL13. *Cell Res*, Vol. 23, No. 12, pp. 1369-79.
- Liang, J., Jaffrey, S.R., Guo, W., Snyder, S.H. & Clardy, J. (1999). Structure of the PIN/LC8 dimer with a bound peptide. *Nat Struct Biol*, Vol. 6, No. 8, pp. 735-40.
- Lichtenthaler, H.K. (1987). Chlorophylls and carotenoids: pigments of photosynthetic biomembranes. *Methods Enzymol*, Vol. 148, pp. 350-382.
- Lim, G.H., Zhang, X., Chung, M.S., Lee, D.J., Woo, Y.M., Cheong, H.S. & Kim, C.S. (2009). A putative novel transcription factor, AtSKIP, is involved in abscisic acid signalling and confers salt and osmotic tolerance in Arabidopsis. *New Phytol*, Vol. 185, No. 1, pp. 103-13.
- Lin, Z., Zhong, S. & Grierson, D. (2009). Recent advances in ethylene research. *J Exp Bot*, Vol. 60, No. 12, pp. 3311-36.

- Lindemose, S., O'Shea, C., Jensen, M.K. & Skriver, K. (2013). Structure, function and networks of transcription factors involved in abiotic stress responses. *Int J Mol Sci*, Vol. 14, No. 3, pp. 5842-78.
- Liu, H. & Stone, S.L. (2010). Abscisic acid increases Arabidopsis ABI5 transcription factor levels by promoting KEG E3 ligase self-ubiquitination and proteasomal degradation. *Plant Cell*, Vol. 22, No. 8, pp. 2630-41.
- Liu, Q., Kasuga, M., Sakuma, Y., Abe, H., Miura, S., Yamaguchi-Shinozaki, K. & Shinozaki, K. (1998). Two transcription factors, DREB1 and DREB2, with an EREBP/AP2 DNA binding domain separate two cellular signal transduction pathways in drought- and low-temperature-responsive gene expression, respectively, in Arabidopsis. *Plant Cell*, Vol. 10, No. 8, pp. 1391-406.
- Liu, Q. & Wen, C.K. (2012). Cooperative ethylene receptor signaling. *Plant Signal Behav*, Vol. 7, No. 8, pp. 1009-13.
- Liu, W.C. & Carnsdagger, H.R. (1961). Isolation of Abscisin, an Abscission Accelerating Substance. *Science*, Vol. 134, No. 3476, pp. 384-5.
- Liu, X., Yue, Y., Li, B., Nie, Y., Li, W., Wu, W.H. & Ma, L. (2007). A G protein-coupled receptor is a plasma membrane receptor for the plant hormone abscisic acid. *Science*, Vol. 315, No. 5819, pp. 1712-6.
- Liu, Y., Zhang, S. & Klessig, D.F. (2000). Molecular cloning and characterization of a tobacco MAP kinase kinase that interacts with SIPK. *Mol Plant Microbe Interact*, Vol. 13, No. 1, pp. 118-24.
- Lohrmann, J. & Harter, K. (2002). Plant two-component signaling systems and the role of response regulators. *Plant Physiol*, Vol. 128, No. 2, pp. 363-9.
- Long, J.A., Ohno, C., Smith, Z.R. & Meyerowitz, E.M. (2006). TOPLESS regulates apical embryonic fate in Arabidopsis. *Science*, Vol. 312, No. 5779, pp. 1520-3.
- Lopez-Molina, L., Mongrand, S. & Chua, N.H. (2001). A postgermination developmental arrest checkpoint is mediated by abscisic acid and requires the ABI5 transcription factor in Arabidopsis. *Proc Natl Acad Sci U S A*, Vol. 98, No. 8, pp. 4782-7.
- Lopez-Molina, L., Mongrand, S., Kinoshita, N. & Chua, N.H. (2003). AFP is a novel negative regulator of ABA signaling that promotes ABI5 protein degradation. *Genes Dev*, Vol. 17, No. 3, pp. 410-8.
- Lopez-Molina, L., Mongrand, S., McLachlin, D.T., Chait, B.T. & Chua, N.H. (2002). ABI5 acts downstream of ABI3 to execute an ABA-dependent growth arrest during germination. *Plant J*, Vol. 32, No. 3, pp. 317-28.
- Lorenzo, O., Chico, J.M., Sanchez-Serrano, J.J. & Solano, R. (2004). JASMONATE-INSENSITIVE1 encodes a MYC transcription factor essential to discriminate between different jasmonate-regulated defense responses in Arabidopsis. *Plant Cell*, Vol. 16, No. 7, pp. 1938-50.
- Lu, B., Chen, F., Gong, Z.H., Xie, H., Zhang, J.H. & Liang, J.S. (2007). Intracellular localization of integrin-like protein and its roles in osmotic stress-induced abscisic acid biosynthesis in *Zea mays*. *Protoplasma*, Vol. 232, No. 1-2, pp. 35-43.
- Lu, B., Wang, J., Zhang, Y., Wang, H., Liang, J. & Zhang, J. (2012). AT14A mediates the cell wall-plasma membrane-cytoskeleton continuum in Arabidopsis thaliana cells. *J Exp Bot*, Vol. 63, No. 11, pp. 4061-9.
- Lu, H., Zhang, C., Albrecht, U., Shimizu, R., Wang, G. & Bowman, K.D. (2013). Overexpression of a citrus NDR1 ortholog increases disease resistance in Arabidopsis. *Front Plant Sci*, Vol. 4, pp. 157.
- Luan, S. (2009). The CBL-CIPK network in plant calcium signaling. *Trends Plant Sci*, Vol. 14, No. 1, pp. 37-42.
- Ludwig, A.A., Romeis, T. & Jones, J.D. (2004). CDPK-mediated signalling pathways: specificity and cross-talk. *J Exp Bot*, Vol. 55, No. 395, pp. 181-8.
- Lukowitz, W., Gillmor, C.S. & Scheible, W.R. (2000). Positional cloning in Arabidopsis. Why it feels good to have a genome initiative working for you. *Plant Physiol*, Vol. 123, No. 3, pp. 795-805.

References

- Lyzenga, W.J., Liu, H., Schofield, A., Muise-Hennessey, A. & Stone, S.L. (2013). Arabidopsis CIPK26 interacts with KEG, components of the ABA signalling network and is degraded by the ubiquitin-proteasome system. *J Exp Bot*, Vol. 64, No. 10, pp. 2779-91.
- Ma, S.Y. & Wu, W.H. (2007). AtCPK23 functions in Arabidopsis responses to drought and salt stresses. *Plant Mol Biol*, Vol. 65, No. 4, pp. 511-8.
- Ma, Y., Szostkiewicz, I., Korte, A., Moes, D., Yang, Y., Christmann, A. & Grill, E. (2009). Regulators of PP2C phosphatase activity function as abscisic acid sensors. *Science*, Vol. 324, No. 5930, pp. 1064-8.
- MacRobbie, E.A. (1998). Signal transduction and ion channels in guard cells. *Philos Trans R Soc Lond B Biol Sci*, Vol. 353, No. 1374, pp. 1475-88.
- Maeda, T., Takekawa, M. & Saito, H. (1995). Activation of yeast PBS2 MAPKK by MAPKKs or by binding of an SH3-containing osmosensor. *Science*, Vol. 269, No. 5223, pp. 554-8.
- Maeda, T., Wurgler-Murphy, S.M. & Saito, H. (1994). A two-component system that regulates an osmosensing MAP kinase cascade in yeast. *Nature*, Vol. 369, No. 6477, pp. 242-5.
- Mahajan, S. & Tuteja, N. (2005). Cold, salinity and drought stresses: an overview. *Arch Biochem Biophys*, Vol. 444, No. 2, pp. 139-58.
- Maksaev, G. & Haswell, E.S. (2012). MscS-Like10 is a stretch-activated ion channel from Arabidopsis thaliana with a preference for anions. *Proc Natl Acad Sci U S A*, Vol. 109, No. 46, pp. 19015-20.
- Mao, X., Zhang, H., Tian, S., Chang, X. & Jing, R. (2009). TaSnRK2.4, an SNF1-type serine/threonine protein kinase of wheat (*Triticum aestivum* L.), confers enhanced multistress tolerance in Arabidopsis. *J Exp Bot*, Vol. 61, No. 3, pp. 683-96.
- Marin, E., Nussaume, L., Quesada, A., Gonneau, M., Sotta, B., Huguency, P., Frey, A. & Marion-Poll, A. (1996). Molecular identification of zeaxanthin epoxidase of *Nicotiana plumbaginifolia*, a gene involved in abscisic acid biosynthesis and corresponding to the ABA locus of Arabidopsis thaliana. *EMBO J*, Vol. 15, No. 10, pp. 2331-42.
- Martin-Rodriguez, J.A., Leon-Morcillo, R., Vierheilig, H., Ocampo, J.A., Ludwig-Muller, J. & Garcia-Garrido, J.M. (2011). Ethylene-dependent/ethylene-independent ABA regulation of tomato plants colonized by arbuscular mycorrhiza fungi. *New Phytol*, Vol. 190, No. 1, pp. 193-205.
- Martinac, B. (2011). Bacterial mechanosensitive channels as a paradigm for mechanosensory transduction. *Cell Physiol Biochem*, Vol. 28, No. 6, pp. 1051-60.
- McCarty, D.R., Hattori, T., Carson, C.B., Vasil, V., Lazar, M. & Vasil, I.K. (1991). The Viviparous-1 developmental gene of maize encodes a novel transcriptional activator. *Cell*, Vol. 66, No. 5, pp. 895-905.
- McKay, J.K., Richards, J.H. & Mitchell-Olds, T. (2003). Genetics of drought adaptation in Arabidopsis thaliana: I. Pleiotropy contributes to genetic correlations among ecological traits. *Mol Ecol*, Vol. 12, No. 5, pp. 1137-51.
- Medrano, H., Escalona, J.M., Bota, J., Gulias, J. & Flexas, J. (2002). Regulation of photosynthesis of C3 plants in response to progressive drought: stomatal conductance as a reference parameter. *Ann Bot*, Vol. 89, Spec No, pp. 895-905.
- Meena, N., Kaur, H. & Mondal, A.K. (2010). Interactions among HAMP domain repeats act as an osmosensing molecular switch in group III hybrid histidine kinases from fungi. *J Biol Chem*, Vol. 285, No. 16, pp. 12121-32.
- Meinhard, M. & Grill, E. (2001). Hydrogen peroxide is a regulator of ABI1, a protein phosphatase 2C from Arabidopsis. *FEBS Lett*, Vol. 508, No. 3, pp. 443-6.
- Meinhard, M., Rodriguez, P.L. & Grill, E. (2002). The sensitivity of ABI2 to hydrogen peroxide links the abscisic acid-response regulator to redox signalling. *Planta*, Vol. 214, No. 5, pp. 775-82.

- Melcher, K., Ng, L.M., Zhou, X.E., Soon, F.F., Xu, Y., Suino-Powell, K.M., Park, S.Y., Weiner, J.J., Fujii, H., Chinnusamy, V., Kovach, A., Li, J., Wang, Y., Peterson, F.C., Jensen, D.R., Yong, E.L., Volkman, B.F., Cutler, S.R., Zhu, J.K. & Xu, H.E. (2009). A gate-latch-lock mechanism for hormone signalling by abscisic acid receptors. *Nature*, Vol. 462, No. 7273, pp. 602-8.
- Melcher, K., Xu, Y., Ng, L.M., Zhou, X.E., Soon, F.F., Chinnusamy, V., Suino-Powell, K.M., Kovach, A., Tham, F.S., Cutler, S.R., Li, J., Yong, E.L., Zhu, J.K. & Xu, H.E. (2010). Identification and mechanism of ABA receptor antagonism. *Nat Struct Mol Biol*, Vol. 17, No. 9, pp. 1102-8.
- Merlot, S., Gosti, F., Guerrier, D., Vavasseur, A. & Giraudat, J. (2001). The ABI1 and ABI2 protein phosphatases 2C act in a negative feedback regulatory loop of the abscisic acid signalling pathway. *Plant J*, Vol. 25, No. 3, pp. 295-303.
- Merlot, S., Mustilli, A.C., Genty, B., North, H., Lefebvre, V., Sotta, B., Vavasseur, A. & Giraudat, J. (2002). Use of infrared thermal imaging to isolate Arabidopsis mutants defective in stomatal regulation. *Plant J*, Vol. 30, No. 5, pp. 601-9.
- Metzker, M.L. (2009). Sequencing technologies - the next generation. *Nat Rev Genet*, Vol. 11, No. 1, pp. 31-46.
- Meyer, K., Leube, M.P. & Grill, E. (1994). A protein phosphatase 2C involved in ABA signal transduction in Arabidopsis thaliana. *Science*, Vol. 264, No. 5164, pp. 1452-5.
- Michelmore, R.W., Paran, I. & Kesseli, R.V. (1991). Identification of markers linked to disease-resistance genes by bulked segregant analysis: a rapid method to detect markers in specific genomic regions by using segregating populations. *Proc Natl Acad Sci U S A*, Vol. 88, No. 21, pp. 9828-32.
- Mikolajczyk, M., Awotunde, O.S., Muszynska, G., Klessig, D.F. & Dobrowolska, G. (2000). Osmotic stress induces rapid activation of a salicylic acid-induced protein kinase and a homolog of protein kinase ASK1 in tobacco cells. *Plant Cell*, Vol. 12, No. 1, pp. 165-78.
- Mishra, N.S., Tuteja, R. & Tuteja, N. (2006). Signaling through MAP kinase networks in plants. *Arch Biochem Biophys*, Vol. 452, No. 1, pp. 55-68.
- Miyata, S., Urao, T., Yamaguchi-Shinozaki, K. & Shinozaki, K. (1998). Characterization of genes for two-component phosphorelay mediators with a single Hpt domain in Arabidopsis thaliana. *FEBS Lett*, Vol. 437, No. 1-2, pp. 11-4.
- Miyazono, K., Miyakawa, T., Sawano, Y., Kubota, K., Kang, H.J., Asano, A., Miyauchi, Y., Takahashi, M., Zhi, Y., Fujita, Y., Yoshida, T., Kodaira, K.S., Yamaguchi-Shinozaki, K. & Tanokura, M. (2009). Structural basis of abscisic acid signalling. *Nature*, Vol. 462, No. 7273, pp. 609-14.
- Mizuno, T. (2005). Two-component phosphorelay signal transduction systems in plants: from hormone responses to circadian rhythms. *Biosci Biotechnol Biochem*, Vol. 69, No. 12, pp. 2263-76.
- Mochizuki, N., Brusslan, J.A., Larkin, R., Nagatani, A. & Chory, J. (2001). Arabidopsis genomes uncoupled 5 (GUN5) mutant reveals the involvement of Mg-chelatase H subunit in plastid-to-nucleus signal transduction. *Proc Natl Acad Sci U S A*, Vol. 98, No. 4, pp. 2053-8.
- Moes, D., Himmelbach, A., Korte, A., Haberer, G. & Grill, E. (2008). Nuclear localization of the mutant protein phosphatase abi1 is required for insensitivity towards ABA responses in Arabidopsis. *Plant J*, Vol. 54, No. 5, pp. 806-19.
- Monks, D.E., Aghoram, K., Courtney, P.D., DeWald, D.B. & Dewey, R.E. (2001). Hyperosmotic stress induces the rapid phosphorylation of a soybean phosphatidylinositol transfer protein homolog through activation of the protein kinases SPK1 and SPK2. *Plant Cell*, Vol. 13, No. 5, pp. 1205-19.
- Monshausen, G.B., Bibikova, T.N., Weisenseel, M.H. & Gilroy, S. (2009). Ca²⁺ regulates reactive oxygen species production and pH during mechanosensing in Arabidopsis roots. *Plant Cell*, Vol. 21, No. 8, pp. 2341-56.
- Moore, J.P., Vre-Gibouin, M., Farrant, J.M. & Driouich, A. (2008). Adaptations of higher plant cell walls to water loss: drought vs desiccation. *Physiol Plant*, Vol. 134, No. 2, pp. 237-45.

References

- Mori, I.C., Murata, Y., Yang, Y., Munemasa, S., Wang, Y.F., Andreoli, S., Tiriach, H., Alonso, J.M., Harper, J.F., Ecker, J.R., Kwak, J.M. & Schroeder, J.I. (2006). CDPKs CPK6 and CPK3 function in ABA regulation of guard cell S-type anion- and Ca²⁺-permeable channels and stomatal closure. *PLoS Biol*, Vol. 4, No. 10, pp. e327.
- Mori, I.C. & Schroeder, J.I. (2004). Reactive oxygen species activation of plant Ca²⁺ channels. A signaling mechanism in polar growth, hormone transduction, stress signaling, and hypothetically mechanotransduction. *Plant Physiol*, Vol. 135, No. 2, pp. 702-8.
- Mouradov, A., Cremer, F. & Coupland, G. (2002). Control of flowering time: interacting pathways as a basis for diversity. *Plant Cell*, Vol. 14 Suppl, pp. S111-30.
- Muller, A.H. & Hansson, M. (2009). The barley magnesium chelatase 150-kd subunit is not an abscisic acid receptor. *Plant Physiol*, Vol. 150, No. 1, pp. 157-66.
- Mundy, J., Yamaguchi-Shinozaki, K. & Chua, N.H. (1990). Nuclear proteins bind conserved elements in the abscisic acid-responsive promoter of a rice rab gene. *Proc Natl Acad Sci U S A*, Vol. 87, No. 4, pp. 1406-10.
- Munnik, T., Ligterink, W., Meskiene, I.I., Calderini, O., Beyerly, J., Musgrave, A. & Hirt, H. (1999). Distinct osmo-sensing protein kinase pathways are involved in signalling moderate and severe hyper-osmotic stress. *Plant J*, Vol. 20, No. 4, pp. 381-8.
- Mustilli, A.C., Merlot, S., Vavasseur, A., Fenzi, F. & Giraudat, J. (2002). Arabidopsis OST1 protein kinase mediates the regulation of stomatal aperture by abscisic acid and acts upstream of reactive oxygen species production. *Plant Cell*, Vol. 14, No. 12, pp. 3089-99.
- Nakagami, H., Kiegerl, S. & Hirt, H. (2004). OMTK1, a novel MAPKKK, channels oxidative stress signaling through direct MAPK interaction. *J Biol Chem*, Vol. 279, No. 26, pp. 26959-66.
- Nakagami, H., Soukupova, H., Schikora, A., Zarsky, V. & Hirt, H. (2006). A Mitogen-activated protein kinase kinase kinase mediates reactive oxygen species homeostasis in Arabidopsis. *J Biol Chem*, Vol. 281, No. 50, pp. 38697-704.
- Nakagawa, Y., Katagiri, T., Shinozaki, K., Qi, Z., Tatsumi, H., Furuichi, T., Kishigami, A., Sokabe, M., Kojima, I., Sato, S., Kato, T., Tabata, S., Iida, K., Terashima, A., Nakano, M., Ikeda, M., Yamanaka, T. & Iida, H. (2007). Arabidopsis plasma membrane protein crucial for Ca²⁺ influx and touch sensing in roots. *Proc Natl Acad Sci U S A*, Vol. 104, No. 9, pp. 3639-44.
- Nakashima, K., Fujita, Y., Kanamori, N., Katagiri, T., Umezawa, T., Kidokoro, S., Maruyama, K., Yoshida, T., Ishiyama, K., Kobayashi, M., Shinozaki, K. & Yamaguchi-Shinozaki, K. (2009a). Three Arabidopsis SnRK2 protein kinases, SRK2D/SnRK2.2, SRK2E/SnRK2.6/OST1 and SRK2I/SnRK2.3, involved in ABA signaling are essential for the control of seed development and dormancy. *Plant Cell Physiol*, Vol. 50, No. 7, pp. 1345-63.
- Nakashima, K., Ito, Y. & Yamaguchi-Shinozaki, K. (2009b). Transcriptional regulatory networks in response to abiotic stresses in Arabidopsis and grasses. *Plant Physiol*, Vol. 149, No. 1, pp. 88-95.
- Nakashima, K., Kiyosue, T., Yamaguchi-Shinozaki, K. & Shinozaki, K. (1997). A nuclear gene, *erd1*, encoding a chloroplast-targeted Clp protease regulatory subunit homolog is not only induced by water stress but also developmentally up-regulated during senescence in Arabidopsis thaliana. *Plant J*, Vol. 12, No. 4, pp. 851-61.
- Nakata, M., Mitsuda, N., Herde, M., Koo, A.J., Moreno, J.E., Suzuki, K., Howe, G.A. & Ohme-Takagi, M. (2013). A bHLH-Type Transcription Factor, ABA-INDUCIBLE BHLH-TYPE TRANSCRIPTION FACTOR/JA-ASSOCIATED MYC2-LIKE1, Acts as a Repressor to Negatively Regulate Jasmonate Signaling in Arabidopsis. *Plant Cell*.
- Nakata, M. & Ohme-Takagi, M. (2013). Two bHLH-type transcription factors, JA-ASSOCIATED MYC2-LIKE2 and JAM3, are transcriptional repressors and affect male fertility. *Plant Signal Behav*, Vol. 8, No. 12.

- Nakayama, H., Yoshida, K., Ono, H., Murooka, Y. & Shinmyo, A. (2000). Ectoine, the compatible solute of *Halomonas elongata*, confers hyperosmotic tolerance in cultured tobacco cells. *Plant Physiol*, Vol. 122, No. 4, pp. 1239-47.
- Nambara, E. & Marion-Poll, A. (2005). Abscisic acid biosynthesis and catabolism. *Annu Rev Plant Biol*, Vol. 56, pp. 165-85.
- Ndimba, B.K., Chivasa, S., Simon, W.J. & Slabas, A.R. (2005). Identification of Arabidopsis salt and osmotic stress responsive proteins using two-dimensional difference gel electrophoresis and mass spectrometry. *Proteomics*, Vol. 5, No. 16, pp. 4185-96.
- Neff, M.M., Turk, E. & Kalishman, M. (2002). Web-based primer design for single nucleotide polymorphism analysis. *Trends Genet*, Vol. 18, No. 12, pp. 613-5.
- Negi, J., Matsuda, O., Nagasawa, T., Oba, Y., Takahashi, H., Kawai-Yamada, M., Uchimiya, H., Hashimoto, M. & Iba, K. (2008). CO₂ regulator SLAC1 and its homologues are essential for anion homeostasis in plant cells. *Nature*, Vol. 452, No. 7186, pp. 483-6.
- Ng, L.M., Soon, F.F., Zhou, X.E., West, G.M., Kovach, A., Suino-Powell, K.M., Chalmers, M.J., Li, J., Yong, E.L., Zhu, J.K., Griffin, P.R., Melcher, K. & Xu, H.E. (2011). Structural basis for basal activity and autoactivation of abscisic acid (ABA) signaling SnRK2 kinases. *Proc Natl Acad Sci U S A*, Vol. 108, No. 52, pp. 21259-64.
- Ning, J., Li, X., Hicks, L.M. & Xiong, L. (2010). A Raf-like MAPKKK gene DSM1 mediates drought resistance through reactive oxygen species scavenging in rice. *Plant Physiol*, Vol. 152, No. 2, pp. 876-90.
- Nishimura, N., Hitomi, K., Arvai, A.S., Rambo, R.P., Hitomi, C., Cutler, S.R., Schroeder, J.I. & Getzoff, E.D. (2009). Structural mechanism of abscisic acid binding and signaling by dimeric PYR1. *Science*, Vol. 326, No. 5958, pp. 1373-9.
- Nishimura, N., Sarkeshik, A., Nito, K., Park, S.Y., Wang, A., Carvalho, P.C., Lee, S., Caddell, D.F., Cutler, S.R., Chory, J., Yates, J.R. & Schroeder, J.I. (2010). PYR/PYL/RCAR family members are major in-vivo ABI1 protein phosphatase 2C-interacting proteins in Arabidopsis. *Plant J*, Vol. 61, No. 2, pp. 290-9.
- Nishimura, N., Yoshida, T., Kitahata, N., Asami, T., Shinozaki, K. & Hirayama, T. (2007). ABA-Hypersensitive Germination1 encodes a protein phosphatase 2C, an essential component of abscisic acid signaling in Arabidopsis seed. *Plant J*, Vol. 50, No. 6, pp. 935-49.
- Niu, Y., Figueroa, P. & Browse, J. (2011). Characterization of JAZ-interacting bHLH transcription factors that regulate jasmonate responses in Arabidopsis. *J Exp Bot*, Vol. 62, No. 6, pp. 2143-54.
- Niyogi, K.K., Grossman, A.R. & Bjorkman, O. (1998). Arabidopsis mutants define a central role for the xanthophyll cycle in the regulation of photosynthetic energy conversion. *Plant Cell*, Vol. 10, No. 7, pp. 1121-34.
- Nongpiur, R., Soni, P., Karan, R., Singla-Pareek, S.L. & Pareek, A. (2012). Histidine kinases in plants: cross talk between hormone and stress responses. *Plant Signal Behav*, Vol. 7, No. 10, pp. 1230-7.
- Nordin, K., Vahala, T. & Palva, E.T. (1993). Differential expression of two related, low-temperature-induced genes in Arabidopsis thaliana (L.) Heynh. *Plant Mol Biol*, Vol. 21, No. 4, pp. 641-53.
- North, H.M., De Almeida, A., Boutin, J.P., Frey, A., To, A., Botran, L., Sotta, B. & Marion-Poll, A. (2007). The Arabidopsis ABA-deficient mutant aba4 demonstrates that the major route for stress-induced ABA accumulation is via neoxanthin isomers. *Plant J*, Vol. 50, No. 5, pp. 810-24.
- Obayashi, T., Hayashi, S., Saeki, M., Ohta, H. & Kinoshita, K. (2009). ATTED-II provides coexpressed gene networks for Arabidopsis. *Nucleic Acids Res*, Vol. 37, No. Database issue, pp. D987-91.
- Ober, E.S. & Sharp, R.E. (2003). Electrophysiological responses of maize roots to low water potentials: relationship to growth and ABA accumulation. *J Exp Bot*, Vol. 54, No. 383, pp. 813-24.
- Ohkuma, K., Lyon, J.L., Addicott, F.T. & Smith, O.E. (1963). Abscission II, an Abscission-Accelerating Substance from Young Cotton Fruit. *Science*, Vol. 142, No. 3599, pp. 1592-3.

References

- Ohta, M., Guo, Y., Halfter, U. & Zhu, J.K. (2003). A novel domain in the protein kinase SOS2 mediates interaction with the protein phosphatase 2C ABI2. *Proc Natl Acad Sci U S A*, Vol. 100, No. 20, pp. 11771-6.
- Ohta, M., Matsui, K., Hiratsu, K., Shinshi, H. & Ohme-Takagi, M. (2001). Repression domains of class II ERF transcriptional repressors share an essential motif for active repression. *Plant Cell*, Vol. 13, No. 8, pp. 1959-68.
- Okamoto, M., Kushiro, T., Jikumaru, Y., Abrams, S.R., Kamiya, Y., Seki, M. & Nambara, E. (2011). ABA 9'-hydroxylation is catalyzed by CYP707A in Arabidopsis. *Phytochemistry*, Vol. 72, No. 8, pp. 717-22.
- Okamoto, M., Kuwahara, A., Seo, M., Kushiro, T., Asami, T., Hirai, N., Kamiya, Y., Koshihara, T. & Nambara, E. (2006). CYP707A1 and CYP707A2, which encode abscisic acid 8'-hydroxylases, are indispensable for proper control of seed dormancy and germination in Arabidopsis. *Plant Physiol*, Vol. 141, No. 1, pp. 97-107.
- Okamoto, M., Tatematsu, K., Matsui, A., Morosawa, T., Ishida, J., Tanaka, M., Endo, T.A., Mochizuki, Y., Toyoda, T., Kamiya, Y., Shinozaki, K., Nambara, E. & Seki, M. (2010). Genome-wide analysis of endogenous abscisic acid-mediated transcription in dry and imbibed seeds of Arabidopsis using tiling arrays. *Plant J*, Vol. 62, No. 1, pp. 39-51.
- Oliver, M.J., Velten, J. & Mishler, B.D. (2005). Desiccation tolerance in bryophytes: a reflection of the primitive strategy for plant survival in dehydrating habitats? *Integr Comp Biol*, Vol. 45, No. 5, pp. 788-99.
- Olsson, A.S., Engstrom, P. & Soderman, E. (2004). The homeobox genes ATHB12 and ATHB7 encode potential regulators of growth in response to water deficit in Arabidopsis. *Plant Mol Biol*, Vol. 55, No. 5, pp. 663-77.
- Opdenakker, K., Remans, T., Vangronsveld, J. & Cuypers, A. (2012). Mitogen-Activated Protein (MAP) Kinases in Plant Metal Stress: Regulation and Responses in Comparison to Other Biotic and Abiotic Stresses. *Int J Mol Sci*, Vol. 13, No. 6, pp. 7828-53.
- Osakabe, Y., Arinaga, N., Umezawa, T., Katsura, S., Nagamachi, K., Tanaka, H., Ohiraki, H., Yamada, K., Seo, S.U., Abo, M., Yoshimura, E., Shinozaki, K. & Yamaguchi-Shinozaki, K. (2013). Osmotic stress responses and plant growth controlled by potassium transporters in Arabidopsis. *Plant Cell*, Vol. 25, No. 2, pp. 609-24.
- Palancade, B. & Bensaude, O. (2003). Investigating RNA polymerase II carboxyl-terminal domain (CTD) phosphorylation. *Eur J Biochem*, Vol. 270, No. 19, pp. 3859-70.
- Pandey, G.K., Cheong, Y.H., Kim, K.N., Grant, J.J., Li, L., Hung, W., D'Angelo, C., Weinl, S., Kudla, J. & Luan, S. (2004). The calcium sensor calcineurin B-like 9 modulates abscisic acid sensitivity and biosynthesis in Arabidopsis. *Plant Cell*, Vol. 16, No. 7, pp. 1912-24.
- Pandey, S., Nelson, D.C. & Assmann, S.M. (2009). Two novel GPCR-type G proteins are abscisic acid receptors in Arabidopsis. *Cell*, Vol. 136, No. 1, pp. 136-48.
- Pandey, S., Zhang, W. & Assmann, S.M. (2007). Roles of ion channels and transporters in guard cell signal transduction. *FEBS Lett*, Vol. 581, No. 12, pp. 2325-36.
- Park, S.Y., Fung, P., Nishimura, N., Jensen, D.R., Fujii, H., Zhao, Y., Lumba, S., Santiago, J., Rodrigues, A., Chow, T.F., Alfred, S.E., Bonetta, D., Finkelstein, R., Provart, N.J., Desveaux, D., Rodriguez, P.L., McCourt, P., Zhu, J.K., Schroeder, J.I., Volkman, B.F. & Cutler, S.R. (2009). Abscisic acid inhibits type 2C protein phosphatases via the PYR/PYL family of START proteins. *Science*, Vol. 324, No. 5930, pp. 1068-71.
- Pauwels, L., Barbero, G.F., Geerinck, J., Tilleman, S., Grunewald, W., Perez, A.C., Chico, J.M., Bossche, R.V., Sewell, J., Gil, E., Garcia-Casado, G., Witters, E., Inze, D., Long, J.A., De Jaeger, G., Solano, R. & Goossens, A. (2010). NINJA connects the co-repressor TOPLESS to jasmonate signalling. *Nature*, Vol. 464, No. 7289, pp. 788-91.
- Pauwels, L. & Goossens, A. (2011). The JAZ proteins: a crucial interface in the jasmonate signaling cascade. *Plant Cell*, Vol. 23, No. 9, pp. 3089-100.

- Pei, Z.M., Kuchitsu, K., Ward, J.M., Schwarz, M. & Schroeder, J.I. (1997). Differential abscisic acid regulation of guard cell slow anion channels in Arabidopsis wild-type and *abi1* and *abi2* mutants. *Plant Cell*, Vol. 9, No. 3, pp. 409-23.
- Pei, Z.M., Murata, Y., Benning, G., Thomine, S., Klusener, B., Allen, G.J., Grill, E. & Schroeder, J.I. (2000). Calcium channels activated by hydrogen peroxide mediate abscisic acid signalling in guard cells. *Nature*, Vol. 406, No. 6797, pp. 731-4.
- Perilli, S., Moubayidin, L. & Sabatini, S. (2009). The molecular basis of cytokinin function. *Curr Opin Plant Biol*, Vol. 13, No. 1, pp. 21-6.
- Peters, J.L., Cnudde, F. & Gerats, T. (2003). Forward genetics and map-based cloning approaches. *Trends Plant Sci*, Vol. 8, No. 10, pp. 484-91.
- Peyronnet, R., Haswell, E.S., Barbier-Brygoo, H. & Frachisse, J.M. (2008). AtMSL9 and AtMSL10: Sensors of plasma membrane tension in Arabidopsis roots. *Plant Signal Behav*, Vol. 3, No. 9, pp. 726-9.
- Phillips, J.R., Fischer, E., Baron, M., van den Dries, N., Facchinelli, F., Kutzer, M., Rahmzadeh, R., Remus, D. & Bartels, D. (2008). *Lindernia brevidens*: a novel desiccation-tolerant vascular plant, endemic to ancient tropical rainforests. *Plant J*, Vol. 54, No. 5, pp. 938-48.
- Pilot, G., Lacombe, B., Gaymard, F., Cherel, I., Boucherez, J., Thibaud, J.B. & Sentenac, H. (2001). Guard cell inward K⁺ channel activity in Arabidopsis involves expression of the twin channel subunits KAT1 and KAT2. *J Biol Chem*, Vol. 276, No. 5, pp. 3215-21.
- Pires, N.D. & Dolan, L. (2012). Morphological evolution in land plants: new designs with old genes. *Philos Trans R Soc Lond B Biol Sci*, Vol. 367, No. 1588, pp. 508-18.
- Pivetti, C.D., Yen, M.R., Miller, S., Busch, W., Tseng, Y.H., Booth, I.R. & Saier, M.H., Jr. (2003). Two families of mechanosensitive channel proteins. *Microbiol Mol Biol Rev*, Vol. 67, No. 1, pp. 66-85, table of contents.
- Poroyko, V., Spollen, W.G., Hejlek, L.G., Hernandez, A.G., LeNoble, M.E., Davis, G., Nguyen, H.T., Springer, G.K., Sharp, R.E. & Bohnert, H.J. (2007). Comparing regional transcript profiles from maize primary roots under well-watered and low water potential conditions. *J Exp Bot*, Vol. 58, No. 2, pp. 279-89.
- Posas, F., Wurgler-Murphy, S.M., Maeda, T., Witten, E.A., Thai, T.C. & Saito, H. (1996). Yeast HOG1 MAP kinase cascade is regulated by a multistep phosphorelay mechanism in the SLN1-YPD1-SSK1 "two-component" osmosensor. *Cell*, Vol. 86, No. 6, pp. 865-75.
- Priest, D.M., Ambrose, S.J., Vaistij, F.E., Elias, L., Higgins, G.S., Ross, A.R., Abrams, S.R. & Bowles, D.J. (2006). Use of the glucosyltransferase UGT71B6 to disturb abscisic acid homeostasis in Arabidopsis thaliana. *Plant J*, Vol. 46, No. 3, pp. 492-502.
- Qi, Z., Kishigami, A., Nakagawa, Y., Iida, H. & Sokabe, M. (2004). A mechanosensitive anion channel in Arabidopsis thaliana mesophyll cells. *Plant Cell Physiol*, Vol. 45, No. 11, pp. 1704-8.
- Qin, F., Shinozaki, K. & Yamaguchi-Shinozaki, K. (2011). Achievements and challenges in understanding plant abiotic stress responses and tolerance. *Plant Cell Physiol*, Vol. 52, No. 9, pp. 1569-82.
- Quintero, F.J., Martinez-Atienza, J., Villalta, I., Jiang, X., Kim, W.Y., Ali, Z., Fujii, H., Mendoza, I., Yun, D.J., Zhu, J.K. & Pardo, J.M. (2011). Activation of the plasma membrane Na⁺/H⁺ antiporter Salt-Overly-Sensitive 1 (SOS1) by phosphorylation of an auto-inhibitory C-terminal domain. *Proc Natl Acad Sci U S A*, Vol. 108, No. 6, pp. 2611-6.
- Radauer, C., Lackner, P. & Breiteneder, H. (2008). The Bet v 1 fold: an ancient, versatile scaffold for binding of large, hydrophobic ligands. *BMC Evol Biol*, Vol. 8, pp. 286.
- Raghavendra, A.S., Gonugunta, V.K., Christmann, A. & Grill, E. (2010). ABA perception and signalling. *Trends Plant Sci*, Vol. 15, No. 7, pp. 395-401.

References

- Raitt, D.C., Posas, F. & Saito, H. (2000). Yeast Cdc42 GTPase and Ste20 PAK-like kinase regulate Sho1-dependent activation of the Hog1 MAPK pathway. *EMBO J*, Vol. 19, No. 17, pp. 4623-31.
- Reeves, W.M., Lynch, T.J., Mobin, R. & Finkelstein, R.R. (2011). Direct targets of the transcription factors ABA-Insensitive(ABI)4 and ABI5 reveal synergistic action by ABI4 and several bZIP ABA response factors. *Plant Mol Biol*, Vol. 75, No. 4-5, pp. 347-63.
- Reiser, V., Raitt, D.C. & Saito, H. (2003). Yeast osmosensor Sln1 and plant cytokinin receptor Cre1 respond to changes in turgor pressure. *J Cell Biol*, Vol. 161, No. 6, pp. 1035-40.
- Reiser, V., Salah, S.M. & Ammerer, G. (2000). Polarized localization of yeast Pbs2 depends on osmostress, the membrane protein Sho1 and Cdc42. *Nat Cell Biol*, Vol. 2, No. 9, pp. 620-7.
- Ren, D., Yang, H. & Zhang, S. (2002). Cell death mediated by MAPK is associated with hydrogen peroxide production in Arabidopsis. *J Biol Chem*, Vol. 277, No. 1, pp. 559-65.
- Ren, H., Santner, A., del Pozo, J.C., Murray, J.A. & Estelle, M. (2008). Degradation of the cyclin-dependent kinase inhibitor KRP1 is regulated by two different ubiquitin E3 ligases. *Plant J*, Vol. 53, No. 5, pp. 705-16.
- Riboni, M., Galbiati, M., Tonelli, C. & Conti, L. (2013). GIGANTEA enables drought escape response via abscisic acid-dependent activation of the florigens and SUPPRESSOR OF OVEREXPRESSION OF CONSTANS. *Plant Physiol*, Vol. 162, No. 3, pp. 1706-19.
- Risk, J.M., Day, C.L. & Macknight, R.C. (2009). Reevaluation of abscisic acid-binding assays shows that G-Protein-Coupled Receptor2 does not bind abscisic Acid. *Plant Physiol*, Vol. 150, No. 1, pp. 6-11.
- Robert, N., Merlot, S., N'Guyen, V., Boisson-Dernier, A. & Schroeder, J.I. (2006). A hypermorphic mutation in the protein phosphatase 2C HAB1 strongly affects ABA signaling in Arabidopsis. *FEBS Lett*, Vol. 580, No. 19, pp. 4691-6.
- Roberts, D.L., Bennett, D.W. & Forst, S.A. (1994). Identification of the site of phosphorylation on the osmosensor, EnvZ, of Escherichia coli. *J Biol Chem*, Vol. 269, No. 12, pp. 8728-33.
- Rodicio, R. & Heinisch, J.J. (2010). Together we are strong--cell wall integrity sensors in yeasts. *Yeast*, Vol. 27, No. 8, pp. 531-40.
- Rodriguez, M.C., Edsgard, D., Hussain, S.S., Alquezar, D., Rasmussen, M., Gilbert, T., Nielsen, B.H., Bartels, D. & Mundy, J. (2010). Transcriptomes of the desiccation-tolerant resurrection plant *Craterostigma plantagineum*. *Plant J*, Vol. 63, No. 2, pp. 212-28.
- Rodriguez, P.L., Benning, G. & Grill, E. (1998). ABI2, a second protein phosphatase 2C involved in abscisic acid signal transduction in Arabidopsis. *FEBS Lett*, Vol. 421, No. 3, pp. 185-90.
- Roelfsema, M.R. & Hedrich, R. (2005). In the light of stomatal opening: new insights into 'the Watergate'. *New Phytol*, Vol. 167, No. 3, pp. 665-91.
- Roelfsema, M.R., Levchenko, V. & Hedrich, R. (2004). ABA depolarizes guard cells in intact plants, through a transient activation of R- and S-type anion channels. *Plant J*, Vol. 37, No. 4, pp. 578-88.
- Rontein, D., Basset, G. & Hanson, A.D. (2002). Metabolic engineering of osmoprotectant accumulation in plants. *Metab Eng*, Vol. 4, No. 1, pp. 49-56.
- Rosado, A., Amaya, I., Valpuesta, V., Cuartero, J., Botella, M.A. & Borsani, O. (2006). ABA- and ethylene-mediated responses in osmotically stressed tomato are regulated by the TSS2 and TOS1 loci. *J Exp Bot*, Vol. 57, No. 12, pp. 3327-35.
- Rubio, S., Rodrigues, A., Saez, A., Dizon, M.B., Galle, A., Kim, T.H., Santiago, J., Flexas, J., Schroeder, J.I. & Rodriguez, P.L. (2009). Triple loss of function of protein phosphatases type 2C leads to partial constitutive response to endogenous abscisic acid. *Plant Physiol*, Vol. 150, No. 3, pp. 1345-55.

- Saez, A., Apostolova, N., Gonzalez-Guzman, M., Gonzalez-Garcia, M.P., Nicolas, C., Lorenzo, O. & Rodriguez, P.L. (2004). Gain-of-function and loss-of-function phenotypes of the protein phosphatase 2C HAB1 reveal its role as a negative regulator of abscisic acid signalling. *Plant J*, Vol. 37, No. 3, pp. 354-69.
- Saez, A., Robert, N., Maktabi, M.H., Schroeder, J.I., Serrano, R. & Rodriguez, P.L. (2006). Enhancement of abscisic acid sensitivity and reduction of water consumption in Arabidopsis by combined inactivation of the protein phosphatases type 2C ABI1 and HAB1. *Plant Physiol*, Vol. 141, No. 4, pp. 1389-99.
- Saito, S., Hirai, N., Matsumoto, C., Ohigashi, H., Ohta, D., Sakata, K. & Mizutani, M. (2004). Arabidopsis CYP707As encode (+)-abscisic acid 8'-hydroxylase, a key enzyme in the oxidative catabolism of abscisic acid. *Plant Physiol*, Vol. 134, No. 4, pp. 1439-49.
- Sakuma, Y., Maruyama, K., Osakabe, Y., Qin, F., Seki, M., Shinozaki, K. & Yamaguchi-Shinozaki, K. (2006). Functional analysis of an Arabidopsis transcription factor, DREB2A, involved in drought-responsive gene expression. *Plant Cell*, Vol. 18, No. 5, pp. 1292-309.
- Sanchez-Barrena, M.J., Martinez-Ripoll, M. & Albert, A. (2013). Structural Biology of a Major Signaling Network that Regulates Plant Abiotic Stress: The CBL-CIPK Mediated Pathway. *Int J Mol Sci*, Vol. 14, No. 3, pp. 5734-49.
- Santiago, J., Dupeux, F., Round, A., Antoni, R., Park, S.Y., Jamin, M., Cutler, S.R., Rodriguez, P.L. & Marquez, J.A. (2009a). The abscisic acid receptor PYR1 in complex with abscisic acid. *Nature*, Vol. 462, No. 7273, pp. 665-8.
- Santiago, J., Rodrigues, A., Saez, A., Rubio, S., Antoni, R., Dupeux, F., Park, S.Y., Marquez, J.A., Cutler, S.R. & Rodriguez, P.L. (2009b). Modulation of drought resistance by the abscisic acid receptor PYL5 through inhibition of clade A PP2Cs. *Plant J*, Vol. 60, No. 4, pp. 575-88.
- Sasaki-Sekimoto, Y., Jikumaru, Y., Obayashi, T., Saito, H., Masuda, S., Kamiya, Y., Ohta, H. & Shirasu, K. (2013). Basic helix-loop-helix transcription factors JASMONATE-ASSOCIATED MYC2-LIKE1 (JAM1), JAM2, and JAM3 are negative regulators of jasmonate responses in Arabidopsis. *Plant Physiol*, Vol. 163, No. 1, pp. 291-304.
- Sasaki, K., Kim, M.H. & Imai, R. (2013). Arabidopsis COLD SHOCK DOMAIN PROTEIN 2 is a negative regulator of cold acclimation. *New Phytol*, Vol. 198, No. 1, pp. 95-102.
- Sato, A., Sato, Y., Fukao, Y., Fujiwara, M., Umezawa, T., Shinozaki, K., Hibi, T., Taniguchi, M., Miyake, H., Goto, D.B. & Uozumi, N. (2009). Threonine at position 306 of the KAT1 potassium channel is essential for channel activity and is a target site for ABA-activated SnRK2/OST1/SnRK2.6 protein kinase. *Biochem J*, Vol. 424, No. 3, pp. 439-48.
- Sauter, A., Davies, W.J. & Hartung, W. (2001). The long-distance abscisic acid signal in the droughted plant: the fate of the hormone on its way from root to shoot. *J Exp Bot*, Vol. 52, No. 363, pp. 1991-7.
- Sauter, A., Dietz, K.J. & Hartung, W. (2002). A possible stress physiological role of abscisic acid conjugates in root-to-shoot signalling. *Plant Cell Environ*, Vol. 25, No. 2, pp. 223-228.
- Schaller, G.E., Doi, K., Hwang, I., Kieber, J.J., Khurana, J.P., Kurata, N., Mizuno, T., Pareek, A., Shiu, S.H., Wu, P. & Yip, W.K. (2007). Nomenclature for two-component signaling elements of rice. *Plant Physiol*, Vol. 143, No. 2, pp. 555-7.
- Schaller, G.E., Kieber, J.J. & Shiu, S.H. (2008). Two-component signaling elements and histidyl-aspartyl phosphorelays. *Arabidopsis Book*, Vol. 6, pp. e0112.
- Schindler, M., Meiners, S. & Cheresch, D.A. (1989). RGD-dependent linkage between plant cell wall and plasma membrane: consequences for growth. *J Cell Biol*, Vol. 108, No. 5, pp. 1955-65.
- Schneeberger, K., Ossowski, S., Lanz, C., Juul, T., Petersen, A.H., Nielsen, K.L., Jorgensen, J.E., Weigel, D. & Andersen, S.U. (2009). SHOREmap: simultaneous mapping and mutation identification by deep sequencing. *Nat Methods*, Vol. 6, No. 8, pp. 550-1.

References

- Schroeder, J.I., Kwak, J.M. & Allen, G.J. (2001). Guard cell abscisic acid signalling and engineering drought hardiness in plants. *Nature*, Vol. 410, No. 6826, pp. 327-30.
- Schumacher, M.A., Goodman, R.H. & Brennan, R.G. (2000). The structure of a CREB bZIP.somatostatin CRE complex reveals the basis for selective dimerization and divalent cation-enhanced DNA binding. *J Biol Chem*, Vol. 275, No. 45, pp. 35242-7.
- Schwartz, S.H., Leon-Kloosterziel, K.M., Koornneef, M. & Zeevaart, J.A. (1997). Biochemical characterization of the *aba2* and *aba3* mutants in *Arabidopsis thaliana*. *Plant Physiol*, Vol. 114, No. 1, pp. 161-6.
- Schwartz, S.H., Qin, X. & Zeevaart, J.A. (2003). Elucidation of the indirect pathway of abscisic acid biosynthesis by mutants, genes, and enzymes. *Plant Physiol*, Vol. 131, No. 4, pp. 1591-601.
- Schweighofer, A., Hirt, H. & Meskiene, I. (2004). Plant PP2C phosphatases: emerging functions in stress signaling. *Trends Plant Sci*, Vol. 9, No. 5, pp. 236-43.
- Seo, M., Aoki, H., Koiwai, H., Kamiya, Y., Nambara, E. & Koshiba, T. (2004). Comparative studies on the *Arabidopsis* aldehyde oxidase (AAO) gene family revealed a major role of AAO3 in ABA biosynthesis in seeds. *Plant Cell Physiol*, Vol. 45, No. 11, pp. 1694-703.
- Seo, M., Peeters, A.J., Koiwai, H., Oritani, T., Marion-Poll, A., Zeevaart, J.A., Koornneef, M., Kamiya, Y. & Koshiba, T. (2000). The *Arabidopsis* aldehyde oxidase 3 (AAO3) gene product catalyzes the final step in abscisic acid biosynthesis in leaves. *Proc Natl Acad Sci U S A*, Vol. 97, No. 23, pp. 12908-13.
- Seung, D., Risopatron, J.P., Jones, B.J. & Marc, J. (2011). Circadian clock-dependent gating in ABA signalling networks. *Protoplasma*.
- Shabala, S.N. & Lew, R.R. (2002). Turgor regulation in osmotically stressed *Arabidopsis* epidermal root cells. Direct support for the role of inorganic ion uptake as revealed by concurrent flux and cell turgor measurements. *Plant Physiol*, Vol. 129, No. 1, pp. 290-9.
- Shang, Y., Yan, L., Liu, Z.Q., Cao, Z., Mei, C., Xin, Q., Wu, F.Q., Wang, X.F., Du, S.Y., Jiang, T., Zhang, X.F., Zhao, R., Sun, H.L., Liu, R., Yu, Y.T. & Zhang, D.P. (2010). The Mg-chelatase H subunit of *Arabidopsis* antagonizes a group of WRKY transcription repressors to relieve ABA-responsive genes of inhibition. *Plant Cell*, Vol. 22, No. 6, pp. 1909-35.
- Sharma, S. & Verslues, P.E. (2010). Mechanisms independent of abscisic acid (ABA) or proline feedback have a predominant role in transcriptional regulation of proline metabolism during low water potential and stress recovery. *Plant Cell Environ*, Vol. 33, No. 11, pp. 1838-51.
- Sharp, R.E. (2002). Interaction with ethylene: changing views on the role of abscisic acid in root and shoot growth responses to water stress. *Plant Cell Environ*, Vol. 25, No. 2, pp. 211-222.
- Sharp, R.E. & LeNoble, M.E. (2002). ABA, ethylene and the control of shoot and root growth under water stress. *J Exp Bot*, Vol. 53, No. 366, pp. 33-7.
- Sharp, R.E., Poroyko, V., Hejlek, L.G., Spollen, W.G., Springer, G.K., Bohnert, H.J. & Nguyen, H.T. (2004). Root growth maintenance during water deficits: physiology to functional genomics. *J Exp Bot*, Vol. 55, No. 407, pp. 2343-51.
- Shatil-Cohen, A., Attia, Z. & Moshelion, M. (2011). Bundle-sheath cell regulation of xylem-mesophyll water transport via aquaporins under drought stress: a target of xylem-borne ABA? *Plant J*, Vol. 67, No. 1, pp. 72-80.
- Sheen, J. (1998). Mutational analysis of protein phosphatase 2C involved in abscisic acid signal transduction in higher plants. *Proc Natl Acad Sci U S A*, Vol. 95, No. 3, pp. 975-80.
- Shen, Q. & Ho, T.H. (1995). Functional dissection of an abscisic acid (ABA)-inducible gene reveals two independent ABA-responsive complexes each containing a G-box and a novel cis-acting element. *Plant Cell*, Vol. 7, No. 3, pp. 295-307.

- Shen, Y.Y., Wang, X.F., Wu, F.Q., Du, S.Y., Cao, Z., Shang, Y., Wang, X.L., Peng, C.C., Yu, X.C., Zhu, S.Y., Fan, R.C., Xu, Y.H. & Zhang, D.P. (2006). The Mg-chelatase H subunit is an abscisic acid receptor. *Nature*, Vol. 443, No. 7113, pp. 823-6.
- Shinohara, N., Taylor, C. & Leyser, O. (2013). Strigolactone can promote or inhibit shoot branching by triggering rapid depletion of the auxin efflux protein PIN1 from the plasma membrane. *PLoS Biol*, Vol. 11, No. 1, pp. e1001474.
- Shinozaki, K. & Yamaguchi-Shinozaki, K. (2007). Gene networks involved in drought stress response and tolerance. *J Exp Bot*, Vol. 58, No. 2, pp. 221-7.
- Shyu, C., Figueroa, P., Depew, C.L., Cooke, T.F., Sheard, L.B., Moreno, J.E., Katsir, L., Zheng, N., Browse, J. & Howe, G.A. (2012). JAZ8 lacks a canonical degron and has an EAR motif that mediates transcriptional repression of jasmonate responses in Arabidopsis. *Plant Cell*, Vol. 24, No. 2, pp. 536-50.
- Shyy, J.Y. & Chien, S. (2002). Role of integrins in endothelial mechanosensing of shear stress. *Circ Res*, Vol. 91, No. 9, pp. 769-75.
- Siegel, R.S., Xue, S., Murata, Y., Yang, Y., Nishimura, N., Wang, A. & Schroeder, J.I. (2009). Calcium elevation-dependent and attenuated resting calcium-dependent abscisic acid induction of stomatal closure and abscisic acid-induced enhancement of calcium sensitivities of S-type anion and inward-rectifying K channels in Arabidopsis guard cells. *Plant J*, Vol. 59, No. 2, pp. 207-20.
- Simpson, S.D., Nakashima, K., Narusaka, Y., Seki, M., Shinozaki, K. & Yamaguchi-Shinozaki, K. (2003). Two different novel cis-acting elements of *erd1*, a *clpA* homologous Arabidopsis gene function in induction by dehydration stress and dark-induced senescence. *Plant J*, Vol. 33, No. 2, pp. 259-70.
- Sims, D.A. & Gamon, J.A. (2002). Relationships between leaf pigment content and spectral reflectance across a wide range of species, leaf structures and developmental stages. *Remote sensing of environment*, Vol. 81, pp. 337-354.
- Sirichandra, C., Gu, D., Hu, H.C., Davanture, M., Lee, S., Djaoui, M., Valot, B., Zivy, M., Leung, J., Merlot, S. & Kwak, J.M. (2009a). Phosphorylation of the Arabidopsis AtrbohF NADPH oxidase by OST1 protein kinase. *FEBS Lett*, Vol. 583, No. 18, pp. 2982-6.
- Sirichandra, C., Wasilewska, A., Vlad, F., Valon, C. & Leung, J. (2009b). The guard cell as a single-cell model towards understanding drought tolerance and abscisic acid action. *J Exp Bot*, Vol. 60, No. 5, pp. 1439-63.
- Skriver, K., Olsen, F.L., Rogers, J.C. & Mundy, J. (1991). cis-acting DNA elements responsive to gibberellin and its antagonist abscisic acid. *Proc Natl Acad Sci U S A*, Vol. 88, No. 16, pp. 7266-70.
- Slauch, J.M., Garrett, S., Jackson, D.E. & Silhavy, T.J. (1988). EnvZ functions through OmpR to control porin gene expression in Escherichia coli K-12. *J Bacteriol*, Vol. 170, No. 1, pp. 439-41.
- Soon, F.F., Ng, L.M., Zhou, X.E., West, G.M., Kovach, A., Tan, M.H., Suino-Powell, K.M., He, Y., Xu, Y., Chalmers, M.J., Brunzelle, J.S., Zhang, H., Yang, H., Jiang, H., Li, J., Yong, E.L., Cutler, S., Zhu, J.K., Griffin, P.R., Melcher, K. & Xu, H.E. (2011). Molecular mimicry regulates ABA signaling by SnRK2 kinases and PP2C phosphatases. *Science*, Vol. 335, No. 6064, pp. 85-8.
- Spollen, W.G., Tao, W., Valliyodan, B., Chen, K., Hejlek, L.G., Kim, J.J., Lenoble, M.E., Zhu, J., Bohnert, H.J., Henderson, D., Schachtman, D.P., Davis, G.E., Springer, G.K., Sharp, R.E. & Nguyen, H.T. (2008). Spatial distribution of transcript changes in the maize primary root elongation zone at low water potential. *BMC Plant Biol*, Vol. 8, pp. 32.
- Stewart, C.R. & Voetberg, G. (1985). Relationship between Stress-Induced ABA and Proline Accumulations and ABA-Induced Proline Accumulation in Excised Barley Leaves. *Plant Physiol*, Vol. 79, No. 1, pp. 24-7.

References

- Stone, S.L., Williams, L.A., Farmer, L.M., Vierstra, R.D. & Callis, J. (2006). KEEP ON GOING, a RING E3 ligase essential for Arabidopsis growth and development, is involved in abscisic acid signaling. *Plant Cell*, Vol. 18, No. 12, pp. 3415-28.
- Strizhov, N., Abraham, E., Okresz, L., Blickling, S., Zilberstein, A., Schell, J., Koncz, C. & Szabados, L. (1997). Differential expression of two P5CS genes controlling proline accumulation during salt-stress requires ABA and is regulated by ABA1, ABI1 and AXR2 in Arabidopsis. *Plant J*, Vol. 12, No. 3, pp. 557-69.
- Sukharev, S.I., Blount, P., Martinac, B., Blattner, F.R. & Kung, C. (1994). A large-conductance mechanosensitive channel in E. coli encoded by mscL alone. *Nature*, Vol. 368, No. 6468, pp. 265-8.
- Sukharev, S.I., Martinac, B., Arshavsky, V.Y. & Kung, C. (1993). Two types of mechanosensitive channels in the Escherichia coli cell envelope: solubilization and functional reconstitution. *Biophys J*, Vol. 65, No. 1, pp. 177-83.
- Sun, D., Wang, H., Wu, M., Zang, J., Wu, F. & Tian, C. (2012). Crystal structures of the Arabidopsis thaliana abscisic acid receptor PYL10 and its complex with abscisic acid. *Biochem Biophys Res Commun*, Vol. 418, No. 1, pp. 122-7.
- Sun, J., Jiang, H., Xu, Y., Li, H., Wu, X., Xie, Q. & Li, C. (2007). The CCCH-type zinc finger proteins AtSZF1 and AtSZF2 regulate salt stress responses in Arabidopsis. *Plant Cell Physiol*, Vol. 48, No. 8, pp. 1148-58.
- Sunkar, R. & Zhu, J.K. (2004). Novel and stress-regulated microRNAs and other small RNAs from Arabidopsis. *Plant Cell*, Vol. 16, No. 8, pp. 2001-19.
- Suzuki, T., Imamura, A., Ueguchi, C. & Mizuno, T. (1998). Histidine-containing phosphotransfer (HPT) signal transducers implicated in His-to-Asp phosphorelay in Arabidopsis. *Plant Cell Physiol*, Vol. 39, No. 12, pp. 1258-68.
- Sze, H., Padmanaban, S., Cellier, F., Honys, D., Cheng, N.H., Bock, K.W., Conejero, G., Li, X., Twell, D., Ward, J.M. & Hirschi, K.D. (2004). Expression patterns of a novel AtCHX gene family highlight potential roles in osmotic adjustment and K⁺ homeostasis in pollen development. *Plant Physiol*, Vol. 136, No. 1, pp. 2532-47.
- Szemenyei, H., Hannon, M. & Long, J.A. (2008). TOPLESS mediates auxin-dependent transcriptional repression during Arabidopsis embryogenesis. *Science*, Vol. 319, No. 5868, pp. 1384-6.
- Szostkiewicz, I., Richter, K., Kepka, M., Demmel, S., Ma, Y., Korte, A., Assaad, F.F., Christmann, A. & Grill, E. (2009). Closely related receptor complexes differ in their ABA selectivity and sensitivity. *Plant J*, Vol. 61, No. 1, pp. 25-35.
- Takase, T., Yasuhara, M., Geekiyanage, S., Ogura, Y. & Kiyosue, T. (2007). Overexpression of the chimeric gene of the floral regulator CONSTANS and the EAR motif repressor causes late flowering in Arabidopsis. *Plant Cell Rep*, Vol. 26, No. 6, pp. 815-21.
- Takeda, S., Gapper, C., Kaya, H., Bell, E., Kuchitsu, K. & Dolan, L. (2008). Local positive feedback regulation determines cell shape in root hair cells. *Science*, Vol. 319, No. 5867, pp. 1241-4.
- Takezawa, D., Komatsu, K. & Sakata, Y. (2011). ABA in bryophytes: how a universal growth regulator in life became a plant hormone? *J Plant Res*, Vol. 124, No. 4, pp. 437-53.
- Tamas, M.J., Rep, M., Thevelein, J.M. & Hohmann, S. (2000). Stimulation of the yeast high osmolarity glycerol (HOG) pathway: evidence for a signal generated by a change in turgor rather than by water stress. *FEBS Lett*, Vol. 472, No. 1, pp. 159-65.
- Tan, B.C., Joseph, L.M., Deng, W.T., Liu, L., Li, Q.B., Cline, K. & McCarty, D.R. (2003). Molecular characterization of the Arabidopsis 9-cis epoxy-carotenoid dioxygenase gene family. *Plant J*, Vol. 35, No. 1, pp. 44-56.
- Tanz, S.K., Castleden, I., Hooper, C.M., Vacher, M., Small, I. & Millar, H.A. (2013). SUBA3: a database for integrating experimentation and prediction to define the SUBcellular location of proteins in Arabidopsis. *Nucleic Acids Res*, Vol. 41, No. Database issue, pp. D1185-91.

- Tao, Q., Guo, D., Wei, B., Zhang, F., Pang, C., Jiang, H., Zhang, J., Wei, T., Gu, H., Qu, L.J. & Qin, G. (2013). The TIE1 transcriptional repressor links TCP transcription factors with TOPLESS/TOPLESS-RELATED corepressors and modulates leaf development in Arabidopsis. *Plant Cell*, Vol. 25, No. 2, pp. 421-37.
- Tao, W., Malone, C.L., Ault, A.D., Deschenes, R.J. & Fassler, J.S. (2002). A cytoplasmic coiled-coil domain is required for histidine kinase activity of the yeast osmosensor, SLN1. *Mol Microbiol*, Vol. 43, No. 2, pp. 459-73.
- Tardieu, F. (2012). Any trait or trait-related allele can confer drought tolerance: just design the right drought scenario. *J Exp Bot*, Vol. 63, No. 1, pp. 25-31.
- Tardieu, F. (2013). Plant response to environmental conditions: assessing potential production, water demand, and negative effects of water deficit. *Front Physiol*, Vol. 4, pp. 17.
- Tatebayashi, K., Tanaka, K., Yang, H.Y., Yamamoto, K., Matsushita, Y., Tomida, T., Imai, M. & Saito, H. (2007). Transmembrane mucins Hkr1 and Msb2 are putative osmosensors in the SHO1 branch of yeast HOG pathway. *EMBO J*, Vol. 26, No. 15, pp. 3521-33.
- Tatebayashi, K., Yamamoto, K., Tanaka, K., Tomida, T., Maruoka, T., Kasukawa, E. & Saito, H. (2006). Adaptor functions of Cdc42, Ste50, and Sho1 in the yeast osmoregulatory HOG MAPK pathway. *EMBO J*, Vol. 25, No. 13, pp. 3033-44.
- Teale, W.D., Paponov, I.A. & Palme, K. (2006). Auxin in action: signalling, transport and the control of plant growth and development. *Nat Rev Mol Cell Biol*, Vol. 7, No. 11, pp. 847-59.
- Teige, M., Scheikl, E., Eulgem, T., Doczi, R., Ichimura, K., Shinozaki, K., Dangl, J.L. & Hirt, H. (2004). The MKK2 pathway mediates cold and salt stress signaling in Arabidopsis. *Mol Cell*, Vol. 15, No. 1, pp. 141-52.
- Thompson, A.J., Jackson, A.C., Parker, R.A., Morpeth, D.R., Burbidge, A. & Taylor, I.B. (2000). Abscisic acid biosynthesis in tomato: regulation of zeaxanthin epoxidase and 9-cis-epoxycarotenoid dioxygenase mRNAs by light/dark cycles, water stress and abscisic acid. *Plant Mol Biol*, Vol. 42, No. 6, pp. 833-45.
- To, J.P., Deruere, J., Maxwell, B.B., Morris, V.F., Hutchison, C.E., Ferreira, F.J., Schaller, G.E. & Kieber, J.J. (2007). Cytokinin regulates type-A Arabidopsis Response Regulator activity and protein stability via two-component phosphorelay. *Plant Cell*, Vol. 19, No. 12, pp. 3901-14.
- To, J.P. & Kieber, J.J. (2008). Cytokinin signaling: two-components and more. *Trends Plant Sci*, Vol. 13, No. 2, pp. 85-92.
- Toledo-Ortiz, G., Huq, E. & Quail, P.H. (2003). The Arabidopsis basic/helix-loop-helix transcription factor family. *Plant Cell*, Vol. 15, No. 8, pp. 1749-70.
- Torres, M.A. & Dangl, J.L. (2005). Functions of the respiratory burst oxidase in biotic interactions, abiotic stress and development. *Curr Opin Plant Biol*, Vol. 8, No. 4, pp. 397-403.
- Tran, L.S., Nakashima, K., Shinozaki, K. & Yamaguchi-Shinozaki, K. (2007a). Plant gene networks in osmotic stress response: from genes to regulatory networks. *Methods Enzymol*, Vol. 428, pp. 109-28.
- Tran, L.S., Urao, T., Qin, F., Maruyama, K., Kakimoto, T., Shinozaki, K. & Yamaguchi-Shinozaki, K. (2007b). Functional analysis of AHK1/ATHK1 and cytokinin receptor histidine kinases in response to abscisic acid, drought, and salt stress in Arabidopsis. *Proc Natl Acad Sci U S A*, Vol. 104, No. 51, pp. 20623-8.
- Tsugama, D., Liu, S. & Takano, T. (2012). Drought-induced activation and rehydration-induced inactivation of MPK6 in Arabidopsis. *Biochem Biophys Res Commun*, Vol. 426, No. 4, pp. 626-9.
- Tsuzuki, T., Takahashi, K., Inoue, S., Okigaki, Y., Tomiyama, M., Hossain, M.A., Shimazaki, K., Murata, Y. & Kinoshita, T. (2011). Mg-chelatase H subunit affects ABA signaling in stomatal guard cells, but is not an ABA receptor in Arabidopsis thaliana. *J Plant Res*, Vol. 124, No. 4, pp. 527-38.

References

- Tsuzuki, T., Takahashi, K., Tomiyama, M., Inoue, S. & Kinoshita, T. (2013). Overexpression of the Mg-chelatase H subunit in guard cells confers drought tolerance via promotion of stomatal closure in *Arabidopsis thaliana*. *Front Plant Sci*, Vol. 4, pp. 440.
- Ulmasov, T., Hagen, G. & Guilfoyle, T.J. (1997). ARF1, a transcription factor that binds to auxin response elements. *Science*, Vol. 276, No. 5320, pp. 1865-8.
- Umehara, M., Hanada, A., Yoshida, S., Akiyama, K., Arite, T., Takeda-Kamiya, N., Magome, H., Kamiya, Y., Shirasu, K., Yoneyama, K., Kyojuka, J. & Yamaguchi, S. (2008). Inhibition of shoot branching by new terpenoid plant hormones. *Nature*, Vol. 455, No. 7210, pp. 195-200.
- Umezawa, T., Okamoto, M., Kushiro, T., Nambara, E., Oono, Y., Seki, M., Kobayashi, M., Koshiba, T., Kamiya, Y. & Shinozaki, K. (2006). CYP707A3, a major ABA 8'-hydroxylase involved in dehydration and rehydration response in *Arabidopsis thaliana*. *Plant J*, Vol. 46, No. 2, pp. 171-82.
- Umezawa, T., Sugiyama, N., Mizoguchi, M., Hayashi, S., Myouga, F., Yamaguchi-Shinozaki, K., Ishihama, Y., Hirayama, T. & Shinozaki, K. (2009). Type 2C protein phosphatases directly regulate abscisic acid-activated protein kinases in *Arabidopsis*. *Proc Natl Acad Sci U S A*, Vol. 106, No. 41, pp. 17588-93.
- Uno, Y., Furihata, T., Abe, H., Yoshida, R., Shinozaki, K. & Yamaguchi-Shinozaki, K. (2000). *Arabidopsis* basic leucine zipper transcription factors involved in an abscisic acid-dependent signal transduction pathway under drought and high-salinity conditions. *Proc Natl Acad Sci U S A*, Vol. 97, No. 21, pp. 11632-7.
- Urao, T., Yakubov, B., Satoh, R., Yamaguchi-Shinozaki, K., Seki, M., Hirayama, T. & Shinozaki, K. (1999). A transmembrane hybrid-type histidine kinase in *Arabidopsis* functions as an osmosensor. *Plant Cell*, Vol. 11, No. 9, pp. 1743-54.
- Vahisalu, T., Kollist, H., Wang, Y.F., Nishimura, N., Chan, W.Y., Valerio, G., Lamminmaki, A., Brosche, M., Moldau, H., Desikan, R., Schroeder, J.I. & Kangasjarvi, J. (2008). SLAC1 is required for plant guard cell S-type anion channel function in stomatal signalling. *Nature*, Vol. 452, No. 7186, pp. 487-91.
- Valdes, A.E., Overnas, E., Johansson, H., Rada-Iglesias, A. & Engstrom, P. (2012). The homeodomain-leucine zipper (HD-Zip) class I transcription factors ATHB7 and ATHB12 modulate abscisic acid signalling by regulating protein phosphatase 2C and abscisic acid receptor gene activities. *Plant Mol Biol*, Vol. 80, No. 4-5, pp. 405-18.
- Veley, K.M., Marshburn, S., Clure, C.E. & Haswell, E.S. (2012). Mechanosensitive channels protect plastids from hypoosmotic stress during normal plant growth. *Curr Biol*, Vol. 22, No. 5, pp. 408-13.
- Verslues, P.E., Agarwal, M., Katiyar-Agarwal, S., Zhu, J. & Zhu, J.K. (2006). Methods and concepts in quantifying resistance to drought, salt and freezing, abiotic stresses that affect plant water status. *Plant J*, Vol. 45, No. 4, pp. 523-39.
- Verslues, P.E. & Bray, E.A. (2006). Role of abscisic acid (ABA) and *Arabidopsis thaliana* ABA-insensitive loci in low water potential-induced ABA and proline accumulation. *J Exp Bot*, Vol. 57, No. 1, pp. 201-12.
- Verslues, P.E. & Juenger, T.E. (2011). Drought, metabolites, and *Arabidopsis* natural variation: a promising combination for understanding adaptation to water-limited environments. *Curr Opin Plant Biol*, Vol. 14, No. 3, pp. 240-5.
- Verslues, P.E. & Zhu, J.K. (2005). Before and beyond ABA: upstream sensing and internal signals that determine ABA accumulation and response under abiotic stress. *Biochem Soc Trans*, Vol. 33, No. Pt 2, pp. 375-9.
- Vlad, F., Rubio, S., Rodrigues, A., Sirichandra, C., Belin, C., Robert, N., Leung, J., Rodriguez, P.L., Lauriere, C. & Merlot, S. (2009). Protein phosphatases 2C regulate the activation of the Snf1-related kinase OST1 by abscisic acid in *Arabidopsis*. *Plant Cell*, Vol. 21, No. 10, pp. 3170-84.
- Walhout, A.J., Temple, G.F., Brasch, M.A., Hartley, J.L., Lorson, M.A., van den Heuvel, S. & Vidal, M. (2000). GATEWAY recombinational cloning: application to the cloning of large numbers of open reading frames or ORFeomes. *Methods Enzymol*, Vol. 328, pp. 575-92.

- Wang, D., Guo, Y., Wu, C., Yang, G., Li, Y. & Zheng, C. (2008a). Genome-wide analysis of CCCH zinc finger family in Arabidopsis and rice. *BMC Genomics*, Vol. 9, pp. 44.
- Wang, L., Kim, J. & Somers, D.E. (2012a). Transcriptional corepressor TOPLESS complexes with pseudoresponse regulator proteins and histone deacetylases to regulate circadian transcription. *Proc Natl Acad Sci U S A*, Vol. 110, No. 2, pp. 761-6.
- Wang, L., Xu, Y., Zhang, C., Ma, Q., Joo, S.H., Kim, S.K., Xu, Z. & Chong, K. (2008b). OsLIC, a Novel CCCH-Type Zinc Finger Protein with Transcription Activation, Mediates Rice Architecture via Brassinosteroids Signaling. *PLoS One*, Vol. 3, No. 10, pp. e3521.
- Wang, L.C., Morgan, L.K., Godakumbura, P., Kenney, L.J. & Anand, G.S. (2012b). The inner membrane histidine kinase EnvZ senses osmolality via helix-coil transitions in the cytoplasm. *EMBO J*, Vol. 31, No. 11, pp. 2648-59.
- Wang, M., Zheng, Q., Shen, Q. & Guo, S. (2013). The critical role of potassium in plant stress response. *Int J Mol Sci*, Vol. 14, No. 4, pp. 7370-90.
- Wang, R.S., Pandey, S., Li, S., Gookin, T.E., Zhao, Z., Albert, R. & Assmann, S.M. (2011). Common and unique elements of the ABA-regulated transcriptome of Arabidopsis guard cells. *BMC Genomics*, Vol. 12, pp. 216.
- Wani, S.H., Singh, N.B., Haribhushan, A. & Mir, J.I. (2013). Compatible solute engineering in plants for abiotic stress tolerance - role of glycine betaine. *Curr Genomics*, Vol. 14, No. 3, pp. 157-65.
- Wasilewska, A., Vlad, F., Sirichandra, C., Redko, Y., Jammes, F., Valon, C., Frei dit Frey, N. & Leung, J. (2008). An update on abscisic acid signaling in plants and more. *Mol Plant*, Vol. 1, No. 2, pp. 198-217.
- Wegener, K.L. & Campbell, I.D. (2008). Transmembrane and cytoplasmic domains in integrin activation and protein-protein interactions (review). *Mol Membr Biol*, Vol. 25, No. 5, pp. 376-87.
- Welsch, R., Maass, D., Voegel, T., Dellapenna, D. & Beyer, P. (2007). Transcription factor RAP2.2 and its interacting partner SINAT2: stable elements in the carotenogenesis of Arabidopsis leaves. *Plant Physiol*, Vol. 145, No. 3, pp. 1073-85.
- Wilkinson, S. & Davies, W.J. (2002). ABA-based chemical signalling: the co-ordination of responses to stress in plants. *Plant Cell Environ*, Vol. 25, No. 2, pp. 195-210.
- Wilkinson, S. & Davies, W.J. (2009). Drought, ozone, ABA and ethylene: new insights from cell to plant to community. *Plant Cell Environ*, Vol. 33, No. 4, pp. 510-25.
- Winter, D., Vinegar, B., Nahal, H., Ammar, R., Wilson, G.V. & Provar, N.J. (2007). An "Electronic Fluorescent Pictograph" browser for exploring and analyzing large-scale biological data sets. *PLoS One*, Vol. 2, No. 8, pp. e718.
- Wohlbach, D.J., Quirino, B.F. & Sussman, M.R. (2008). Analysis of the Arabidopsis histidine kinase ATHK1 reveals a connection between vegetative osmotic stress sensing and seed maturation. *Plant Cell*, Vol. 20, No. 4, pp. 1101-17.
- Wu, F.Q., Xin, Q., Cao, Z., Liu, Z.Q., Du, S.Y., Mei, C., Zhao, C.X., Wang, X.F., Shang, Y., Jiang, T., Zhang, X.F., Yan, L., Zhao, R., Cui, Z.N., Liu, R., Sun, H.L., Yang, X.L., Su, Z. & Zhang, D.P. (2009). The magnesium-chelatase H subunit binds abscisic acid and functions in abscisic acid signaling: new evidence in Arabidopsis. *Plant Physiol*, Vol. 150, No. 4, pp. 1940-54.
- Wu, Y. & Cosgrove, D.J. (2000). Adaptation of roots to low water potentials by changes in cell wall extensibility and cell wall proteins. *J Exp Bot*, Vol. 51, No. 350, pp. 1543-53.
- Wurzinger, B., Mair, A., Pfister, B. & Teige, M. (2011). Cross-talk of calcium-dependent protein kinase and MAP kinase signaling. *Plant Signal Behav*, Vol. 6, No. 1, pp. 8-12.

References

- Xie, Q., Guo, H.S., Dallman, G., Fang, S., Weissman, A.M. & Chua, N.H. (2002). SINAT5 promotes ubiquitin-related degradation of NAC1 to attenuate auxin signals. *Nature*, Vol. 419, No. 6903, pp. 167-70.
- Xiong, L., Ishitani, M., Lee, H. & Zhu, J.K. (2001). The Arabidopsis LOS5/ABA3 locus encodes a molybdenum cofactor sulfurase and modulates cold stress- and osmotic stress-responsive gene expression. *Plant Cell*, Vol. 13, No. 9, pp. 2063-83.
- Xiong, L., Lee, H., Ishitani, M. & Zhu, J.K. (2002). Regulation of osmotic stress-responsive gene expression by the LOS6/ABA1 locus in Arabidopsis. *J Biol Chem*, Vol. 277, No. 10, pp. 8588-96.
- Xiong, L. & Zhu, J.K. (2003). Regulation of abscisic acid biosynthesis. *Plant Physiol*, Vol. 133, No. 1, pp. 29-36.
- Xu, J. & Chua, N.H. (2012). Dehydration stress activates Arabidopsis MPK6 to signal DCP1 phosphorylation. *EMBO J*, Vol. 31, No. 8, pp. 1975-84.
- Xu, J., Li, H.D., Chen, L.Q., Wang, Y., Liu, L.L., He, L. & Wu, W.H. (2006a). A protein kinase, interacting with two calcineurin B-like proteins, regulates K⁺ transporter AKT1 in Arabidopsis. *Cell*, Vol. 125, No. 7, pp. 1347-60.
- Xu, J., Yang, J.Y., Niu, Q.W. & Chua, N.H. (2006b). Arabidopsis DCP2, DCP1, and VARICOSE form a decapping complex required for postembryonic development. *Plant Cell*, Vol. 18, No. 12, pp. 3386-98.
- Xu, Q., Porter, S.W. & West, A.H. (2003). The yeast YPD1/SLN1 complex: insights into molecular recognition in two-component signaling systems. *Structure*, Vol. 11, No. 12, pp. 1569-81.
- Xu, Z.J., Nakajima, M., Suzuki, Y. & Yamaguchi, I. (2002). Cloning and characterization of the abscisic acid-specific glucosyltransferase gene from adzuki bean seedlings. *Plant Physiol*, Vol. 129, No. 3, pp. 1285-95.
- Xu, Z.Y., Lee, K.H., Dong, T., Jeong, J.C., Jin, J.B., Kanno, Y., Kim, D.H., Kim, S.Y., Seo, M., Bressan, R.A., Yun, D.J. & Hwang, I. (2012). A vacuolar beta-glucosidase homolog that possesses glucose-conjugated abscisic acid hydrolyzing activity plays an important role in osmotic stress responses in Arabidopsis. *Plant Cell*, Vol. 24, No. 5, pp. 2184-99.
- Xue, T., Wang, D., Zhang, S., Ehltling, J., Ni, F., Jakab, S., Zheng, C. & Zhong, Y. (2008). Genome-wide and expression analysis of protein phosphatase 2C in rice and Arabidopsis. *BMC Genomics*, Vol. 9, pp. 550.
- Yamaguchi-Shinozaki, K. & Shinozaki, K. (1993). Characterization of the expression of a desiccation-responsive rd29 gene of Arabidopsis thaliana and analysis of its promoter in transgenic plants. *Mol Gen Genet*, Vol. 236, No. 2-3, pp. 331-40.
- Yamaguchi-Shinozaki, K. & Shinozaki, K. (1994). A novel cis-acting element in an Arabidopsis gene is involved in responsiveness to drought, low-temperature, or high-salt stress. *Plant Cell*, Vol. 6, No. 2, pp. 251-64.
- Yamaguchi-Shinozaki, K. & Shinozaki, K. (2005). Organization of cis-acting regulatory elements in osmotic- and cold-stress-responsive promoters. *Trends Plant Sci*, Vol. 10, No. 2, pp. 88-94.
- Yamaguchi-Shinozaki, K. & Shinozaki, K. (2006). Transcriptional regulatory networks in cellular responses and tolerance to dehydration and cold stresses. *Annu Rev Plant Biol*, Vol. 57, pp. 781-803.
- Yamaguchi, M. & Sharp, R.E. (2010). Complexity and coordination of root growth at low water potentials: recent advances from transcriptomic and proteomic analyses. *Plant Cell Environ*, Vol. 33, No. 4, pp. 590-603.
- Yamaguchi, M., Valliyodan, B., Zhang, J., Lenoble, M.E., Yu, O., Rogers, E.E., Nguyen, H.T. & Sharp, R.E. (2009). Regulation of growth response to water stress in the soybean primary root. I. Proteomic analysis reveals region-specific regulation of phenylpropanoid metabolism and control of free iron in the elongation zone. *Plant Cell Environ*, Vol. 33, No. 2, pp. 223-43.
- Yamanaka, T., Nakagawa, Y., Mori, K., Nakano, M., Imamura, T., Kataoka, H., Terashima, A., Iida, K., Kojima, I., Katagiri, T., Shinozaki, K. & Iida, H. (2010). MCA1 and MCA2 that mediate Ca²⁺ uptake have distinct and overlapping roles in Arabidopsis. *Plant Physiol*, Vol. 152, No. 3, pp. 1284-96.

- Yan, J., Zhang, C., Gu, M., Bai, Z., Zhang, W., Qi, T., Cheng, Z., Peng, W., Luo, H., Nan, F., Wang, Z. & Xie, D. (2009). The Arabidopsis CORONATINE INSENSITIVE1 protein is a jasmonate receptor. *Plant Cell*, Vol. 21, No. 8, pp. 2220-36.
- Yang, Y., Sulpice, R., Himmelbach, A., Meinhard, M., Christmann, A. & Grill, E. (2006). Fibrillin expression is regulated by abscisic acid response regulators and is involved in abscisic acid-mediated photoprotection. *Proc Natl Acad Sci U S A*, Vol. 103, No. 15, pp. 6061-6.
- Yang, Z.B., Eticha, D., Fuhrs, H., Heintz, D., Ayoub, D., Van Dorsselaer, A., Schlingmann, B., Rao, I.M., Braun, H.P. & Horst, W.J. (2013). Proteomic and phosphoproteomic analysis of polyethylene glycol-induced osmotic stress in root tips of common bean (*Phaseolus vulgaris* L.). *J Exp Bot*, Vol. 64, No. 18, pp. 5569-86.
- Yin, P., Fan, H., Hao, Q., Yuan, X., Wu, D., Pang, Y., Yan, C., Li, W., Wang, J. & Yan, N. (2009). Structural insights into the mechanism of abscisic acid signaling by PYL proteins. *Nat Struct Mol Biol*, Vol. 16, No. 12, pp. 1230-6.
- Yoo, S.D., Cho, Y. & Sheen, J. (2009). Emerging connections in the ethylene signaling network. *Trends Plant Sci*, Vol. 14, No. 5, pp. 270-9.
- Yoshida, R., Hobo, T., Ichimura, K., Mizoguchi, T., Takahashi, F., Aronso, J., Ecker, J.R. & Shinozaki, K. (2002). ABA-activated SnRK2 protein kinase is required for dehydration stress signaling in Arabidopsis. *Plant Cell Physiol*, Vol. 43, No. 12, pp. 1473-83.
- Yoshida, R., Umezawa, T., Mizoguchi, T., Takahashi, S., Takahashi, F. & Shinozaki, K. (2006a). The regulatory domain of SRK2E/OST1/SnRK2.6 interacts with ABI1 and integrates abscisic acid (ABA) and osmotic stress signals controlling stomatal closure in Arabidopsis. *J Biol Chem*, Vol. 281, No. 8, pp. 5310-8.
- Yoshida, T., Fujita, Y., Sayama, H., Kidokoro, S., Maruyama, K., Mizoi, J., Shinozaki, K. & Yamaguchi-Shinozaki, K. (2010). AREB1, AREB2, and ABF3 are master transcription factors that cooperatively regulate ABRE-dependent ABA signaling involved in drought stress tolerance and require ABA for full activation. *Plant J*, Vol. 61, No. 4, pp. 672-85.
- Yoshida, T., Nishimura, N., Kitahata, N., Kuromori, T., Ito, T., Asami, T., Shinozaki, K. & Hirayama, T. (2006b). ABA-hypersensitive germination3 encodes a protein phosphatase 2C (AtPP2CA) that strongly regulates abscisic acid signaling during germination among Arabidopsis protein phosphatase 2Cs. *Plant Physiol*, Vol. 140, No. 1, pp. 115-26.
- Young, N.F., Ferguson, B.J., Antoniadis, I., Bennett, M.H., Beveridge, C.A. & Turnbull, C.G. (2014). Conditional Auxin Response and Differential Cytokinin Profiles in Shoot Branching Mutants. *Plant Physiol*, Vol. 165, No. 4, pp. 1723-1736.
- Yu, H., Braun, P., Yildirim, M.A., Lemmens, I., Venkatesan, K., Sahalie, J., Hirozane-Kishikawa, T., Gebreab, F., Li, N., Simonis, N., Hao, T., Rual, J.F., Dricot, A., Vazquez, A., Murray, R.R., Simon, C., Tardivo, L., Tam, S., Svrikapa, N., Fan, C., de Smet, A.S., Motyl, A., Hudson, M.E., Park, J., Xin, X., Cusick, M.E., Moore, T., Boone, C., Snyder, M., Roth, F.P., Barabasi, A.L., Tavernier, J., Hill, D.E. & Vidal, M. (2008). High-quality binary protein interaction map of the yeast interactome network. *Science*, Vol. 322, No. 5898, pp. 104-10.
- Yunta, C., Martinez-Ripoll, M. & Albert, A. (2011). SnRK2.6/OST1 from Arabidopsis thaliana: cloning, expression, purification, crystallization and preliminary X-ray analysis of K50N and D160A mutants. *Acta Crystallogr Sect F Struct Biol Cryst Commun*, Vol. 67, No. Pt 3, pp. 364-8.
- Zeller, G., Henz, S.R., Widmer, C.K., Sachsenberg, T., Ratsch, G., Weigel, D. & Laubinger, S. (2009). Stress-induced changes in the Arabidopsis thaliana transcriptome analyzed using whole-genome tiling arrays. *Plant J*, Vol. 58, No. 6, pp. 1068-82.
- Zhang, X., Henriques, R., Lin, S.S., Niu, Q.W. & Chua, N.H. (2006). Agrobacterium-mediated transformation of Arabidopsis thaliana using the floral dip method. *Nat Protoc*, Vol. 1, No. 2, pp. 641-6.

References

- Zhang, X., Jiang, L., Wang, G., Yu, L., Zhang, Q., Xin, Q., Wu, W., Gong, Z. & Chen, Z. (2013). Structural insights into the abscisic acid stereospecificity by the ABA receptors PYR/PYL/RCAR. *PLoS One*, Vol. 8, No. 7, pp. e67477.
- Zhang, X., Zhang, Q., Xin, Q., Yu, L., Wang, Z., Wu, W., Jiang, L., Wang, G., Tian, W., Deng, Z., Wang, Y., Liu, Z., Long, J., Gong, Z. & Chen, Z. (2012). Complex structures of the abscisic acid receptor PYL3/RCAR13 reveal a unique regulatory mechanism. *Structure*, Vol. 20, No. 5, pp. 780-90.
- Zhao, R., Sun, H.L., Mei, C., Wang, X.J., Yan, L., Liu, R., Zhang, X.F., Wang, X.F. & Zhang, D.P. (2011a). The Arabidopsis Ca(2+) -dependent protein kinase CPK12 negatively regulates abscisic acid signaling in seed germination and post-germination growth. *New Phytol*, Vol. 192, No. 1, pp. 61-73.
- Zhao, R., Wang, X.F. & Zhang, D.P. (2011b). CPK12: A Ca (2+) -dependent protein kinase balancer in abscisic acid signaling. *Plant Signal Behav*, Vol. 6, No. 11.
- Zhu, J., Alvarez, S., Marsh, E.L., Lenoble, M.E., Cho, I.J., Sivaguru, M., Chen, S., Nguyen, H.T., Wu, Y., Schachtman, D.P. & Sharp, R.E. (2007a). Cell wall proteome in the maize primary root elongation zone. II. Region-specific changes in water soluble and lightly ionically bound proteins under water deficit. *Plant Physiol*, Vol. 145, No. 4, pp. 1533-48.
- Zhu, J.K. (2002). Salt and drought stress signal transduction in plants. *Annu Rev Plant Biol*, Vol. 53, pp. 247-73.
- Zhu, S.Y., Yu, X.C., Wang, X.J., Zhao, R., Li, Y., Fan, R.C., Shang, Y., Du, S.Y., Wang, X.F., Wu, F.Q., Xu, Y.H., Zhang, X.Y. & Zhang, D.P. (2007b). Two calcium-dependent protein kinases, CPK4 and CPK11, regulate abscisic acid signal transduction in Arabidopsis. *Plant Cell*, Vol. 19, No. 10, pp. 3019-36.

Lebenslauf

Persönliche Daten

Name	Jin Huang
Geboren	Am 04 Januar 1982, in Shaanxi, V.R. China
Nationalität	Chinesisch
Familienstand	Ledig

Ausbildungen

1997-2000	Gymnasium Xiaan, Shaanxi Provenz, V.R. China
2000-2004	Studium von Bachelor an der Sichuan Universität mit Studiengang der Biotechnologie, Sichuan Provenz, V.R. China
2005-2008	Studium von Master an der Sichuan Universität in Studiengang der chemikalischen und molukularen Biologie , Sichuan Provenz, V.R. China
2008-2014	Promotion im Lehrstuh für Botanik der Technische Universität München

Publikation

Christmann, A., Grill, E. & Huang, J. (2013). Hydraulic signals in long-distance signaling. *Curr Opin Plant Biol*, Vol. 16, No. 3, pp. 293-300.

Acknowledgments

This work was performed in the laboratory of Prof. Dr. Erwin Grill at the Institute of Botany of Technische Universität München. I would like to thank with a deep sense of gratitude for Prof. Dr. Erwin Grill accepting me in his laboratory, for the excellent working conditions provided, and the consistent support, teaching and interesting scientific discussions during my Ph. D. time.

I extend my gratitude to Prof. Dr. Kay Schnneitz and Prof. Dr. Ralph Hüchelhoven for participation in my committee.

I would like to thank Dr. Alexander Christmann for his help, patience, scientific and valuable discussions and suggestions from the beginning to the end during my Ph. D. time in this laboratory. I gratefully acknowledge the scientific advices and supports of Dr. Farhah Assaad and Dr. Pascal Braun. Thanks also to Prof. Dr. Christine Gietl for sincere care and valuable discussion.

I specially thank Ting Cao for cooperation and scientific discussion. I am deeply appreciative to many of my colleagues who helped me at the beginning during my Ph. D. time: Dr. Arthur Korte, Dr. Simone Demmel, Dr. Christian Wellmann, Dr. Izabela Szostkiewicz, Dr. Michal Kepka and Dr. Stefan Fuchs. Thanks to C. Eltschig, C. Heidersberger, C. Kornbauer, L. Berngehrer, J. Berger, C. Klaus, L. Held, M. Shimmit, J. Reischenbeck, Z. Yang, G. Czap, K. Hill, N. Kowalski, N. Pleißner, F. Mayer, M. Ruschhaupt, S. Tischer, C. Wunschel, M. Papacek, K. Gläser, K. Rybak, A. Steiner and T. Höwing for their understanding and indispensable cooperation.

I would like to thank Beate Seelinger for her help in daily life and bureaucracy.

I am very grateful to Dr. Tim-Matthias Strom from Helmholtz Center Munich Human Genetic Institute, for providing an opportunity and assistance for next generation sequencing (NGS) and data analysis. I also thank to Prof. Dr. Jutta Ludwig-Müller from the Institut für Botanik of Technische Universität Dresden for GC-MS analysis of ABA quantification.

Finally, I want to express my sincere gratitude to my parents for their help, support, patience, and encouragement during all my life.

This work is supported by Deutsche Forschungsgemeinschaft. And my living in Germany is funded by the State Scholarship fund from the China Scholarship Council of the P.R. China.